Mirroring Enzymes:

The Role of H-Bonding In HQuin-BAM Catalyzed Asymmetric Aza-Henry Reactions:

A DFT Study into the Reactivity, Mechanism, and Origins of Selectivity

Seyedeh Maryamdokht Taimoory, M.Sc.

Department of Chemistry

A dissertation submitted in partial fulfilment of the

requirements for the degree of

Doctor of Philosophy

Faculty of Mathematics and Science, Brock University

St. Catharines, Ontario

To my Family.

Abstract

The exact mechanistic understanding of various organocatalytic systems in asymmetric reactions such as Henry and *aza*-Henry transformations is important for developing and designing new synthetic organocatalysts. The focus of this dissertation will be on the use of density functional theory (DFT) for studying the asymmetric *aza*-Henry reaction. The first part of the thesis is a detailed mechanistic investigation of a poorly understood chiral bis(amidine) (BAM) Brønsted acid catalyzed *aza*-Henry reaction between nitromethane and *N*-Boc phenylaldimine. The catalyst, in addition to acting as a Brønsted base, serves to simultaneously activate both the electrophile and the nucleophile through dual H-bonding during C–C bond formation and is thus essential for both reaction rate and selectivity. Analysis of the H-bonding interactions revealed that there was a strong preference for the formation of a homonuclear positive charge-assisted H-bond, which in turn governed the relative orientation of substrate binding. Attracted by this well-defined mechanistic investigation, the other important aspect of my PhD research addressed a detailed theoretical analysis accounting for the observed selectivity in diastereoselective versions of this reaction. A detailed inspection of the stereodetermining C–C bond forming transition states for monoalkylated nitronate addition to a range of electronically different aldimines, revealed that the origins of stereoselectivity were controlled by a delicate balance of different factors such as steric, orbital interactions, and the extent of distortion in the catalyst and substrates. The structural analysis of different substituted transition states established an interesting dependency on matching the shape and size of the catalyst (host molecule) and substrates (guest molecules) upon binding, both being key factors governing selectivity, in essence, offering an analogy to positive cooperative binding effect of catalytic enzymes and substrates in Nature. In addition, both intra-molecular (intra-host) and inter-

molecular (host-guest, guest-guest) stabilizing interactions play a key role to the high π-facial selectivity. The application of dispersion-corrected functionals (i.e., ωB97X-D and B3LYP-D3) was essential for accurately modeling these stabilizing interactions, indicating the importance of dispersion effects in enantioselectivity. As a brief prelude to more extensive future studies, the influence of a triflate counterion on both reactivity and selectivity in this reaction was also addressed.

Acknowledgements

I am extremely grateful to the following people. Without their guidance and help, the completion of this thesis would not have been possible.

First and foremost, I would like to express my sincere appreciation to my research supervisor, Professor Travis Dudding for his mentoring, encouragement and for giving me an opportunity to work under his guidance. His immense knowledge and endless patience helped me throughout my time in his group. Alongside with the chemistry, he taught me the significance of learning from failure and being strong.

I would like to extend my special appreciation to my supervisory committee members: Professor Heather Gordon, and Professor Art van der Est for their guidance, encouragement, insightful suggestions and generous support over the years, for both being brilliant teachers, for their participation on my committee and for their valuable comments on this thesis.

I would also like to thank Professor Georgii Nikonov and Professor Jeffrey Atkinson for being in my candidacy examination.

I want to thank the Dudding group members. I would like to specifically thank Lee Belding for his assistance and most importantly his friendship. I would also like to thanks all my friends.

I gratefully acknowledge the Ontario Trillium Scholarships for financial support. I would also like to thank Sharcnet for computing resources.

Last but not least, words cannot express how grateful I am to my father and mother, my sister, Neda, and my brother, Nima; their unwavering love and support provided me inspiration

to pursue my dreams, without them none of this would have been possible. I'd like to express my greatest appreciation and love to my husband, Iraj, because of you I made it this far.

.

Table of Contents

List of Schemes

List of Figures

List of Tables

Abbreviations

BAM	bis(amidine)
BCP	bond critical point
BINAP	2,2'-bis(diphenylphosphino)-1,1'-binaphthyl
BINOL	1,1'-bi-2-naphthol
B3LYP	Becke 3-parameter (exchange), Lee, Yang, Parr
Bu	butyl
(±)CAHBs	positive or negative charge-assisted hydrogen bonds
calcd	calculated
CP	cyclopentadiene
DFT	Density Functional Theory
DHAP	dihydroxyacetone phosphate
DMF	dimethylformamide
ee	enantiomeric excess
hDA	hetero-Diels-Alder cycloaddition reaction
HDV	hepatitis delta virus
HOMO	highest occupied molecular orbital
IEFPCM	integral equation formalism polarizable continuum model
IHBs	isolated hydrogen bonds
IUPAC	International Union of Pure and Applied Chemistry
LUMO	lowest unoccupied molecular orbital
m	meta
Me	methyl
MM	molecular mechanics
MO	molecular orbital
NBO	natural bond orbitals
MVK	methyl vinyl ketone
o	ortho
OTf	trifluoromethanesulfonate
p	para
PA	proton affinity
PAHBs	polarization-assisted hydrogen bonds
PES	potential energy surface
Pr	propyl
PTC	phase transfer catalysis
p-Tol-BINAP	2,2′-bis(di-*p*-tolylphosphino)-1,1′-binaphthyl
py	pyridine
QM	quantum mechanics
QTAIM	quantum theory of atoms in molecules
RAHBs	resonance-assisted hydrogen bonds
rt.	room temperature
TADDOL	(*α,α,α',α'*-tetraaryl-1,3-dioxolane-4,5-dimethanol)
TFA	trifluoroacetic acid
TFOH	trifluoromethanesulfonic acid
TFPB	3,5-bis(trifluoromethyl) phenyl) borate

THF	tetrahydrofuran
TMS	trimethylsilyl
TS	transition state

1. Introduction

1.1. H-Bond Catalysis

1.1.1. H-Bond Definition and Classification

The hydrogen bond (H-Bond)[1] plays a crucial role in nearly all of life's chemical processes. For example, the hydrogen bond is essential in DNA base pairing, cell-signaling, and enzymatic activity. In addition to its significance as a structural determining factor, hydrogen bonding plays a central role in catalysis in both the acceleration of chemical reactions and as the primary source of stereocontrol. In a related, but chemically distinct context, the recent emergence of the field of organocatalysis, which encompasses processes mediated by small organic molecules that in many ways are similar in composition and function to enzymes, has brought with it a number of H-bond catalyzed methodologies.[2] Thus, to gain a comprehensive understanding of the fundamentals of H-bond catalysis, a brief definition and discussion of H-bonding is required.

The primary definition of the H-bonding phenomenon is attributed to G.N. Lewis, who first categorized H-bonding as A:H:B-type bonding and described the H-bonding concept as,[3] *''an atom of hydrogen [that] may at times be attached to two electron pairs of two different atoms, thus acting as a loose bond between these atoms''* Pauling and several researchers[4] were the first to identify the general principle of this interaction and paved the way for the creation of the modern concept of H-bonding. In 2002, Steiner *et al.* defined H-bonding as,[5] *"An X-H···A interaction is called a hydrogen bond, if 1. It constitutes a local bond, and 2. X-H acts as a proton donor to A."* The best understanding of the H-bonding motif was reported by IUPAC (International Union of Pure and Applied Chemistry) which recently updated its definition as,[6] *"A fractional chemical bond of coordinative A–H…B Lewis acid–base type, associated with the*

partial intermolecular A–H…:B↔A:…H–B resonance (3-center/4-electron proton-sharing) commonly originating in the $n_B \rightarrow \sigma^*_{AH}$ *donor–acceptor interaction between the lone pair* n_B *of the Lewis base and the hydride antibond* σ^*_{AH} *of the Lewis acid".*

Notably, there are numerous studies focused on the strength and nature of H-bonding and its classification.[7] For example, Desiraju and Steiner[8] classified H-bonds as weak, moderate and strong, based on the geometrical parameters and the energetic aspects of such interactions. Rozas *et al.*[9] characterized H-bond interactions according to the topological parameters derived from the Quantum Theory of Atoms in Molecules (QTAIM).[10] The most comprehensive and interesting aspect of a H-bond classification was proposed by Gilli *et al.*[11] (Table 1) who divided H-bonds as positive or negative charge-assisted H-bonds (±CAHBs), resonance-assisted H-bonds (RAHBs), polarization-assisted H-bonds (PAHBs), and ordinary or isolated H-bonds (IHBs). Although there has been extensive discussion of the definition and identification of this important interaction, the main goal of this dissertation will be to explain the importance of H-bonding in catalysis.

Table 1. A recent classification of H-bond based on its strength.[11]

	Strong	**Moderate**	**Weak**
H-Bond nature	mostly covalent	mostly electrostatic	electrostatic
Bond lengths	D-H ≈ H…A	D-H < H…A	D-H << H…A
H···A (Å)	*1.2-1.5*	*1.5-2.2*	*2.2-3.2*
D···A (Å)	*2.2-2.5*	*2.5-3.2*	*3.2-4.0*
D-H…A angle (°)	*165-180*	*130-180*	*90-150*
Energy (kcal mol^{-1})	*15-45*	*4-15*	*< 4*
Typical H-Bonds	Charge-assisted: $[H_2O{\cdot\cdot}H{\cdot\cdot}OH_2]^+$; proton sponges $[=N{\cdot\cdot}H{\cdot\cdot}N=]^+$	-O-H···O=; -O-H···N=; -N-H···O=; -N-H···N=; σ-Cooperative or polarization-assisted: ···O-H···O-H···	C-H···O; C-H···N; O/N-H···π bonds Ordinary or Isolated H-Bond

1.1.2. H-Bond in Biocatalysis

To realize the potential of H-bond catalysts in accelerating chemical reactions and performing asymmetric transformations, a detailed mechanistic analysis of their actions is certainly required. Understanding how enzymes (Nature's catalysts), utilize H-bonds to carry out different enzyme-catalyzed reactions, allows organic chemists to design and develop a wide range of H-bond mediated asymmetric reactions.

The multifunctional role of serine proteases and other biocatalysts has triggered numerous studies[12] researching various synthetic catalyst systems, which rely on the simultaneous activation of a nucleophile and an electrophile. Mechanistically, the distortion of the amide group at the time of substrate binding and the structural rearrangement of the enzyme affect the favorable alignment of catalytic residues and in turn increase their catalytic activities.

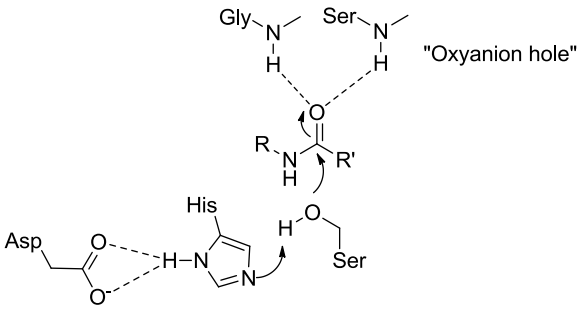

Scheme 1. Serine protease: Acceleration of amide hydrolysis by bifurcated H-bonding, multiple noncovalent catalyst–substrate interactions and bifunctional catalysis.

Type II aldolases such as L-fuculose 1-phosphate aldolase are one of the few classes of enzyme, that use H-bonding interactions to catalyze enantioselective reactions. As highlighted in Scheme 2, in this stereoselective aldol reaction of dihydroxyacetone phosphate (DHAP) with L-lactaldehyde, the phenolic hydroxy groups of Tyr and the carboxylic acid group in the Glu residue, affect the favored orientation and activation of the electrophile.[13]

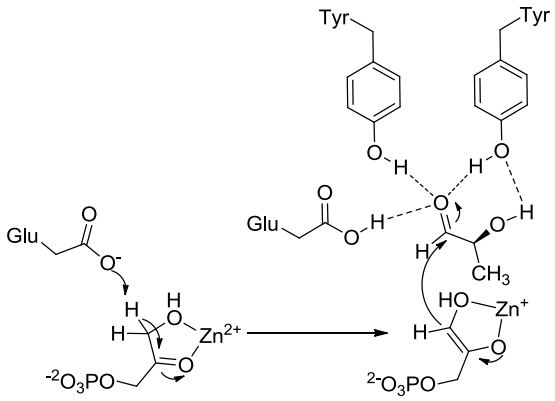

Scheme 2. Type II aldolase: Bifunctional catalysis in stereoselective aldol reaction.

Organic chemists are particularly interested in studying the exact action of RNA enzymes in catalysis, as these details have allowed them to develop a variety of H-bond catalysts that mimic enzymes.[14] For example, probing the catalytic mechanism of a naturally found ribozyme, [15] hepatitis delta virus (HDV), highlighted the H-bond mediated bifunctional role of HDV in phosphoryl transfer reactions. As shown in Scheme 3, cleavage of a phosphodiester bond of the HDV ribozyme occurs through a general acid/base catalysis mechanism, in which the phosphate electrophile is activated by H-bonding with the protonated form of cytosine 75 as an H-bond donor (a general acid catalysis), while the nucleophilic 2'-hydroxy group is activated by a ribozyme-bound hydrated metal hydroxide (a general base catalysis).

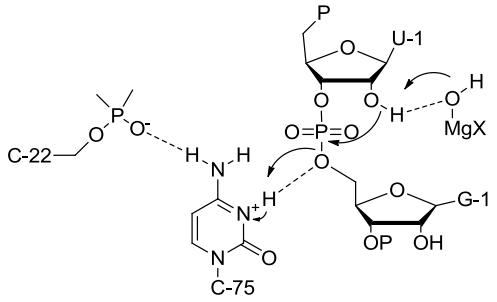

Scheme 3. The hepatitis delta virus ribozyme: Acceleration of a phosphoryl transfer by bifunctional catalysis.

1.1.3. H-Bonding in Small Organic Synthetic Catalysis

As mentioned in Section 1.1.2, Nature uses the H-bond as a powerful element to activate and orient substrates in enzymatic catalysis. Through well-organized H-bonding networks, enzymes have achieved unparalleled efficiency that has rarely been equaled by chemists. As a result, the concepts behind enzyme-mediated transformation, in which H-bond activation plays an important role, are actively being applied to catalyst design.[16] With the aim of mimicking Nature's efficiency, organic catalysts are being developed with substrate-specific cavities, chiral backbones, and multiple activation sites, many of which rely on the use of hydrogen bond motifs.[17] In this regard, the synthesis of chiral organocatalysts with H-bonding sites has attracted substantial attention in recent years.[18] Research in this area has covered a number of Lewis- and Brønsted acid subtypes, such as (thio)ureas, diols, phosphoric acids, and guanidinium/amidinium ion catalysts, which importantly, from a mechanistic point of view, are thought to affect the H-bond catalysis through distinctly different modes of action.[19]

1.1.4. Chiral Lewis-, Brønsted Acid Hydrogen Bond Organocatalysis

The application of organocatalysts in asymmetric transformations has received considerable attention in recent years due to the presence of their different modes of activation and the structural simplicity of the majority of organocatalysts. Mechanistically, catalytic modes of activation can be categorized based on the type of interactions between substrate and catalyst (covalent or noncovalent), the nature of the applied organocatalyst (Lewis base, Lewis acid, Brønsted base, and Brønsted acid),[20] or a combination of these aspects (bifunctional organocatalysis).

Among different organocatalysts, Lewis- (H-bonding) and Brønsted acid organocatalysts are capable of catalyzing a great variety of H-bond mediated organic reactions and are useful

tools in asymmetric synthesis.[21] From a mechanistic point of view, this area of organocatalysis is further subdivided into three main classes of catalysis: 1) Brønsted acid activation organocatalysis (Scheme 4a,b), in which a complete proton transfer from a catalyst to the substrate occurs, which renders the substrate more electrophilic toward nucleophilic attack; 2) H-bonding activation organocatalysts, in which the catalyst increases the electrophilic character of the substrate by means of H-bonding interaction (Scheme 4c); and 3) H-bonding activation catalysts with anion-binding, in which the chiral organocatalyst increases either the acidic nature of an achiral Brønsted acid (Scheme 4d) or the nucleophilic character of substrate (Scheme 4e).[22]

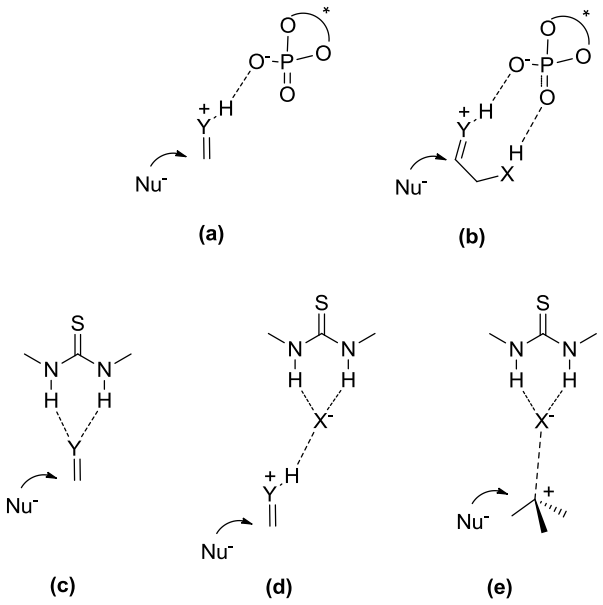

Scheme 4. Different kinds of organocatalysis: (a, b) Brønsted acid activation, (c) H-bonding activation; and (d, e) H-bond donor activation organocatalysis by anion-binding.

Since H-bonding interactions play a central role in all these areas of organocatalysis, understanding the spectrum of H-bonding reactivity is essential for continued development in the area of catalytic design. Although there has been extensive research in the area of

organocatalyzed asymmetric transformations, the focus of this dissertation will be on chiral Lewis-, Brønsted acid H-bond organocatalysts and their applications in accelerating chemical reactions such as the aldol, Henry, and *aza*-Henry reactions and in controlling asymmetric induction.

1.1.4.1. O-H Based Chiral H-Bond/Brønsted Acid Organocatalysts (Diols, Biphenols, and Phosphoric Acid-Based Organocatalysts)

The O-H based class of chiral organocatalysts such as TADDOL (*α*,*α*,*α*',*α*'-tetraaryl-1,3-dioxolane-4,5-dimethanol) and BINOL (1,1'-bi-2-naphthol) derivatives, as well as chiral phosphoric acids, are capable of highly enantio- and diastereoselective catalysis employing either single or double H-bonding interactions.[23]

Chiral BINOL and BINOL-based phosphoric acid derivatives are one of the most important types of organocatalysts in the area of Brønsted acid activation organocatalysis. In 1999, Yamamoto *et al*.[24] proposed the application of Lewis acid assisted chiral Brønsted acids, as well as Brønsted acid assisted chiral Lewis acids, in different asymmetric transformations. Since Yamamoto's initial reports, a wide class of chiral alcohols have been designed and successfully applied as asymmetric H-bond catalysts.

In pioneering research, Schaus and co-workers[25] discovered the role of BINOL-based organocatalysts, (**1** and **2** in Scheme 5) as chiral Brønsted acids (H-bond catalysts) in reactions of electron deficient alkenes with aldehydes (Morita-Baylis-Hillman reactions). A particularly interesting mechanistic feature of these binaphthol-derived Brønsted acids was the formation of dual H-bonding that was essential for both their catalytic actions and enantioselectivity.

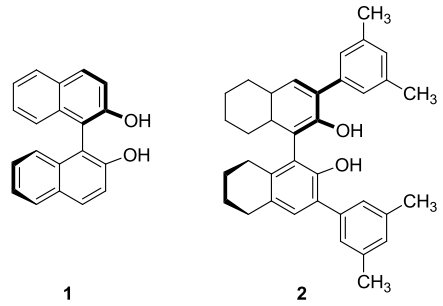

Scheme 5. Schaus BINOL-derived Brønsted acid organocatalysts.

Attracted by the discovery of the BINOL skeleton, the groups of Akiyama[26] and Terada[27] developed novel phosphoric acid catalysts (**3**, **4** in Scheme 6). This new family of chiral Bronsted acid organocatalysts were successfully applied in highly enantioselective Mannich-type reactions. It was found that substitution at the 3-position of the catalyst's naphthyl ring with aryl functional groups was important for achieving high selectivity. Although at that time a detailed mechanism of this phosphoric acid catalyzed Mannich reaction was not revealed, it was proposed that the aldimine substrate was activated by the catalyst via formation of an iminium salt. These successful achievements paved the way for the use of these relatively strong Brønsted acid organocatalysts in large classes of asymmetric transformations.

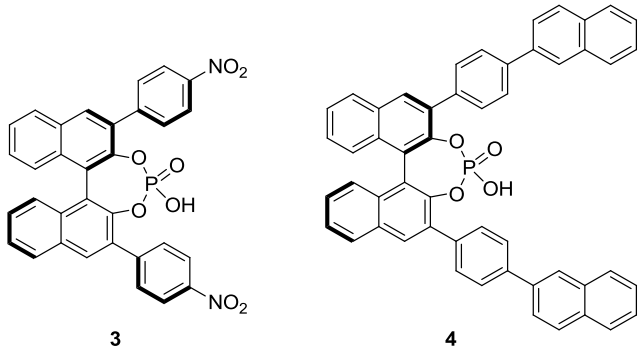

Scheme 6. Initial reports by Akiyama and Terada of chiral phosphoric acids.

The enantioselective hetero-Diels-Alder (hDA) cycloaddition reaction, proposed by Rawal,[28] is one of the important classes of H-bond promoted asymmetric transformations. In 2004, Rawal and co-workers reported a chiral alcohol (**5** in Scheme 7a), TADDOL (*α,α,α',α'*-tetraaryl-1,3-dioxolane-4,5-dimethanol)-catalyzed enantioselective hetero-Diels−Alder reaction of aldehydes with activated dienes and have since reported numerous related organocatalyzed processes. The authors highlighted the importance of H-bonding on both the rate and the enantioselectivity of the cycloaddition. Accordingly, it was suggested that H-bonding not only affected the preferred conformation of the TADDOL catalyst, but, acting as a Brønsted acid catalyst, it also activated the dienophile (Scheme 7b).

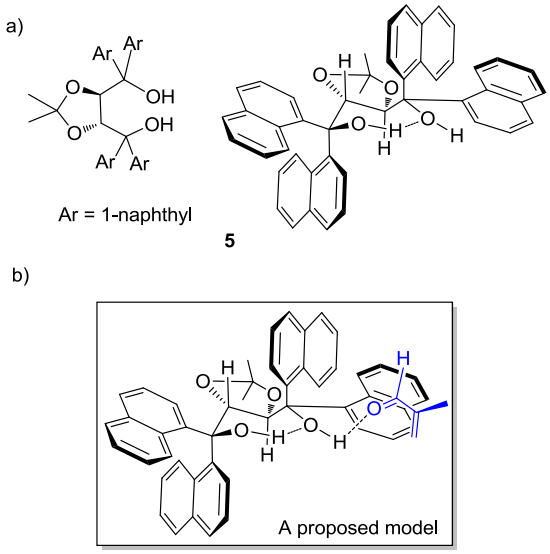

Scheme 7. a) Solid-state structures of TADDOL **5**, b) a proposed working model for the activation of dienophile in TADDOL catalyzed hetero-Diels–Alder reactions.

The importance of these findings led to detailed theoretical studies from Domingo, Dudding, Houk and others[29] which have established that the (*R,R*)-TADDOL-catalyzed hDA reactions occur through different binding modes. The theoretical investigation of TADDOL-based organocatalysis will be discussed in detail throughout section 1.3.

1.1.4.2. N-H Based Chiral H-Bond/Brønsted Acid Organocatalysts (Peptides, Urea/Thiourea, Guanidinium, Amidinum)

The application of organocalysts containing N-H groups for catalysis has been extensively investigated by both experimental and theoretical research groups. For example, among different classes of synthetic peptides, cyclic dipeptides, cyclo[(*R*)-His-(*R*)-Phe] or cyclo[(*S*)-His-(*S*)-Phe], are thought to be potential catalysts for asymmetric synthesis. Using this family of organocatalyst, Inoue and co-workers studied the asymmetric addition of hydrogen cyanide to benzaldehyde.[30] This synthetic cyclic catalyst (**6** in Scheme 8a) was developed to be analogous to the enzyme hydroxynitrilase lyase (oxynitrilase) which catalyzes the same reaction. In their mechanistic analysis, the author proposed that the benzaldehyde substrate was activated via formation of mono-coordinated H-bonding with catalyst **6**, and hydrogen cyanide interacting with the imidazolyl functionality of the histidine. The generated cyanide ion then attacked the *Si* face of the activated carbonyl group (Scheme 8b).

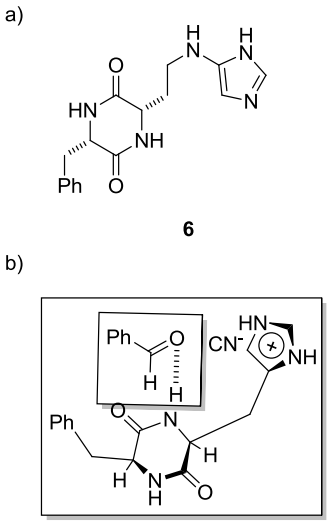

Scheme 8. a) Inoue's dipeptide catalyst, and b) a proposed model for the asymmetric addition of hydrogen cyanide to benzaldehyde.[30]

Several years after Inoue's work, Lipton *et al.* reported the first example of an analogous cyclic dipeptide (**7** in Scheme 9), which catalyzed the enantioselective Strecker reaction.[31] Both catalysts **6** and **7** have almost similar structures and the same mechanistic actions, albeit they catalyze formation of enantiomers.

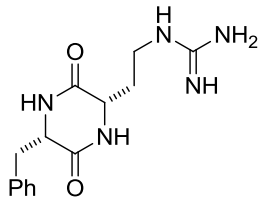

7

Scheme 9. Lipton's **7** dipeptide catalyst.[31]

To explore further these novel organocatalysts, their mechanistic actions were further investigated using different computational and experimental techniques that highlighted the critical role of H-bonds and noncovalent interactions in controlling reactivity and selectivity of dipeptide-mediated asymmetric reations, such as enantioselective hydrocyanation of aldehydes (Figure 1).[32]

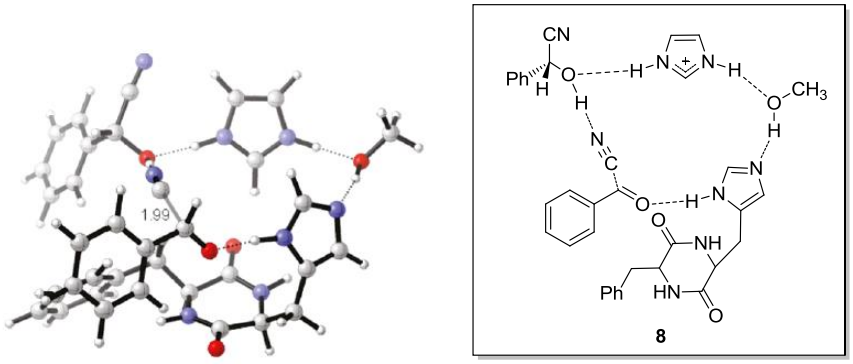

8

Figure 1. Model transition state **8** for dipeptide-catalyzed enantioselective hydrocyanation of aldehydes.

A new class of organocatalysts based on urea/thiourea (Scheme 10), was designed and developed by Jacobsen and coworkers.[33] Their initial studies revealed the power of these chiral

catalysts for the asymmetric Strecker reaction. However, at that time, the origin of high enantioselectivity and the exact mechanism of catalysis were poorly understood.

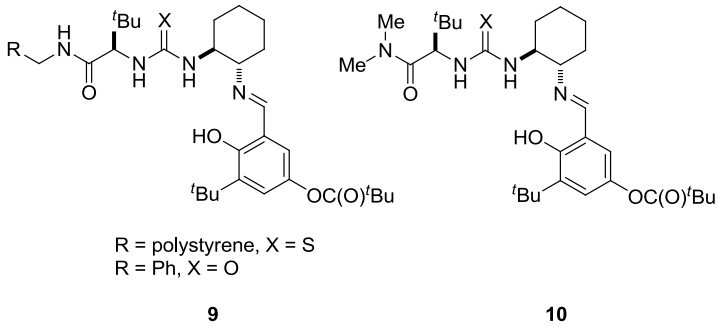

Scheme 10. Jacobsen's urea/thiourea chiral organocatalysts.

The use of urea/thiourea based catalysts was widely investigated and successfully extended to a variety of asymmetric transformations. Different experimental and theoretical research groups have identified the exact mechanistic functions of thiourea-based organocatalysts in numerous asymmetric reactions.[34] For example, through an eloquent series of spectroscopic experiments, DFT calculations, and kinetic rate studies, Jacobson *et al.* reported that the thioureas mediated enantioselective cyanosilylations of ketones, acyl-Pictet Spengler reactions, Mannich-type reactions and the aza-Baylis-Hillman reaction function by means of bifurcated H-bonding mode of action, as illustrated by the minimum energy geometry of a catalyst-imine complex **11** and **11'** (Figure 2).[35]

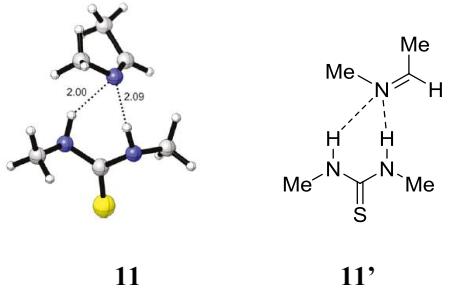

Figure 2. The key role of thiourea functionality and bifurcated H-bonding for catalysis.

Very recently, various thiourea organocatalysts have been designed, which are effective anion stabilizers. The group of Jacobsen in combination with Seidel and others have pioneered this conceptually unique approach to asymmetric organocatalysis, in which chemo-, regio-, and stereoselective induction is carried out by formation of a bifurcated H-bond stabilized anion (i.e., a pseudochiral anion).[36]

Following Jacobsen's initial work of applying thioureas in asymmetric organocatalysis, Takemoto *et al*.[37] reported the first example of an achiral thiourea (**13** in Scheme 11) catalyzed addition of cyanide to nitrones. Achiral ureas and thioureas were then used in synthetically important organic transformations such as allylation reactions, Claisen rearrangements, Diels–Alder cycloadditions and dipolar cycloaddition processes.[38] Although this class of achiral catalyst was applied in a relatively small range of reactions, their chiral equivalents catalyze a wide range of asymmetric reactions. For example, a few months after Takemoto's report of the achiral thiourea **13** catalyst, it was changed into a chiral bifunctional catalyst (**14** in Scheme 11) and used in both Michael and aza-Henry reactions.[39]

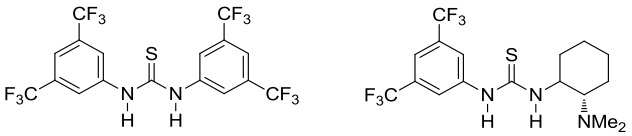

Scheme 11. Achiral and chiral thiourea organocatalysts.

The field of bifunctional asymmetric organocatalysis, involving the synergistic activation of both electrophile and nucleophile, has received considerable attention. The bifunctional thiourea-based organocatalyst with a H-bonding site and a Brønsted basic functional group, was first developed by Takemoto and represented in Figure 3.[40] Since then, the bifunctional role of

different substituted thiourea catalysts and the importance of the bifurcated H-bond in both activation and orientation of substrates have been investigated by different research groups.[41]

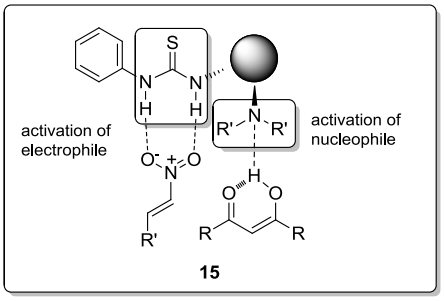

Figure 3. Bifunctional role of thiourea catalysts in simultaneous activation of electrophile and nucleophile.

Chiral guanidinium and amidinium ions (structural relatives of thiourea organocatalysts), were used to catalyze different asymmetric reactions via formation of dual (bifurcated), as well as single, H-bonding interactions.[42] Ground-breaking research in this field was performed by Corey and coworkers in asymmetric Strecker reactions, highlighting the potential of both single H-bonding and double H-bonding in the activation of imine substrates.[43] In their mechanistic analysis, it was proposed that a complex of guanidinium cyanide was initially generated from the cyclic guanidine catalyst (**16** in Scheme 12a) and hydrogen cyanide, then the H-bond mediated addition of cyanide ion to the imine electrophile produced the desired adduct with high yield and enantioselectivity (Scheme 12b).

a)

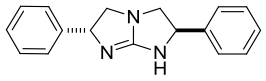

16

b)

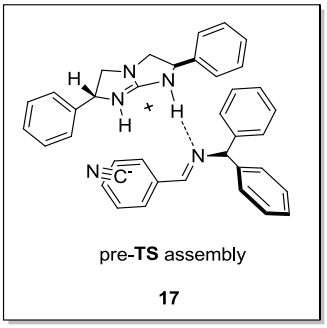

17

Scheme 12. a) The structure of a cyclic guanidine catalyst, and b) pre-transition state assemblies **17** for the guanidine catalyzed Strecker reaction.

Supporting this H-bond mediated asymmetric transformation, Han *et al.* investigated a detailed mechanistic scenario, using DFT methods.[44] These calculations revealed two competitive reaction paths for the bicyclic guanidine catalyzed Strecker reaction of HCN and methanimine. Pathway A involves the isomerization of HCN to HNC, followed by its addition to methanimine (**18** in Scheme 13), while pathway B (**19** in Scheme 13) involves the HCN addition to methanimine to obtain aminoisoacetonitrile, followed by its isomerization to aminoacetonitrile product. The mechanistic pathway A was the energetically favored and the Strecker reaction most likely occurs through HNC.[45]

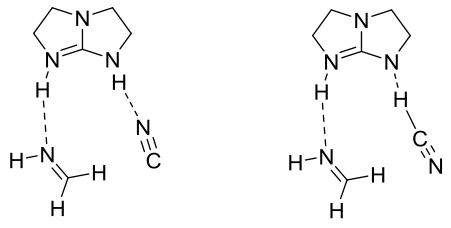

18 **19**

Scheme 13. The proposed models for the reaction of HCN (or HNC) and methanimine with guanidine.[44]

Since then, guanidine-based organocatalysts have been used successfully to promote highly enantioselective reactions such as the Diels-Alder cycloaddition reactions[46] and (aza)-Henry reactions.[47]

A slightly different Brønsted acid catalyst based on a protonated chiral ligand was reported by Kotsuki and coworkers[48] to catalyze the Michael addition reaction of ketones to nitroolefins. The desired 1,4-products were achieved in excellent yields with high enantio- and diastereoselectivities using chiral pyrrolidine-pyridine complexed with an achiral protic acid (**20** in Scheme 14).

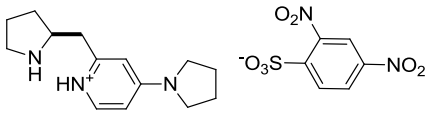

chiral pyrrolidine-pyridine
protic acid
20

Scheme 14. Chiral pyrrolidine-pyridine conjugated base catalyst in combination with a protic acid.

Four years earlier than Kotsuki's report,[50] a new class of achiral, (**21** in Scheme 15) and chiral, (**22** in Scheme 15) amidinium based catalysts was introduced by Göbel *el al.* to accelerate Diels–Alder cycloaddition reactions.[49] The achiral amidinium catalyst, (**21** in Scheme 15) highlighted the potential of the tetrakis (3,5-bis(trifluoromethyl)phenyl) borate (TFPB) counterion in increasing the catalytic activity. In addition, moderate enantioselectivity was attained employing the chiral amidinium catalyst (**22** in Scheme 15), in which the positive H-bond-mediated activation of dienophiles increased rates of cycloaddition reactions. Thus, the mode of action of these classes of organocatalysts is enhancing the electrophilicity of substrate via formation of hydrogen bonded ion pairs.[50]

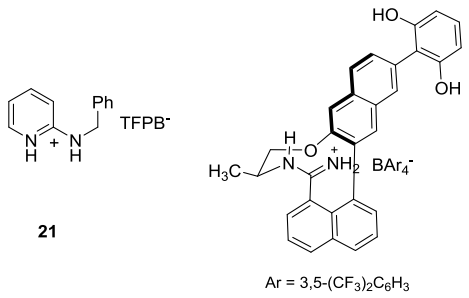

21 22

Scheme 15. An achiral and a chiral amidinium based organocatalysts.

These same authors also reported Diels-Alder cycloaddition reactions employing the chiral bis(amidinium) salt (**23** in Scheme 16) as a catalyst to access synthetically important compounds.[51] The author anticipated that the H-bond mediated binding of dienophiles with the chiral salt **23** increased the rate of the Diels-Alder reaction with dienes. The only limitation of this catalytic system was the moderate enantioselectivity (15-47%). In addition, it was suggested that due to the large distance between the amidinium groups, the catalyst was not able to bind properly to substrate. To gain further knowledge of amidinium-based catalyzed asymmetric reactions, Göbel *el al*. also investigated the alternative bisamidine (**24** in Scheme 16) catalyzed asymmetric Diels-Alder and Friedel-Crafts reactions.[52] It was suggested that the planar conformation of this mono-protonated catalyst (**24** in Scheme 16) with appropriate orientation of the H-bond donors (N-H groups) may lead to optimal substrate binding.

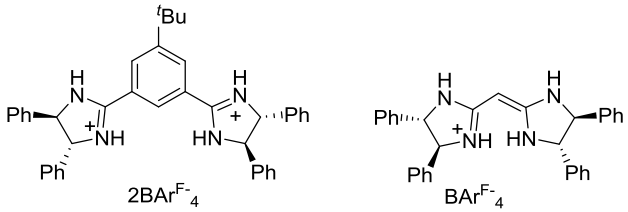

23 24

Scheme 16. Göbel's chiral bis(amidinium) salts **23**, **24**.

Another important early development using protonated amines as catalysts, was Johnston *et al.*'s advancement of a class of chiral bis(amidine) (BAM) Brønsted acid catalysts [e.g., HQuin-BAM **25** in Scheme 17].[53] High enantioselectivity and diastereoselectivity of the aza-Henry reaction was achieved by protonation of a diaminocyclohexane-derived bisamidine ligand, using trifluoromethanesulfonic acid (TfOH). Thus, the catalyst system was based on a chiral BisAMidine ligand (BAM)-protic acid complex (**25** in Scheme 17) which was able to catalyze efficiently asymmetric *aza*-Henry reactions of nitroalkanes with *N*-Boc arylaldimines. However, at the time, the underlying mechanistic details are poorly understood, despite the impressive extension of this work by Johnston.[54]

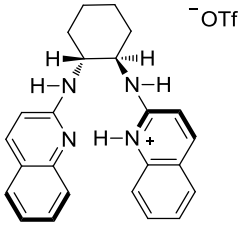

25

Scheme 17. Johnston's amidinium-based organocatalyst.

A particularly interesting aspect of this amidinium-based organocatalyst (**25** in Scheme 17) and its analogues was the postulated involvement of a polar ionic H-bond with greater ability to activate electrophiles owing to the positive charged nature. Furthermore, stereoinduction can be improved by optimizing the achiral counterion.[55]

1.2. *Aza*-Henry (Nitro-Mannich) Reactions

1.2.1. Historical

The nucleophilic addition of nitroalkane nucleophiles **27** to imine electrophiles **26** and related compounds (*aza*-Henry or nitro-Mannich reaction) is an important synthetic approach to formation of C-C bonds with simultaneous generation of vicinal stereogenic nitro- and amino-

substituted centres (Scheme 18). The resulting *β*-nitroamine product **28** is a valuable target that allows access to other synthetically useful structural motifs such as α-amino acids, 1,2-diamines and monoamines via nitro reduction, and the Nef reaction.[56]

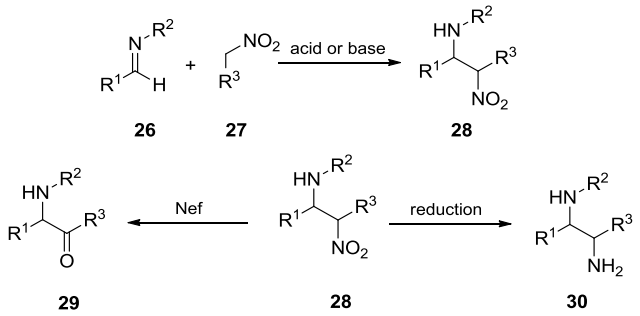

Scheme 18. *aza*-Henry reaction.

The *aza*-Henry reaction is named after Louis Henry, who published the first example of the addition of a nitroalkane nucleophile to an aldehyde electrophile (Henry reaction).[57] The following year, he also reported the first nitro-Mannich reaction (*aza*-Henry) in the addition of nitroalkanes to two equivalent hemiaminals (Scheme 19).[58] In 1901, Mousset and coworkers investigated the application of the synthesized nitroisopentane in both the Henry and *aza*-Henry reactions (Scheme 19).[59]

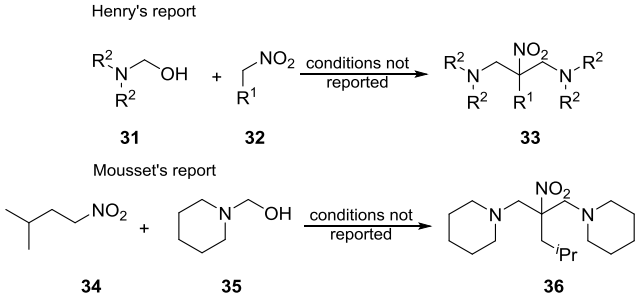

Scheme 19. The first examples of the reported nitro-Mannich reactions.

Almost 30 years later, Cerf de Mauny presented a detailed study of the experimental procedures based on the original theory proposed by Henry.[60] Cerf's description of the nitro-Mannich reaction was later revised by Senkus[61] to describe the reaction of different substituted nitroalkanes with formaldehyde and a range of primary amines. Senkus' report was the first example of a nitro-Mannich reaction using primary amines (Scheme 20). At the same time, Johnson studied and further extended the analogous reaction using secondary amines[62] and primary arylamines (Scheme 20).[63]

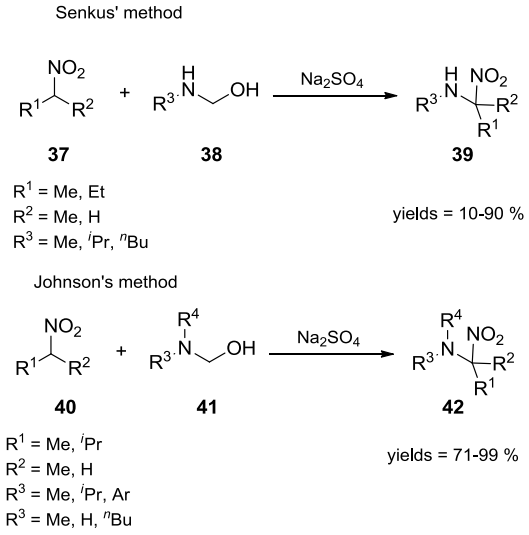

Scheme 20. Senkus' and Johnson's nitro-Mannich reaction.

Further development occured in 1950, when Hurd and Strong reported the first nitro-Mannich reaction between nitroalkanes **44** and the electrophile *N*-protected benzylimine **43** to achieve the final products **45** (Scheme 21).[64]

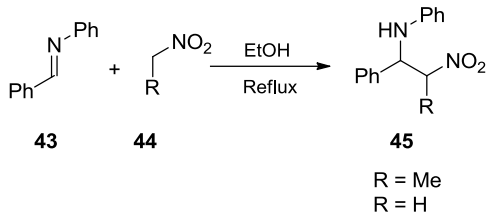

Scheme 21. The first nitro-Mannich reaction between nitroalkanes **44** and a pre-formed imine **43**.

The nucleophilic additions of nitroalkanes to imines was thoroughly investigated in the 20th century, however, there were limitations in both yield and selectivity and most of the related works were focused on racemic derivatives. The first acyclic asymmetric *aza*-Henry reaction between a pre-formed imine and metal nitronates was reported by Anderson *et al.*[65] to afford the desired products in good yields and diastereoselectivity (Scheme 22). Later, Anderson *et al.* investigated a catalytic variant of this reaction using a Lewis acid catalyst.[66]

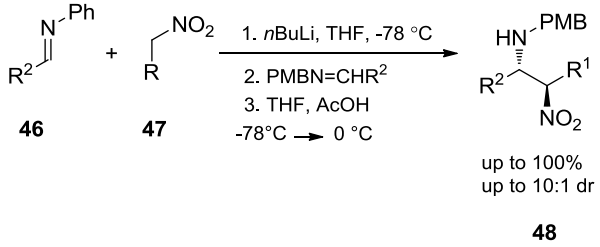

Scheme 22. The first acyclic diastereoselective nitro-Mannich reaction.

The success of this class of catalysts in a variety of asymmetric *aza*-Henry reactions was further reported by several research groups. For example, Shibasaki *et al.*[67] proposed the first catalytic asymmetric nitro-Mannich reaction employing the heterobimetallic complex **52** (Scheme 23). A significant advancement in this area was further reported by the same group using different modified catalytic systems.

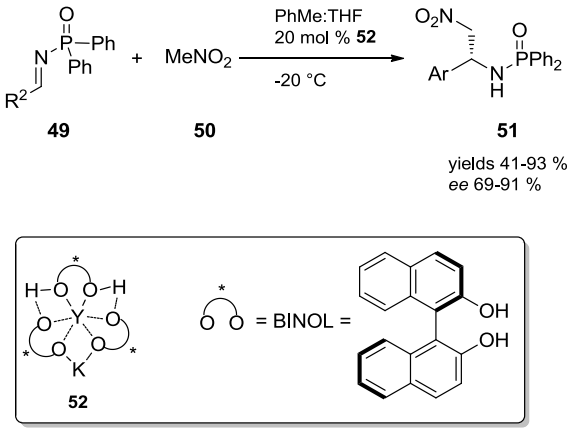

Scheme 23. The first direct catalytic enantioselective nitro-Mannich reaction.

In addition, Jørgensen *et al.*[68] reported the first catalytic asymmetric *aza*-Henry reaction of TMS-nitronates **53** with ethylglyoxylate-N-PMP-imine **54** in presence of Cu(II) Box catalysts **56** achieving products **55** in high yields and with high enantio- and diastereoselectivities (Scheme 24). Applying the same catalyst, Jørgensen also reported a direct variant of the asymmetric *aza*-Henry reaction.[69]

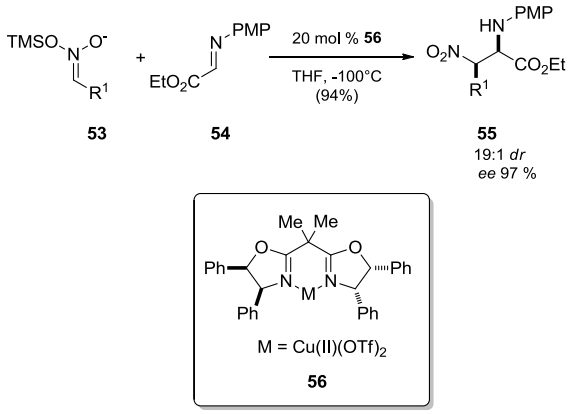

Scheme 24. Asymmetric Lewis acid catalyzed indirect nitro-Mannich reaction.

There have been significant advancements in the catalytic asymmetric *aza*-Henry reaction using different chiral Lewis acid catalysts, H-bond organocatalysts, chiral Brønsted acids, phase transfer, and Brønsted base catalysts. The focus of the following sections (Section 1.2.2) is on

the use of H-bond organocatalysts to promote asymmetric *aza*-Henry reactions. We will also review the theoretical investigation of the reaction mechanism and origin of selectivity to elucidate further the important role of H-bonding in catalysis (Section 1.3).

1.2.2. Organocatalyzed Asymmetric *aza*-Henry Reactions

The organocatalyzed asymmetric *aza*-Henry reactions have gained considerable attention in recent years. The first example of organocatalyzed *aza*-Henry reaction was proposed by Takemoto *et al.* in chiral thiourea promoted reaction of nitroalkane with *N*-protected imines. The final product was achieved in good yield and moderate enantio- and diastereoselectivity (Scheme 25).[70]

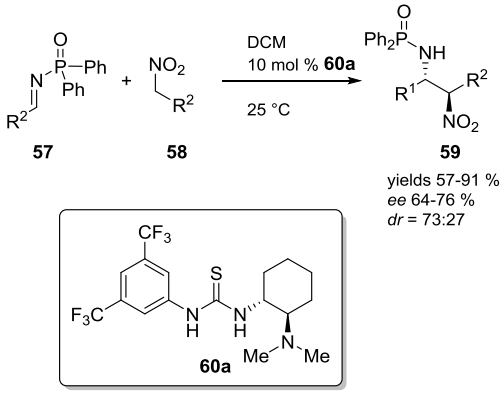

Scheme 25. The first organocatalytic nitro-Mannich reaction.

In 2005, Jacobsen and coworkers, disclosed the thiourea **60b** catalyzed asymmetric *aza*-Henry reaction between nitroethane and *N*-Boc arylimines (Scheme 26).[71] The desired adducts were obtained with yields and stereoselectivities similar to those reported by Takemoto's procedure. However, an external base was required due to the absence of an appropriate basic site in the thiourea skeleton (Scheme 26).

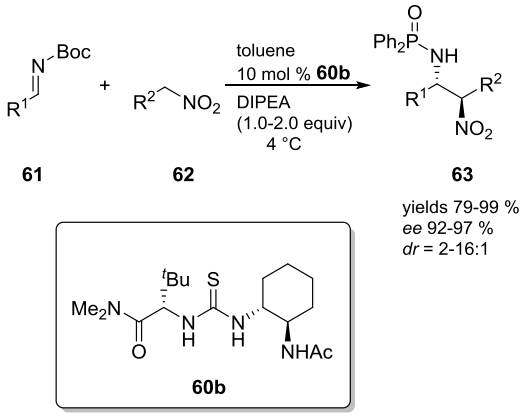

Scheme 26. Jacobsen's thiourea catalyzed nitro-Mannich.

Motivated by the good results achieved by Jacobsen and others, Takemoto later reported an improved variant of the asymmetric *aza*-Henry reaction using the same thiourea catalyst **60a** as well as *N*-Boc imines instead of *N*-phosphinoyl imines (Scheme 27).[72] The bifunctional thiourea catalyst, in addition to acting as a base for deprotonation, served to simultaneously coordinate and activate both the electrophile and the nucleophile through formation of the H-bond mediated ternary complex **67** (Scheme 27).

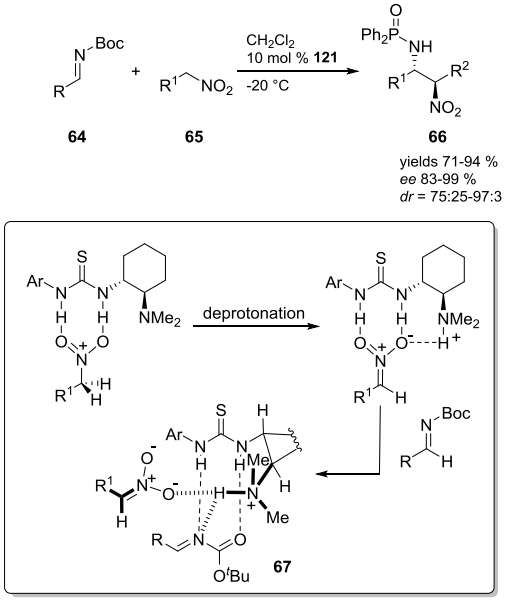

Scheme 27. Thiourea **60a** catalyzed nitro-Mannich reactions of *N*-Boc imines.

Since the above initial advancements, the thiourea-based catalyzed asymmetric *aza*-Henry reaction is considered as being an effective means for obtaining synthetically valuable products. It is also noteworthy that a large number of synthetically useful strategies using thioureas with different chiral frameworks for carrying out highly enantio- and diastereoselective *aza*-Henry reactions have been reported, including those by Schaus, Ricci, Chang, Ellman and others.[75-77] For instance, Schaus and Ricci[73] investigated the asymmetric *aza*-Henry reactions employing hydroquinine-based **71** and quinine-based thioureas **75** to access a wide class of synthetically valuable scaffolds in excellent yields and good enantio- and diastereoselectivities (Scheme 28).

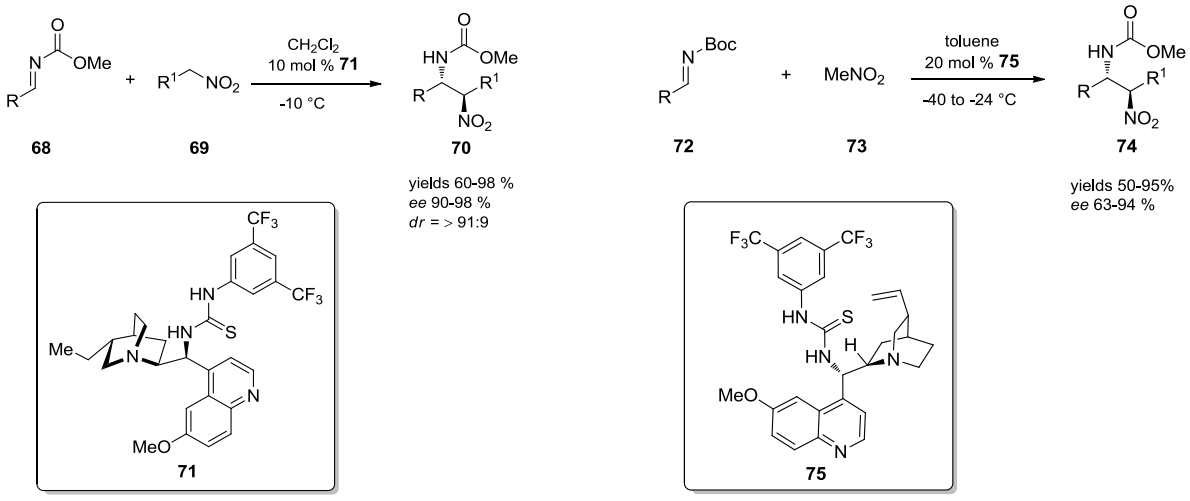

Scheme 28. Schaus's hydroquinine-based **71** and Ricci's quinine-based **75** thiourea catalyzed asymmetric aza-Henry reactions.

In 2007, Chang *et al.*[74] synthesized *β*-nitroamine products in excellent yields and good to excellent enantioselectivities using a chiral oxazoline-thiourea **79** catalyst in the asymmetric *aza*-Henry reactions of nitromethane and nitroethane with electronically different *N*-Boc aryl imines (Scheme 29). However, the relative stereochemistry of the major diastereomers was not elucidated. At the same time, the Ellman group reported the application of a chiral *N*-sulfinyl-

urea based organocatalyst **83** for the asymmetric *aza*-Henry reaction. More specifically, the asymmetric *aza*-Henry reaction of nitroalkane (**81**) with *N*-Boc imines (**80**) afforded the desired product **82** in high enantio- and diastereoselectivities (Scheme 29).[75]

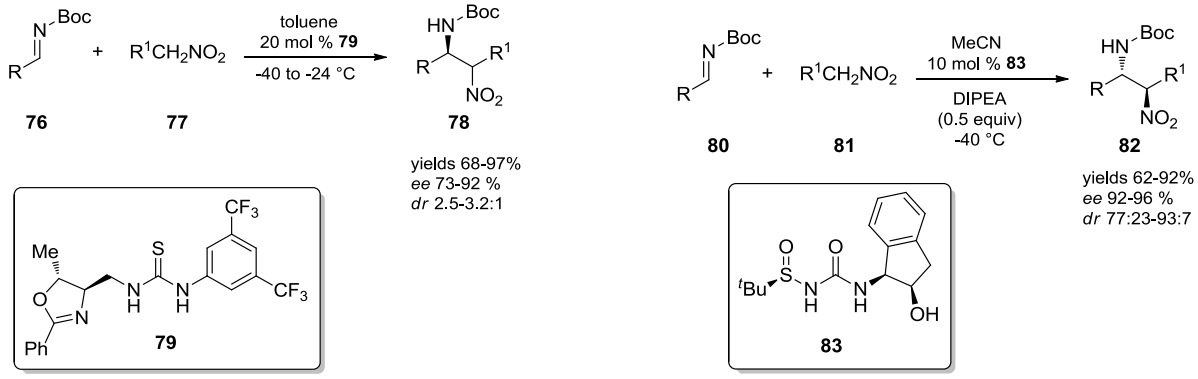

Scheme 29. Chang's **79** and Ellman's **83** thiourea catalyzed asymmetric *aza*-Henry reactions.

In 2008, the groups of Zhou and Wulff[76] reported the catalytic enantio- and diastereoselective *aza*-Henry reaction of *N*-Boc arylimines with a number of nitroalkanes using novel chiral glycosyl-thiourea **87** and bis-thiourea BINAM-based catalysts **91**, respectively (Scheme 30). Applying these novel classes of thiourea-based organocatalysts, the *β*-nitroamine products were formed in good to excellent yields and enantioselectivities, and with low to good *anti* diastereoselectivities (Scheme 30).

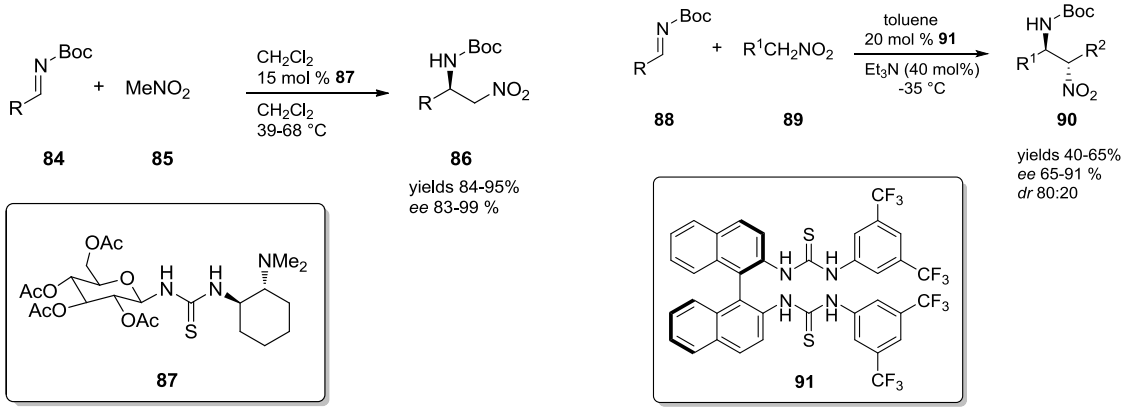

Scheme 30. Zhou's **87** and Wulff's **91** thiourea catalyzed asymmetric *aza*-Henry reactions.

Notably, a mechanistic working model, **92** for the catalytic action of a novel bis-thiourea **91** catalyzed *aza*-Henry reaction was also proposed by Wulff, in which both the imine electrophile and nitronate species were coordinated and activated via formation of H-bonding interactions (Figure 4).

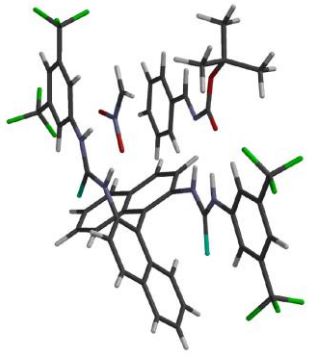

92

Figure 4. Catalyst-substrate complex **92**, a proposed model for the bis-thiourea **91** catalyzed *aza*-Henry reaction.[76]

A key organocatalytic *aza*-Henry reaction was performed by Wang and co-workers[77] in 2008 applying bifunctional amine-thiourea-based catalyst **96** (Scheme 31). Moreover, the same authors have advanced a doubly stereocontrolled asymmetric protocol in the *aza*-Henry reaction of nitroalkanes **98** to in situ generated *N*-Boc imines **97** using a new designed rosin-derived thiourea based organocatalyst **100** (Scheme 31).[78]

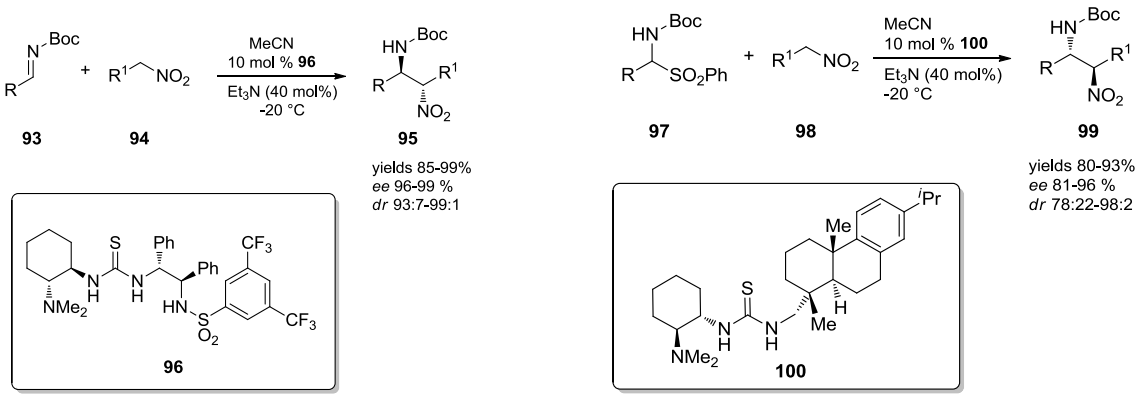

Scheme 31. Wang's thiourea **96** and **100** mediated *aza*-Henry reactions.[77]

Fewer studies of the asymmetric *aza*-Henry reaction under phase-transfer catalysis (PTCs) conditions have been carried out. But, notably, the Palomo and Hererra groups[79] independently investigated the cinchona derived **104** phase-transfer catalyzed *aza*-Henry reactions between α-amidosulfones and different susbtituted nitroalkanes. The final β-nitroamines were obtained in good yields and enantioselectivities (Scheme 32). Palomo *et al*. further extended these phase transfer promoted *aza*-Henry reactions using different substituted electrophiles and nucleophiles.[80] Notably, the computationally based mechanistic study of this approach was proposed by the same group to evaluate and complement the experimental methodology that will be discussed in detail throughout the section 1.3.

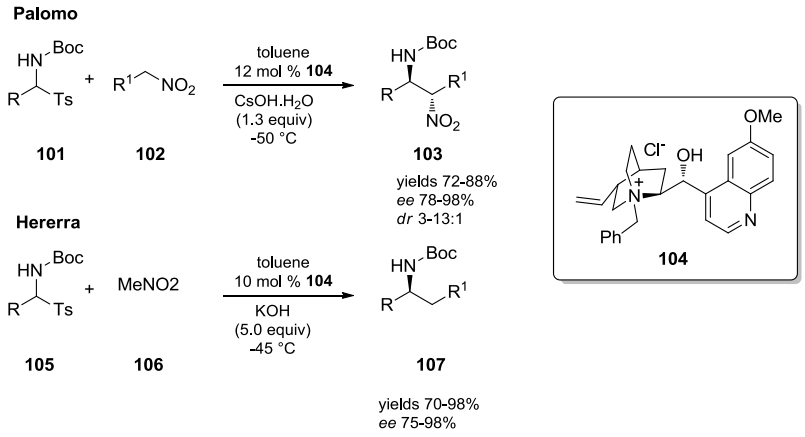

Scheme 32. *N*-benzyl quininium chloride phase-transfer catalyzed *aza*-Henry reactions.

Recently, an analogous *N*-benzotriazole-cinchona based phase transfer catalyst **111** for reactions of α-amidosulfones **108** with nitroalkanes **109** was developed by He and coworkers (Scheme 33).[81] The use of *N*-benzotriazole-cinchona based catalytic system **111** instead of *N*-benzyl quininium chloride **104** lead to the formation of the opposite enantiomer of *β*-nitroamines **110**. This cinchona-based phase transfer catalyst resembles the catalyst reported by the groups of Palomo and Herrera.[79]

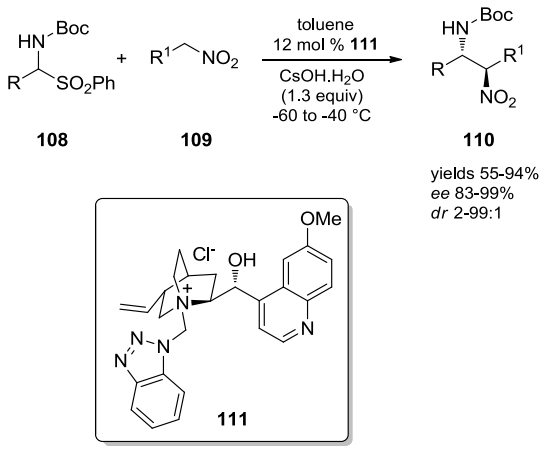

Scheme 33. *N*-benzotriazole-cinchona based catalyzed *aza*-Henry reactions.

Nagasawa proposed a bifunctional guanidine-bisthiourea, **115**, as a different type of PTC catalyst in a highly stereoselective *aza*-Henry protocol (Scheme 34).[82]

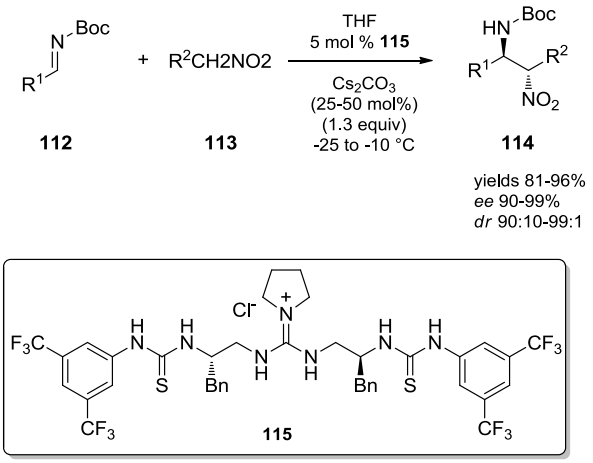

Scheme 34. Bis-thiourea phase-transfer catalyzed *aza*-Henry reactions.

Despite these organocatalytic advances in promoting *aza*-Henry reactions, further development of these systems for studying *aza*-Henry and the related asymmetric processes is still required. One under-explored example is the use of charged H-bond catalysts capable of both inducing asymmetry and accelerating the reaction. The week after the initial report by Takemoto in 2004, Johnston and co-workers[83] reported that a Brønsted acid can act as a chiral proton organocatalyst **119** for the asymmetric *aza*-Henry reaction of nitroalkanes **117** and a number of electron poor arylaldimines **116** to afford *β*-nitroamine products **118**, which are useful precursors to chiral 1,2-diamines (Scheme 35). Imporantly, it was found that the more electron deficient arylaldimines **116** led to better enantioselectivity; yet, the observed high *anti* versus *syn* diastereoselectivities were almost identical for all the reported substituents. Although the origin of selectivity and a stereochemical model was not proposed at that time, their initial experimental results indicated a key role of a chiral proton (*i.e.* a so-called polar ionic H-bond) in both reactivity and selectivity.[83]

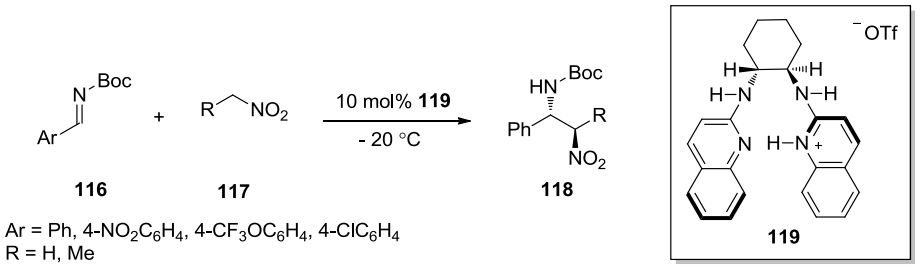

Scheme 35. Enantioselective chiral proton catalyzed *aza*-Henry reactions.

Johnston *et al.* further extended the application of the chiral proton catalyst and its modified structures as bifunctional organocatalysts (Scheme 36), which showed higher efficacy in asymmetric *aza*-Henry reactions.[84] Given the continued applications of HQuin-BAM derivatives as organocatalysts as well as my interest in how the nature of H-bonding affects asymmetric catalysis, I report within this dissertation, a detailed DFT-based investigation of the HQuin−BAM catalyzed *aza*-Henry reactions.

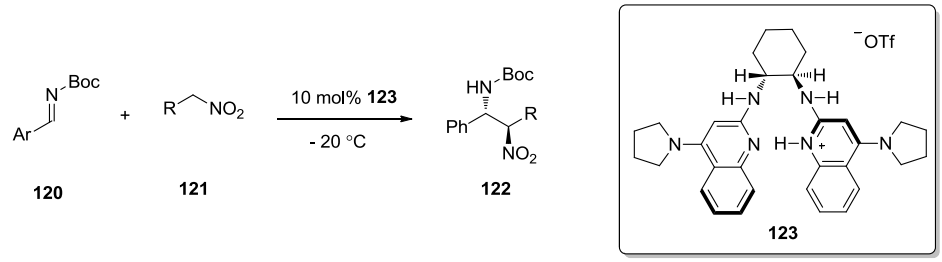

Scheme 36. Chiral proton catalyzed *aza*-Henry reactions.

1.3. Theoretical Studies of Chiral Lewis-, Brønsted Acid H-Bond Organocatalysis (Mechanism, Reactivity and Origins of Selectivity)

Much of the mechanistic understanding of the organocatalyzed asymmetric reactions has come from detailed, computationally-based studies or combined computational and experimental investigations.[85] In this vein, quantum chemical computations, particularly with density functional theory (DFT), can provide a solid foundation and rationale for the experimental

development of an effective organocatalytic synthetic methodology. For example, an understanding of the mechanism of the catalytic actions of the most important class of Lewis (H-bonding) and Brønsted (proton-transfer) acid organocatalysts including (thio)ureas, diols, phosphoric acids, guanidinium/amidinium ions is crucial for developing and designing new organocatalytic reactions. Therefore, the application of theoretical methods based on quantum mechanical calculations would be of great assistance for studying these catalytic reactions.

1.3.1. Density Functional Theory[86]

Density Functional Theory (DFT) describes molecular properties as functionals of electron density. As shown in equation 1, electronic energy in DFT is symbolized as $E[\vec{\rho}(r)]$, indicating that energy is a functional of electron density and in turn, is a function of position, where $\langle T[\vec{\rho}(r)]\rangle$ is the average kinetic energy, $\langle V_{NE}[\vec{\rho}(r)]\rangle$ is the average nuclear-electronic attraction, and $\langle V_{ee}[\vec{\rho}(r)]\rangle$ is the average electron-electron repulsion.

$$E[\vec{\rho}(r)] = \langle T[\vec{\rho}(r)]\rangle + \langle V_{NE}[\vec{\rho}(r)]\rangle + \langle V_{ee}[\vec{\rho}(r)]\rangle \qquad \textbf{Eq. (1)}$$

$V_{NE} = -\sum_{\alpha}\int \frac{Z_\alpha \rho(r)}{r_\alpha} dr$, in which r_α is the distance of electron from nucleus, α and Z_α is the charge on nucleus α, the $\langle T[\vec{\rho}(r)]\rangle$ is defined based on the kinetic energy of a hypothetical non-interacting electron gas, T_s with a perturbation, ΔT, and the $\langle V_{ee}[\vec{\rho}(r)]\rangle$ is defined as a function of average electron separation, $\frac{1}{2}\iint \frac{\vec{\rho}(r_1)\vec{\rho}(r_2)}{r_{12}} d\tau_1 d\tau_2$, with a perturbation ΔV_{ee}. The two unknown functions, ΔV_{ee} and ΔT are called the exchange-correlation energy, E_{xc}. Thus, the energy functional, is shown in equation Eq. (2):

$$E = -\sum_{\alpha}\int \frac{Z\vec{\rho}(r)}{r_\alpha} d\vec{r} + \frac{1}{2}\iint \frac{\vec{\rho}(r_1)\vec{\rho}(r_2)}{\vec{r}_{12}} d\tau_1 d\tau_2 + T_s + E_{XC} \qquad \textbf{Eq. (2)}$$

The first three terms in Eq (2) are calculated functionals of ρ but the last term E_{XC} is an unknown functional having small contribution to the energy. However, the accuracy of the calculated energy depends on the accuracy of this term E_{XC} which includes exchange and correlation energy.

One standard DFT-based functional, the B3LYP exchange-correlation functional, includes a gradient corrected correlation functional, a density functional exchange term, and a Hartree-Fock (HF) exchange term. The presence of HF exchange makes B3LYP a hybrid density functional.

1.3.2. DFT-Based Computational Methods for Organocatalysis

Using Density Functional Theory (DFT), different qualitative and quantitative quantum mechanical methods have been applied to various H-bond mediated asymmetric processes which have provided insight into the selectivity, reactivity, and mechanism of these reactions.[87] DFT has become a preferred method for studying organocatalytic reactions because of the availability of many newly developed density functional theory (DFT) techniques with the ability to calculate large chemical systems with high accuracy and low cost. The success of these new DFT functionals and, especially, the poor performance of the standard DFT-based functional (i.e. B3LYP), have led to studies of DFT techniques for the prediction of organic reactions. These studies show the success of new DFT-based functionals in overcoming some of the important limitations of B3LYP, such as its inability to describe medium-long range type correlation interactions and its poor performance in accounting for dispersion interactions,[88] which are important in determining selectivities. Generally, DFT methods obtain accurate results for most chemical problems, but for larger chemical compounds or noncovalently bound molecules, they underestimate the London dispersion forces. Thus, to allow standard DFT-based functionals to

account for dispersive interactions, a set of empirical corrections,[89] known as the dispersion energy correction are added to the total Kohn-Sham energy, E_{DFT}:

$$E_{DFT\text{-}D} = E_{DFT} + E_{disp} \qquad \textbf{Eq. (3)}$$

The dispersion term is

$$E_{disp} = -\sum_{A,B} \frac{C_6^{AB}}{r_{AB}^6} \qquad \textbf{Eq. (4)}$$

where C_6 is the dispersion coefficient and r_{AB}^6 is the inter-atomic distance between atoms A and B. It is noteworthy that the significance of dispersion interactions for accurately modeling organic structures using different DFT-based functionals has attracted considerable attention.[90] For example, Rzepa *et al*.[91] investigated the effects of dispersion interactions on the stereoselectivity of the proline mediated aldol reaction using both B3LYP and B3LYP-D3. Interestingly, it was found that D3 corrections reduced the energy differences between the stereoisomeric transition states. Recent progress, specifically in calculation of dispersion effects, allows for more reliable models to be calculated for prediction of the reaction mechanism, reactivity and selectivity.[92] In this dissertation, to gain a more accurate treatment of dispersion interactions, we applied both the Grimme's dispersion corrected functional B3LYP-D3[93] and long-range corrected (LRC) exchange-correlation functional with inclusion of dispersion correction, ωB97X-D,[94] in accurate calculation of the interaction energy which depends on the intermolecular and intramolecular distance.

1.3.3. Theoretical Analysis of O-H Based Chiral H-Bond/Brønsted Acid Organocatalysis

In combination with the experimental studies, the mechanism of the chiral O-H based H-bond catalysis, such as diols and phosphoric acids, has also been explored theoretically using different quantum mechanical approaches.[95]

The stereochemical outcome of TADDOL catalyzed asymmetric reactions is well-understood and a number of theoretical models for analyzing the origins of stereoselection have been predicted. For example, in 2006, the group of Wu,[96] reported both experimental and theoretical investigations of the H-bond mediated enantioselective hetero-Diels-Alder (hDA) cycloaddition reaction of Danishefsky's diene (*trans*-1-methoxy-3-trimethylsilyloxy-1,3-butadiene) with benzaldehyde. Mechanistically, several possible H-bonding interaction modes between catalyst and substrate were proposed, of which the *trans*-**124** complex with a single H-bond mode of activation was found to be the best catalytic mode of action (Figure 5).

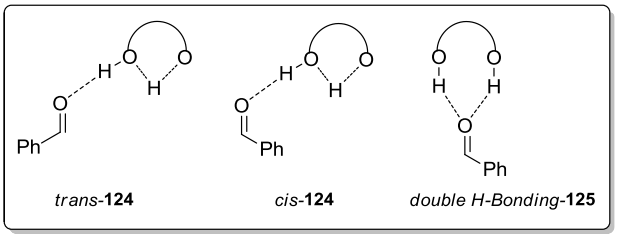

Figure 5. Possible intermolecular H-bonding interactions between benzaldehyde and TADDOL.

Thus, in the calculated lowest-energy transition structure (**126** in Figure 6) for this TADDOL catalyzed hDA cycloaddition reaction, the benzaldehyde substrate was activated via formation of a single H-bond, as *trans*-**124** in Figure 5, with one of the hydroxy groups of the catalyst. This intermolecular H-bond was mainly responsible for the stabilization of the transition state with zwitterionic character. As well, the intramolecular H-bond within the catalyst system facilitated this intermolecular H-bond with the substrate and highlighted the cooperative role of H-bonding motifs (Figure 6).

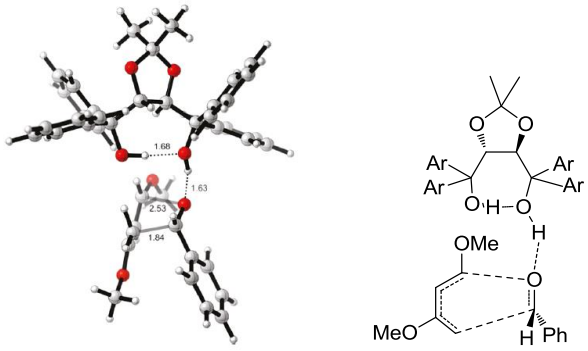

TS-*endo*-*Si*-126

Figure 6. Transition state of the TADDOL catalyzed hDA cycloaddition.

To rationalize the sense of stereoinduction, the same author proposed a quadrant diagram in which the structural features of enantiomeric transition states were exactly elucidated; a detailed comparison of the steric hindrances, and in turn their effect on enantioselctivity, were analyzed (Figure 7).

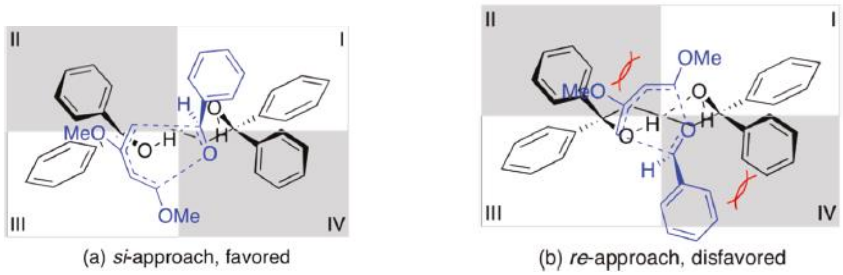

127a **127b**

Figure 7. Quadrant diagram representive of the transition states for the (*Si*) vs (*Re*) approach.[96]

The following year, Houk *et al.* reported a comprehensive theoretical study of TADDOL catalyzed hetero-Diels-Alder and Diels-Alder reactions using 1-dialkylamino-3-substituted-1,3-butadienes. In their calculations, the truncated form of catalyst, 1,4-butanediol, was used initially

as the H-bond organocatalyst and it was proposed to activate the substrate via the above-mentioned cooperative binding mode (Figure 8).[97]

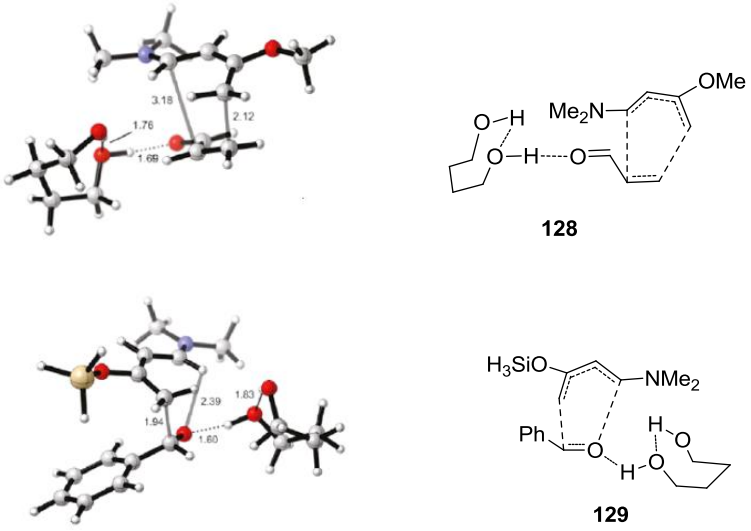

Figure 8. Transition structures for the 1,4-butanediol catalyzed Diels Alder and hetero-DielsAlder reactions.[97]

Two years later, Gomez-Bengoa and coworkers[98] analyzed the double H-bonding interactions between substrate and catalyst (double H-bonding-**125** in Figure 5) and found that the cooperative binding mode in Diels-Alder cycloaddition reaction was the favoured mode of binding. The significance of this cooperative H-bond catalysis has also been established by different research groups such as Domingo, Dudding, Houk and others.[99] Applying quantum mechanics (QM) and quantum mechanics/molecular mechanics (QM/MM), Houk and Dudding[100] studied the exact origin of stereoinduction and the observed high π-facial selectivity in the TADDOL catalyzed hDA reaction. Inspection of enantiodeterminig transition states (*Si*) **TS-130a**, (*Re*) **TS-130b** revealed the key roles of both the stabilizing CH-π interaction as well as destabilizing steric interactions on optimal orientation of the substrate and high π-facial selectivity (Figure 9).

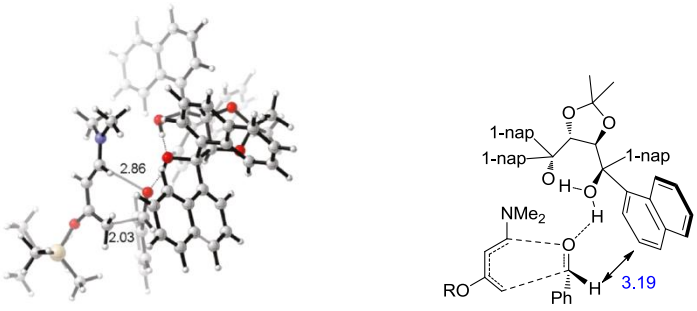

(*Si*) **TS-130a**, 0.0 kcal/mol

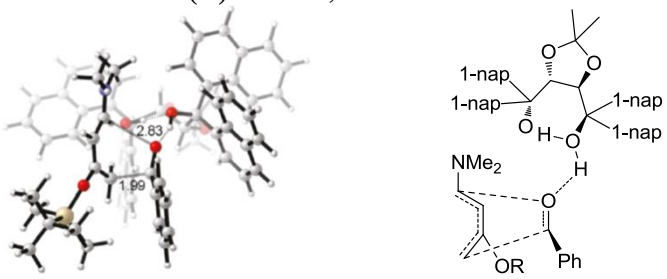

(*Re*) **TS-130b**, 1.5 kcal/mol

Figure 9. Enantiodetermining transition states for TADDOL catalyzed had reaction.

BINOL-based phosphoric acids is the other successful class of H-bond organocatalysts, which were initially explored in Mannich-type reactions by the research groups of Terada and Akiyama.[101] A detailed computational investigation of these organocatalysts in different asymmetric reactions provided insight into their mechanistic actions.[102] For instance, following the preliminary computational study by the Terada group of the BINOL-based phosphoric acid catalyzed asymmetric Mannich reaction,[101] Yamanaka and co-workers[103] published both experimental and theoretical investigations of an analogous chiral Brønsted acid catalyzed asymmetric Mannich reaction. A DFT-based mechanistic analysis of this chiral Brønsted acid catalyzed enantioselective Mannich reaction of aldimines with enolates revealed the efficacy of a dicoordinated H-bonding mode of action (the two-point H-bonding interaction, **131** in Scheme 37) over the mono-coordinated one (**132** in Scheme 37). It was found that this asymmetric transformation involved the rate-determining proton transfer to the imine, followed by the

nucleophilic addition through formation of a cyclic zwitterionic transition state in a dicoordination pathway which was 3.4 kcal/mol lower in energy than the analogue transition state of mono-coordinated pathway.

dicoordination Pathway
131

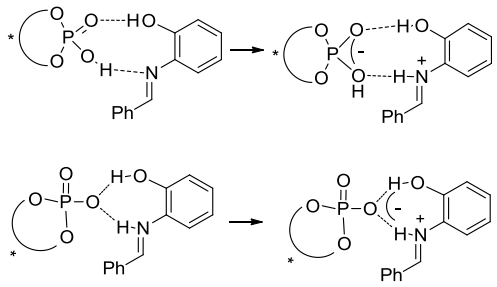

132

mono-coordination Pathway

Scheme 37. Chiral phosphoric acid catalyzed nucleophilic addition to aldimine.

Consistent with experimental observations, *Re* face attack [(*Re*) **TS-133a** in Figure 10] was energetically favoured over the *Si* face by 5.7 kcal/mol [(*Si*) **TS-133b** in Figure 10]. A detailed inspection of the origin of enantioselectivity revealed the importance of noncovalent stacking-type interactions between the catalyst and substrate as well as other controlling elements of selectivity.[104] In the energetically favoured (*Re*) **TS-133a**, the stabilizing stacking interaction between the catalyst and iminium *N*-aryl substrate fixed the geometry of the electrophile toward attack by the nucleophile. On the other hand, the energetically unfavorable *Si* face experienced a destabilizing steric hindrance between the catalyst and the trimethylsilyl group of the nucleophile or the aromatic ring of the electrophile (Figure 10).

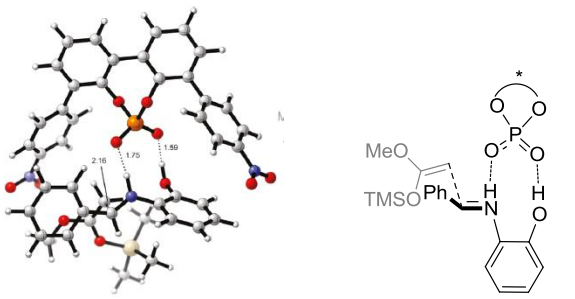

(*Re*) **TS-133a**, 0.0 kcal/mol

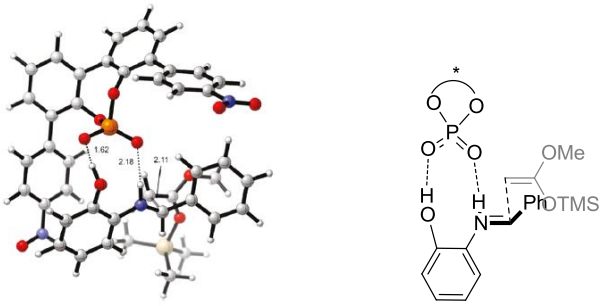

(*Si*) **TS-133b**, 5.7 kcal/mol

Figure 10. Calculated transition states for the *Re* and *Si* face attack of enolate to aldimine.[104]

Gong and co-workers[105] also highlighted the key role of stabilizing H-bond and stacking-type interactions in controlling the regio- and stereoselectivity of chiral phosphoric acid mediated asymmetric 1,3-dipolar cycloaddition reactions. The transition structure leading to the major enantiomer (**TS-134a** in Scheme 38) had significantly stronger stabilizing H-bonding interactions between the methyleneindoline, the azomethine ylide and catalyst. The transition structure corresponding to the unfavorable *Si*-facial attack (**TS-134b** in Scheme 38) did not experience H-bond stabilization with the same strength. As well, the stabilizing stacking-type interaction between substrates was responsible for the stability of the major enantiomeric transition structure (**TS-134a** in Scheme 38) compared to the minor regioisomeric transition state (**TS-135** in Scheme 38).

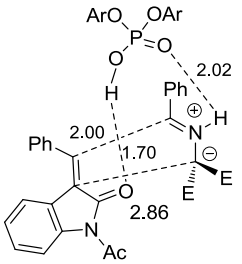

E = CO_2Et

major enantiomer
TS-134a, 0.0 kcal/mol

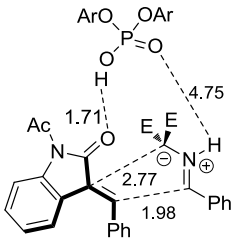

minor enantiomer
TS-134b, 1.5 kcal/mol

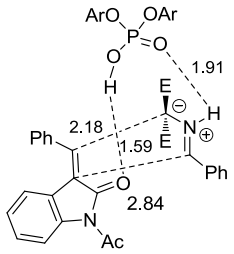

minor regioisomer
TS-135, 1.6 kcal/mol

Scheme 38. Major and minor transition states for the chiral phosphoric acid catalyzed 1,3-dipolar cycloaddition.[105]

The same group also revealed the mechanistic aspects of chiral phosphoric acid catalyzed Biginelli-type reactions.[106] The preferred catalytic mode of action involved H-bond activation of the imine substrate with the phosphoric acid proton to form a zwitterionic iminium and stabilization of the enol substrate via formation of an H-bond with the oxygen of the P=O group (Mechanism B in Scheme 39). Thus, the BINOL-phosphoric acid catalyzed Biginelli reaction proceeded via simultaneous activation of the imine substrate by formation of 6-membered cyclic H-bonding interaction with the OH group of phosphoric acid and activation of the enol substrate via H-bonding between its OH group and the Lewis basic site of the catalyst. Mechanism B led to the formation of the major (*S*) product via the energetically favored (*S*)-**TS**. On the other hand, the (*R*)-**TS**, which generates the minor (*R*) enantiomer is predicted to proceed through

mechanism A. It was found that the presence of a stronger H-bond between the enol and catalyst in the (*S*)-**TS** was responsible for the 1.1 kcal/mol free energy differences between two enantiomeric transition structures.

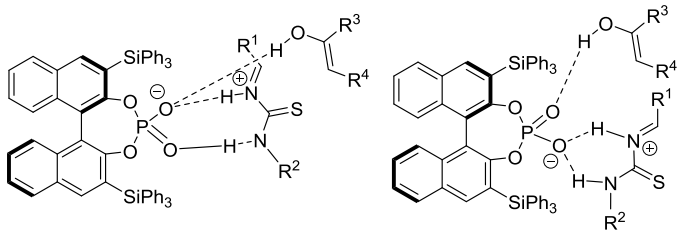

Scheme 39. Proposed activation mechanisms for an organocatalyzed Biginelli reaction.

In 2009, Shi *et al.*[107] investigated the mechanism of the BINOL-based chiral phosphoric acid catalyzed hydrophosphonylation reaction of imines. In their mechanistic analysis, it was predicted that the addition of the phosphonate to protonated imines proceeded via rate-determining transition structures (*R*)-**TS-138a** and (*S*)-**TS-138b**. The 5.2 kcal/mol energy difference between (*R*)-**TS-138a** and (*S*)-**TS-138b** was primarily due to the presence of steric clashes between the catalyst aromatic group and the *para*-methoxyphenyl group of imine in the unfavorable transition state (*S*)-**TS-138b** (Figure 11).

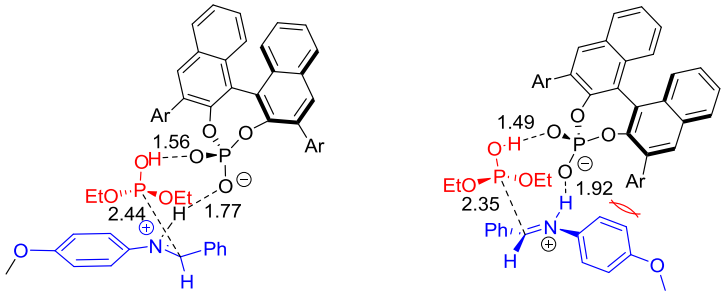

(*R*)-**TS-138a**, 0.0 kcal/mol (*S*)-**TS-138b**, 5.2 kcal/mol

Figure 11. Enantiomeric transition states for the hydrophosphonylation of 4-methoxyphenyl-protected imine catalyzed by phosphoric acid catalyst.[107]

1.3.4. Theoretical Analysis of N-H Based Chiral H-Bond/Brønsted Acid Organocatalysts

Based on the initial investigation of the H-bond activation of electrophiles by the groups of Kelly, Etter, Curran, and others in the 1990s,[108] Jacobsen explored the catalytic role of (thio)urea organocatalysts for highly enantioselective hydrocyanation of imine electrophiles (Strecker reactions) and further extended the potential of this organocatalyst to other asymmetric reactions of imines and their derivatives.[109] For example, in 2007, Jacobsen *et al.*[110] reported the use of thiourea-based catalysis in the asymmetric Pictet-Spengler-type cyclization of hydroxylactams. The mechanism of this cyclization reaction was investigated using both experimental and DFT techniques. These studies revealed that this thiourea mediated transformation proceeded via an S_N1-type mechanism. The addition of the indole to the generated *N*-acyliminium ion was followed by alkyl migration. In this proposed anion-binding mechanism, the activation of substrate and stereoselective induction occured via the transient formation of a short-lived bifurcated H-bond stabilized anion **140** (Scheme 40).

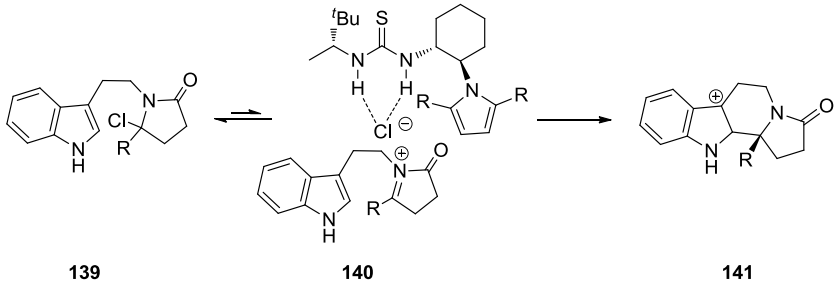

Scheme 40. Proposed reaction mechanism for the thiourea catalyzed asymmetric Pictet-Spengler type cyclization of hydroxylactams.[110]

In a recent kinetic and computational study of the (thio)urea catalyzed imine hydrocyanation reaction, the same group proposed a new mechanism of H-bond catalysis in which, instead of direct activation of the imine, the thiourea catalyzed the reaction via formation

of a catalyst-bound iminium-cyanide complex.[111] The origin of the observed enantioselectivity was attributed to both stabilizing and destabilizing noncovalent interactions between substrate and catalyst (Figure 12).

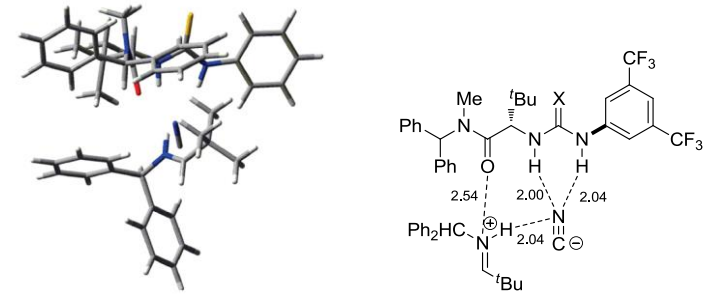

(*Re*) **TS-142a**, 0.0 kcal/mol

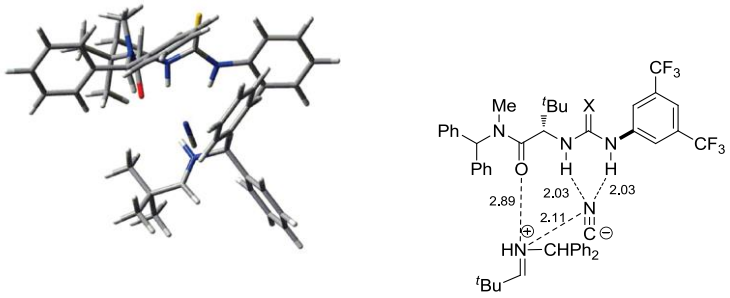

(*Si*) **TS-142b**, 2.4 kcal/mol

Figure 12. Enantiodetermining transition states of the urea/thiourea catalyzed imine hydrocyanation reaction.

A few years after Jacobsen's initial reports, Schreiner and co-workers[112] performed pioneering theoretical studies of thioureas in Diels-Alder cycloaddition reactions. Applying different experimental and theoretical tools, it was found that the thiourea catalyzed the cycloaddition reaction of *N*-acyloxazolidinone with cyclopentadiene through formation of bidentate H-bonding interactions with both carbonyl groups of the substrate similar to how weak Lewis acids coordinate (Figure 13).

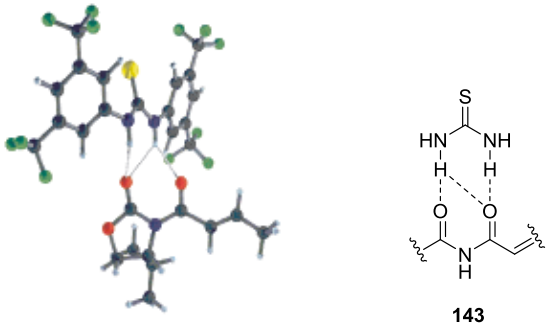

Figure 13. The preferred binding mode of the complexed model of thiourea based organocatalysis.

To study the way in which H-bond interactions affected the reactivity and selectivity of thiourea mediated cycloaddition reactions, Fu *et al.*[113] also reported a DFT-based analysis of the Diels–Alder reaction between cyclopentadiene (CP) and methyl vinyl ketone (MVK). The authors predicted that the thiourea (urea) organocatalysts were attractive alternatives to Lewis acid catalysts, since they could accelerate the reaction in a similar way. The mechanistic features, reactivity and the exact origin of *endo* selectivity showed that the preferred formation of the *endo* transition state (*endo*-**TS-144a** in Figure 14) with the *s-cis* conformer of the methyl vinyl ketone dienophile was found to be due to a balanced combination of steric interactions, H-bonds, solvent effects, and electrostatic factors (Figure 14).

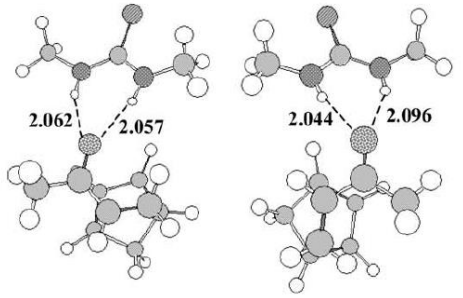

endo-**TS-144a**, *s-cis* MVK
29.4 kcal/mol

endo-**TS-144b**, *s-trans* MVK
31.0 kcal/mol

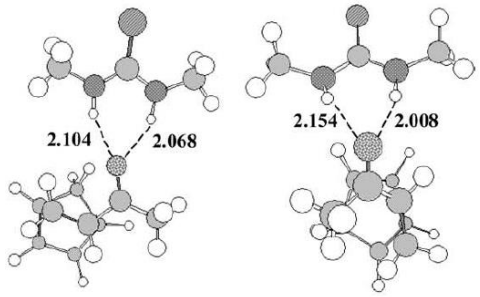

exo-**TS-144c**, *s-cis* MVK
30.4 kcal/mol

exo-**TS-144d**, *s-trans* MVK
32.3 kcal/mol

Figure 14. Transition structures of the thiourea catalyzed cycloaddition between cyclopentadiene (CP) and methyl vinyl ketone (MVK).

Recently, computational methods were extensively used to design a wide array of novel bifunctional H-bond organocatalysts.[114] Different research groups, such as those of Liu, Chen, Simon and Goodman, studied the mechanistic aspects of numerous organocatalyzed asymmetric reactions to clarify further the catalytic role of the new designed organocatalysts.[115] These computationally-based studies highlighted the ability of using computational tools as a basis for catalyst design.

For example, different bifunctional thiourea-based organocatalysts have been designed by combination of a thiourea group with an amine functional group or the second thiourea functionality. Using DFT, different quantum mechanical methods have been applied to various bifunctional thiourea catalyzed asymmetric reactions, such as Michael reactions, which have

provided insight into the selectivity, reactivity, and mechanism of these addition reactions.[116] In 2006, Tsogoeva and Schmatz[117] highlighted the bifunctional role of a thiourea catalyst in simultaneously enhancing the nucleophilic character of the ketone and the electrophilic nature of the nitro-alkene via formation of double H-bonding interactions in the Michael addition reaction. Although it was found by Takemoto and others[118] that in thiourea catalyzed Michael addition reactions both oxygen atoms of the nitro group are coordinated to the catalyst by H-bonding, the theoretical studies by Tsogoeva and Schmatz showed that the double coordinated transition state was less stable than the mono-coordinated transition state. The observed facial selectivity was found to be due to the presence of tighter H-bonding between the thiourea and nitro-alkene substrate in the energetically favored (*R*)-**TS-145a**, as well as destabilizing electrostatic interactions between the phenyl group and oxygen in the minor (*S*)-**TS-145b**.

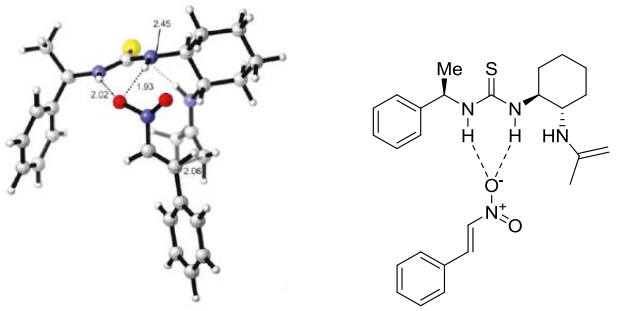

(*R*)-**TS-145a**, 0.0 kcal/mol

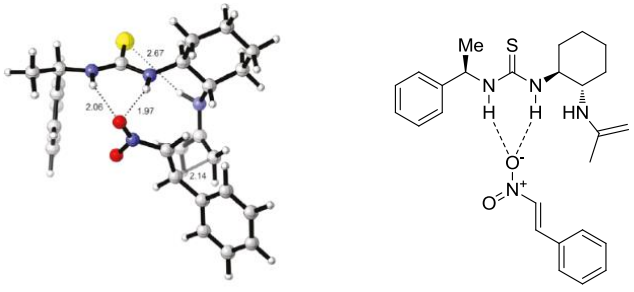

(*S*)-**TS**-145b, 1.3 kcal/mol

Figure 15. (*R*)-**TS** *vs* (*S*)-**TS** of the formation of enantiomeric products in thiourea catalyzed Michael addition reaction.

Notably, in DFT-based investigations of the bifunctional thiourea mediated Michael addition reaction, Papai and co-workers[119] predicted that double H-bond activation of either the nitro-olefin (proposed by Takemoto) **146** or the dicarbonyl substrate **147** was energetically possible, which in turn led to the formation of the major *R*-configured product (Scheme 41).

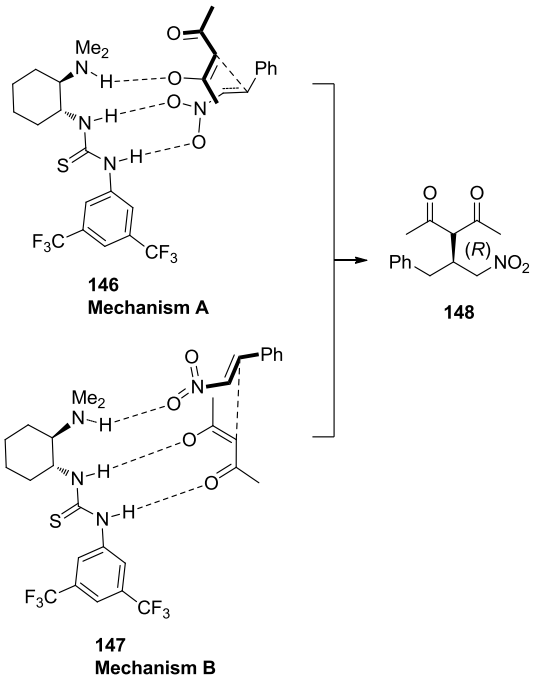

Scheme 41. Two proposed mechanistic pathways for the bifunctional thiourea catalyzed Michael addition of acetylacetone to nitrostyrene.

The transition states producing the major *R* enantiomer for both mechanisms **A** [(*R*)-$\mathbf{TS_A}$**-149**] and **B** [(*R*)-$\mathbf{TS_B}$**-150**] are shown in Figure 16 and are energetically favoured over transition states generating the *S* enantiomer by 2.6 and 2.4 kcal/mol, respectively. The author suggested that the observed enantioselectivity originated from the eclipsing-type C–C forming bonds in the energetically unfavoured (*S*)-**TS**, as opposed to the favorable staggered-type in (*R*)-**TS**.

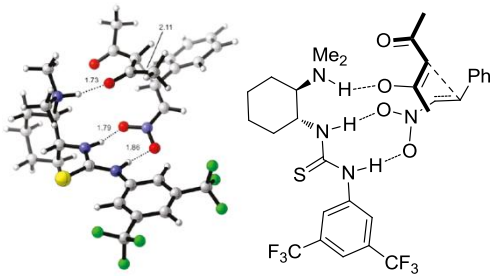

(*R*)-**TS$_A$-149**

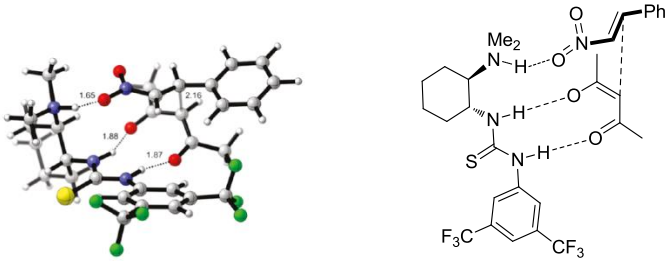

(*R*)-**TS$_B$-150**

Figure 16. Bifunctional thiourea catalyzed Michael addition for the major (*R*) transition structures via pathways **A** and **B** illustrated in Scheme 41.

In 2007, the Chen group[120] reported the thiourea promoted Michael addition of aryl and alkyl cyanoacetates to vinyl ketones. Importantly, steric clashes between the vinyl ketone and aryl group of cyanoacetate were found to play a key role in controlling the (*Re*) attack (**TS-151b** in Figure 17) of the Z-enolate of the cyanoacetate, producing the major *S* enantiomer over (*Si*) attack (**TS-151a** in Figure 17), yielding the minor *R* enantiomer.

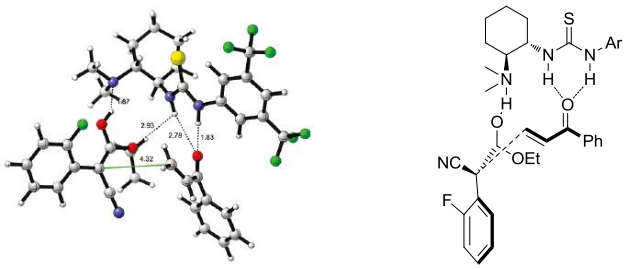

(*Si*) **TS-151a**

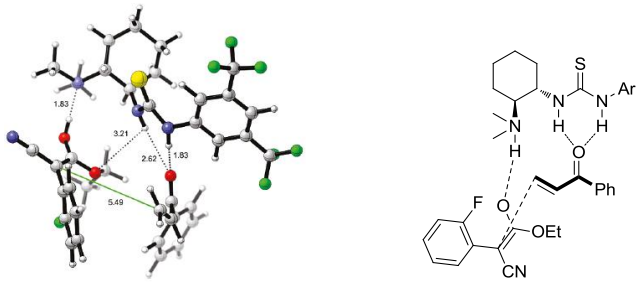

(*Re*) **TS-151b**

Figure 17. The proposed enantiodetermining transition states in the Michael addition of *R*-2-fluorophenyl cyanoacetate to phenyl vinyl ketone.

An analogous urea-based organocatalyst was also investigated by Liu *et al.*[121] in the *α*-amination reaction. In this mechanistic study, the bifunctional role of the urea catalyst in simultaneous coordination and activation of the dicarbonyl substrate to the urea and of the azodicarboxylate to the tertiary amine group was found to be significantly favoured. The lowest-energy transition states, (*Re*) **TS-152a**, (*Si*) **TS-152b** (Scheme 42), producing the enantiomeric adducts were in good qualitative agreement with experimental observations; however, the origin of enantioselectivity was not explored.

urea-dicarbonyl activation azodicarboxylate activation

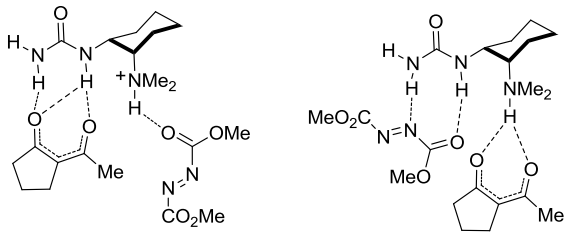

(*Re*) **TS-152a**, 2.7 kcal/mol (*Si*) **TS-152b**, 7.8 kcal/mol

Scheme 42. Lowest energy transition state for the enantiomeric products of the *α*-amination reaction.

Notably, a number of structurally modified and novel variants of bifunctional thiourea-based organocatalysts have been designed and mechanistically investigated in different asymmetric reactions. For example, Zhong *et al.*[122] reported a DFT-based study of a highly enantioselective cinchona-derived thiourea mediated domino Michael-Henry reaction, in which a new catalytic activation mode was proposed (pre-complex-**153**, Figure 18). Mechanistically, it was predicted that this new bifunctional catalytic system promoted the domino reaction through activation of a 1,3-dicarbonyl substrate by the thiourea motif and the acidic proton of the phenyl ring and at the same time the stabilization and mono-coordination (contrasting the dual mode of activation proposed by Takemoto) of the nitro group by the tertiary amine (pre-complex-**153**, Figure 18).

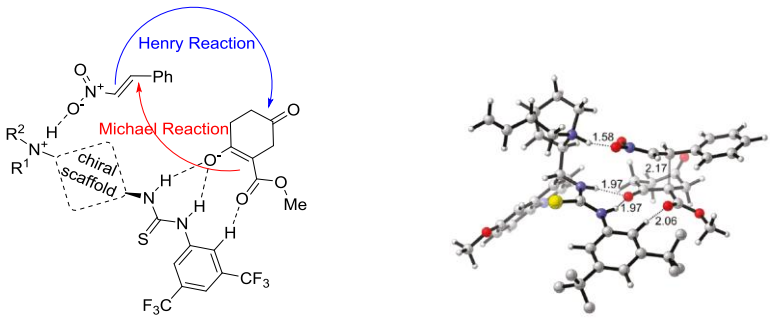

Pre-complex-**153**
catalyst activation mode

(*R*,*S*)-**TS-154**

Figure 18. a) Proposed H-bond mode of activation **153** in which the chiral scaffold represented the chiral cinchona fragment. b) The lowest energy Michael addition transition structure **154**.[122]

Furthermore, applying different quantum mechanical approaches, Simon and Goodman[123] studied the mechanism of the aminoindanol-derived thiourea catalyzed enantioselective hydroxylamine addition to pyrazole crotonates. To explain the role of this novel thiourea-based organocatalyst, they predicted two mechanistic pathways **A** and **B**. The **TS_B-156** of a truncated model system in pathway **B** was energetically favoured over **TS_A-155** in pathway **A** (Figure 19). Thus, following mechanism **B**, the DFT-based calculations led to a 1.6 kcal/mol energy difference between the enantiodetermining transition states producing the major (*S*) enantiomeric product, in agreement with the experimental results for the actual system (calculated *ee*% = 88%; experimental *ee*% = 72%).

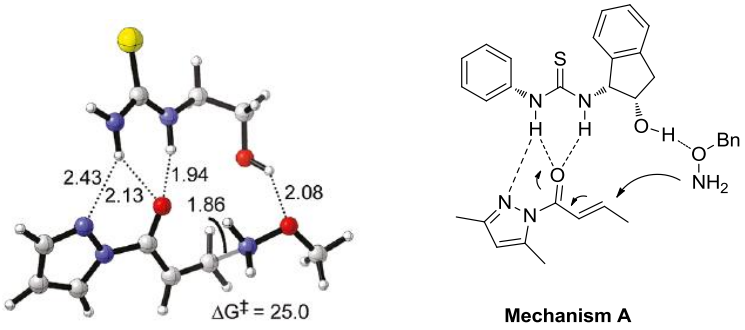

TS_A-155

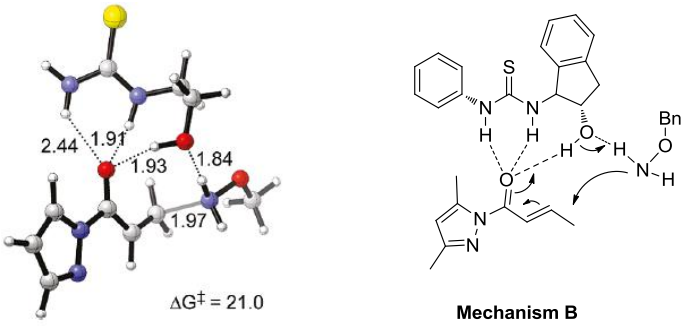

TS_B-156

Figure 19. Proposed mechanisms for the conjugate addition of amines to pyrazole crotonates.

Very recently, the groups of Houk[124] and Kitagaki[125] studied the mechanism of a novel chiral cyclophane-based bisthiourea catalyst in the asymmetric Henry reaction between different substituted aldehydes and nitroalkanes (Figure 20). Kitagaki *et al.*[124] showed that the origin of the high enantioselectivity resulted from dual H-bond activation of the electrophile and nucleophile, as well as the presence of steric clashes in the less stable transition state, while Houk *et al.*[123] predicted that the observed stereoselectivity mainly originated from differences in H-bond strength in stereodetermining transition states.

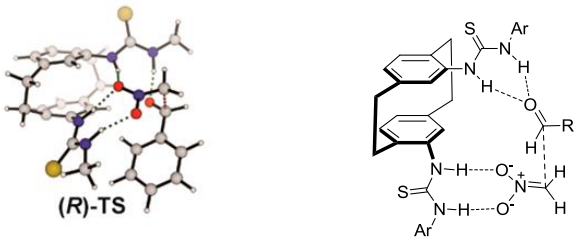

(*R*)-**TS-157a**, 0.0 kcal/mol

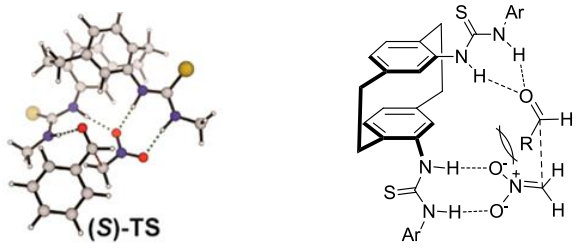

(*S*)-**TS-157b**, 3.8 kcal/mol

Figure 20. Plausible enantiomeric transition state model in cyclophane-based bisthiourea catalyzed the asymmetric Henry reaction.

Different theoretical techniques have also been applied to guanidinium mediated asymmetric transformations which provided insight into the selectivity, reactivity, and the mechanistic features of these classes of H-bond organocatalysis. For example, the groups of Goodman[126] and Rice[127] independently reported comprehensive computational studies of the guanidine catalyzed ring-opening-metathesis. In a more recent theory-based report, Rice and co-workers[126] proposed two mechanisms for the ring-opening polymerization reaction (Figure 21). The first mechanistic path, (**A** in Figure 21) involved catalyst mediated nucleophilic ring-opening of the lactide followed by proton donation to the opened alkoxide. The second predicted mechanism, (**B** in Figure 21) was catalyst promoted H-bond activation of both the lactide and alcohol substrates. Interestingly, their predicted results were consistent with the earlier calculations performed by Goodman *et al.*,[125] in which the transition states (**TS_B-160** in Figure

21) related to the acid-base mechanistic pathway were energetically favoured, which highlighted the bifunctional role of the guanidine H-bond catalyst.

Pathway **A**: Dual activation of lactide substrate.

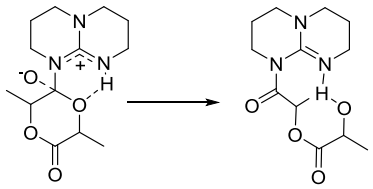

TS_A-158 **159**

Pathway **B**: H-bond mediated activation of lactide and alcohol substrates.

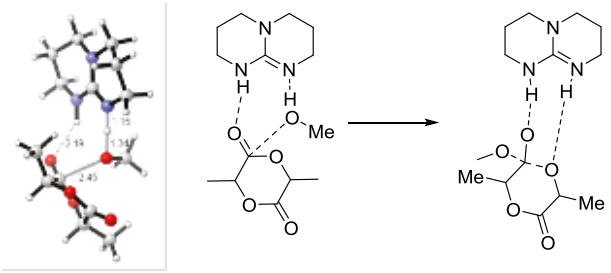

TS_B-160 **161**

Figure 21. Two proposed mechanisms **A**, **B** for the organocatalyzed ring-opening polymerization of L-lactide.

A slightly different type of Brønsted acid organocatalyst was theoretically investigated by Najera and coworkers,[128] in the highly enantioselective Michael addition of 1,3-dicarbonyls to nitroalkenes. The catalyst was derived from protonated cyclohexanediamine-benzimidazole using TFA. In the mechanism of the Michael addition, activation of the nucleophile via formation of a bifurcated H-bond (**162** in Scheme 43) was energetically favoured over coordination and activation of the nitroalkene electrophile (**163** in Scheme 43). This result is consistent with the activation mode proposed by Papai[129] in the cyclohexanediamine-thiourea-based (Scheme 41) catalyzed Michael addition. Furthermore, an energy difference of 2.6

kcal/mol was predicted, in favor of the (*R*)-**TS-162a**, however the exact analysis of factors responsible for the observed enantioselectivity were not elucidated (Scheme 43).

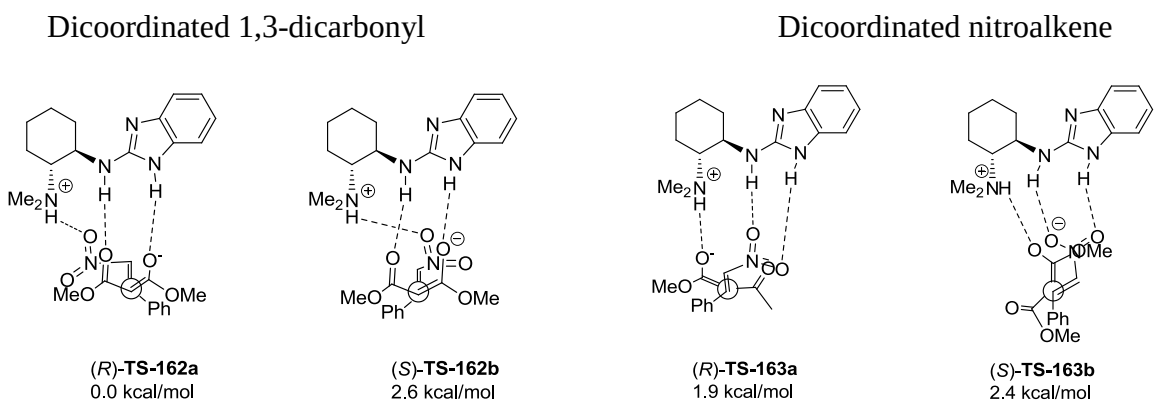

Scheme 43. Enantiomeric transition states for the Michael addition reaction of 1,3-dicarbonyls to nitroalkenes.

In 2009, Feng and Hu,[130] reported a different class of amine-amide type organocatalyst for the highly enantioselective asymmetric nitroaldol reaction. A preliminary theoretical study revealed that the high facial selectivity was due to stronger H-bonding between the catalyst and the substrate in the energetically favoured transition state structure (*R*)-**TS-164a** (Figure 22).

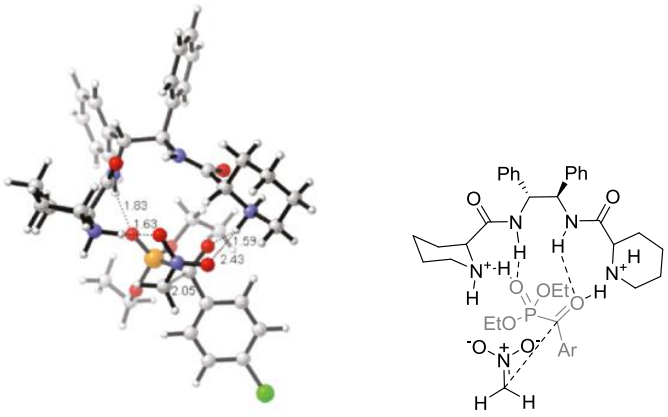

major (*R*)-**TS**-164a, 0.0 kcal/mol

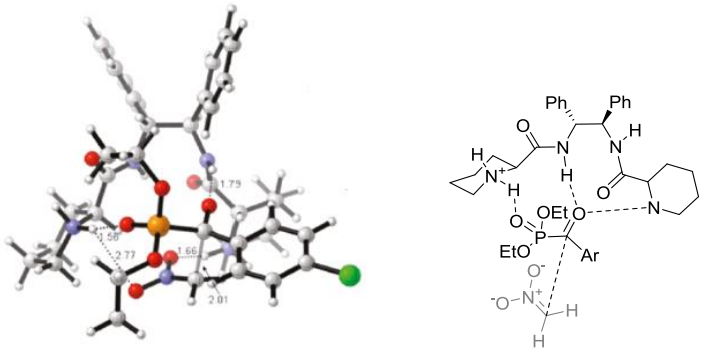

minor (*S*)-**TS-164b**, 3.7 kcal/mol

Figure 22. Major (*R*) and minor (*S*) transition structures for the nitroaldol reaction.

Ooi *et al.* pioneered[131] a class of phosphazene-based organocatalysis. In their mechanistic analysis of aldol reaction, they proposed that the phosphazene initially deprotonates the nucleophile, then interacts via H-bonding with both the pre-formed nucleophile and electrophile. Building on this work, the group of Simón and Paton,[132] recently published a DFT and molecular mechanics based study of the nitro and phospho-aldol addition reactions catalyzed by a chiral phosphazene catalyst. This theory-based study suggested that the catalyst simultaneously interacts by H-bonding interactions with the pre-formed nucleophile and the electrophile, followed by a proton transfer to the aldehyde in conjuction with a C–C bond formation step. The observed stereo- and diastereoselectivity was proposed to be due to stabilizing noncovalent

interactions, steric clashes, the conformational preference of the reactants, and the distortion energy (Figure 23).

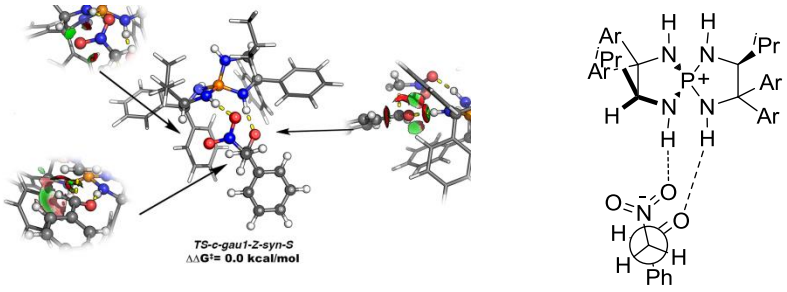

(*S*)-**TS-165a**, 0.0 kcal/mol

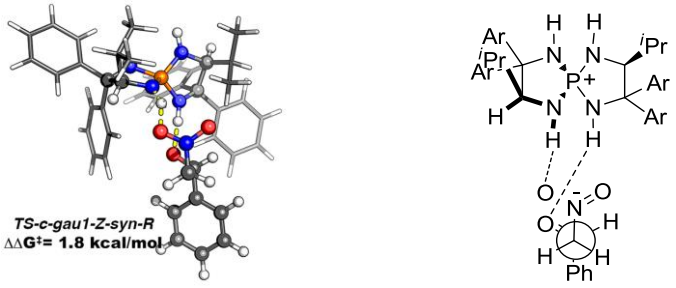

(*R*)-**TS-165b**, 1.8 kcal/mol

Figure 23. Most stable enantiomeric transition states for the reaction of nitromethane with benzaldehyde catalyzed by Phosphazene.

Although cinchona alkaloids have been employed in a wide range of asymmetric transformations, the observed high stereoselectivity has only in some cases been rationalized. Recently, the origins of stereocontrol by cinchona-based organocatalysts with different catalytic actions, such as H-bonding interactions[133] and phase-transfer catalysis[134] have been revealed. For example, in 2014, Houk[135] explained the way in which cinchona derived amines catalyzed asymmetric electrophilic α-fluorination of cyclic ketones. The author proposed that there was a close correlation between the conformational preferences of the generated cyclic fluorine transfer transition state and the observed stereoselectivity. The conformational preference (chair

conformer in **TS-166a**) in the fluorine transfer cyclic transition state determined the sense and level of enantioinduction (Figure 24).

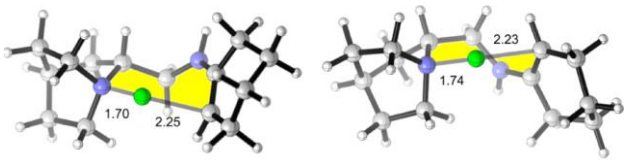

TS-166a, 0.0 kcal/mol **TS-166b**, 4.1 kcal/mol

Figure 24. The proposed fluorination transition structures derived from truncated substrate and catalyst in an asymmetric electrophilic α-fluorination of cyclic ketone.

Building upon these findings, the same group used various computational techniques[136] to investigate the origins of asymmetric induction in cinchona-catalyzed intramolecular aldol reaction. Mechanistically, it was found that both the preferred arrangement of the diketone substituent (axial *vs* equatorial) on the generating chair cyclohexane and the favoured conformation (boat−chair *vs* crown) of a H-bonded nine-membered cyclic transition state in enamine formation and intramolecular aldol addition steps, controlled the sense of stereoinduction (Figure 25).

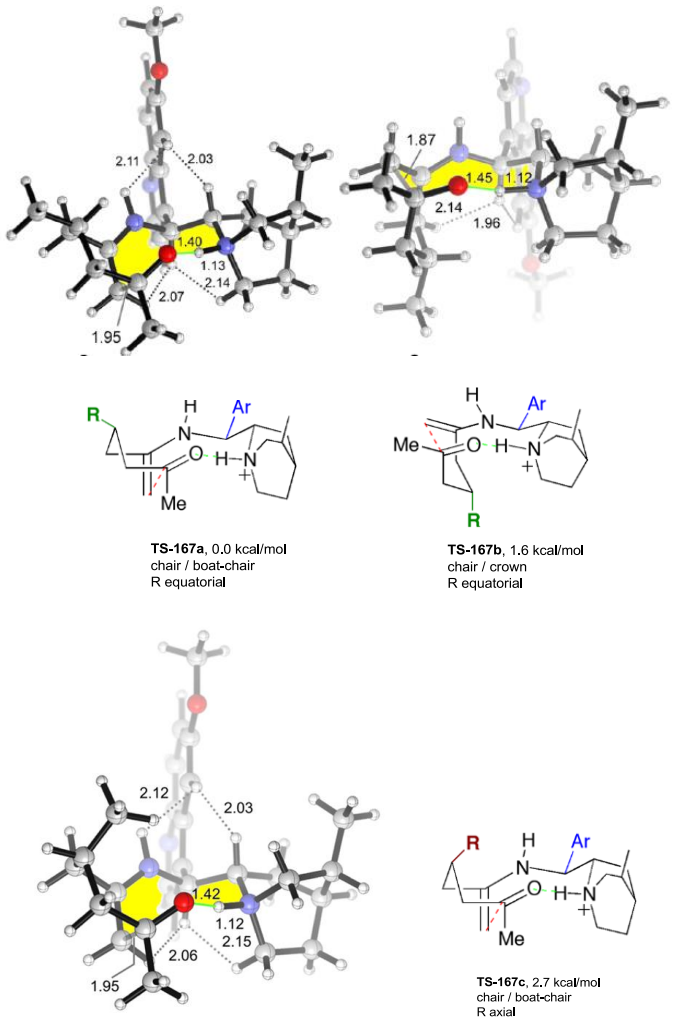

Figure 25. Lowest energy stereoisomeric transition states of cinchona alkaloid mediated intramolecular aldol reaction.

In spite of these theoretical reports, further development of these tools for studying H-bond promoted organocatalytic asymmetric processes is highly desirable. One important class is H-bond organocatalysts that activate both the electrophile and nucleophile. These families of H-bond organocatalyst have been applied in a variety of asymmetric reactions, but a theory-based study of their mechanistic functions is still needed. This thesis describes a DFT-based study of a class of successful, yet mechanistically under-developed, bifunctional chiral bis(amidine) (BAM) Brønsted acid catalysts [e.g., HQuin-BAM, **25** in Scheme 17] for the asymmetric *aza*-Henry reaction.

2. Results and Discussions

2.1. The Role of H-Bonding in Enantioselective HQuin-BAM *Aza*-Henry Reaction of Nitromethane with N-Boc phenylaldimine

Nucleophilic addition to carbonyl and imine double bonds represents one of the most important C-C bond forming reactions. Compared to carbonyl compounds, imines are relatively strong H-bond acceptors and are among the best potential electrophilic substrates for asymmetric H-bond catalysis. It is therefore not surprising that the majority of applications of asymmetric H-bonding catalysis have been in the context of nucleophilic addition to imines. The nucleophilic addition of carbons to electrophilic imines (*aza*-Henry reactions) represents one of the most attractive C-C bond forming reactions because it allows access to a wide variety of synthetically valuable targets. Organocatalytic asymmetric versions of *aza*-Henry reactions are also of interest for the synthesis of highly optically-enriched materials under mild conditions. Accordingly, the H-bond mediated chiral proton (HQuin-BAM) catalyzed asymmetric *aza*-Henry reaction is considered as being an effective way of preparing important chiral targets such as 1,2-diamines, and cyclic amines. Given the continued applications of HQuin-BAM derivatives as catalysts, as well as my interest in how the nature of H-bonding affects asymmetric catalysis and the importance of H-bonding to the mechanism, I report herein a detailed mechanistic investigation of the HQuin−BAM catalyzed *aza*-Henry reaction pioneered by Johnston and coworkers.[55] The outcome of this work was published in the journal ACS Catalysis,[137] which represents the first theoretical investigation into the function of HQuin-BAM as an organocatalyst. As shown in Scheme 44, the optimized conditions reported by Johnston *et al.*[138] for the enantioselective *aza*-Henry reaction of nitromethane **168** and *N*-Boc phenylaldimine **169** employed 10 mol % (HQuin-BAM)•HOTf catalyst **171** and nitromethane as solvent. It appeared from the initial

reports that the counterion was trifluoromethanesulfonate (triflate). For simplicity, an explicit triflate counteranion was omitted in our calculations, as its effects on mechanistic aspects and stereochemical outcome of this chiral proton catalyzed *aza*-Henry reaction were expected to be negligible.

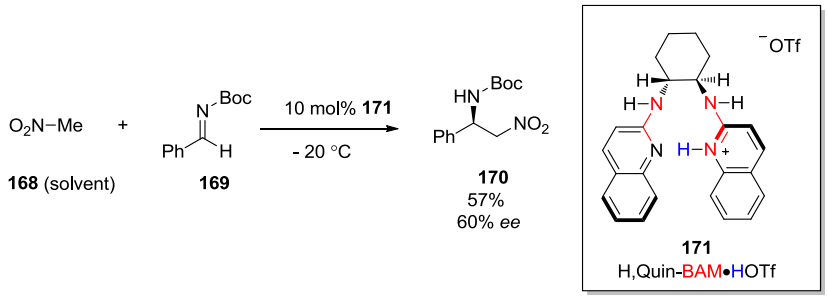

Scheme 44. HQuin-BAM catalyzed enantioselective *aza*-Henry reaction.

At the beginning of this study, working under the assumption that C–C bond formation between *N*-Boc phenylaldimine and either an in situ-derived nitroenolate (i.e., nitronate) or nitroenol species was stereodetermining, three possible mechanistic scenarios were investigated: namely, addition modes **A**, **B**, and **C** (Scheme 45). These three mechanistic pathways were modeled using the Gaussian 09 suite of programs at the ωB97X-D/6-31G(d) level of theory with the IEFPCM[139] dielectric continuum solvation model and the default parameters for nitromethane as solvent (ε = 35.87). Addition mode **A** corresponds to nucleophilic attack of nitroenol to a catalyst-bound *N*-Boc phenylaldimine, whereas in addition mode **B**, a catalyst activated nitronate adds to an unactivated *N*-Boc phenylaldimine. Last, addition mode **C** involves activation of both the nitronate nucleophile and the *N*-Boc phenylaldimine electrophile during C–C bond formation.

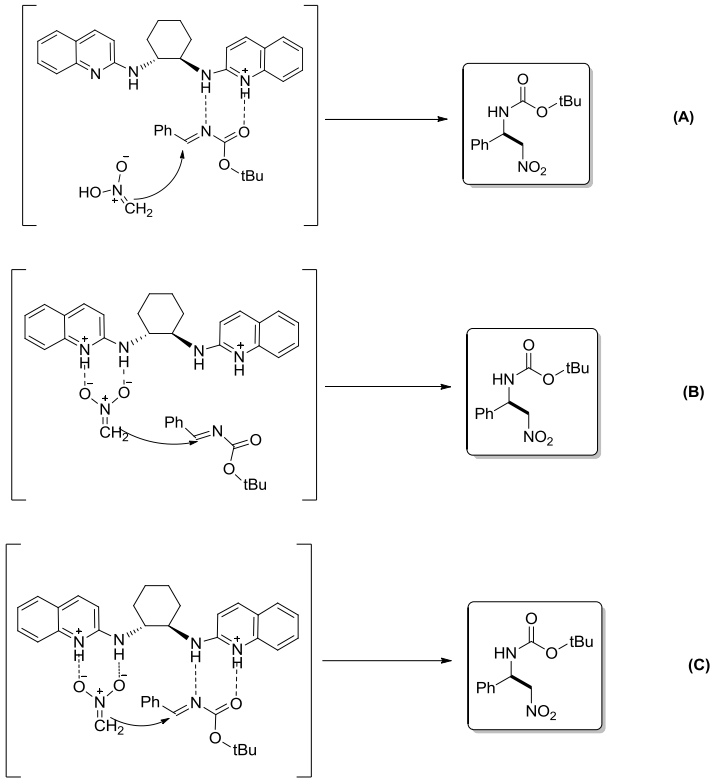

Scheme 45. Three possible C–C bond forming events, addition modes **A**, **B**, and **C**.

2.1.1. Analysis of Different H-Bonding Activation Modes (Uncatalyzed, A, B, C) through a Series of Truncated Models

When initially considering the HQuin-BAM catalytic system, two key functions were identified: hydrogen bond (H-bond) activation and chiral induction. To properly understand the nature of the first of these variables (H-bond activation), it was important that it be investigated in the absence of the chiral environment. To achieve this, we initially examined the effect of achiral catalyst 2-(methylamino)pyridine-1-ium on the reaction between nitromethane and a truncated aldimine, *N*-methyl methylenecarbamate (Figure 26-28). From the computed addition mode **A**, two possible binding orientations between the aldimine and the catalyst (**TS-A172** and **TS-A173**, Figure 26) were found. In both orientations, the lowest energy transition states possessed C–C bond forming distances of 2.0 Å and a synclinal arrangement with respect to the

approaching nitronate nucleophile (N−C−C−N dihedral angle, θ = 34.0° for **TS-A172** and θ=31.0° for **TS-A173**). These similarities suggest that the 0.8 kcal/mol energetic preference for **TS-A172** over **TS-A173** is exclusively a result of the difference in H-bonding interactions between the two transition states (Figure 26). As a result, to better understand these H-bonding interactions, we turned to natural bond orbital (NBO) analysis.[140] Generally, natural bond orbital analysis is used to quantify the electronic donor−acceptor interactions as second-order perturbation energies (ENBO). Accordingly, a subsequent natural bond order (NBO) analysis revealed that the homonuclear H-bonds (in which the donor and acceptor atoms are the same) in both structures are stronger than the heteronuclear H-bonds (in which the donor and acceptor atoms are different), most probably as a result of better pK_a matching. The concept of proton affinity (PA) and pK_a matching ("PA/pK_a Equalization Principle") has been thoroughly investigated both theoretically and experimentally since the 1960s.[141] According to this principle, the strength of H-bonding interactions can be explained in terms of matching between the acidic-basic properties of the H-bond donor and acceptor atoms. For example, a small difference in these properties between H-bond donor and acceptor atoms results in formation of strong H-bonds, while large differences results in weaker bonds. It was found that the homonuclear positive charge assisted H-bond (homonuclear (+)CAHB, i.e., N^+−H3···N1) present in **TS-A172** displayed a significantly stronger stabilization energy (ENBO = 43.8 kcal/mol) than the neutral homonuclear H-bond present in **TS-A173** (ENBO = 29.3 kcal/mol), thus suggesting that the preferred binding alignment is a consequence of maximizing the strength of the positive charged assisted H-bond. The better orbital overlap between the donor orbital and the acceptor NBO orbital[142] in the homonuclear H-bond (N^+−H3···N1) in **TS-A172** compared to the heteronuclear H-bond (N^+−H3···O2) in **TS-A173** was observed from the plotted NBO orbitals using the

Chemcraft computational package (Figure 26a). It is significant that truncated models corresponding to the anticlinal alignment of nitroenol with respect to the imine components shows the same results regarding the two features of H-bonding interactions, however, they are energetically disfavored compared to **TS-A172** and **TS-A173** (see Section 4.1.2). Attracted by the importance of the subtle differences in H-bonding modes, Bader's Quantum Theory of Atoms in Molecules (QTAIM)[143] was also applied to further probe these interactions. In general, the Bader's theory of atom in molecules is a very useful tool for describing electronic charge density in hydrogen bonded systems. According to the AIM theory, existence of a bond path between the donor and the acceptor atoms containing a (3, -1) bond critical point (BCP) confirm the presence of bonds in this system. In particular, the electronic charge density [ρ(r)] and its Laplacian [$\nabla^2\rho$(r)] at the bond critical point (BCP) were used to evaluate the H-bond strength. Interestingly, all the results obtained from QTAIM analysis on truncated models were consistent with the second-order perturbation interaction energies in the NBO approach. As can be observed in Figure 26b, the ρ(r) for the homonuclear (+)CAHB, i.e., N^+−H3···N1 in **TS-A172** is higher than that of the heteronuclear H-bond (N^+−H3···O2) in **TS-A173** which shows that ρ(r) increases as the H-bond strength increases. In line with these findings, the $\nabla^2\rho(r)$ values also increased in magnitude in the same way (Figure 26b).

The efficacy of the homonuclear (+)CAHB was also evident in Johnston's[117] experimental results in the increased activation of aldimine electrophiles, which supports the preference for the so-called polar ionic H-bonding framework.

a)

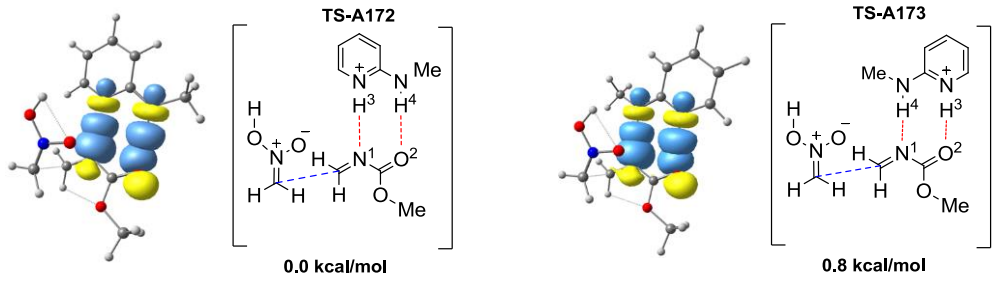

TS-A172	Bond Distance (Å)	ΔE_{NBO} (kcal/mol)	TS-A173	Bond Distance (Å)	ΔE_{NBO} (kcal/mol)
$N^1...(N^+)H^3$	1.75	43.8	$N^1...(N)H^4$	1.87	29.3
$O^2...(N)H^4$	1.86	14.4	$O^2...(N^+)H^3$	1.76	21.0

b)

TS-A172	ρ(r) (e/au^3)	$\nabla^2\rho$(r) (e/au^5)	E(x) (kcal/mol)	TS-A173	ρ(r) (e/au^3)	$\nabla^2\rho$(r) (e/au^5)	E(x) (kcal/mol)
$N^1...(N^+)H^3$	0.0463	0.1460	12.1	$N^1...(N)H^4$	0.0405	0.1119	9.9
$O^2...(N)H^4$	0.0322	0.0840	7.5	$O^2...(N^+)H^3$	0.0373	0.1020	9.5

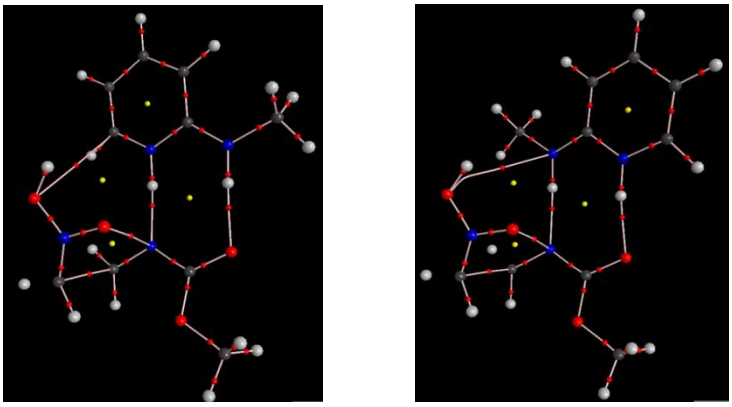

Figure 26. a) ωB97X-D/6-31G(d) calculated transition states with relative activation barriers and overlap of n and σ* orbitals in 3D orbital rendering for addition mode **A**. b) The related molecular graph and topological properties by QTAIM.

With the insight gained from **TS-A172** and **TS-A173** depicted in Figure 26, we next investigated truncated models **TS-B172** and **TS-B173** (Figure 27). The addition mode **B** involves

nucleophilic addition of an *in situ* generated bicoordinated H-bond stabilized nitronate to a free electrophile (Figure 27). However, this time, because of the absence of H-bonding to the aldimine electrophile, the two comparative substrate orientations (analogous to those in addition mode **A**) were almost isoenergetic ($\Delta G^{\ddagger}$ = 0.2 kcal/mol). In both transition states, **TS-B172** and **TS-B173**, the C–C bond-forming distances (2.33 and 2.31 Å) were slightly elongated when compared with **TS-A172** and **TS-A173**, whereas θ_{NCCN} maintained a similar synclinal alignment of 39.4° and 38.1°.

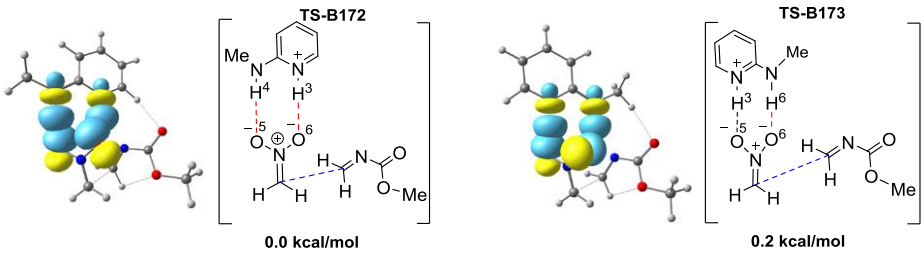

Figure 27. ωB97X-D/6-31G(d) calculated transition states with relative activation barriers and overlap of n and σ* orbitals in 3D orbital rendering for addition mode **B**.

Lastly, addition mode **C**, which is effectively a combination of addition modes **A** and **B**, involving catalyst activation of the *N*-Boc phenylaldimine electrophile and stabilization of the nucleophilic nitronate, was found to be considerably favoured (Figure 28). Once again, natural bond orbital (NBO) analysis and topological analysis of the electron density (QTAIM) are used to understand the nature and key role of the H-bond interactions. Interestingly, the data obtained from NBO analysis is consistent with the QTAIM findings (Figure 28). Similar to addition mode **A**, in addition mode **C**, the preferential H-bonding alignment is that with the strongest homonuclear (+)CAHB (N^{+}–H3···N1). However, the steric imposition caused by the presence of a second catalyst fragment forces the substrates into a nearly synperiplanar arrangement (**TS-**

C172 $\theta_{(NCCN)}$ = 14.0° and **TS-C173** $\theta_{(NCCN)}$ = −15.0°). Even though a synclinal arrangement is preferred in addition modes **A** and **B** (*vida infra*), this factor is apparently balanced by simultaneous coordination and activation of both electrophilic and nucleophilic components. Thus, the H-bond stabilization of both substrates reduces the activation energy required for C–C bond formation (Table 2).

a)

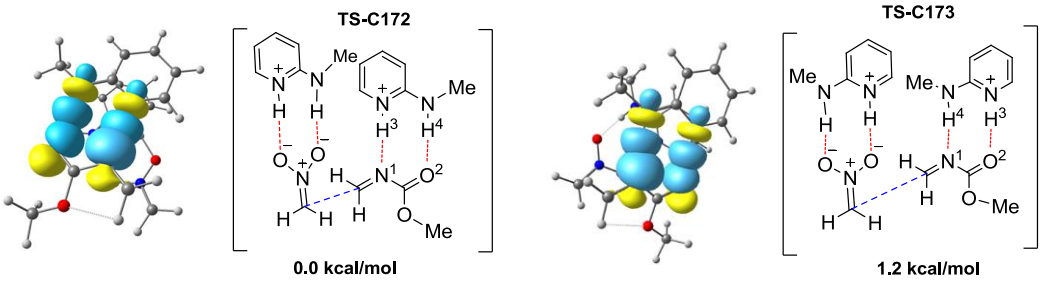

TS-C172	Bond Distance (Å)	ΔE_{NBO} (kcal/mol)	**TS-C173**	Bond Distance (Å)	ΔE_{NBO} (kcal/mol)
$N^1...(N^+)H^3$	1.78	38.5	$N^1...(N)H^4$	1.90	25.6
$O^2...(N)H^4$	1.89	14.3	$O^2...(N^+)H^3$	1.80	20.6

b)

TS-C172	ρ(r) (e/au^3)	$\nabla^2\rho$(r) (e/au^5)	E(x) (kcal/mol)	**TS-C173**	ρ(r) (e/au^3)	$\nabla^2\rho$(r) (e/au^5)	E(x) (kcal/mol)
$N^1...(N^+)H^3$	0.0450	0.1168	11.1	$N^1...(N)H^4$	0.0370	0.1131	9.7
$O^2...(N)H^4$	0.0304	0.0927	8.0	$O^2...(N^+)H^3$	0.0351	0.0955	8.6

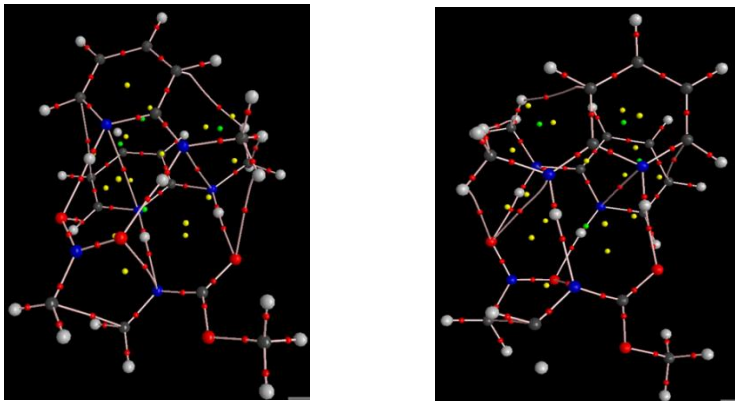

Figure 28. a) ωB97X-D/6-31G(d) calculated transition states with relative activation barriers and overlap of n and σ* orbitals in 3D orbital rendering for addition mode **C**. b) The related molecular graph and topological properties by QTAIM.

One can conclude from the truncated models, **A**, **B**, and **C**, that the activation barrier to C–C bond formation is reduced upon either activation of the aldimine electrophile or stabilization of the nitronate nucleophile, with dual activation/stabilization being preferred. The calculations above show that the formation of a homonuclear (+)CAHB directs the preferred arrangement between the aldimine and the HQuin-BAM catalyst. Thus, it can be said that the catalyst acts in a manner similar to an enzyme, in which subtle pK_a differences in the H-bond donors guide the substrates into appropriate binding alignment for optimal transition state stabilization. The truncated model systems **A**, **B**, and **C** provide a deeper understanding of the H-bonding modes responsible for both substrates binding orientation and catalysis.

To further highlight the potential of H-bond organocatalysis, we also modeled the uncatalyzed nucleophilic attack of nitronate on a truncated aldimine, *N*-methyl methylenecarbamate, and compared the energetics of the H-bond catalyzed reaction with the uncatalyzed *aza*-Henry reaction. As shown in Figure 29, for the nucleophilic addition of the nitronate on the aldimine in the absence of catalyst, the $\mathbf{TS}_{uncat}$ with synclinal attack of the substrates (**TS-D172**) was energetically favored over the analogue $\mathbf{TS}_{uncat}$ with anticlinal attack (**TS-D173**). Thus, in line with addition modes **A**, **B** and **C**, the nucleophilic addition of the nitronate on the aldimine was calculated to proceed via $\mathbf{TS}_{uncat}$ with synclinal attack orientation (**TS-D172**).

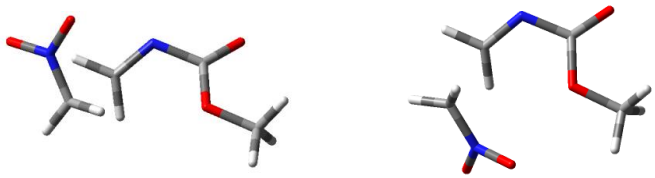

TS-D172
0.0 kcal/mol

TS-D173
0.002 kcal/mol

Figure 29. ωB97X-D/6-31G(d) calculated C–C bond forming transition states of uncatalyzed *aza*-Henry reaction between nitronate and aldimine.

Importantly, the uncatalyzed addition of nitronate to aldimine (**TS-D172**, **TS-D173**), was found to be energetically disfavored with respect to addition modes **A**, **B**, and **C** (Table 2). This observation suggests that the H-bond catalyst imparts between 10 and 27 kcal/mol stabilization to the C–C bond-forming transition state when bound to the nitronate nucleophile, the electrophile, or both (Table 2).

Table 2. Isodesmic reaction schemes for comparison of truncated model systems **A**-**D**.[a]

	Isodesmic Reaction Scheme	Net Charge	Relative Energy (kcal/mol)
Scenario A	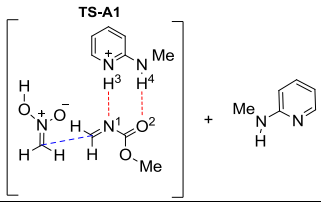	+1	21.2
Scenario B	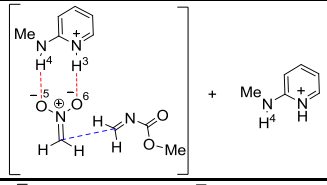	+1	10.7
Scenario C	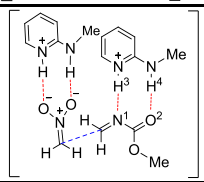	+1	0
Scenario D	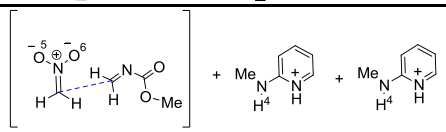	+1	27.1

[a]Relative energy of transition states with respect to the most stable transition structure of Scenario C.

Given the above findings, (1) the detailed electronic characteristics of the complementary set of bicoordinate H-bonds in **TS-C172**, (2) the more favorable endergonicity $\Delta G^{\ddagger}$ of **TS-C172** compared to other truncated modes, (3) the computed metrics of **TS-C172**, it is suggested that the catalytic events of HQuin-BAM medited enantioselective C–C bond formation may proceed via a transition state assembly similar to that of **TS-C172** in Figure 28.

2.1.2. Enantiodetermining Transition States for HQuin-BAM Catalyzed *aza*-Henry Reaction (Experimental Model System)

In order to investigate the effect of the constrained and the role of the chiral diamine motif, enantioselective C–C bond forming transition states were computed in the presence of the asymmetric HQuin-BAM catalytic system (**171** in Scheme 44). Once again, the H-bonding modes in this catalytic system were investigated through three mechanistic scenarios: **A**, **B**, and **C**. A comparison of the relative energy of the HQuin-BAM catalyzed *aza*-Henry reaction of nitromethane with *N*-Boc phenylaldimine proceeding via addition modes **A**, **B** and **C**, are shown in Table 3 and the related optimized transition state structures are depicted in Section 4.3.

Table 3. Computed relative energies for the three different enantioselective C–C bond forming transition state scenarios in HQuin-BAM catalyzed aza-Henry reaction of nitronate with *N*-Boc aldimine.

	ωB97X-D/6-31G(d) $\Delta G^{\ddagger}$ (kcal/mol)
Addition Mode C	
pro-(*R*)-TS174a	0.0
pro-(*S*)-TS174b	2.4
pro-(*R*)-TS174c	3.2
pro-(*S*)-TS174d	6.8
Addition Mode B	
pro-(*R*)-TS175a	10.6
pro-(*S*)-TS175b	18.5
pro-(*R*)-TS175c	18.6
pro-(*S*)-TS175d	16.9
Addition Mode A	
pro-(*R*)-TS176a	21.2
pro-(*S*)-TS176b	21.0
pro-(*R*)-TS176c	21.8
pro-(*S*)-TS176d	21.0

Consistent with the truncated models, transition states for nitronate addition to *N*-Boc phenylaldimine computed in the presence of HQuin-BAM catalyst were found to be significantly favoured when both nucleophile and electrophile were coordinated to catalyst (pathway **C**). Table 4 represents a comparison of relative transition state energies of each addition modes **A**, **B**, and **C**.

Table 4. Computed relative energies for the three different pro-(*R*) enantiomeric transition state scenarios in HQuin-BAM catalyzed aza-Henry reaction of nitronate with *N*-Boc aldimine.

	Transition State	Net Charge	Relative Energy (kcal/mol)
Scenario A	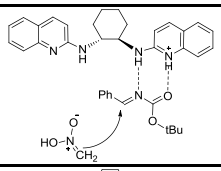	+1	21.8
Scenario B	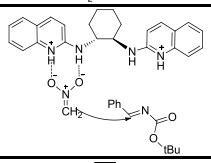	+1	18.6
Scenario C	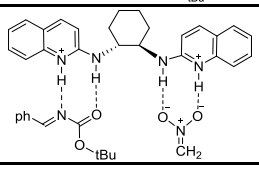	+1	0

Notably, the strong homonuclear (+)CAHB (N^+-H3···N1), such as that present in the achiral truncated models, was found in both the lowest energy enantiomeric transition states (**pro-(*R*)-TS174a** and **pro-(*S*)-TS174b**, Figure 30), further supporting the preference for this important H-bonding framework (e.g. so-called polar ionic H-bond), even in the presence of the chiral diamine backbone.

Given the analogous H-bonding framework in both **pro-(*R*)-TS174a** and **pro-(*S*)-TS174b** in Figure 30, analysis of these two transition states was carried out to gain initial insight into the factors contributing to asymmetric induction. Since the lowest energy pro-(*R*) and pro-(*S*) transition states both possessed optimal, homonuclear, charge assisted H-bonds (originally referred to as polar ionic H-bonds by Johnston)[55] between the catalyst and electrophile (pyridinium N^+-H…imine N), the preferential H-bonding network remains the same irrespective of the enantiofacial mode of addition. Consistent with the experimental results of Johnston, the pro-(*R*) transition state energy was energetically favoured than that of the pro-(*S*) transition state

by 2.3 kcal/mol (corresponding to 98% ee). The ratio of enantiodetermining C–C bond formation transition states is obtained based on the following formula:

$$A = (N_{pro(R)\text{-}TS} / N_{pro(S)\text{-}TS}) = e^{-(E_{pro(S)\text{-}TS} - E_{pro(R)\text{-}TS})/KT} \qquad \textbf{Eq. (5)}$$

$$\%\ ee = (1-A)/(1+A)100 \qquad \textbf{Eq. (6)}$$

where E is the calculated Gibbs free energy, and K is the Boltzmann constant and T is the temperature in Kelvin. In addition, the free energies of activation for these diastereomeric transition states were calculated to be 3.5 (**pro-(*R*)-TS174a**) and 5.9 kcal/mol (**pro-(*S*)-TS174b**), showing the kinetic preference for the experimentally observed *R*-**170** adduct. The difference in the transition state arrangement results in a more effective H-bonding network in pro-(*R*) and, in turn, better activation of *N*-Boc phenylaldimine and nitroenolate substrates, as evidenced by H-bond strength. This observation was supported by the greater sum of second-order perturbation energies, evaluated by NBO analysis of the four point H-bond network (124.1 kcal/mol for **pro-(*R*)-TS174a** vs 94.2 kcal/mol for **pro-(*S*)-TS174b**, Figure 30).

pro-(*R*)-TS174	Bond Distance (Å)	ΔE_{NBO} (kcal/mol)
$N^1...(N)H^{3a}$	1.82	31.2
$N^2...(N^+)H^{4a}$	1.71	26.9
$O^5...(N)H^{3b}$	1.76	24.7
$O^6...(N^+)H^{4b}$	1.63	41.3
ΔE_{NBO}(total)		**124.1**

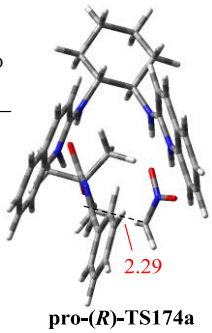

pro-(*R*)-TS174a
0.0 kcal/mol

pro-(*S*)-TS174b	Bond Distance (Å)	ΔE_{NBO} (kcal/mol)
$N^1...(N)H^{3a}$	1.74	36.3
$N^2...(N^+)H^{4a}$	1.84	11.0
$O^5...(N^+)H^{3b}$	1.85	16.4
$O^6...(N^+)H^{4b}$	1.66	30.5
ΔE_{NBO}(total)		**94.2**

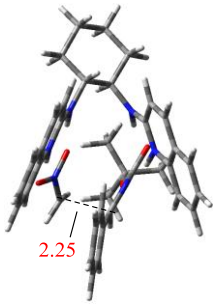

pro-(*S*)-TS174b
2.4 kcal/mol

Figure 30. ωB97X-D/6-31G(d) calculated C–C bond forming transition states for addition mode **C**.

Computations overestimated the selectivity observed experimentally by Johnston, however, the estimation improves with higher levels of theory (Table 5).

Table 5. Computed energies of enantiomeric transition states with different DFT-based functionals and basis sets, increasing level of theory from left to right.

	ωB97X-D/6-31G(d) ΔG (kcal/mol)	**ωB97X-D/6-31+G(d,p) ΔG (kcal/mol)**	**B3LYP-D3/6-31G(d) ΔG (kcal/mol)**
pro-(*R*)-TS174a	0.0	0.0	0.0
pro-(*S*)-TS174b	2.3 (96%)	1.4 (83%)	1.2 (77%)

To further elucidate the factors governing the enantioselectivity and trace the rather subtle structural differences which accounted for the 2.3 kcal/mol energetic difference between **pro-(*R*)-TS174a** and **pro-(*S*)-TS174b** in Figure 30, a distortion/interaction analysis (Figure 31, Eqs 5−7) was carried out. The distortion/interaction energy consists of: (1) the interaction energy (Eq

5) between HQuin-BAM catalyst and the two substrates in their transition state geometry, where **I** denotes the full transition state assembly, **II** represents the catalyst in its transition state geometry, and **III** relates to the reacting substrates unperturbed from their transition state geometry; (2) the distortion within the catalyst backbone at the transition state, compared with its ground state (Eq 6); (3) the distortion/interaction energy between the two reacting components (Eq 5) at the transition state (**III**), relative to their ground states (**IV** and **V**). Although, the interaction energy (Eq 5) was expectedly large for both **pro-(*R*)-TS174a** and **pro-(*S*)-TS174b** (E_{int} = -51.8 and -51.5 kcal/mol, respectively), the energy difference between the two enantiofacial addition modes was minimal (ΔE_{int} = 0.3 kcal/mol), likely as a result of the analogous H-bonding network. On the other hand, the amount of catalyst distortion (Eq 6) was small relative to that of the interaction energy ($E_{dist(cat)}$ = 9.2 and 9.8 kcal/mol), although it contributed slightly to the energetic preference for the pro-(*R*) stereofacial mode of addition ($\Delta E_{dist(cat)}$ = 0.6 kcal/mol). Finally, the substrate distortion/interaction (Eq 7) had the smallest energetic contribution ($E_{dist/int(subs)}$ = 4.9 and 4.0 kcal/mol) but the largest influence on the energetic difference between the two stereofacial addition modes ($\Delta E_{dist/int(subs)}$ = 0.9 kcal/mol) and was the overriding factor contributing to facial selectivity in the enantioselective HQuin-BAM catalyzed *aza*-Henry reaction between nitromethane and *N*-Boc phenylaldimine.

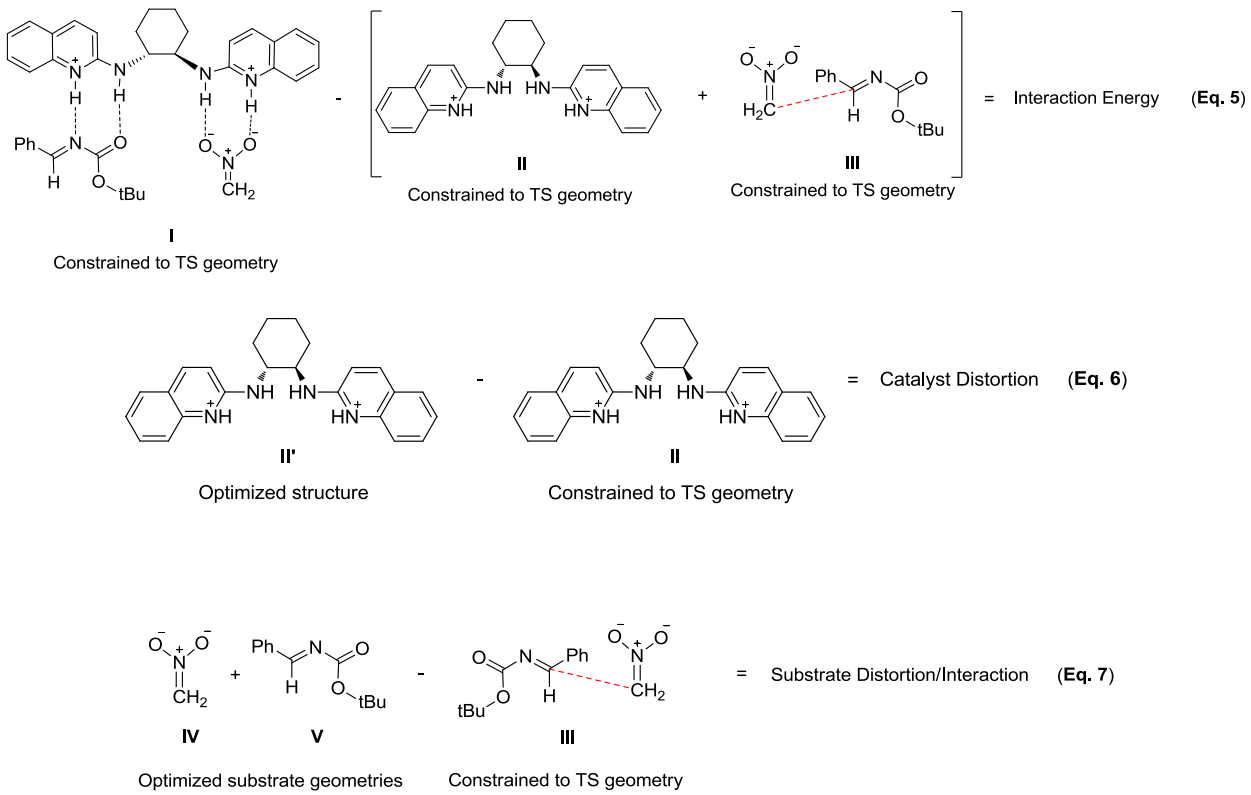

Figure 31. Distortion/interaction analysis (eqs 5−7) for the ωB97X-D/6 31G(d) calculated enantiodetermining C–C bond forming transition states for aza-Henry reaction of nitronate and *N*-Boc aldimine catalyzed by HQuin-BAM.

A comparison of the two stereofacial addition modes, $\mathbf{III}_{\text{pro}(S)}$ and $\mathbf{III}_{\text{pro}(R)}$, also showed a significant difference in attack orientation of substrates between the two stereofacial addition modes (as defined by the dihedral angle θ_{NCCN}). Even in the truncated models without all steric and structural parameters related to the catalyst backbone, the ideal substrate arrangement is synclinal, with an angle of θ = 30−40°; therefore, this angle is expected to be optimal. Interestingly, in the energetically favoured transition state, **pro-(*R*)-TS174a** in Figure 30, the nitronate and *N*-Boc phenylaldimine share a synclinal attack orientation $\theta_{\text{pro}(R)}$ = 39.1°, while in **pro-(*S*)-TS174b** in Figure 30, they approach each other at an wider angle of $\theta_{\text{pro}(S)}$ = −51.1°. The origin of this favoured attack trajectory was due to the secondary orbital overlap between the two substrates at the transition state geometry, as observed from the HOMO orbitals depicted in

Figure 32. Furthermore, a subsequent application of NBO analysis indicated that synclinal attack of substrates optimizes the secondary orbital interactions between the nitronate oxygen atom and the antibonding orbital of carbonyl group in *N*-Boc phenylaldimine (Figure 32; **pro-(*R*)-TS174a**, $E_{(NBO)}$ = 2.6; **pro-(*S*)-TS174b**, $E_{(NBO)}$ = 0.6 kcal/mol).

a) b)

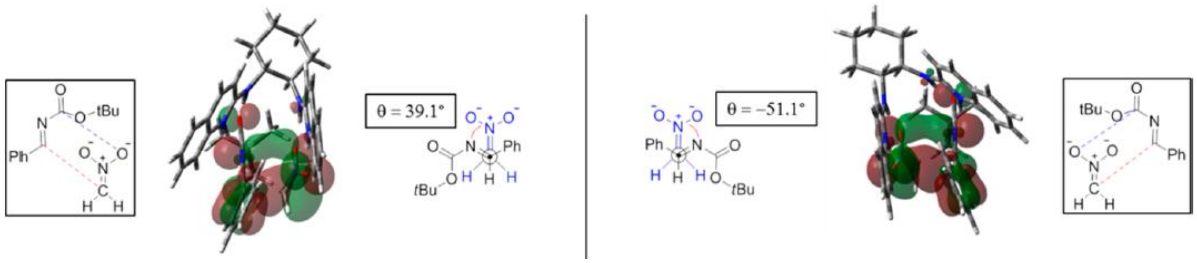

Figure 32. Depiction of the substrate alignment and secondary orbital interactions within the ωB97X-D/6-31G(d) calculated transition states a) **pro-(*R*)-TS174a** and b) **pro-(*S*)-TS174b**. 3D models represent the HOMO orbital.

Further supporting the importance of this orbital interaction, analysis of the energy of interaction between the deformed fragments, comprised of orbital interaction (ΔE_{orb}), attractive electrostatic interaction (ΔE_{elec}), and steric interaction (ΔE_{Pauli}) was performed by Energy Decomposition Analysis technique (EDA) on enantioselective *aza*-Henry reaction of nitromethane to *N*-Boc phenylaldimine, using the computational chemistry package ADF (Amsterdam Density Functional). This analysis revealed that the orbital interaction (ΔE_{orb}) accounts for charge transfer (i.e., donor–acceptor interactions) was the dominant factors controlling the observed enantioselectivity (Table 6).

Table 6. Energy decomposition analysis for the calculated enantiodetermining transition states for addition reaction of nitronate to *N*-Boc phenylaldimine.

	ΔE_{Pauli} (kcal/mol)	ΔE_{elec} (kcal/mol)	ΔE_{orb} (kcal/mol)	ΔE_{int} (kcal/mol)
pro-(*R*)-TS174a	0.083	-0.106	-0.414	-0.438
pro-(*S*)-TS174b	0.081	-0.132	-0.308	-0.359

Taken together, the specific binding mode of substrate directed by the asymmetric H-bonding framework of the chiral HQuin-BAM organocatalyst, along with secondary orbital interactions, leads to the observed stereoinduction. Further research was essential to trace properly the detailed origins of both enantio- and diastereoselectivity in HQuin-BAM promoted asymmetric *aza*-Henry reactions. To this end, the second part of my research program focused on an analysis of the origins of enantio- and diastereoselectivity, using monosusbtituted nitroalkane and electron deficient *N*-Boc arylaldimines (see Section 2.2).

2.1.3. The Mechanistic pathway of HQuin-BAM Catalyzed Asymmetric *aza*-Henry Reaction

Having determined the initial factor controlling the sense of enantioinduction, my attention next turned towards mapping a complete reaction pathway that represents the bifunctional activation/stabilization role of the catalyst, within the potential energy surface (PES) of the enantioselective HQuin-BAM catalyzed *aza*-Henry reaction of nitromethane with *N*-Boc phenylaldimine reported by Johnston and co-workers.[117] Elucidation of the reaction mechanism began with analyzing the most stable complexes formed between the HQuin-BAM catalyst **171** and *N*-Boc phenylaldimine **169** or nitromethane **168**. Not surprisingly, it was found that coordination of the *N*-Boc phenylaldimine (**INT-2** in Figure 34) is thermodynamically favoured over coordination of nitromethane (**INT-1** in Figure 34), indicating that the chiral proton

activated the aldimine electrophile to render it more electrophilic for attack by the nucleophile. Thus, it is likely that the reaction path begins with coordination of *N*-Boc phenylaldimine to the catalyst (**INT-2** in Figure 34), followed by docking of nitromethane (**INT-3** in Figure 34), which undergoes subsequent catalyst facilitated deprotonation. It is important to mention that formation of nitroenol may take place through tautomerization, however, given the equilibrium constant between nitromethane and nitroenol, it is more likely that the catalyst facilitates deprotonation. In other words, a reaction scenario involving coordination of free nitroenol to attain **INT-4** in Figure 34 is doubtful, due to the low equilibrium constant between nitromethane and nitroenol (1.1×10^{-7}) at room temperature, which is too small to rationalize a substantial formation of the nitroenol nucleophile.[144] Furthermore, according to the reported experimental reaction conditions, there were only less than 0.01 equivalents of nitroenol at equilibrium, using 0.4 mL of nitromethane.[117] Further supporting our prediction, it is important to mention that Jørgensen *et al.*[145] reported an analogous indirect/direct catalytic asymmetric *aza*-Henry reaction using different Cu(II) Box salts **180**, **184** (Scheme 46). More specifically, in the direct variant, an external base was used together with the chiral Cu(II) Box catalyst **184**. It was determined that addition of an external base allowed direct nucleophilc attack of nitroalkane to electrophile (Scheme 46b), rather than preformation of the nucleophile, as was observed in the indirect reaction (Scheme 46a).

a)

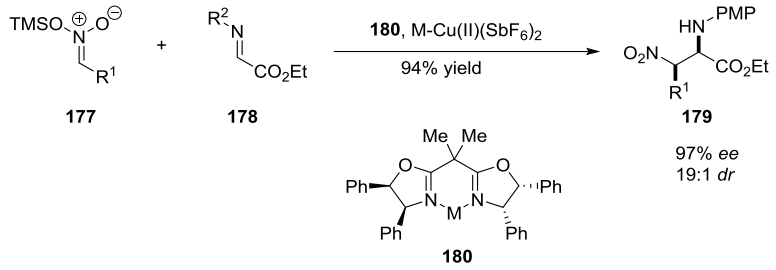

b)

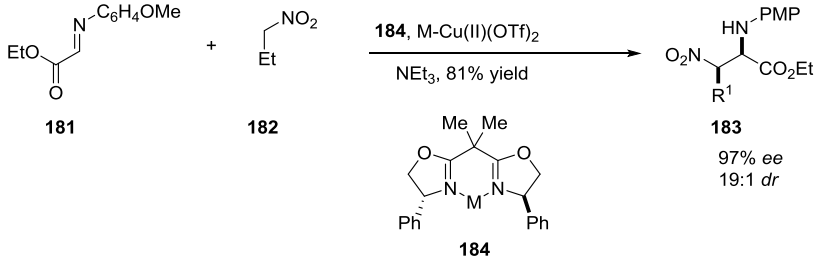

Scheme 46. a) An indirect and b) a direct catalytic asymmetric *aza*-Henry reaction using different Cu(II) Box salts.

Therefore, in our catalytic system, the quinoline ring in the HQuin-BAM catalyst functions as a Brønsted base to deprotonate nitromethane. Accordingly, two competing deprotonation transition states were modeled (**TS-E1** and **TS-E2**, Figure 33). The lowest energy deprotonation transition state, **TS-E2**, possesses a N···H bond-forming distance of 1.22 Å and a C···H bond breaking distance of 1.50 Å. As shown in Figure 34, the preferred transition state, in which *N*-Boc phenylaldimine is already coordinated to the protonated half of the HQuin-BAM catalyst, as opposed to deprotonation via a free catalyst (**TS-E1**), is energetically favoured.

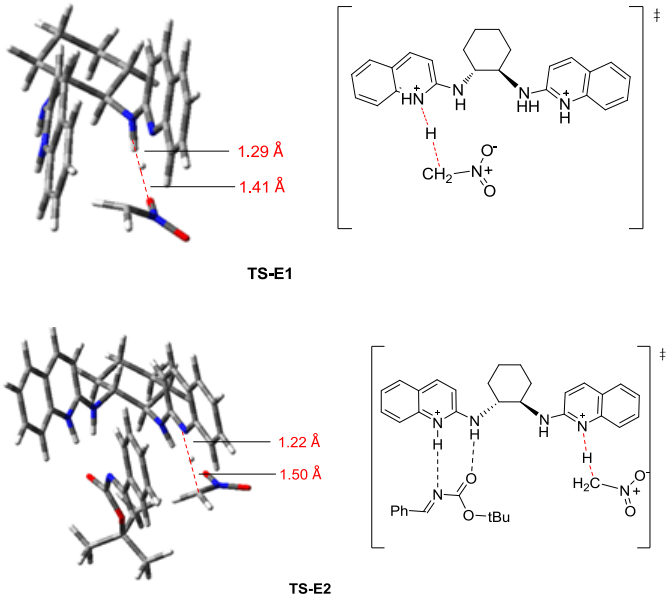

Figure 33. ωB97X-D/6-31G(d) calculated deprotonation transition states.

The transition state **TS-E2** was more stable than **TS-E1** ($\Delta\Delta G^{\ddagger}$ = 0.9 kcal/mol) due to the fact that coordination of the electrophilic *N*-Boc phenylaldimine to the HQuin-BAM catalyst (intermediate **INT-2** in Figure 34) is energetically favoured over coordination of nucleophilic nitromethane (intermediate **INT-1** in Figure 34). Regardless, deprotonation of nitromethane is calculated to be rate-limiting. An interesting feature of this mechanistic pathway is that deprotonation becomes rate limiting, while C–C bond formation remains selectivity determining. The intermediate product of **TS-E2** is **INT-4**, a charge separated complex generated from a subtle shift in the nitronate alignment. In this charge-separated intermediate, **INT-4**, H-bond contacts between the diprotonated BAM catalyst and nitro group stabilize the negatively charged nitroenolate (Figure 34). At this point in the mechanism, the BAM catalyst possesses four strong H-bond donors. It is significant that the four-point H-bond network formed by the BAM catalyst in this conformation is easily amenable to the stabilization/activation motif exemplified in the

preferred C–C bond forming mode and the catalyst coordinated substrates are in close proximity and in proper alignment for enantiodetermining C–C bond formation, **pro-(*R*)-TS174a** in Figure 30. The direct product of enantioselective C–C bond formation is the charge-separated complex (**INT-5** in Figure 34). In the final step in the reaction mechanism, the resulting charge-separated intermediate (**INT-5**) then undergoes proton transfer from the protonated quinoline system to the amide nitrogen atom, via **TS-F** (Figure 34). Subsequent processing along the reaction coordinate leads directly to the H-bonded complex, which results in product formation and catalyst regeneration. In fact the enolizable proton from the nitromethane goes back to the free ligand, which in turn leads to formation of the final product and regeneration of the catalyst, further emphasizing that the reaction was catalytic in the chiral proton complex (Figure 34).

To sum up, the DFT studies show that for the HQuin-BAM catalyzed *aza*-Henry reaction between nitromethane and *N*-Boc phenylaldimine, deprotonation of nitromethane by the catalyst is the rate-limiting step, while C–C bond formation is enantiodetermining. The successful mapping of the reaction mechanism for the HQuin-BAM catalyzed *aza*-Henry reaction has provided models for assessing the bifunctional role of this organocatalyst. Within this mechanistic scenario, the HQuin-BAM catalyst fulfills both acid and base roles, as a Brønsted base and an H-bond donor to deprotonate nitromethane and activate the generated nitronate by a quinoline ring H-bond acceptor. This shows that the quinoline ring of the catalyst plays an important role in both the deprotonation and the asymmetric step. Following proton transfer, the catalyst bears four H-bonding sites, allowing it to provide the bifunctional activation/stabilization role in enantioselective C–C bond formation step. The final transition state (**TS-F** in Figure 34) on the potential energy surface shows that the proton which activates the imide nitrogen via the (+)CAHB interaction is released to the final product. In other words, the HQuin-BAM catalyst,

in addition to acting as a Brønsted base to generate a nitroenolate, served subsequently as a Brønsted acid to simultaneously activate the electrophile and stabilize the nucleophile through H-bonding during C–C bond formation and is thus essential for both reaction rate and selectivity. Of particular interest, analysis of H-bonding schemes in truncated simple systems (**TS-A172-173**, **TS-B172-173**, and **TS-C172-173**, Figures 26-28) and enantioselective C–C bond-forming transition states (**pro(*R*)-TS174a**, **pro(*S*)-TS174b**, Figure 30) highlighted the relative 'potency' of (+)CAHBs in catalysis (e.g. so-called polar ionic H-bonds) and showed this strength and ability to act as strong activators in H-bond catalysis.

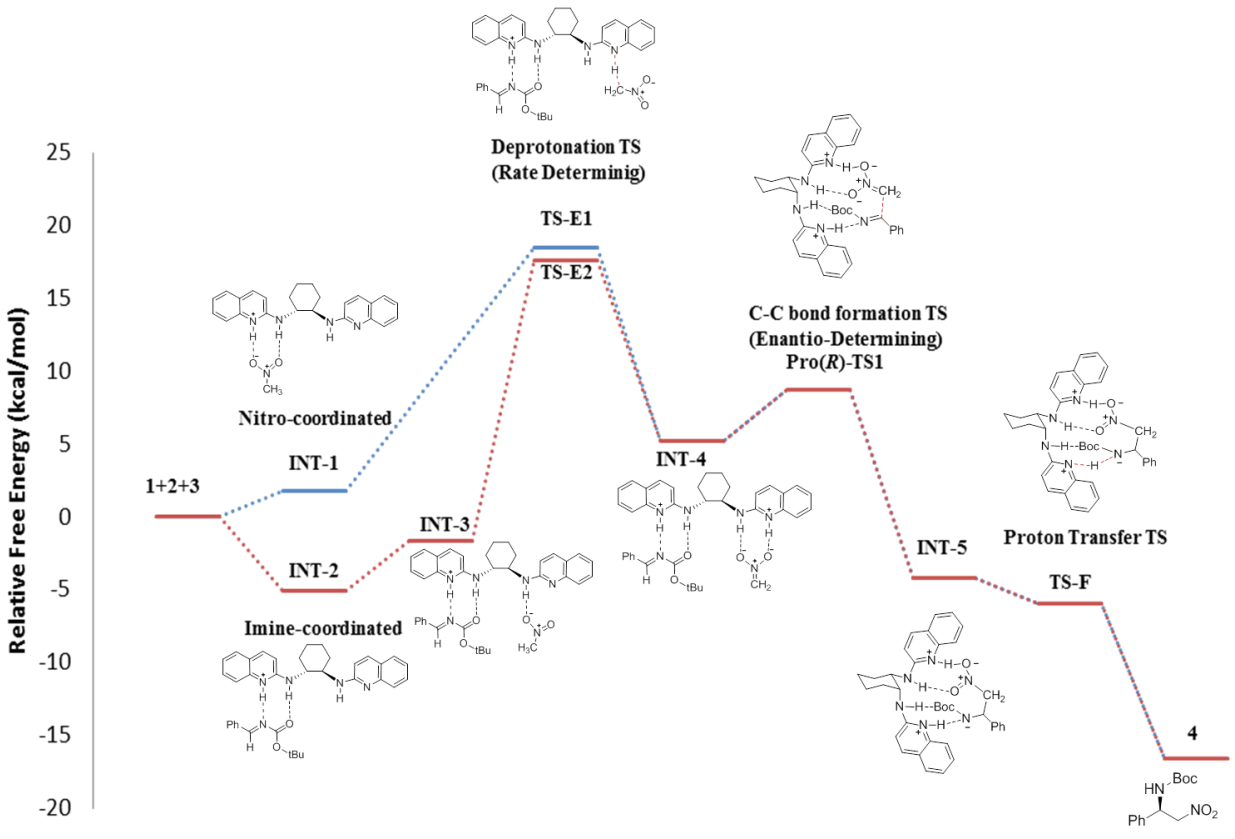

Figure 34. ωB97X-D/6-31G(d) calculated relative free energy diagram of the HQuin-BAM catalyzed enantioselective *aza*-Henry reaction.

2.2. Insight from DFT Studies into the Exact Origins of Enantio- & Diastereoselectivity in HQuin-BAM Catalyzed *Aza*-Henry Reactions of Nitroethane with Electron Deficient Aldimines

The design of a new H-bond organocatalyst for asymmetric transformations depends on a detailed understanding of the important factors controlling the sense of stereoinduction in these processes. Thus, the study of the exact origins of catalysis and stereoselectivity is of great interest. From the computational investigation in the preceeding chapter of the initial factor controlling the sense of enantioinduction in HQuin-BAM catalyzed *aza*-Henry reaction, it may be possible to understand the detailed factors controlling stereoselection in related diastereoselective processes (Scheme 47). The experimentally reported finding from Johnston *et al*. [117] that HQuin-BAM **171** catalyzes the addition of nitroethane **186** to *N*-Boc phenylaldimine **185** to afford (*1R,2S*)-anti product as the major stereoisomer in 59% ee with 14:1 *anti*/*syn* dr, is a good starting point for such a study (Scheme 47).

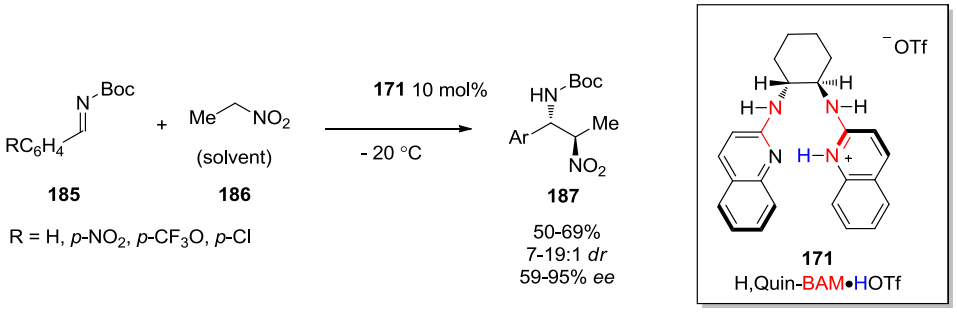

Scheme 47. HQuin-BAM catalyzed asymmetric *aza*-Henry reactions of nitroethane with *N*-Boc arylaldimines.

Accordingly, an initial series of transition state searches were performed in which the relative dihedral angle (θ_{NCCN}) and (*Re*)- vs (*Si*)-stereofacial mode of nitronate addition to *N*-Boc aldimine as well as the in versus out orientation of the *N*-Boc aldimine with respect to the

HQuin-BAM catalyst were varied. Ultimately, emerging from these searches was the finding of low energy (*Re*)- and (*Si*)-selective transition states having distinct characteristic structural aspects (Figure 35). Notwithstanding, present throughout the series was the occurrence of a positive charged assisted hydrogen bond (+)CAHB, that as crucial directing element for *N*-Boc aldimine and nitronate addition, was of paramount importance for aligning the substrates in an optimal attack geometry akin to stabilizing charge build up during the C–C bond forming process, and allowing for effective transmission of catalyst based chirality to the substrates in the stereodetermining transition states.

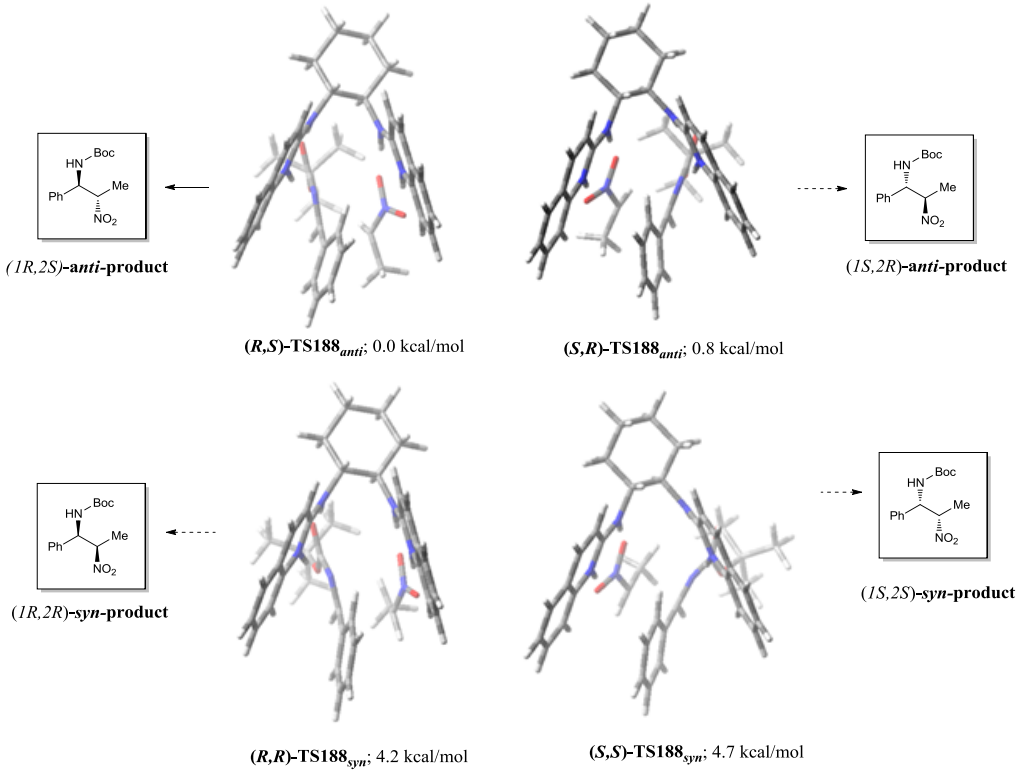

Figure 35. ωB97X-D/6-31G(d) calculated C–C bond forming enantiomeric and diastereomeric transition states of monoalkylated nitronate addition to *N*-Boc phenylaldimine.

Within the subset of these stereodetermining transition states, the two most favorable were (*R*,*S*)-**TS188**$_{anti}$ and (*S*,*R*)-**TS188**$_{anti}$ leading to *anti* diastereomeric products having relative free

energies of 0.0 and 0.8 kcal/mol relative to the most stable transition state, whereas *syn*-product forming (*R,R*)-**TS188**$_{syn}$ and (*S,S*)-**TS188**$_{syn}$ were 4.2 and 4.7 kcal/mol higher in energy (Table 7). The addition of a monoalkylated nitronate nucleophile to a range of electronically different *N*-Boc arylaldimines (*p*-OCF_3-, *p*-Cl, *p*-NO_2-arylaldimines) was also modeled at the ωB97X-D/6-31G(d) level of theory with the IEFPCM dielectric continuum solvation model and the default parameters for nitroethane as the solvent (**TS189-TS191,** see Section 4.4). Single-point calculations were also performed at B3LYP/6-31G(d), ωB97X-D/6-311+G(d,p), and B3LYP-D3/6-311+G(d,p) levels on ωB97X-D/6-31G(d) optimized geometries. Thermal corrections from the vibrational frequencies at the ωB97X-D/6-31G(d) level on the optimized geometries were combined with the electronic energies of the above mentioned methods to gain the free energies. The free energy corrections were calculated using the Truhlar's quasiharmonic approximation,[146] in which the harmonic oscillator approximation in the calculations of the vibrational partition functions was used and vibrational frequencies lower than 100 cm^{-1} were set to 100 cm^{-1} (Table 7). As experimentally observed, for all these substituted transition states (**TS188-TS191**) our calculation predicts an enantiomeric excess of 66-95%, in favor of the (*1R,2S*)-configured products with the (*1R*)-absolute configuration at the benzylic carbon and *anti* diastereoselection. Notably, the application of a dispersion-uncorrected functional (i.e. B3LYP) led to the wrong sign for the relative stability of the stereodetermining transition states, however, this observation was expected due to the poor performance of the B3LYP functional in accounting for dispersion interactions.[147] The underestimation of medium- and long-range type dispersion forces is a main limitation of B3LYP. Thus, both a long-range corrected (LRC) exchange-correlation functional with inclusion of dispersion correction, ωB97X-D and the Grimme's dispersion corrected functional B3LYP-D3 within the IEFPCM model were used. Interestingly, there was a fairly

reliable correlation between predicted and experimentally measured enantioselectivities with both dispersion inclusive functionals (ωB97X-D and B3LYP-D3) and fairly reliable results with the experimental enantioselectivity were obtained with these functionals for all substituted transition states. Notably, the energy difference between the stereodetermining transition states did not change significantly when the larger basis set including polarization functions on the hydrogen atoms as well as diffuse functions [i.e., 6-311+G(d,p)] was used (Table 7).

Table 7. Computed relative energies of stereo-detremining transition states with respect to the most stable transition structure in reaction of nitronate with (a) *N*-Boc phenylaldimine (**TS188**), (b) *p*-OCF_3-arylaldimine (**TS189**), (c) *p*-Cl-arylaldimine (**TS190**), and (d) *p*-NO_2-arylaldimine (**TS191**) with dispersion corrected functionals and different basis sets.[a,b]

	ωB97X-D/6-31G(d) ΔG (kcal/mol)	**ωB97X-D/6-311+G(d,p) ΔG (kcal/mol)**	**B3LYP-D3/6-311+G(d,p) ΔG (kcal/mol)**
(*R*,*S*)-TS188$_{anti}$	0.0	0.0	0.0
(*S*,*R*)-TS188$_{anti}$	0.8	1.3	0.9
(*R*,*R*)-TS188$_{syn}$	4.2	4.3	4.1
(*S*,*S*)-TS188$_{syn}$	4.7	5.0	4.6

	ωB97X-D/6-31G(d) ΔG (kcal/mol)	**ωB97X-D/6-311+G(d,p) ΔG (kcal/mol)**	**B3LYP-D3/6-311+G(d,p) ΔG (kcal/mol)**
(*R*,*S*)-TS189$_{anti}$	0.0	0.0	0.0
(*S*,*R*)-TS189$_{anti}$	1.5	1.3	1.3
(*R*,*R*)-TS189$_{syn}$	3.5	3.5	3.4
(*S*,*S*)-TS189$_{syn}$	5.0	4.4	4.3

	ωB97X-D/6-31G(d) ΔG (kcal/mol)	**ωB97X-D/6-311+G(d,p) ΔG (kcal/mol)**	**B3LYP-D3/6-311+G(d,p) ΔG (kcal/mol)**
(*R*,*S*)-TS190$_{anti}$	0.0	0.0	0.0
(*S*,*R*)-TS190$_{anti}$	1.0	1.1	0.8
(*R*,*R*)-TS190$_{syn}$	4.1	3.8	3.7
(*S*,*S*)-TS190$_{syn}$	5.8	5.1	4.5

	ωB97X-D/6-31G(d) ΔG (kcal/mol)	**ωB97X-D/6-311+G(d,p) ΔG (kcal/mol)**	**B3LYP-D3/6-311+G(d,p) ΔG (kcal/mol)**
(*R*,*S*)-TS191$_{anti}$	0.0	0.0	0.0
(*S*,*R*)-TS191$_{anti}$	1.8	2.2	1.6
(*R*,*R*)-TS191$_{syn}$	3.3	3.3	3.1
(*S*,*S*)-TS191$_{syn}$	5.2	4.7	4.3

[a] *Single point calculations and thermal corrections were performed at B3LYP/6-31G(d), ωB97X-D/6-311+G(d,p), and B3LYP-D3/6-311+G(d,p) levels on ωB97X-D/6-31G(d) optimized geometries.* [b]*The computed energies of the stereodetermining transition states using the dispersion-uncorrected functional B3LYP/6-31G(d) are depicted in Section 4.4.*

2.2.1. Factors Controlling Diastereoselectivity: *Anti*/*Syn* Selectivity

As for the basis of the energetic difference between stereo-determining transition states a breakdown of the factors contributing to diastereo- vis-à-vis enantioinduction was undertaken to disentangle these two aspects. On this front, the origin of *anti*/*syn*-diastereocontrol was addressed first. Arising from this endeavor was the finding that a decisive factor controlling diastereoinduction was the presence of a sterically unfavorable interaction between the nitronate methyl and the aldimine *N*-Boc protecting group in the higher energy transition states. Ultimately, this has the effect of distorting the *N*-Boc group from planarity (C_{Ph}-C_{CN}-N_{CN}-C_{CO} dihedral angle, τ_{imine} = 177° for (*R*,*S*)-**TS188**$_{anti}$, 179° for (*S*,*R*)-**TS188**$_{anti}$ and τ_{imine} = 169° for (*R*,*R*)-**TS188**$_{syn}$, 166° for (*S*,*S*)-**TS188**$_{syn}$) and consequently reducing conjugation between the carbonyl and phenyl group. Accordingly, the computed NBO resonance stabilization energy for delocalization of electron pairs in the *N*-Boc phenylaldimine system supports this loss in conjugation with values of 99, 99, 95, and 93 kcal/mol for (*R*,*S*)-**TS188**$_{anti}$, (*S*,*R*)-**TS188**$_{anti}$, (*R*,*R*)-**TS188**$_{syn}$, and (*S*,*S*)-**TS188**$_{syn}$, respectively (Table 8). This resonance stabilization energy was evaluated by second-order perturbation theory, in which delocalization of the donor orbitals to the acceptor NBO orbitals on the entire *N*-Boc phenylaldimine conformer were summed (see Appendix, Table 8A, for the substituted **TS189**-**TS191**). In addition, in the transition state structure featuring *anti* approach of the nitronate nucleophile, a stabilizing donor-acceptor $CH_{vinyl}\cdots O$ type interaction between the vinylic nitronate C-H bond and the *tert*-butoxy oxygen of the *N*-Boc protecting group is present. An NBO analysis revealed the presence of this stabilizing donor-acceptor interaction involving donation of an alkoxy oxygen lone pair (a *tert*-butoxy oxygen lone pair) into a σ*-orbital of a vinylic C–H bond of the nitronate in *anti* diastereomeric transition states (Figure 36; (*R*,*S*)-**TS188**$_{anti}$, E(NBO) = 1.4 kcal/mol; (*S*,*R*)-

TS188$_{anti}$, E(NBO) = 1.9 kcal/mol). Whereas, in (*R*,*R*)-**TS188**$_{syn}$ and (*S*,*S*)-**TS188**$_{syn}$, the *syn* nucleophilic attack of the nitronate leads to the loss of this stabilizing $CH_{vinyl}\cdots O$ interaction and the formation of unfavorable alkyl-alkyl based steric repulsion between the nitronate methyl and *N*-Boc protecting group.

Table 8. The evaluated resonance stabilization energy and C_{Ph}-C_{CN}-N_{CN}-C_{CO} dihedral angle of the *N*-Boc phenylaldimine within the optimized transition state geometries.

(*R*,*S*)-**TS188**$_{anti}$

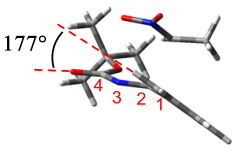

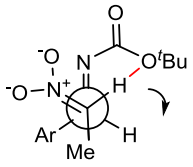

LP(O)... BD*(C-H)
= 1.4 kcal/mol

Donor NBO	Acceptor NBO	*E(2)* (kcal/mol)	C_{ph}-C_{CN}-N_{CN}-C_{CO} (degree)
BD N32-C33	BD* N32-C34	1.50	-177°
BD N32-C33	BD* C34-O35	51.1	
BD C33-C63	BD* N32-C33	1.52	
BD C33-C63	BD* N32-C34	4.31	
BD C63-C66	BD* C33-C63	2.89	
BD C63-C65	BD* N32-C33	29.3	
BD C63-C65	BD* C33-C63	2.66	
BD C34-O35	BD* C34-O35	1.60	
LP N32	BD* C34-O35	4.20	
E(2)(delocalization)		99.1	

(*S*,*R*)-**TS188**$_{anti}$

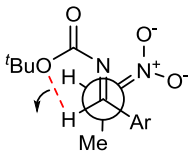

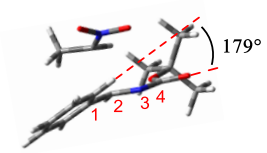

LP(O)... BD*(C-H)
= 1.9 kcal/mol

Donor NBO	Acceptor NBO	*E(2)* (kcal/mol)	C_{ph}-C_{CN}-N_{CN}-C_{CO} (degree)
BD N36-C42	BD* N36-C37	1.50	-179°
BD N36-C42	BD* C37-O38	50.7	
BD C42-C51	BD* N36-C37	4.38	
BD C42-C51	BD* N36-C42	1.59	
BD C51-C53	BD* N36-C42	30.2	
BD C51-C53	BD* C42-C51	2.70	
BD C51-C54	BD* C42-C51	2.89	
BD C37-O38	BD* C37-O38	1.54	
LP N36	BD* C37-O38	3.42	
E(2)(delocalization)		98.9	

(*R*,*R*)-**TS188**$_{syn}$

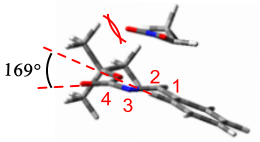

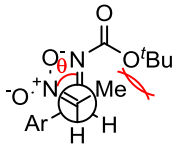

Donor NBO	Acceptor NBO	*E(2)* (kcal/mol)	C_{ph}-C_{CN}-N_{CN}-C_{CO} (degree)
BD N32-C33	BD* N32-C34	1.43	-169°
BD N32-C33	BD* C34-O35	52.4	
BD C33-C62	BD* N32-C33	1.46	
BD C33-C62	BD* N32-C34	4.23	
BD C62-C65	BD* N32-C33	25.9	
BD C62-C64	BD* C33-C62	2.54	
BD C62-C65	BD* C33-C62	2.90	
BD C34-O35	BD* C34-O35	1.50	
LP N 32	BD* C34-O35	3.58	
E(2)(delocalization)		95.0	

(*S*,*S*)-**TS188**$_{syn}$

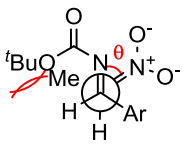

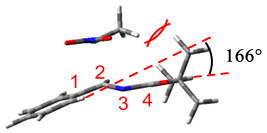

Donor NBO	Acceptor NBO	*E(2)* (kcal/mol)	C_{ph}-C_{CN}-N_{CN}-C_{CO} (degree)
			-166°
BD N36-C42	BD* N36-C37	1.56	
BD N36-C42	BD* C37-O38	47.5	
BD C42-C50	BD* N36-C37	4.16	
BD C42-C50	BD* N36-C42	1.60	
BD C50-C53	BD* N36-C42	26.3	
BD C50-C52	BD* N36-C42	2.38	
BD C50-C52	BD* C42-C50	2.57	
BD C50-C53	BD* C42-C50	2.93	
BD C37-O38	BD* C37-O38	1.48	
LP N 36	BD* C37-O38	2.74	
E(2)(delocalization)		93.2	

Our calculated stability of the diastereomeric *anti* transition states, (*R*,*S*)-**TS188**$_{anti}$-**TS191**$_{anti}$ and (*S*,*R*)-**TS188**$_{anti}$-**TS191**$_{anti}$ compared with the *syn* transition states, (*R*,*R*)-**TS188**$_{syn}$-**TS191**$_{syn}$ and (*S*,*S*)-**TS188**$_{syn}$-**TS191**$_{syn}$ were overestimated, albeit their energetic trends gave us a qualitative picture of the origin of the *anti*/*syn* diastereoselectivity.

2.2.2. Factors Controlling Enantioselectivity: (*Si*)/(*Re*)-Enantioface

Meanwhile, the apparent factor contributing to the difference in (*Si*) vs (*Re*) transition state stabilities was the ability of the catalyst to adopt flexible conformations, as seen by measured separation distances between the quinoline rings of the catalyst (evaluated as the distance between the centroids of two quinoline ring systems), which was shorter in the case of the (*Si*) nucleophilic mode of addition (Figure 36). This folded conformation linked with a reduced dihedral angle (θ_{NCCN}) around the forming C−C bond in the (*Si*) enantiofacial addition modes, as evidenced by (*R*,*S*)-**TS188**$_{anti}$ and (*R*,*R*)-**TS188**$_{syn}$ having dihedrals θ_{NCCN} of 36.0°-38.0°, while in (*S*,*R*)-**TS188**$_{anti}$ and (*S*,*S*)-**TS188**$_{syn}$ corresponding to (*Re*)-enantiofacial nucleophilic addition, this angle was noticeably larger spanning a range from 52.0°-59.0°.

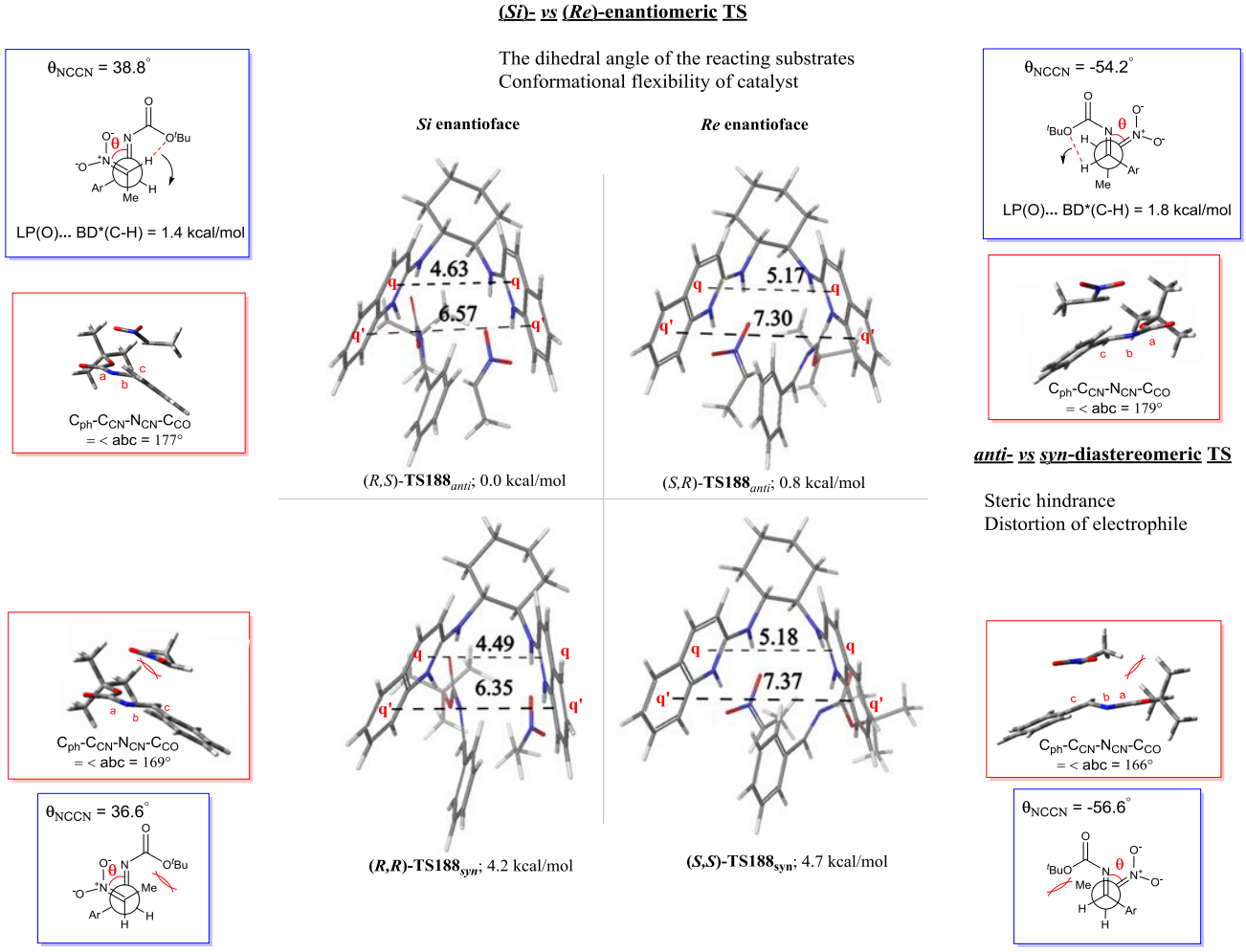

Figure 36. ωB97X-D/6-31G(d) calculated C– C bond forming enantio- and diastereomeric transition states for addition reaction of nitronate to *N*-Boc phenylaldimine.

It is important to mention that the enantio- and diastereoselectivity of the HQuin-BAM catalyzed *aza*-Henry reaction of nitroethane with more electrophilic *p*-OCF_3-, *p*-Cl, *p*-NO_2-arylaldimines, **TS189-191** showed the same trends as the nitroethane addition to *N*-Boc phenylaldimine, **TS188** (Figures 37). For instance, in all the reactions considered, the catalyst adopted a more closed conformation and the reactants approached one another at angles of 36.0°-39.0° and therefore, the major products resulted from attack of the *N*-Boc arylaldimines (*Si*) enantioface. Mirroring (*R,S*)-**TS189**$_{anti}$ as well were closed catalyst binding pockets in *anti*(*R,S*)-

TS189$_{anti}$ and (*R*,*S*)-**TS191**$_{anti}$, which reinforced the intramolecular (intra-host) and intermolecular (host-guest) non-covalent attractive interactions.

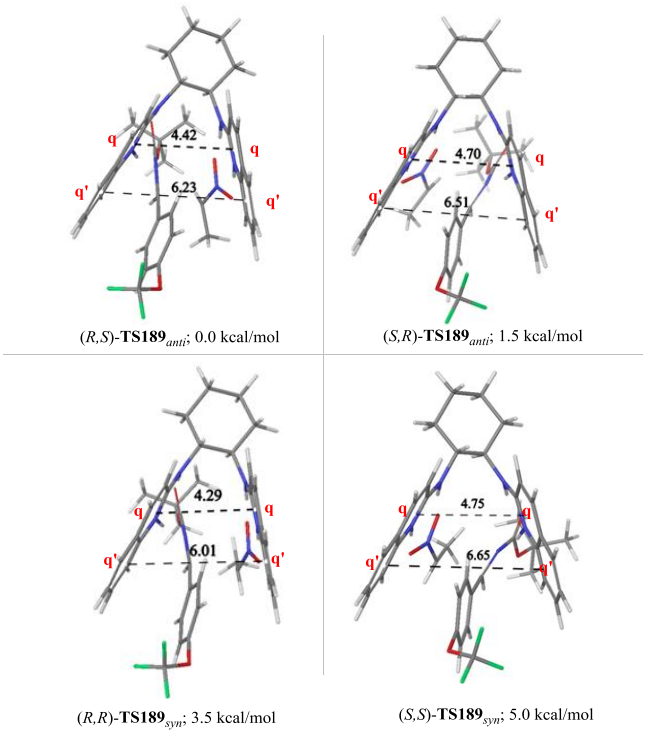

(*R*,*S*)-**TS189**$_{anti}$; 0.0 kcal/mol

(*S*,*R*)-**TS189**$_{anti}$; 1.5 kcal/mol

(*R*,*R*)-**TS189**$_{syn}$; 3.5 kcal/mol

(*S*,*S*)-**TS189**$_{syn}$; 5.0 kcal/mol

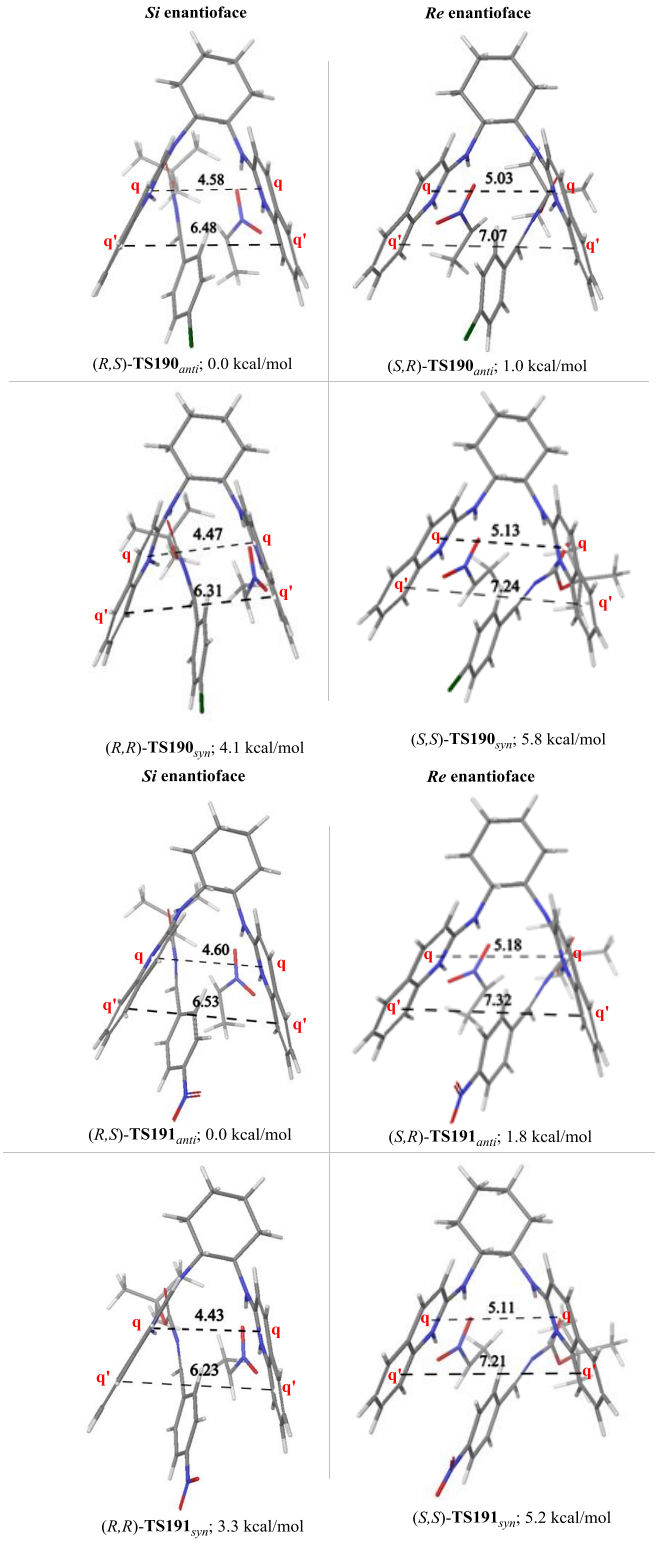

Figure 37. ωB97X-D/6-31G(d) calculated C–C bond forming enantio- and diastereomeric transition states, **TS189-TS191**, for reaction of nitronate to *N*-Boc arylaldimines.

2.2.3. General Overview of the Origins of Enantiocontrol

Taken together, the high π-facial selectivity in HQuin-BAM catalyzed *aza*-Henry reactions can be well-understood within the context of three factors, namely substrate, catalyst, and substrate-catalyst based interactions.

2.2.3.1. Substrate-Based Interactions

Turning first to the substrate localized interactions and consistent with a preliminary computational study of the mechanism of the HQuin-BAM catalyzed *aza*-Henry reaction in Section 2.1.2., substrate based interactions comprised of distortion energy and the energy of interaction between the deformed substrates (i.e., orbital interactions, attractive electrostatic interactions, and steric interactions) were found to be important factors governing selectivity as shown by distortion/interaction analysis (Table 9, 9A in the Appendix). However, it was found from our initial results obtained by Energy Decomposition Analysis (EDA) on the enantioselective *aza*-Henry reaction of nitromethane to *N*-Boc phenylaldimine (Table 6) that the orbital interaction (ΔE_{orb}) was the dominant factor controlling the observed enantioselectivity.

Table 9. Distortion/interaction analysis for the calculated stereo-determining transition states in addition of nitronate to *N*-Boc phenylaldimine (**TS188**).

	(*R*,*S*)-**TS188**$_{anti}$	(*S*,*R*)-**TS188**$_{anti}$	**ΔE**	(*R*,*R*)-**TS188**$_{syn}$	(*S*,*S*)-**TS188**$_{syn}$	**ΔE**
Interaction Energy (E_{int}) (kcal/mol)	-64.8	-64.2	0.60	-63.1	-62.2	0.88
Catalyst Distortion ($E_{dist/cat}$) (kcal/mol)	5.20	5.86	0.66	5.17	5.49	0.32
Substrate Distortion/Interaction ($E_{dist/int}$) (kcal/mol)	1.05	1.94	0.89	1.90	1.0	0.90

Both electrophile and nucleophile within the optimized enantiodetermining (*Si*)- and (*Re*)-transition states possessed several notable structural features. Their C_{nitro}•••C_{imine} bond forming distances were similar, at 2.23 Å-2.24 Å. Each enantiomeric transition state possessed several stabilizing orbital interactions and an electrostatic interaction between *N*-Boc aldimine and nitronate substrates. Accordingly, analysis of the structural parameters of both electrophile and nucleophile within the optimized stereodetermining transition states revealed that a synclinal attack orientation present in (*R*,*S*)-**TS188**$_{anti}$ and (*R*,*R*)-**TS188**$_{syn,}$ (θ_{NCCN} = 36.0^{o}-38.0^{o}) optimized the secondary orbital interactions between the nitronate and aldimine. Of these transition structures, the secondary orbital interactions were greater in those with (*1R*) configuration at benzylic carbon, (*R*,*S*)-**TS188**$_{anti}$ and (*R*,*R*)-**TS188**$_{syn,}$ as deemed by NBO analysis (Figure 38). These interactions corresponded to donor-acceptor orbital interactions between the nitronate oxygen atoms and the antibonding orbital of C=O, N=C and C_{Ar}–C_{Ar} groups in *N*-Boc phenylaldimine (Figure 38).

It is noteworthy that the same scenario was also observed in the substituted transition states having more electrophilic aldimines, **TS189-191** (Figure 39).

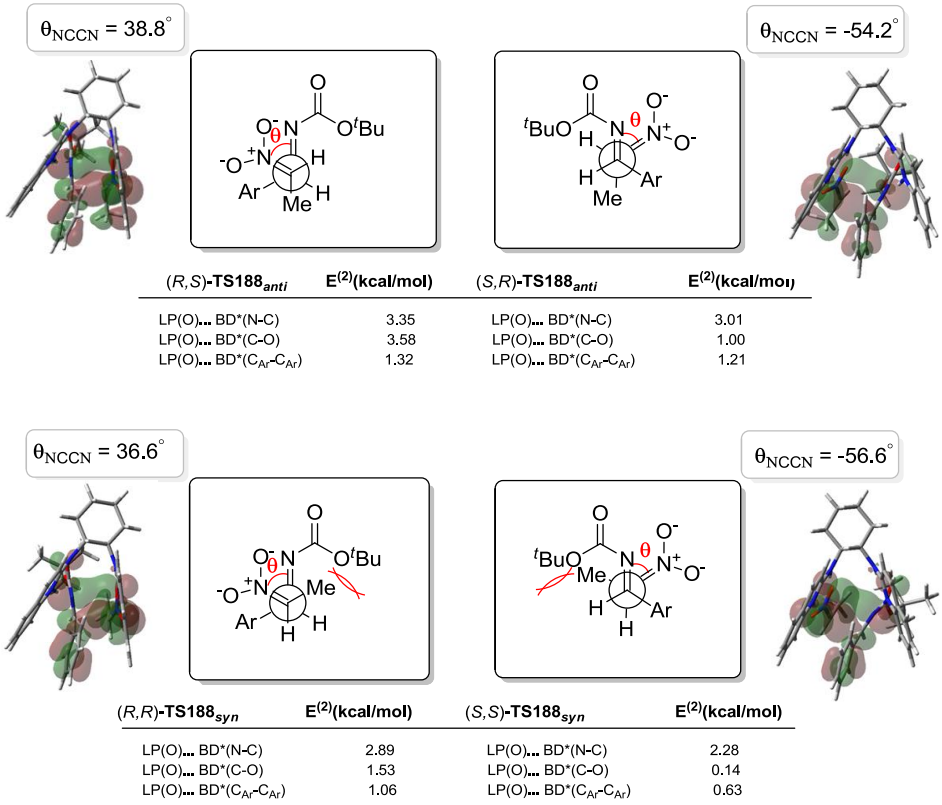

Figure 38. Depiction of the substrate alignment and secondary orbital interactions within the ωB97X-D/6-31G(d) calculated stereo-determining C–C bond forming transition states **TS188**. 3D models represent the HOMO orbital.

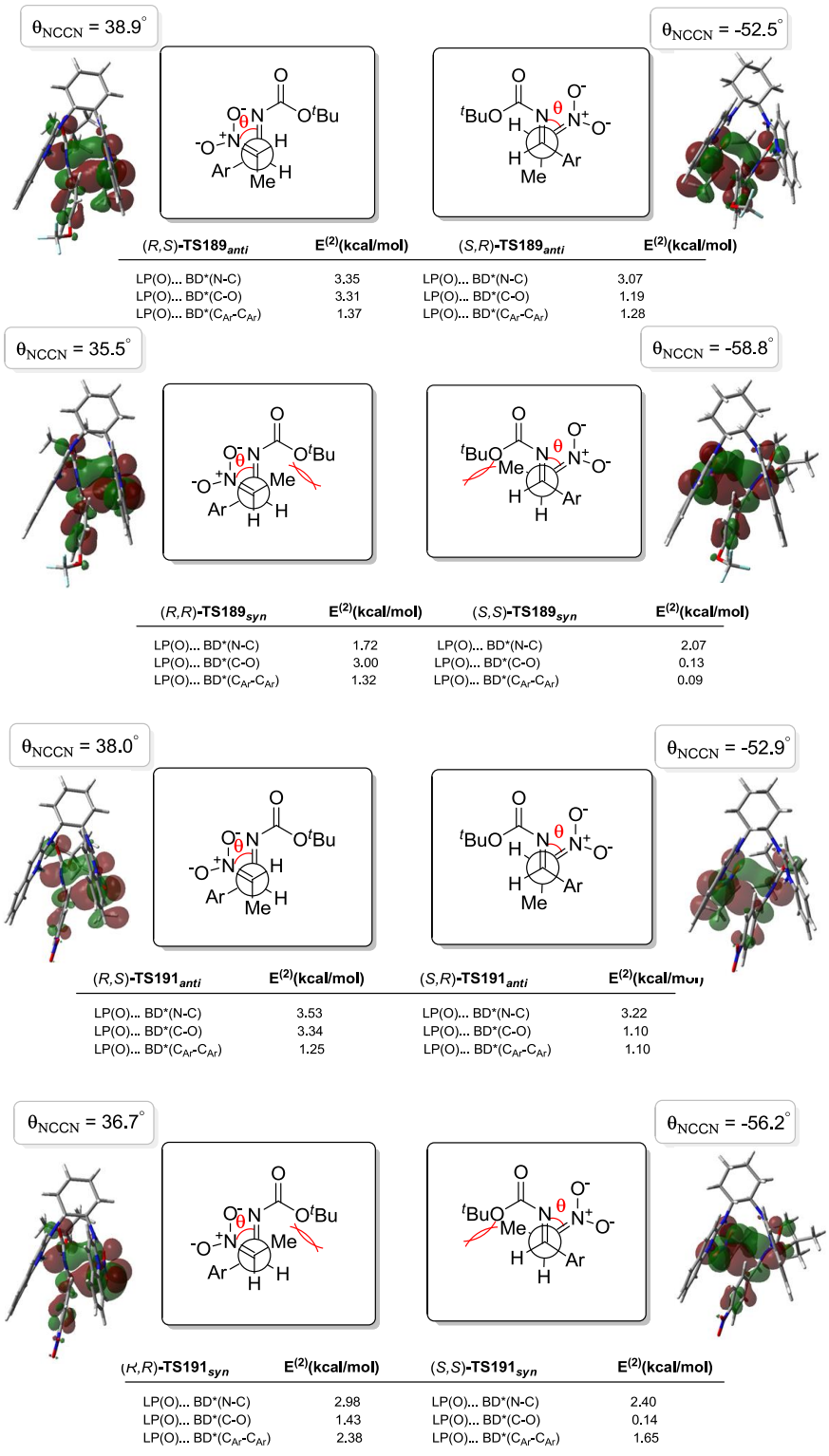

Figure 39. Depiction of the substrate alignment and secondary orbital interactions for transition states **TS189** and **TS191**. 3D models represent the HOMO orbital.

Additionally, in all the optimized C–C bond forming transition states, (*R*,*S*)-**TS188**$_{anti}$, (*R*,*R*)-**TS188**$_{syn}$, (*S*,*R*)-**TS188**$_{anti}$, and (*S*,*S*)-**TS188**$_{syn}$, the aldimine nitrogen is stabilized through a weak electrostatic contact to a nitronate nitrogen ($C_{nitro}N^{\delta+}\bullet\bullet\bullet N^{\delta-}C_{imine}$), however, this interaction is much weaker in energetically unfavored (*Re*)-enantiomers, (*S*,*R*)-**TS188**$_{anti}$, (*S*,*S*)-**TS188**$_{syn}$. Accordingly, this electrostatic type interaction between a partial positive nitrogen of nitronate (N_{12}, natural charge = 0.456) and the aldimine nitrogen (N_{32}, natural charge = -0.697, distance 2.91 Å) in (*R*,*S*)-**TS1**$_{anti}$, was stronger than the analogues interaction between the nitronate (N_{46}, natural charge = 0.398) and the aldimine (N_{36}, natural charge = -0.693, distance 3.00 Å) in (*S*,*R*)-**TS1**$_{anti}$. The same scenario involving stabilization of partial charge via an electrostatic-type interaction in energetically less favorable *syn*-diastereomers (*R*,*R*)-**TS188**$_{syn}$, (*S*,*S*)-**TS188**$_{syn}$ were also present between nitronate (N_{12}, natural charge = 0.464) and the aldimine (N_{32}, natural charge = -0.706, distance 2.89 Å) for (*R*,*R*)-**TS188**$_{syn}$, and between nitronate (N_{45}, natural charge = 0.463) and the aldimine nitrogen (N_{36}, natural charge = -0.702, distance 3.03 Å) for (*S*,*S*)-**TS188**$_{syn}$.

2.2.3.2. Catalyst-Substrate (Host-Guest) and Catalyst-Based (Intra-Host) Interactions

Another factor contributing to difference in (*Si*) over (*Re*) transition state stabilities was the ability of the HQuin-BAM catalyst adopting two different conformations (closed/open), as judged by the relative distances between the ring centroids of two quinoline ring systems ($d_{q\cdots q}$, $d_{q'\cdots q'}$) of the respective catalyst fragments. Within the series the shorter distance was found in energetically favored (*Si*)-enantioface, whereas the (*Re*) higher energy transition states had a more open binding pocket ($d_{q\cdots q}$ = 4.63 Å, $d_{q'\cdots q'}$ = 6.57 Å for (*R*,*S*)-**TS188**$_{anti}$ versus $d_{q\cdots q}$ = 5.17 Å, $d_{q'\cdots q'}$ = 7.30 Å for (*S*,*R*)-**TS188**$_{anti}$ as well as $d_{q\cdots q}$ = 4.49 Å, $d_{q'\cdots q'}$ = 6.35 Å for (*R*,*R*)-**TS188**$_{syn}$ versus $d_{q\cdots q}$ = 5.18 Å, $d_{q'\cdots q'}$ = 7.37 Å for (*S*,*S*)-**TS188**$_{syn}$) in addition to the catalyst fragment

being more distorted with respect to their ground state geometries, respectively (Figure 36). The extent of distortion in the catalyst at the time of substrate binding was larger in the energetically unfavored (*Re*) transition state structures relative to (*Si*) analogues ($E_{dist/cat}$ = 5.20 kcal/mol for (*R,S*)-**TS188**$_{anti}$ vs 5.86 kcal/mol for (*S,R*)-**TS188**$_{anti}$ as well as $E_{dist/cat}$ = 5.17 kcal/mol for (*R,R*)-**TS188**$_{syn}$ vs 5.49 kcal/mol for (*S,S*)-**TS188**$_{syn}$ kcal/mol in Table 9, Figure 36; see Appendix Table 9A for substituted transition states **TS189-191**). Associated with this more closed vice versa open binding pocket of the catalyst were several metrical outcomes on substrate-catalyst based (host-guest) interactions. For instance, to produce the final products with (*1R*)/(*1S*) absolute configuration at the benzylic carbon, the flexible catalyst must undergoes conformational changing to accommodate the approaching substrates. More specifically, the catalyst undergoes less geometrical rearrangement in the favored (*Si*) enantiofacial modes of addition, (*R,S*)-**TS188**$_{anti}$ and (*R,R*)-**TS188**$_{syn}$, as a synclinal attack orientation of the substrates accommodated appropriately in the closed binding pocket of the catalyst, which in turn resulted in better transmission of catalyst-based induction of chirality to the substrates. Conversely, in the unfavored (*Re*)-enantiomers, (*S,R*)-**TS188**$_{anti}$ and (*S,S*)-**TS188**$_{syn}$, having a wider dihedral angles (θ_{NCCN}) of 52.0^{o}-59.0^{o} between the nitronate and aldimine substrates, the catalyst manifold must undergo greater geometrical reorganization to accommodate these transition state assemblies (Figure 36). The above scenario establish an interesting dependency on matching the shape and size of the catalyst (host molecule) and substrates (guest molecules) upon binding, both being key factors governing selectivity, in essence, offering an analogy to positive cooperative binding effect of catalytic enzymes and substrates in Nature.

Notably, the source of catalyst based substrate activation and associated transition state stabilization could be further traced to a greater number of stronger favorable intra- and

intermolecular stabilizing interactions in (*R*,*S*)-**TS188**$_{anti}$ and (*R*,*R*)-**TS188**$_{syn}$. For instance, a comparison of the relative energetics for C–C bond forming transition states (*R*,*S*)-**TS188**$_{anti}$, (*R*,*R*)-**TS188**$_{syn}$, (*S*,*R*)-**TS188**$_{anti}$, and (*S*,*S*)-**TS188**$_{syn}$ differed substantially when using the dispersion-uncorrected functional B3LYP versus the dispersion corrected functionals ωB97X-D and B3LYP-D3. Importantly, the results from the latter two dispersion corrected functionals, were more in line with the reported enantio- and diastereoselectivies (Table 6). Notably also, the intermolecular interactions (e.g., H-bonding network and noncovalent interactions) responsible for substrates binding and activation were all stronger in the (*Si*) transition states, as confirmed by the larger value of interaction energy (E_{int} = -64.8 kcal/mol for (*R*,*S*)-**TS188**$_{anti}$ versus -64.2 kcal/mol for (*S*,*R*)-**TS188**$_{anti}$ as well as E_{int} = -63.1 kcal/mol for (*R*,*R*)-**TS188**$_{syn}$ versus -62.2 kcal/mol for (*S*,*S*)-**TS188**$_{syn}$ kcal/mol).

Accordingly, the transition structure leading to the major (*Si*) enantiomer, (*R*,*S*)-**TS188**$_{anti}$, (*R*,*R*)-**TS188**$_{syn}$, had also stronger H-bonding interactions between the two unbound substrates and catalyst (tight host-guest interactions). However, the transition state structure corresponding to the unfavorable *Re*-facial attack, (*S*,*R*)-**TS188**$_{anti}$ and (*S*,*S*)-**TS188**$_{syn}$, did not experience H-bond stabilization with the same strength. This observation was further supported by the greater second-order perturbation energies, evaluated by NBO analysis of the H-bond networks (ΔE_{NBO}(total) = 131.1 kcal/mol for (*R*,*S*)-**TS188**$_{anti}$ vs 96.7 kcal/mol for (*S*,*R*)-**TS188**$_{anti}$ as well as ΔE_{NBO}(total) = 130.3 kcal/mol for (*R*,*R*)-**TS188**$_{syn}$ vs 118.6 kcal/mol for (*S*,*S*)-**TS188**$_{syn}$ in Figure 40).

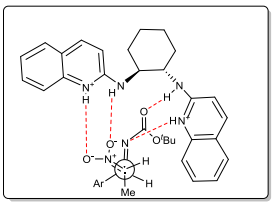

(*R*,*S*)-**TS188**$_{anti}$ 0.0 kcal/mol	Bond Distance (Å)	ΔE_{NBO} (kcal/mol)
O...(N)H	1.79	29.5
N...(N^+)H	1.83	28.0
O...(N)H	1.81	30.0
O...(N^+)H	1.70	43.6
ΔE_{NBO}(total)		**131.1**

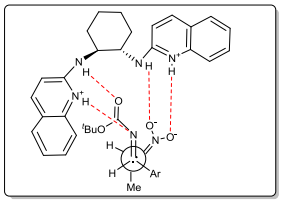

(*S*,*R*)-**TS188**$_{anti}$ 0.8 kcal/mol	Bond Distance (Å)	ΔE_{NBO} (kcal/mol)
O...(N)H	1.82	14.4
N...(N^+)H	1.76	32.0
O...(N)H	1.85	17.3
O...(N^+)H	1.69	33.0
ΔE_{NBO}(total)		**96.7**

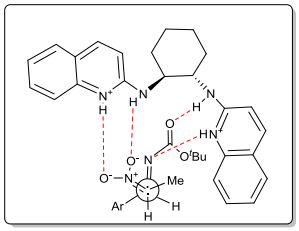

(*R*,*R*)-**TS188**$_{syn}$ 0.0 kcal/mol	Bond Distance (Å)	ΔE_{NBO} (kcal/mol)
O...(N)H	1.76	33.0
N...(N^+)H	1.88	23.7
O...(N)H	1.84	27.2
O...(N^+)H	1.67	46.4
ΔE_{NBO}(total)		**130.3**

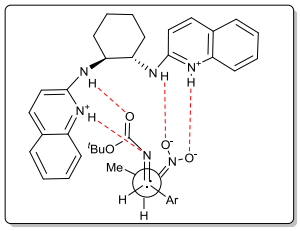

(*S*,*S*)-**TS188**$_{syn}$ 0.8 kcal/mol	Bond Distance (Å)	ΔE_{NBO} (kcal/mol)
O...(N)H	1.88	15.8
N...(N^+)H	1.77	36.2
O...(N)H	1.79	27.5
O...(N^+)H	1.69	39.1
ΔE_{NBO}(total)		**118.6**

Figure 40. Calculated NBO donor-acceptor orbital interactions present in the H-bonding networks of **TS188**.

In an effort to better understand the inter- and intramolecular non-covalent interactions, we turned to the NCI approach[148] which allows one to visualize non-covalent interactions and identify their nature as either repulsive or attractive by plotting the magnitude of the electron density signed by the second eigenvalue of the density Hessian, sign(λ_2)ρ, versus regions of very low-reduced density gradient $s(r)$. These isosurfaces represent both favorable and unfavorable interactions between unbound atoms, as defined by the sign of the second Hessian eigenvalue of the density (λ_2) and the map coloring specifies the strength as well as (un)favorable nature of the interactions. The green and yellow isosurfaces correspond to weakly attractive and weakly repulsive interactions respectively, whereas the boundaries of the coloring scheme used for the isosurfaces are defined by a (rainbow) scale with red being repulsive and blue attractive

interactions (Figure 41). Thus, the values of ρ(r), called NCI interaction critical points ((+/-)ρ_{ICP}), allows us to assess the interaction strength and the sign of (λ_2)ρ, allows discrimination of the different types of weak interactions. The larger the absolute values of (-)ρ_{ICP} associated with density accumulation (sign(λ_2)ρ < 0), the stronger the observed stabilizing non-covalent interaction. For ease of viewing, those NCI isosurface regions of greatest importance are highlighted in Figure 41-43. Inspection of the NCI isosurfaces of (*Si*)- *vs* (*Re*)-enantiofacial nucleophilic addition (*R,S*)-**TS188**$_{anti}$ and (*R,R*)-**TS188**$_{syn}$ revealed the significance of stabilizing intra-host and host-guest non-covalent interactions (sign(λ_2)ρ < 0) as apparent from the large NCI isosurface densities in these two structures, whereas in the less energetically favorable enantio-determining (*S,R*)-**TS188**$_{anti}$ and (*S,S*)-**TS188**$_{syn}$ the density of the NCI isosurfaces was less (Figure 41).

With respect to the intra-host interactions, a $\pi_{Ar}\cdots\pi_{Ar}$ type stacking (highlighted as A, Figure 41) was present in (*R,S*)-**TS188**$_{anti}$ and (*R,R*)-**TS188**$_{syn}$, as seen by the NCI isosurface plots with ρ_{ICP} having values of -0.0037 and -0.0039. The low density values (i.e., ρ(r) < 0.005 au) and the negative sign of λ_2 associated with this intra-host interaction were diagnostic of weakly attractive bonding interactions, such as induced dipole-induced dipole (London dispersion forces) interactions. Meanwhile this interaction was not present in the analogues enantiomeric (*S,R*)-**TS188**$_{anti}$ and (*S,S*)-**TS188**$_{syn}$. Visible in both (*Si*)- and (*Re*)-transition states, (*R,S*)-**TS188**$_{anti}$, (*R,R*)-**TS188**$_{syn}$, (*S,R*)-**TS188**$_{anti}$ and (*S,S*)-**TS188**$_{syn}$ were two isolated NCI isosurface regions originating from intra-host interactions between the quinoline rings and the chiral 1,2-diaminocyclohexane backbone of the catalyst (highlighted as B, Figure 41). This interaction, however, was stronger in the energetically favored (*Si*)-selective transition states (ρ_{ICP} = -0.0114

for (*R*,*S*)-**TS188**$_{anti}$ versus -0.0107 for (*S*,*R*)-**TS188**$_{anti}$ as well as ρ_{ICP} = -0.0111 for (*R*,*R*)-**TS188**$_{syn}$ versus -0.0104 for (*S*,*S*)-**TS188**$_{syn}$ kcal/mol).

An array of stabilizing host-guest N^{+}-H•••π_{Ar}-type (highlighted as C, Figure 41) and π_{Ar}•••π_{Ar}, CH_{Ar}•••π_{Ar} (highlighted as D, Figure 41) interactions between the *N*-Boc phenylaldimines and the catalyst quinoline ring systems were also present. Interestingly, the isosurfaces associated with these intermolecular stabilizing interactions were significantly stronger (more negative $(-)\rho_{ICP}$) in the (*Si*)-selective addition modes. As depicted in Figure 41, the ρ_{ICP} values associated with N^{+}-H•••π_{Ar}-type interactions (highlighted as C) were -0.0069 for (*R*,*S*)-**TS188**$_{anti}$ versus -0.0054 for (*S*,*R*)-**TS188**$_{anti}$ as well as ρ_{ICP} = -0.0053 for (*R*,*R*)-**TS188**$_{syn}$ versus -0.0046 for (*S*,*S*)-**TS188**$_{syn}$, while the ρ_{ICP} values associated with π_{Ar}•••π_{Ar}, CH_{Ar}•••π_{Ar} interactions (highlighted as D) were -0.0067 for (*R*,*S*)-**TS188**$_{anti}$ versus -0.0052 for (*S*,*R*)-**TS1**$_{anti}$ as well as -0.0067 for (*R*,*R*)-**TS188**$_{syn}$ versus -0.0045 for (*S*,*S*)-**TS188**$_{syn}$. The higher densities (i.e., $0.005 < \rho(r) < 0.05$ au) associated with these host-guest NCI interactions was consistent with their stronger non-covalent character. These stronger and broader host-guest noncovalent interactions between the catalyst and *N*-Boc phenylaldimine in the energetically favored (*Si*)-enantioface, fixed the geometry of the *N*-Boc phenylaldimine toward attack by the nucleophile.

Further supporting this interpretation, are the QTAIM findings which show that in most cases, there is concentrated charge density at the bond critical points (BCPs) in close proximity to the corresponding NCI interaction critical points associated with these various interactions (Figure 41 and Figure 41A in the Appendix). According to QTAIM,[149] gradient analysis of the electron density scalar field (ρ) identified a (3,-1) critical point that defines a bond path for which the charge density ρ_{BCP}, the properties of the Laplacian of the charge density $\nabla^2\rho(r)$ and its three curvatures at the interatomic critical points were determined. In general, the charge density is

locally concentrated if $\nabla^2\rho(r) < 0$ (covalent bonds), but is depleted when $\nabla^2\rho(r) > 0$ (e.g., for closed shell type interactions such as ionic bonds, H-bonds and van der Waals interactions). In addition, depending on the type of interaction, the second eigenvalue (λ_2) of the electron-density Hessian (second derivative) matrix can be either positive or negative. Accordingly, the related Laplacians ($\nabla^2 \rho(r)$ = 0.01 to 0.04) at these BCPs were all positive, thus suggestive of "closed shell" type interactions. In addition, the negative sign and low value of the second density Hessian eigenvalue (λ_2 = -0.001 to -0.007) confirmed further the van der Waals character of these interactions.[150]

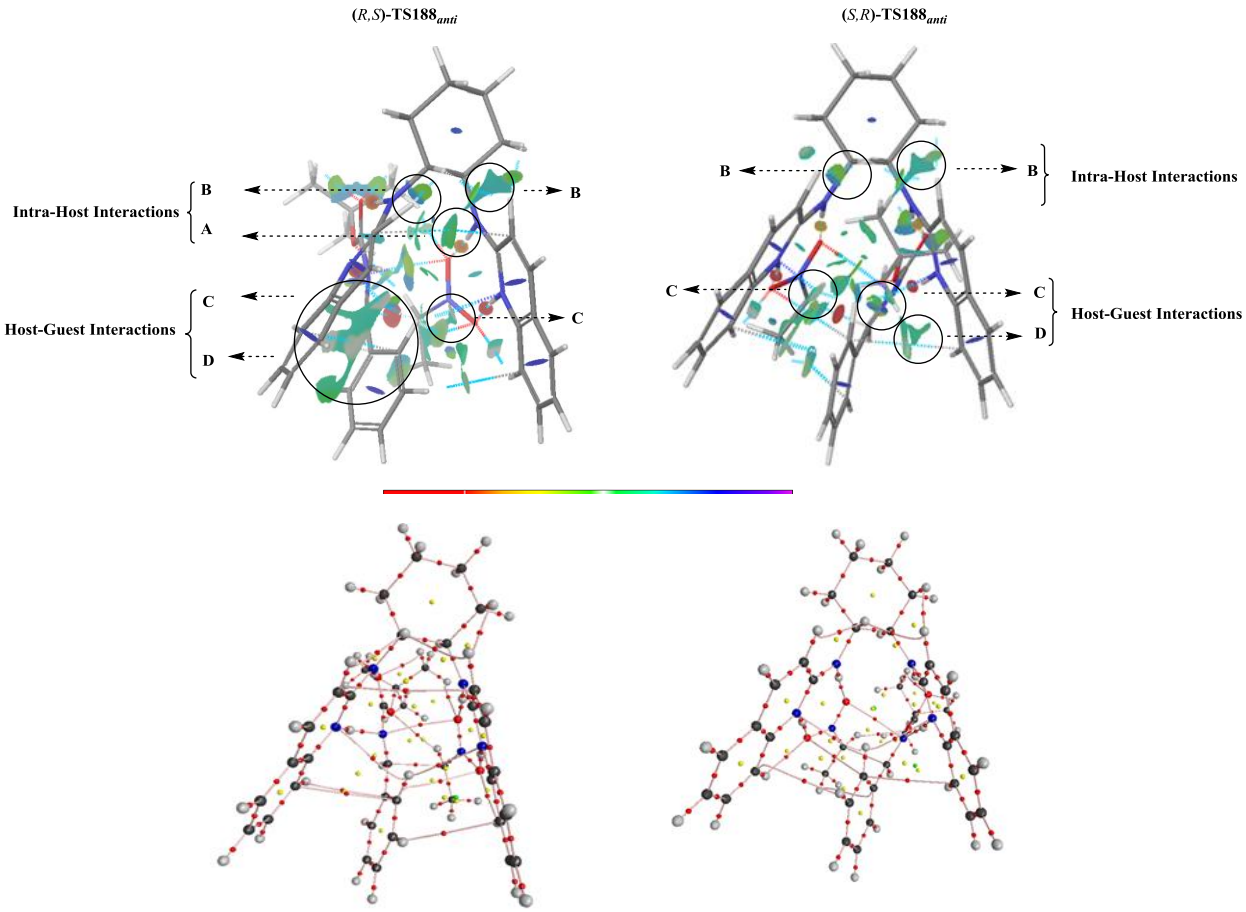

	Non-Covalent Interactions	$(-)\rho_{ICP}$	ρ_{BCP}
(*R*,*S*)-**TS188**$_{anti}$	**Intra-Host**		
	A	-0.0037	0.0037
	B	-0.0114	0.0113
	Host-Guest		
	C	-0.0069	0.0068
	D	-0.0067	0.0072
(*S*,*R*)-**TS188**$_{anti}$	**Intra-Host**		
	A	-0.0107	0.0113
	B		
	Host-Guest		
	C	-0.0054	0.0064
	D	-0.0052	0.0061

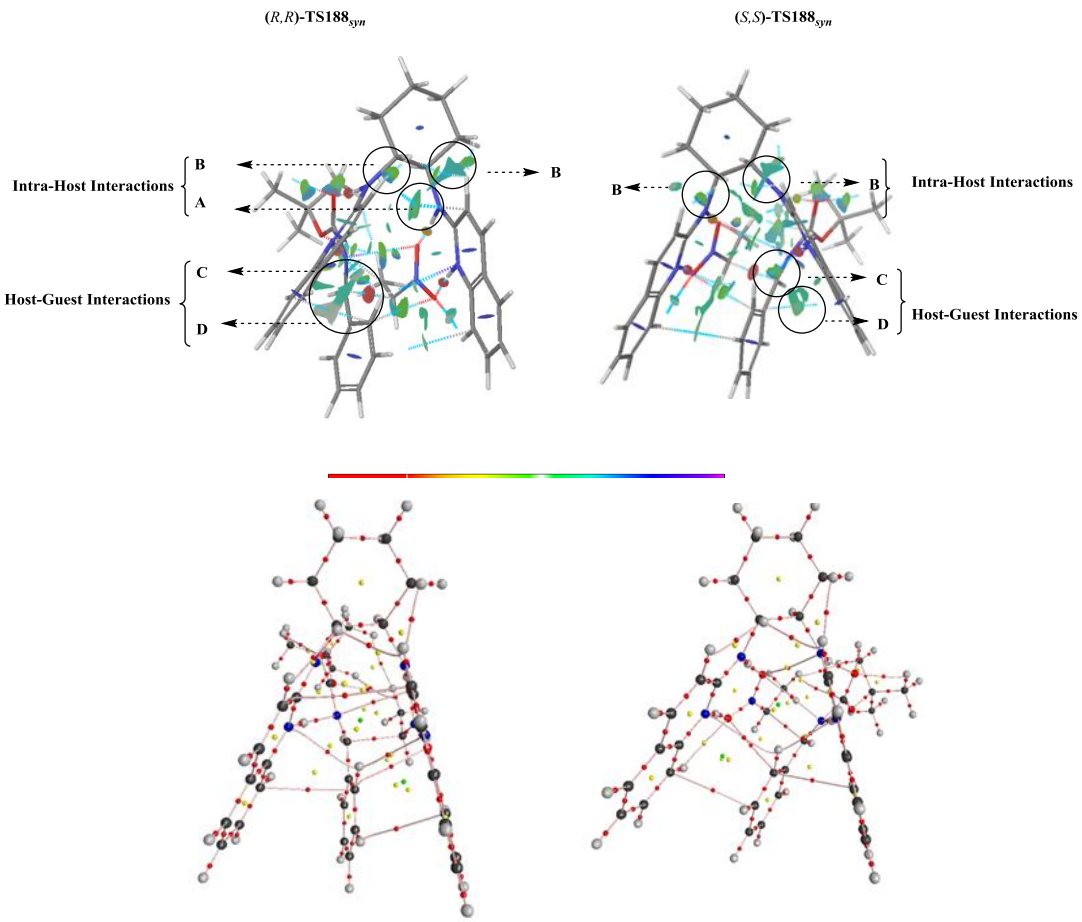

	Non-Covalent Interactions	$(-)\rho_{ICP}$	ρ_{BCP}
(*R*,*R*)-**TS188**$_{syn}$	**Intra-Host** B	 -0.0039 -0.0111	 0.0039 0.0111
	Host-Guest C D	 -0.0053 -0.0067	 0.0056 0.0073
(*S*,*S*)-**TS188**$_{syn}$	**Intra-Host** A B	 - -0.0104	 - 0.0108
	Host-Guest C D	 -0.0046 -0.0045	 0.0068 0.0059

Figure 41. a) B3LYP-D3/6-31G(d,p) gradient isosurfaces with s = 0:5 au representing non-covalent interactions. The surfaces are colored on a rainbow scale based on values of sign(λ_2) between -0.04 to 0.04 au, b) The QTAIM molecular graph showing bond critical points and bond paths were obtained from the B3LYP-D3/6-31G(d,p) electron density.

In a like manner, the substituted transition states, **TS189-TS191**, presented the same intra-host and host-guest stabilizing non-covalent interactions, however, with larger values of $(-)\rho_{ICP}$ (Figure 42-43 and Table 10A in Appendix). Comparison of these enantiodetermining transition states suggests that the electron deficient aldimines within transition state geometry are stabilized through a series of significantly stronger $\pi_{Ar}\bullet\bullet\bullet\pi_{Ar}$ and $CH_{Ar}\bullet\bullet\bullet\pi_{Ar}$ donor–acceptor type non-covalent interactions with the quinoline ring of catalyst.

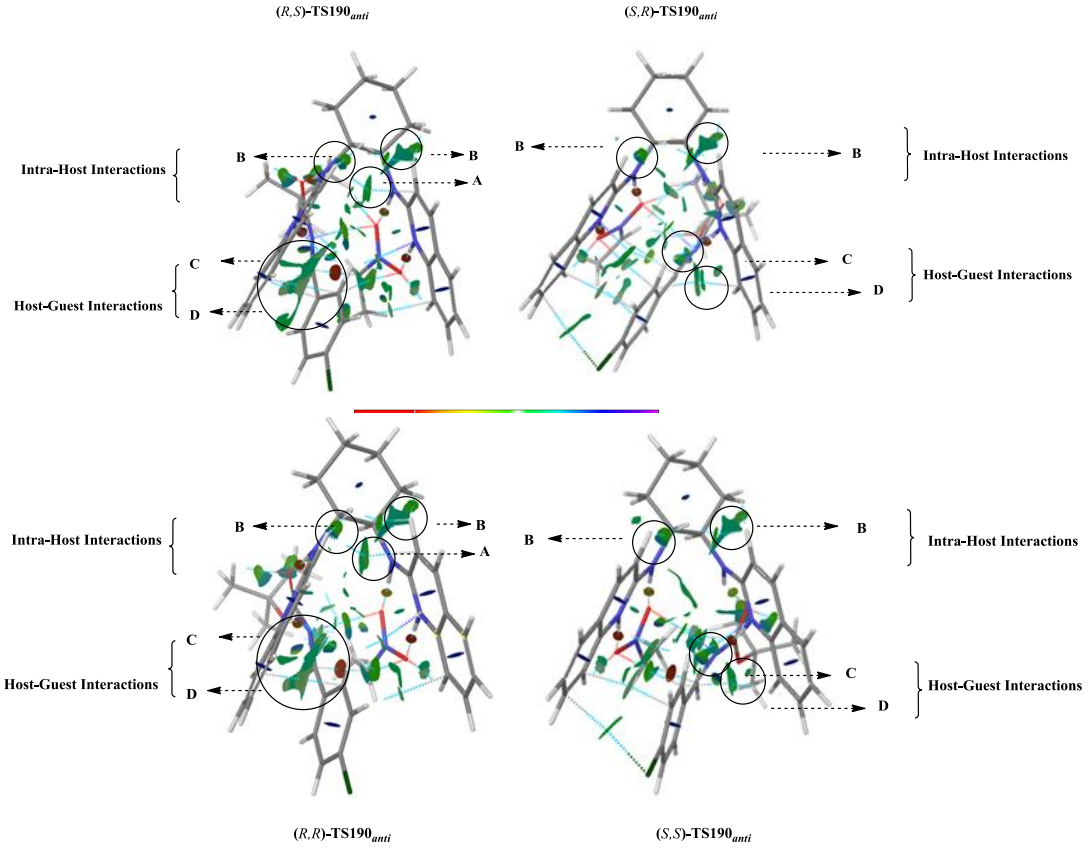

Figure 42. NCI gradient isosurfaces representing the intra-host and host-guest non-covalent interactions in **TS190**.

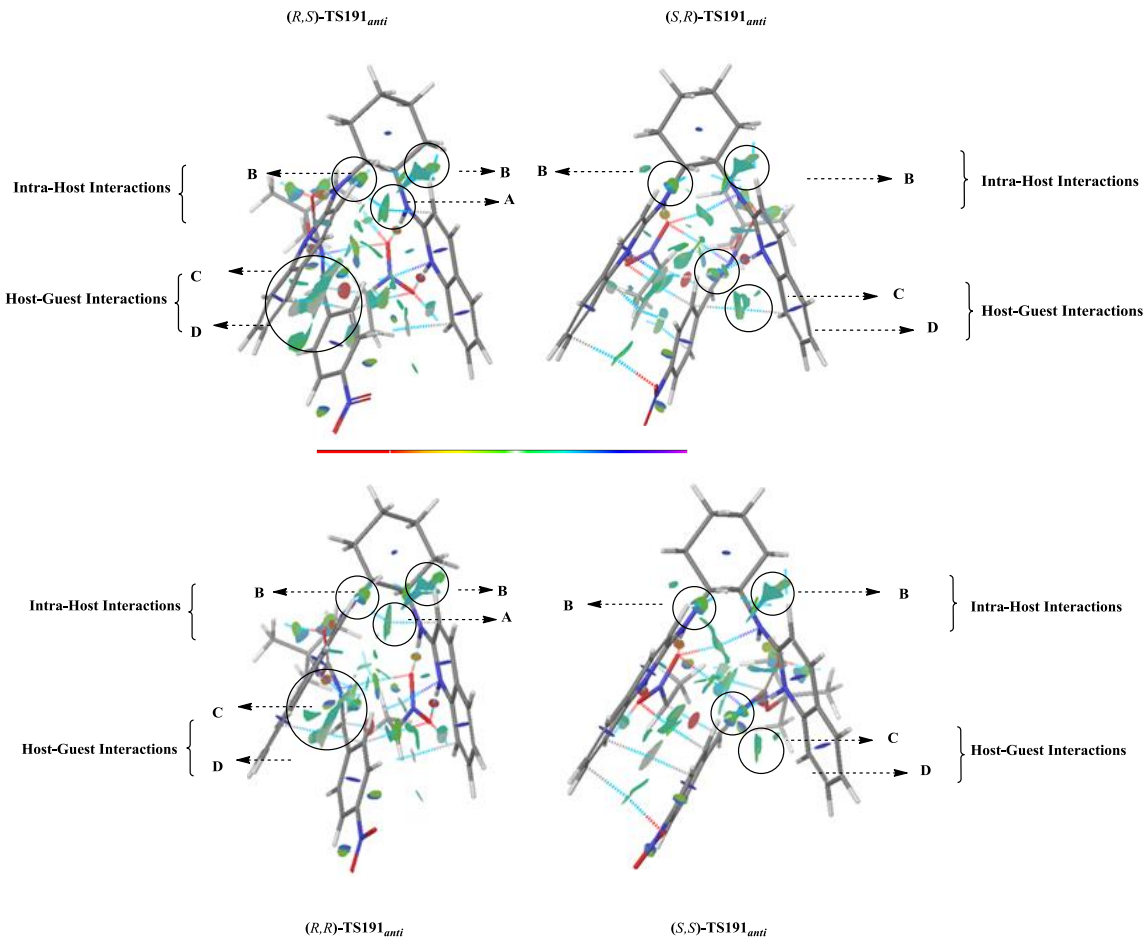

Figure 43. NCI gradient isosurfaces representing the intra-host and host-guest non-covalent interactions in **TS191**.

Taken together, similar to enzymes, the intra-molecular (intra-host) and inter-molecular (host-guest and guest-guest) stabilizing interactions organized HQuin-BAM into a proper closed conformation, selectively shield one face of the electrophile toward attack by nucleophile which in turn make the *Si*-face of the *N*-Boc aldimines available to the nitronate and consequently predicted the observed absolute configuration of the major products. The preference for the transition state leading to product with the (*1R*)-absolute configuration (*Si* enantioface) over the ones with (*1S*)-configuration (*Re* enantioface) at the benzylic carbon was centered around the extent of distortion in the catalyst motif and substrates, the observed positive cooperativity in

host-guest binding, which maximized the strength of key interactions (e.g., hydrogen bonding, stacking type, and orbital interactions) and in turn allow for optimal binding.

2.3. Initial Screening of Counterion Effect (Positive Cooperativity in the Binding of Guest-Host Molecules)

Finally, in an effort to begin understanding the potential influence of the achiral counterion on substrate binding, reactivity and selectivity, the HQuin-BAM-triflate complex that catalyzes the enantioselective *aza*-Henry reaction of nitromethane with *N*-Boc phenylaldimine was considered. A structural analysis of the enantiodeterming C–C bond-forming transition structures complexed with the triflate counterion, **pro-(*R*)-TS174a** and **pro-(*S*)-TS174b**, in the HQuin-BAM catalyzed *aza*-Henry reaction of nitromethane with *N*-Boc phenylaldimine was undertaken. This analysis included a molecular electrostatic potential (MEP) surface map over the optimized structures of **pro-(*R*)-TS174a** and **pro-(*S*)-TS174b** using the ωB97X-D/6-31G(d) method. Generally, these MEP surfaces generated around the transition state structures were used to recognize the reactive sites for electrophilic (areas of high negative charge) and nucleophilic (areas of high positive charge) attack. The MEP was used to identify qualitatively the important sites for triflate counterion interaction, and to see if binding of the counterion to either active site or allosteric site alters the binding affinity of the HQuin-BAM for the substrates (Figure 44). In these surfaces, the blue colours are the most nucleophilic or most positive regions. These plotted electrostatic potential surfaces of the enantiomeric *aza*-Henry transition states predictes that the counterion would bind most favourably to the catalyst backbone, which in turn allows allosteric-like regulation of the catalyst binding site. Ultimately, this cooperative interaction result in improved reactivity and selectivity. It is noteworthy that such cooperative interactions also play an important role in different natural processes such as the allosteric oxygenation of hemoglobin

and protein folding.[151] Notable also, the same scenario in stability of stereodetermining transition states was observed in enantio- and diastereoselective *aza*-Henry reaction of nitroethane with *N*-Boc phenylaldimine (Figure 45). Importantly, our initial investigations showed the cooperative effect of the counterion on energetic aspects of the optimized enantiomeric transition states, however, involvement of counterion did not perturb the proposed bifunctional role of the catalyst and the correct substrate binding alignment (Figure 44, 45).

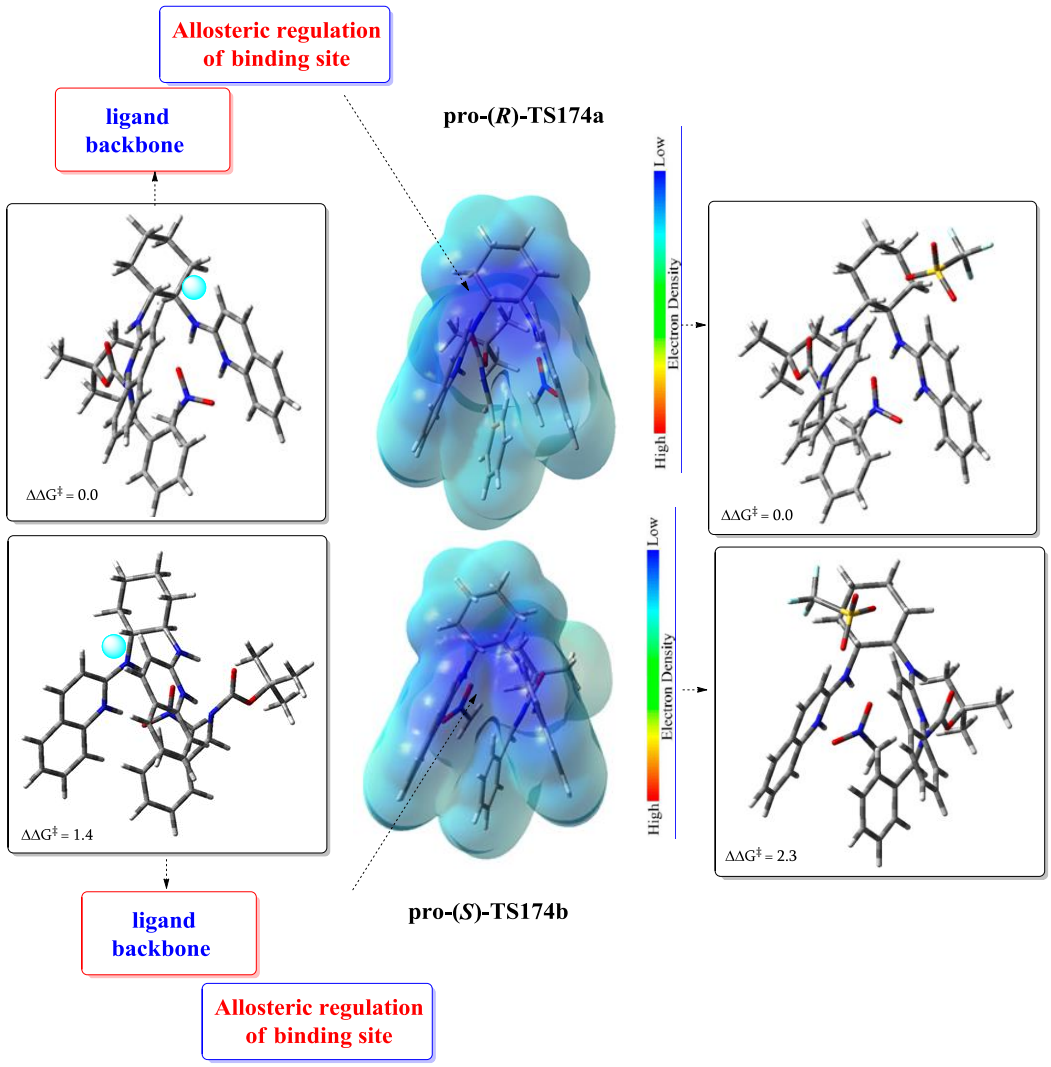

Figure 44. Enantiodetermining transition states without counterion (left) with corresponding Molecular Electrostatic Potential surface (MEP) [Red regions are negative and blue regions are positive (middle)]. Transition state with counterion (right). The blue dot on ligand backbone (left) represents the possible position of counterion.

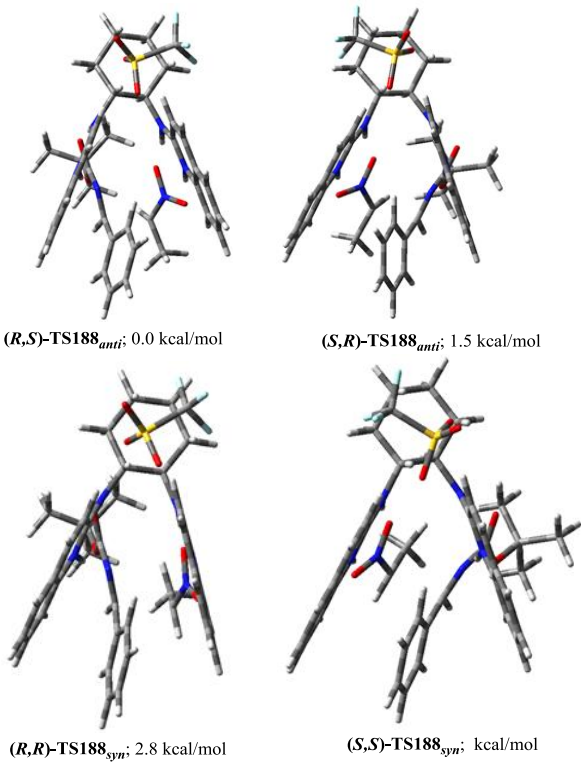

Figure 45. ωB97X-D/6-31G(d) calculated enantiomeric and diastereomeric transition states for addition reaction of monoalkylated nitronate to *N*-Boc phenylaldimine in presence of counterion.

3. Conclusions & Future Work

In this dissertation, a detailed mechanism of the HQuin-BAM catalyzed *aza*-Henry reactions between nitroalkanes and *N*-Boc arylaldimines was studied using density functional theory. Deprotonation of nitroalkane by the catalyst was revealed to be the rate-limiting step, and C–C bond formation was found to be enantiodetermining. The catalyst, in addition to acting as a Brønsted base to generate a nitroenolate, served subsequently as a Brønsted acid to simultaneously activate the electrophile and stabilize the nucleophile through dual H-bonding during C–C bond formation and is thus essential for both reaction rate and selectivity. The

influence of H-bonding in this catalytic system was also investigated through a series of truncated models and the chiral diamine motif. Analysis of the H-bonding interactions revealed that there was a strong preference for the formation of homonuclear (+)CAHB, which in turn governed the relative orientation of substrate binding. Furthermore, a direct correlation between the dihedral angle (θ_{NCCN}) of the reacting substrates and facial selectivity in enantioselective version of this reaction was observed. This relationship was found to be a consequence of optimal secondary interactions and orbital overlap.

To the best of our knowledge, this work presents the first theoretical example of a mechanistic investigation of the HQuin−BAM organocatalyzed *aza*-Henry reactions pioneered by Johnston and coworkers.

Additionally, a DFT-based analysis of the exact origins of enantio- and diastereoselectivity, specifically factors contributing to high π-facial selectivity, in the HQuin-BAM catalyzed *aza*-Henry reactions between nitroethane and electron deficient aldimines was investigated. As experimentally observed, the calculation predicts an enantiomeric excess of 66-95%, in favor of the (*1R,2S*)-configured products with the (*1R*)-absolute configuration at the benzylic carbon and *anti* diastereoselection. There is a fairly reliable correlation between experimentally measured enantioselectivities and those predicted with dispersion inclusive functionals (ωB97X-D and B3LYP-D3). Satisfactory agreement with the experimental enantioselectivities was obtained with these functionals for all substituted transition states. A detailed inspection of the stereodetermining C–C bond-forming transition states for nitronate addition to *N*-Boc arylaldimines, **TS188**-**TS191**, revealed that the origin of enantio- and diastereoselectivity was governed by (1) substrate-based interactions, (2) catalyst-based interactions, and (3) intermolecular catalyst-substrate interactions. All of these controlling factors

originate in whole or in part from donor-acceptor interactions, steric interactions, intra- and intermolecular stabilizing interactions and the distortion of the substrates and catalyst in the transition states, which ultimately lead to the formation of (*1R,2S*)-configured *anti* products. Emerging from this DFT-based study was the finding that the stronger stabilizing host-guest, intra-host and guest-guest interactions in the energetically favoured (*Si*) enantiodetermining transition states, associated with the preferred more closed conformer of the catalyst on binding to substrates with the synclinal attack orientation. The disfavored transition states (*Re* enantioface) with an open conformer of the catalyst was shown to have a more distorted geometry than the favoured ones with a more closed binding pocket. In the favorable (*Si)* enantiofacial mode of nucleophilic addition to aldimines, a synclinal attack orientation for C–C bond formation fits well in the closed binding pocket of the catalyst, which in turn allows effective transmission of catalyst-based chirality to the substrates and highlights the ability of the catalyst to distinguish between (*Si*)- versus (*Re*)-enantiofaces. Mechanistically, the catalyst imposes a specific substrate binding alignment, plays multiple roles in the transformation, imparts a chiral environment, and undergoes geometrical rearrangement on binding to its susbtrates, thus strongly resembling the actions of an enzyme. The insight gained into the effect of different H-bonding modes on the preferred binding arrangement should facilitate future advancements in H-bond based organocatalysis. A priori knowledge of substrate binding alignment to a given catalyst will facilitate computationally based catalyst screening as well as the rational design of future catalysts.

Ongoing efforts in our laboratory are focusing on further exploration of the catalyst structure and its modified derivatives and application of this methodology to other H-bond catalyzed asymmetric transformations. For instance, a comprehensive theoretical study will be

carried out to rationalize how the reactivity and stereoselectivity observed are enhanced by alternative substituents on both substrates and catalyst. Currently, the counterion effect and the electronic and steric parameters of different counterions are being investigated. Further exploration of allosteric regulation by counterions in other H-bond catalyzed asymmetric transformations is underway.

4. Experimental

4.1. HQuin-BAM Catalyzed Enantioselective *aza*-Henry Reaction of Nitromethane and *N*-Boc phenylaldimine

All structures were computed using the Gaussian 09 suite of programs[152] at the ωB97X-D[153]/6-31G(d) level of theory, implementing the integrated equation formalism polarized continuum solvation model (IEFPCM)[140] to account for solvent effects (default solvent parameters for nitromethane were used). All minima were confirmed by the presence of only real vibrational frequencies, and transition states were confirmed to have one imaginary frequency. Thermochemical quantities were evaluated at 253 K, and the IRC methodology was used to obtain the minima on either side of each transition state. Natural bond orbital analysis (NBO) Version 3.1 as implemented in Gaussian 09 was used. For simplicity, the triflate counterion was omitted from these initial calculations.

4.2. A DFT Insight into the Exact Origins of Enantio- & Diastereoselectivity in HQuin-BAM Catalyzed *Aza*-Henry Reaction of Nitroethane with *N*-Boc Arylaldimines

All calculations were performed with the Gaussian 09 suite of programs. Structure analysis, including visualization of imaginary transition state frequencies and Molecular Electrostatic Potential (MEP) surface map, was performed using GaussView v5.0.8.4.

To evaluate the strength and nature of key inter- and intramolecular interactions and their density characteristics, both QTAIM and the non-covalent interactions (NCI) index analysis were applied. A topological analysis of the electron density were carried out with Bader's quantum theory of atoms in molecules (QTAIM) using the AIM2000 software.[154] The non-covalent interactions (NCI) index analysis was performed using Jaguar program and visualized with

Maestro 10.1.[155] QTAIM and NCI analysis were performed at the B3LYP-D3/6-311+G(d,p) using ωB97X-D/6-31G(d)/IEFPCM as input geometries for single-point calculations.

4.3. Selected DFT Calculated Transition state Geometries & Thermochemical Data for *aza*-Henry Reaction of Nitromethane and *N*-Boc phenylaldimine

Uncatalyzed addition of nitronate to aldimine
TS-D172 (synclinal rearrangement)

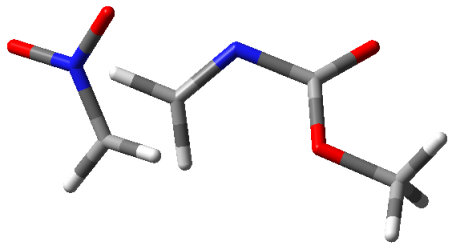

# opt=(calcfc,ts,noeigen) freq=noraman ωB97X-D/6-31g(d) scrf=(iefpcm,so
lvent=nitromethane,smd) geom=connectivity temperature=253

Zero-point correction=	0.123877 (Hartree/Particle)
Thermal correction to Energy=	0.132101
Thermal correction to Enthalpy=	0.132902
Thermal correction to Gibbs Free Energy=	0.092614
Sum of electronic and zero-point Energies=	-566.707877
Sum of electronic and thermal Energies=	-566.699653
Sum of electronic and thermal Enthalpies=	-566.698852
Sum of electronic and thermal Free Energies=	-566.739140

-1 1

C	-1.80003600	-0.61447400	0.11764200
O	-2.75188400	-1.26564600	0.49917800
O	-1.86521500	0.70463200	-0.13705800
N	-0.52440000	-1.14886400	-0.03956500
C	0.19412700	-0.73767500	-1.02835800
C	-3.15242800	1.30189100	0.02488300
H	-3.01187600	2.36404100	-0.17731000
H	-3.86944700	0.87815200	-0.68349500
H	-3.52087600	1.15975400	1.04407700
H	-0.19190500	-0.09057900	-1.81836100
H	1.16861900	-1.19810700	-1.18271800
C	1.82248200	1.15156400	-0.49901800
H	1.24821100	1.87858600	0.05742800
H	2.07402000	1.28435700	-1.54176500
N	2.56749600	0.28720800	0.20770700
O	2.45448400	0.22607800	1.46768900
O	3.33970400	-0.52162000	-0.40052700

Uncatalyzed addition of nitronate to aldimine

TS-D173 (anticlinal rearrangement)

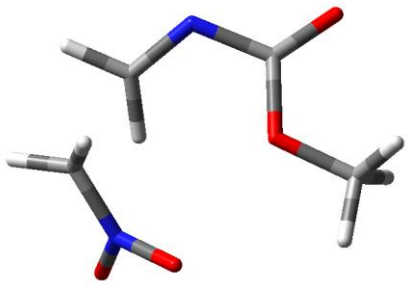

# opt=(calcfc,ts,noeigen) freq=noraman ωB97X-D/6-31g(d) scrf=(iefpcm,so
lvent=nitromethane,smd) geom=connectivity temperature=253

Zero-point correction=	0.123891 (Hartree/Particle)
Thermal correction to Energy=	0.132093
Thermal correction to Enthalpy=	0.132894
Thermal correction to Gibbs Free Energy=	0.092767
Sum of electronic and zero-point Energies=	-566.706242
Sum of electronic and thermal Energies=	-566.698039
Sum of electronic and thermal Enthalpies=	-566.697238
Sum of electronic and thermal Free Energies=	-566.737366

-1 1

C	1.82179100	-0.37841600	-0.05664700
O	3.02886300	-0.22754600	-0.10427100
O	0.95736300	0.64008300	0.06298200
N	1.19737600	-1.61520700	-0.17857800
C	0.04540200	-1.76431500	0.39936900
C	1.50884000	1.94822100	0.14292400
H	0.65043500	2.61961300	0.15880200
H	2.10119600	2.06844600	1.05476700
H	2.13813300	2.16083500	-0.72604200
H	-0.36717800	-1.06665700	1.13128100
H	-0.41261300	-2.74946200	0.33982600
C	-1.98234600	-0.93203100	-0.73821200
H	-2.50076300	-1.76552300	-0.28443700
H	-1.87199200	-0.86502900	-1.81291300
N	-2.08568100	0.24768200	-0.08268600
O	-2.34858300	0.24146700	1.15735300
O	-1.87279400	1.33720800	-0.68069500

Nitroenol adds to a catalyst bound aldimine
TS-A172 (synclinal arrangement)

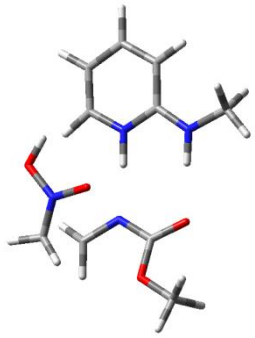

# opt=(calcfc,ts,noeigen) freq=noraman ωB97X-D/6-31g(d) scrf=(iefpcm,so
lvent=nitromethane,smd) geom=connectivity temperature=253

Zero-point correction=	0.289481 (Hartree/Particle)
Thermal correction to Energy=	0.303726
Thermal correction to Enthalpy=	0.304527
Thermal correction to Gibbs Free Energy=	0.250659
Sum of electronic and zero-point Energies=	-910.365693
Sum of electronic and thermal Energies=	-910.351447
Sum of electronic and thermal Enthalpies=	-910.350646
Sum of electronic and thermal Free Energies=	-910.404515

1 1

N	-1.42508300	1.94088200	0.23052300
H	-0.43223500	1.94971100	-0.02146900
C	-1.98030700	3.14497400	0.81855100
H	-2.76166200	3.57575500	0.18297900
H	-2.39798900	2.94907200	1.81177000
H	-1.17173000	3.86987500	0.91685800
C	1.94832600	0.98002400	-0.53253800
O	1.40101500	2.05270800	-0.31168000
O	3.26123500	0.79679200	-0.37234900
N	1.24870700	-0.13258100	-0.95825800
C	1.91412700	-1.23664100	-1.28169900
C	4.01575900	1.93336600	0.06404400
H	3.64043900	2.29681700	1.02325700
H	5.04032600	1.57776700	0.16968000
H	3.96792700	2.73114100	-0.68056700
C	-3.50341900	-1.50846800	-0.68846800
C	-4.18837100	-0.43106900	-0.08770800
C	-3.53805700	0.73414600	0.23432900
C	-2.15170400	0.85572900	-0.03806000
N	-1.52879700	-0.20657300	-0.60883900
C	-2.16911800	-1.35568400	-0.93517400
H	-4.00851600	-2.42959500	-0.94889100
H	-5.24924800	-0.52119200	0.12300300
H	-4.06474900	1.56103500	0.69328000
H	-1.54737600	-2.11632100	-1.39167300
H	-0.49460200	-0.14470800	-0.79806700
H	2.96754200	-1.19470700	-1.55915200
H	1.32373000	-2.01242400	-1.76552100
C	2.35030100	-2.27006500	0.37111000

H	3.21958800	-1.70776000	0.68739500
H	2.44849900	-3.30084500	0.05527400
N	1.24813800	-1.97185000	1.06608700
O	1.00180600	-0.87926600	1.55150600
O	0.21933800	-2.86387900	0.94057000
H	-0.53307200	-2.42146800	1.38454400

Nitroenol adds to a catalyst bound aldimine
TS-A172 (anticlinal arrangement)

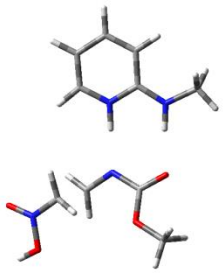

# opt=(calcfc,ts,noeigen) freq=noraman ωB97X-D/6-31g(d) scrf=(iefpcm,so
lvent=nitromethane,smd) geom=connectivity temperature=253

Zero-point correction= 0.289205 (Hartree/Particle)
Thermal correction to Energy= 0.303758
Thermal correction to Enthalpy= 0.304560
Thermal correction to Gibbs Free Energy= 0.249159
Sum of electronic and zero-point Energies= -910.355194
Sum of electronic and thermal Energies= -910.340640
Sum of electronic and thermal Enthalpies= -910.339839
Sum of electronic and thermal Free Energies= -910.395240

1 1

N	-2.70100600	1.31763100	0.01191500
H	-1.75043400	1.68797300	-0.08668000
C	-3.77164600	2.27193400	0.22829400
H	-4.54185300	2.19040400	-0.54601700
H	-4.23923500	2.13667500	1.20977100
H	-3.33799000	3.27122400	0.18254700
C	0.86942600	1.73435400	-0.25417200
O	-0.08291000	2.49091100	-0.09577100
O	2.13550400	2.14068600	-0.10146700
N	0.71240700	0.40823400	-0.57508400
C	1.78513300	-0.31322000	-0.88749500
C	2.32357100	3.51724100	0.24416600
H	3.40186100	3.65420600	0.32088600
H	1.91530800	4.16910700	-0.53144700
H	1.84695100	3.73894800	1.20169400
C	-3.05855900	-2.79650300	-0.01713400
C	-4.20947300	-2.00714800	0.18856500
C	-4.13759000	-0.63592000	0.20523100
C	-2.88383500	-0.00329100	0.01139800
N	-1.80184200	-0.79961500	-0.18504900
C	-1.86826900	-2.15224200	-0.20076000

H	-3.10596100	-3.87779000	-0.03094400
H	-5.17052200	-2.48883100	0.33834100
H	-5.02102100	-0.03090900	0.36547300
H	-0.92450100	-2.65755000	-0.36595800
H	-0.86335100	-0.34752800	-0.33482600
H	2.69361400	0.17596000	-1.24481000
H	1.58301700	-1.29756800	-1.30979100
C	2.54430800	-1.00798900	0.79017500
H	1.73147300	-1.64058500	1.12315600
H	2.78596700	-0.09679200	1.32253600
N	3.60777400	-1.69837100	0.34874100
O	3.61700300	-2.82999000	-0.10306600
O	4.74838900	-0.96118900	0.24555400
H	5.37307200	-1.54874200	-0.22919000

Nitroenol adds to a catalyst bound aldimine
TS-A173 (synclinal arrangement)

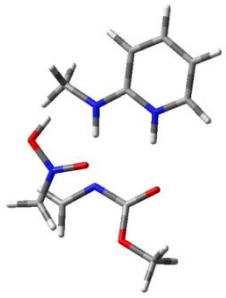

# opt=(calcfc,ts,noeigen) freq=noraman ωB97X-D/6-31g(d) scrf=(iefpcm,so
lvent=nitromethane,smd) geom=connectivity temperature=253

Zero-point correction=	0.290077 (Hartree/Particle)
Thermal correction to Energy=	0.304222
Thermal correction to Enthalpy=	0.305024
Thermal correction to Gibbs Free Energy=	0.251691
Sum of electronic and zero-point Energies=	-910.364853
Sum of electronic and thermal Energies=	-910.350708
Sum of electronic and thermal Enthalpies=	-910.349907
Sum of electronic and thermal Free Energies=	-910.403240

1 1

C	1.73825400	1.20759200	-0.56779200
O	0.85016100	2.05002600	-0.46495900
O	3.01504100	1.48891300	-0.30367300
N	1.47763800	-0.08466200	-0.96723500
C	2.47698900	-0.96040400	-1.03129600
C	3.30206000	2.83129500	0.10448100
H	4.37689300	2.85789700	0.28170800
H	3.03156200	3.53684800	-0.68408100
H	2.76182000	3.07658500	1.02157300
N	-1.25168900	-1.03629900	-0.92937600
H	-0.28220100	-0.70038400	-1.04731200

H	3.51312900	-0.62968500	-1.11083400
H	2.24040900	-1.89900000	-1.52912700
C	2.80144000	-1.73434100	0.77129600
H	3.43915800	-0.96251300	1.18369000
H	3.19510400	-2.72782600	0.59779100
N	1.54299500	-1.67200300	1.22304500
O	0.96627600	-0.63950000	1.52400900
O	0.78768600	-2.78974200	1.01111400
C	-2.14508100	-0.19878100	-0.40376900
C	-4.33244500	0.41726900	0.39974200
C	-2.53832400	1.97310100	0.51301800
C	-3.85115000	1.69354500	0.76055000
H	-5.37371500	0.16728600	0.57624500
H	-2.06725000	2.92173300	0.73843400
H	-4.49445200	2.43699600	1.21300100
C	-1.58794300	-2.36616600	-1.40278400
H	-0.67881800	-2.81743800	-1.80102500
H	-1.96783100	-2.99798200	-0.59218200
H	-2.33857600	-2.32934500	-2.19956000
C	-3.50638500	-0.51794100	-0.17195700
H	-3.87599600	-1.49766000	-0.44662900
N	-1.72613000	1.04647100	-0.05373100
H	-0.74730200	1.33050400	-0.24840700
H	-0.12944000	-2.48913900	1.17694500

Nitroenol adds to a catalyst bound aldimine
TS-A173 (anticlinal arrangement)

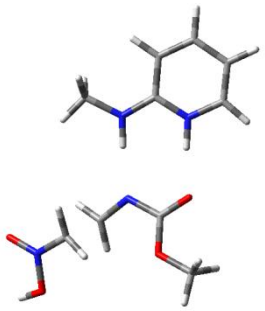

# opt=(calcfc,ts,noeigen) freq=noraman ωB97X-D/6-31g(d) scrf=(iefpcm,so
lvent=nitromethane,smd) geom=connectivity temperature=253

Zero-point correction= 0.289215 (Hartree/Particle)
Thermal correction to Energy= 0.303827
Thermal correction to Enthalpy= 0.304628
Thermal correction to Gibbs Free Energy= 0.248836
Sum of electronic and zero-point Energies= -910.354229
Sum of electronic and thermal Energies= -910.339617
Sum of electronic and thermal Enthalpies= -910.338816
Sum of electronic and thermal Free Energies= -910.394608

1 1

C	0.68445600	1.58542100	-0.11772900

O	-0.41102000	2.11116900	0.07760700
O	1.82464100	2.27852700	-0.02803300
N	0.81709200	0.25603700	-0.40983500
C	1.99663300	-0.20240700	-0.82183400
C	1.70129300	3.67311100	0.27440200
H	2.72185100	4.05173800	0.32419000
H	1.14620200	4.18800300	-0.51313100
H	1.20005700	3.81370400	1.23445800
N	-1.48428100	-1.43519000	0.06389700
H	-0.63738900	-0.85696200	-0.06223700
H	2.72429700	0.47313900	-1.27780900
H	1.98728000	-1.21926500	-1.21557500
C	3.06057800	-0.63467600	0.76504900
H	2.38641200	-1.31098700	1.27469000
H	3.26240300	0.34840500	1.17139100
N	4.12788300	-1.25772000	0.23809300
O	4.20909100	-2.42954100	-0.08564300
O	5.14374700	-0.42530300	-0.12041100
C	-2.67099500	-0.83389700	0.02963100
C	-5.08186900	-0.78650300	0.03769100
C	-3.84959000	1.24362100	-0.07755500
C	-5.06427600	0.62269100	-0.04133100
H	-6.03205700	-1.30999200	0.07006400
H	-3.71826600	2.31694900	-0.13532700
H	-5.97813400	1.20172400	-0.07055700
C	-1.31940500	-2.87376500	0.13807700
H	-0.24913100	-3.08207300	0.17020200
H	-1.78063800	-3.28125700	1.04373000
H	-1.74882800	-3.37537000	-0.73638400
C	-3.91703600	-1.51115300	0.07144000
H	-3.93184500	-2.59207900	0.12891100
N	-2.70068900	0.52397700	-0.04099000
H	-1.80590200	1.05096900	-0.04275200
H	5.76323100	-0.99983900	-0.61722600

Activated nitronate adds to an unactivated aldimine

TS-B172

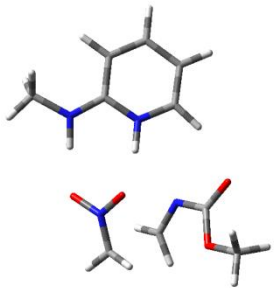

# opt=(calcfc,ts,noeigen) freq=noraman ωB97X-D/6-31g(d) scrf=(iefpcm,so
lvent=nitromethane,smd) geom=connectivity temperature=253

Zero-point correction= 0.276172 (Hartree/Particle)

Thermal correction to Energy=	0.290244
Thermal correction to Enthalpy=	0.291045
Thermal correction to Gibbs Free Energy=	0.237778
Sum of electronic and zero-point Energies=	-909.927108
Sum of electronic and thermal Energies=	-909.913036
Sum of electronic and thermal Enthalpies=	-909.912235
Sum of electronic and thermal Free Energies=	-909.965502

0 1

C	2.41092900	-1.03927500	0.20873200
O	2.04333400	-2.13447400	-0.18499300
O	3.54583600	-0.46829300	-0.23073300
N	1.68720600	-0.29342300	1.12810200
C	2.25391600	0.76198300	1.64307400
C	4.29297900	-1.21880800	-1.18704300
H	5.15136700	-0.59756600	-1.44479300
H	4.63206500	-2.16604600	-0.75947900
H	3.69187900	-1.41584900	-2.07839300
N	-2.59087400	1.27602700	-0.38649800
H	-1.71800500	1.80799400	-0.24935100
H	3.32462500	0.95502900	1.58467700
H	1.69540300	1.30319500	2.40442500
C	2.01397300	2.49858900	0.14433900
H	2.81065000	2.16512100	-0.50373300
H	2.09273700	3.39019900	0.75039600
N	0.78365300	2.10174500	-0.18316200
O	0.63444500	1.14035800	-1.00304800
O	-0.23659800	2.57795600	0.41466300
C	-2.54093400	-0.03688000	-0.15624300
C	-3.49311100	-2.21829600	0.21420800
C	-1.12933500	-1.93210500	0.20467900
C	-2.20167200	-2.76886000	0.34315200
H	-4.36321200	-2.85957900	0.31458000
H	-0.08964800	-2.24001500	0.26659500
H	-2.05074500	-3.82270500	0.53903500
C	-3.83631600	2.01172200	-0.47723000
H	-3.59353600	3.05302800	-0.69263100
H	-4.46214700	1.62697500	-1.28876900
H	-4.40599500	1.97084500	0.45896900
C	-3.67349600	-0.87904900	-0.03179500
H	-4.66424100	-0.45192100	-0.12225200
N	-1.31530800	-0.61306000	-0.04017900
H	-0.48165700	-0.01622800	-0.20946000

Activated nitronate adds to an unactivated aldimine

TS-B173

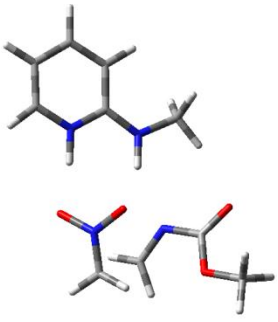

# opt=(calcfc,ts,noeigen) freq=noraman ωB97X-D/6-31g(d) scrf=(iefpcm,so
lvent=nitromethane,smd) geom=connectivity temperature=253

Zero-point correction= 0.275920 (Hartree/Particle)
Thermal correction to Energy= 0.289952
Thermal correction to Enthalpy= 0.290754
Thermal correction to Gibbs Free Energy= 0.237513
Sum of electronic and zero-point Energies= -909.926777
Sum of electronic and thermal Energies= -909.912744
Sum of electronic and thermal Enthalpies= -909.911943
Sum of electronic and thermal Free Energies= -909.965183

0 1

C	2.68440700	-0.94064300	0.16982100
O	2.48240500	-2.08508300	-0.19425000
O	3.70912600	-0.20743100	-0.30085200
N	1.87181100	-0.28756000	1.09068800
C	2.30684700	0.82542300	1.60725500
C	4.55018100	-0.84986000	-1.25709400
H	3.98039200	-1.12867200	-2.14752400
H	5.31358500	-0.11619700	-1.51726000
H	5.01695500	-1.74134100	-0.83025200
N	-2.39242000	0.66483100	-0.13125800
H	-1.55253300	1.29666900	-0.04349100
H	3.34541100	1.14791600	1.54500900
H	1.68303300	1.30291100	2.36025900
C	1.86637300	2.52388400	0.06976200
H	2.69031300	2.26014400	-0.57618100
H	1.85593600	3.42754400	0.66255100
N	0.68565900	1.98357300	-0.22901500
O	0.61219400	0.99228800	-1.00920700
O	-0.37463500	2.37896400	0.38048400
C	-0.73560700	-2.54330400	0.53648100
H	-1.05172900	-3.16195400	-0.31177800
N	-1.01383100	-1.14021900	0.30080300
H	-0.21408300	-0.50916900	0.21070300
H	-1.23980500	-2.90098200	1.44088300
H	0.34313700	-2.64319900	0.65770700
C	-3.59171400	1.24327800	-0.37307800
C	-4.73660400	0.49911300	-0.42235300
H	-5.69108000	0.97091100	-0.61708400
C	-4.62519500	-0.88958500	-0.20274800
H	-5.51507600	-1.51081000	-0.22842500
C	-3.40760000	-1.47409800	0.04315500
H	-3.32243500	-2.54027200	0.20951900
C	-2.23959300	-0.66826900	0.07457500
H	-3.56224300	2.31658000	-0.51722500

Activated nitronate adds to an activated aldimine

TS-C172

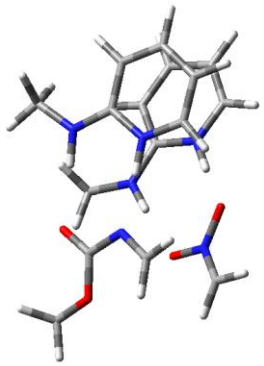

# opt=(calcfc,ts,noeigen) freq=noraman ωB97X-D/6-31g(d) scrf=(iefpcm,so
lvent=nitromethane,smd) geom=connectivity temperature=253

Zero-point correction=	0.427383 (Hartree/Particle)
Thermal correction to Energy=	0.447652
Thermal correction to Enthalpy=	0.448454
Thermal correction to Gibbs Free Energy=	0.381756
Sum of electronic and zero-point Energies=	-1253.136987
Sum of electronic and thermal Energies=	-1253.116718
Sum of electronic and thermal Enthalpies=	-1253.115917
Sum of electronic and thermal Free Energies=	-1253.182614

1 1

C	1.26812900	0.32855800	1.72493500
N	0.63068700	1.50006000	1.69111100
C	2.65672700	0.18206300	1.96456800
H	-0.34996200	1.51692500	1.39869100
N	0.54864800	-0.79784100	1.49210700
N	1.52847300	-0.57933300	-1.52351300
C	1.37083500	0.77089400	-1.53244300
C	2.54161800	1.56952600	-1.56538800
N	0.13009700	1.24782600	-1.47467500
H	-0.64480300	0.57046700	-1.47096400
N	-2.25437900	-0.59457100	1.16043200
C	-2.79007500	0.62331600	0.73354900
O	-2.13403900	1.65302600	0.78636300
O	-4.04993900	0.58270800	0.32178600
C	-4.59321700	1.81213400	-0.17112900
H	0.67186800	-1.18025100	-1.44460200
C	-2.99601800	-1.65304400	1.16693100
H	-4.06854500	-1.62970400	0.98616700
C	-2.81823000	-2.62239700	-1.14096200
H	-3.78175000	-2.25621900	-1.46204400
H	-2.61714500	-3.66283800	-0.93283400
N	-1.77930000	-1.82691300	-1.33315800
O	-0.59080600	-2.23882600	-1.07722700
O	-1.95828800	-0.61130100	-1.67028300
H	-4.05111000	2.12999400	-1.06500700

H	-4.54161100	2.58988300	0.59359600
H	-5.63166200	1.59385900	-0.41793900
H	-2.55856200	-2.57231700	1.54606700
C	-0.17972900	2.66226900	-1.51785500
H	0.15622000	3.11650400	-2.45666500
H	-1.26064800	2.76828600	-1.43586200
H	0.28204000	3.19665900	-0.68148800
C	3.77108900	0.95912600	-1.60197100
C	2.73926600	-1.18375200	-1.56535400
C	3.88896700	-0.44643700	-1.60881600
H	4.85337600	-0.93638600	-1.64009600
H	4.66637000	1.57245900	-1.62438800
H	2.71462500	-2.26641400	-1.55356500
H	2.44766400	2.64811400	-1.56130100
C	1.29689500	2.77072600	1.90160400
H	2.05837500	2.95762200	1.13567900
H	0.54149600	3.55502800	1.84546900
H	1.76789400	2.81097000	2.88912400
C	3.21050000	-1.07443600	1.96410100
C	1.08985900	-2.03947800	1.48872000
C	2.42268700	-2.22004800	1.72557000
H	2.85293300	-3.21303000	1.71685800
H	4.27554800	-1.18352700	2.14200600
H	3.26263100	1.06206100	2.13814000
H	0.39545600	-2.83831300	1.26411100
H	-0.48153900	-0.71342800	1.32324200

Activated nitronate adds to an activated aldimine

TS-C173

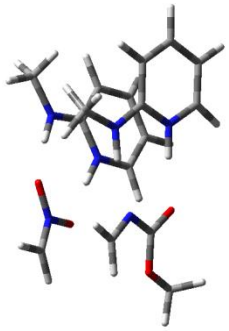

# opt=(calcfc,ts,noeigen) freq=noraman ωB97X-D/6-31g(d) scrf=(iefpcm,so
lvent=nitromethane,smd) geom=connectivity temperature=253

Zero-point correction=	0.427484 (Hartree/Particle)
Thermal correction to Energy=	0.447757
Thermal correction to Enthalpy=	0.448558
Thermal correction to Gibbs Free Energy=	0.382375
Sum of electronic and zero-point Energies=	-1253.135589
Sum of electronic and thermal Energies=	-1253.115316
Sum of electronic and thermal Enthalpies=	-1253.114515

Sum of electronic and thermal Free Energies= -1253.180698

1 1

C	-1.44316400	0.35652700	-1.61829800
N	-1.17714200	-0.95809000	-1.38308300
C	-3.76265200	-0.26076600	-1.85491100
C	-2.13019800	-1.92346600	-1.38210000
C	-2.79495600	0.71160100	-1.86363100
C	-3.43881500	-1.61304000	-1.61246100
H	-3.04154000	1.74781200	-2.05568800
H	-4.79520400	0.01799700	-2.03942100
H	-0.20434800	-1.24927600	-1.18398700
N	-0.43439000	1.21887100	-1.56950000
H	0.51448400	0.85321200	-1.41212500
N	-1.19232200	1.75106200	1.50675000
C	-1.42350600	0.44997700	1.67551400
C	-1.67353700	-2.31466700	2.01733900
C	-2.70651000	-0.12728600	1.84424200
N	-0.35249200	-0.38533500	1.66083000
C	-0.45525400	-1.72419500	1.83663400
C	-2.81532700	-1.48592900	2.01001800
H	-3.58191900	0.50949400	1.83640000
H	-3.79896500	-1.92747100	2.13438500
H	0.60595900	0.02593400	1.52633300
N	2.22648000	0.03257300	-1.37160200
C	2.34866200	-1.23425200	-0.80052000
O	1.37241700	-1.96583500	-0.68217700
O	3.57068000	-1.60052500	-0.44776500
C	3.69880700	-2.89041000	0.16212800
H	-0.23050300	2.03323200	1.27181000
C	3.28438400	0.74702200	-1.56117800
H	4.29615300	0.37159100	-1.42018000
C	3.65758500	1.98077700	0.62897900
H	4.44846500	1.32071900	0.95133000
H	3.82551900	2.99111100	0.28667200
N	2.42060800	1.64457800	0.94971900
O	1.43831600	2.41736400	0.69206700
O	2.19232300	0.47971400	1.43775700
C	-0.57712700	2.64270800	-1.79760700
H	-0.81515000	2.85930700	-2.84502300
H	-1.35640800	3.07051300	-1.16036800
H	0.37223200	3.10864000	-1.53528500
C	-2.24946000	2.73999100	1.44114600
H	-2.93951600	2.53856300	0.61343700
H	-2.81860400	2.77405800	2.37631100
H	-1.78504600	3.71380800	1.28270200
H	-1.77105600	-2.92524000	-1.18347800
H	-4.19497900	-2.38713000	-1.60604500
H	0.48083200	-2.26642000	1.80478400
H	-1.75047500	-3.38567800	2.15253800
H	3.14148400	-2.92002000	1.10138000
H	3.33721200	-3.66969800	-0.51200000
H	4.76376200	-3.01894300	0.35188100
H	3.15894800	1.71496100	-2.03899300

Nitromethane coordinated

INT-1

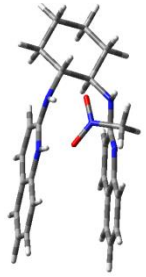

---

opt=calcfc freq=noraman ωB97X-D/6-31g(d) scrf=(iefpcm,solvent=nitrome thane,smd) geom=connectivity temperature=253

Zero-point correction=	0.511413 (Hartree/Particle)
Thermal correction to Energy=	0.531143
Thermal correction to Enthalpy=	0.531944
Thermal correction to Gibbs Free Energy=	0.467380
Sum of electronic and zero-point Energies=	-1392.657757
Sum of electronic and thermal Energies=	-1392.638028
Sum of electronic and thermal Enthalpies=	-1392.637226
Sum of electronic and thermal Free Energies=	-1392.701790

1 1

C	2.90454600	-0.12206400	0.92979800
C	0.59766000	0.65417400	1.48065900
N	-0.26907000	1.53855100	1.01986200
C	-1.12756200	-0.77549900	2.35851000
C	-1.60442200	1.30455800	1.20855200
C	0.19883800	-0.52568400	2.19162300
C	-2.09314400	0.14004300	1.85575900
H	0.94391000	-1.20094600	2.59562200
H	-1.46049600	-1.66767800	2.88216900
H	0.05282700	4.15159900	0.15554300
O	1.52656800	2.63180800	-1.54166600
N	0.37400800	3.04513000	-1.54331300
N	1.93705500	0.91523600	1.27552100
H	2.07609800	1.78502700	0.76985400
O	-0.56968300	2.42067800	-2.00237900
C	0.11924500	4.35612000	-0.91604500
H	-0.81841000	4.74709800	-1.30335900
H	0.96572500	5.00425000	-1.13493000
H	2.52086300	-1.08131100	1.28701300
C	3.10781600	-0.21335900	-0.60202300
H	3.54507800	0.74113300	-0.91745600
C	4.10979500	-1.30598200	-0.98385100
H	3.74241300	-2.29237400	-0.67975700
H	4.22491100	-1.31979400	-2.07257600
C	5.45157100	-1.03988700	-0.29479800
H	5.87601300	-0.10265300	-0.67979000
H	6.15782700	-1.83810800	-0.54677200
C	5.28299200	-0.93688500	1.22311800

H	4.95282300	-1.90797200	1.61703100
H	6.24448800	-0.71118500	1.69697300
C	4.25559800	0.13249600	1.60293400
H	4.61899200	1.12380400	1.29789000
H	4.10599600	0.16117000	2.68735500
N	1.83442300	-0.25275700	-1.33659600
H	1.60111900	0.65303900	-1.73678000
C	0.78961100	-1.06456700	-1.13897000
C	-1.56016300	-2.56466500	-0.72985400
C	0.86044600	-2.37093900	-0.56548100
N	-0.42397000	-0.60229600	-1.49875000
C	-1.60806900	-1.28828100	-1.31770100
C	-0.27928500	-3.08575300	-0.37535200
H	1.82199400	-2.77483700	-0.28453100
H	-0.22350800	-4.07505900	0.06851200
H	-0.48748600	0.35343800	-1.85605300
C	-3.48580500	-0.07157500	1.97683300
C	-4.37635000	0.84725900	1.47293000
H	-5.44550500	0.68200900	1.56358400
C	-3.89499700	2.01025200	0.83271900
H	-4.60197500	2.73354500	0.43629800
C	-2.54394400	2.23712100	0.70285500
H	-2.17698900	3.12760000	0.20440100
H	-3.83680100	-0.97511700	2.46894900
C	-2.77000100	-3.24954200	-0.49398500
C	-3.97239200	-2.66966300	-0.83389700
H	-4.90396200	-3.19285800	-0.64560500
C	-3.99702900	-1.39248100	-1.42595900
H	-4.94831300	-0.93862400	-1.68469000
C	-2.82981800	-0.69989500	-1.67448800
H	-2.84801600	0.28950100	-2.12075600
H	-2.73265200	-4.23343400	-0.03617000

N-Boc-phenylaldimine coordinated
INT-2

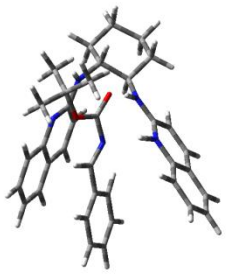

---

opt=calcfc freq=noraman ωB97X-D/6-31g(d) scrf=(iefpcm,solvent=nitrome thane,smd) geom=connectivity temperature=253

Zero-point correction=	0.712173 (Hartree/Particle)
Thermal correction to Energy=	0.739825
Thermal correction to Enthalpy=	0.740627
Thermal correction to Gibbs Free Energy=	0.657451

Sum of electronic and zero-point Energies= -1818.855676
Sum of electronic and thermal Energies= -1818.828023
Sum of electronic and thermal Enthalpies= -1818.827222
Sum of electronic and thermal Free Energies= -1818.910398

1 1

C	3.01849900	1.75226500	0.30485400
C	0.81853900	2.39390700	-0.62000200
N	-0.27525200	1.99120600	-1.29448700
C	-0.32439700	4.45914500	-0.11627400
C	-1.41304100	2.75576500	-1.45549700
C	0.78463900	3.68455500	0.00271800
C	-1.46708200	4.02843800	-0.86121200
H	1.64077400	4.02574000	0.56830400
H	-0.35312900	5.43227900	0.36474100
H	-0.35407400	0.98548900	-1.51037800
N	1.85464600	1.56079800	-0.55627200
H	1.77547800	0.67137200	-1.05845500
C	3.73026600	0.40051700	0.53223600
C	4.82505300	0.58314000	1.59163800
C	5.84571800	1.62934800	1.13119800
C	5.17257500	2.95350400	0.76027400
C	4.04499800	2.74659200	-0.25558300
N	2.86278200	-0.74350500	0.76445800
C	1.75235000	-0.87942900	1.54680100
C	-0.60870200	-1.23026600	2.94936800
C	1.39837100	0.06231700	2.56882400
N	1.02188000	-1.95412900	1.28855600
C	-0.13888500	-2.14276500	1.97002800
C	0.22605500	-0.11542200	3.24079700
H	2.05028100	0.89327300	2.80691600
H	-0.07856800	0.59212000	4.00748100
N	-0.64152300	-0.87357300	-1.11085800
C	-1.74060200	-1.47639500	-0.81994400
C	0.40655500	-1.58461800	-1.72239300
O	1.42942800	-0.98954200	-2.02888100
O	0.16983300	-2.86496700	-1.91794000
C	1.15241300	-3.77892900	-2.52824100
H	2.90679400	-1.45733300	0.05029000
H	2.66113900	2.13635100	1.26608200
H	4.22996100	0.15509000	-0.41236800
H	5.31353400	-0.38248500	1.75797300
H	4.36963700	0.88911200	2.54236200
H	6.37832600	1.23919000	0.25338800
H	6.59488800	1.79026900	1.91411800
H	5.91109900	3.65397300	0.35549800
H	4.75467200	3.41712300	1.66421900
H	3.56291700	3.70217800	-0.48418600
H	4.44495100	2.35089400	-1.19813200
H	-1.91081000	-2.51695600	-1.10390400
C	1.37534300	-3.37643700	-3.98060200
H	0.42317800	-3.34408100	-4.52004700
H	1.86074800	-2.40076000	-4.05423500
H	2.01870500	-4.11965700	-4.46234200
C	2.44280400	-3.78516500	-1.71596700
H	2.22532100	-3.93069800	-0.65332900

H	3.07011400	-4.61523500	-2.05631000
H	3.00153400	-2.85599900	-1.84362600
C	0.44696400	-5.12587500	-2.43316900
H	0.25986500	-5.39096800	-1.38748000
H	-0.50878800	-5.10132600	-2.96629000
H	1.07466200	-5.90169000	-2.88158300
C	-2.81843000	-0.80984100	-0.09614100
C	-4.91703800	0.41499500	1.26859400
C	-4.08977100	-1.39716500	-0.08704500
C	-2.59819500	0.37757400	0.61527900
C	-3.64539600	0.98939200	1.28991800
C	-5.13813700	-0.78075200	0.58660200
H	-4.25158100	-2.33326500	-0.61474600
H	-1.60039500	0.79964400	0.65670700
H	-3.47069500	1.91079700	1.83672400
H	-6.12445400	-1.23369800	0.58449400
H	-5.73598200	0.89501300	1.79613000
C	-2.64310100	4.79407200	-0.99665600
H	-2.68433800	5.77682900	-0.53641500
C	-3.72083800	4.29188100	-1.69396600
H	-4.62873600	4.87769100	-1.79287300
C	-3.64823600	3.01339700	-2.27839000
H	-4.50232300	2.62272600	-2.82249400
C	-2.50767500	2.24464000	-2.16840900
H	-2.44711800	1.25658300	-2.61394600
C	-0.93566900	-3.27276700	1.65442900
H	-0.56956000	-3.96595300	0.90257000
C	-2.14992000	-3.46278500	2.27246700
H	-2.75770000	-4.32499100	2.01249400
C	-2.62477300	-2.54205200	3.23373200
H	-3.59000500	-2.70162500	3.70436700
C	-1.86126900	-1.44744000	3.56902800
H	-2.21203400	-0.73058200	4.30728800

Deprotonation transition state

TS-E1

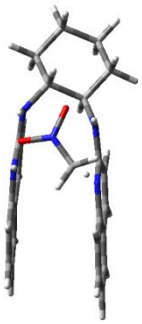

---

opt=(calcfc,ts,noeigen) freq=noraman ωB97X-D/6-31g(d) scrf=(iefpcm,so lvent=nitromethane,smd) geom=connectivity temperature=253

Zero-point correction= 0.506822 (Hartree/Particle)

Thermal correction to Energy= 0.525474
Thermal correction to Enthalpy= 0.526275
Thermal correction to Gibbs Free Energy= 0.464338
Sum of electronic and zero-point Energies= -1392.632581
Sum of electronic and thermal Energies= -1392.613930
Sum of electronic and thermal Enthalpies= -1392.613128
Sum of electronic and thermal Free Energies= -1392.675065

1 1

C	2.66653600	-0.12208100	0.97910900
C	0.28987400	0.56863400	1.37158600
N	-0.65262600	1.42230400	0.96560100
C	-1.39885700	-0.88783600	2.28927900
C	-1.98942000	1.18806600	1.18800300
C	-0.08333500	-0.61559900	2.08881800
C	-2.41164600	0.00587800	1.83327900
H	0.68094800	-1.28105100	2.46871300
H	-1.69159900	-1.79160600	2.81599400
H	-0.37483200	2.35706300	0.12356100
O	2.13980100	2.91621900	-1.01336400
N	1.00301100	2.81197300	-1.50892200
N	1.58190300	0.84969000	1.08177700
H	1.77016500	1.74818600	0.64105600
O	0.82942900	2.11163500	-2.54062400
C	-0.09374600	3.34419700	-0.84683900
H	-0.95578000	3.43455300	-1.50127100
H	0.17474900	4.21784100	-0.25826300
H	2.26618000	-1.10637600	1.23067700
C	3.20839900	-0.17563800	-0.47131600
H	3.66238400	0.79848300	-0.68144300
C	4.30710100	-1.23215800	-0.60568600
H	3.90433500	-2.23052900	-0.39876800
H	4.67230300	-1.23397100	-1.63779300
C	5.44603100	-0.93030100	0.37342600
H	5.91764800	0.02155800	0.09435100
H	6.21550700	-1.70544300	0.29205700
C	4.93523700	-0.83913600	1.81364300
H	4.55958200	-1.82225800	2.12866700
H	5.75515900	-0.57798500	2.49129300
C	3.81036800	0.19080900	1.94626900
H	4.19270300	1.19743400	1.72939500
H	3.41275900	0.20393700	2.96660000
N	2.13199100	-0.26929200	-1.47451900
H	1.99268900	0.60276400	-1.98526400
C	1.00923900	-0.99726400	-1.32841400
C	-1.45667700	-2.30127400	-0.94574600
C	0.96519400	-2.29155800	-0.73091500
N	-0.15040600	-0.46040100	-1.75031200
C	-1.38783200	-1.04284300	-1.56991000
C	-0.23072200	-2.91481500	-0.55336600
H	1.89010200	-2.76376000	-0.43131800
H	-0.26199500	-3.89726600	-0.09229200
H	-0.12569500	0.49159500	-2.13233900
C	-3.79061100	-0.23875900	2.00611400
C	-4.71966400	0.66955100	1.55124100
H	-5.78026900	0.48005000	1.68115100

C	-4.29043500	1.85393400	0.91975500
H	-5.02647000	2.57093400	0.56901900
C	-2.94987600	2.11922800	0.74033300
H	-2.62819700	3.03640400	0.25868500
H	-4.10064500	-1.15526800	2.50037800
C	-2.72410000	-2.87350800	-0.70763300
C	-3.86718200	-2.19712100	-1.07056300
H	-4.84232600	-2.63204000	-0.87856800
C	-3.77580800	-0.93321200	-1.68651700
H	-4.68294500	-0.40172500	-1.95579300
C	-2.55110900	-0.35425800	-1.94484600
H	-2.47156200	0.62320900	-2.41062500
H	-2.77759600	-3.84511100	-0.22596400

Deprotonation transition state

TS-E2

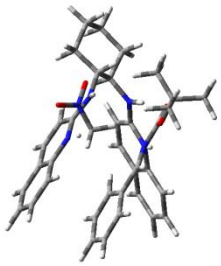

# opt=(calcfc,ts,noeigen) freq=noraman ωB97X-D/6-31g(d) scrf=(iefpcm,so
lvent=nitromethane,smd) geom=connectivity temperature=253

Zero-point correction= 0.760586 (Hartree/Particle)
Thermal correction to Energy= 0.791826
Thermal correction to Enthalpy= 0.792627
Thermal correction to Gibbs Free Energy= 0.701861
Sum of electronic and zero-point Energies= -2063.725057
Sum of electronic and thermal Energies= -2063.693817
Sum of electronic and thermal Enthalpies= -2063.693015
Sum of electronic and thermal Free Energies= -2063.783782

1 1

C	-1.28898100	2.86405100	-1.18073900
C	0.80346500	2.75270100	0.14337400
N	1.41825000	2.12435300	1.16393200
C	2.92998400	3.69022000	-0.49575000
C	2.76730700	2.23083200	1.43853400
C	1.59798100	3.56717100	-0.72636100
C	3.56761500	3.02679500	0.60043200
H	1.11982500	4.09428000	-1.54139600
H	3.53437300	4.31277500	-1.14885100
H	0.88360800	1.39388000	1.65530900
O	-3.61862400	-3.65327400	-1.69818900
N	-3.27019600	-2.71130300	-0.97752400

N	-0.50655500	2.56903500	0.00849300
H	-0.99075200	2.09145500	0.77431300
O	-3.82964300	-1.58558200	-1.07941400
C	-2.25114300	1.69508700	-1.47694000
C	-2.95171200	1.93684000	-2.81881500
C	-3.73207300	3.25460600	-2.77840800
C	-2.83731000	4.43259700	-2.38183900
C	-2.09501800	4.16167200	-1.06918900
N	-1.68715300	0.35195900	-1.33660500
C	-0.58487300	-0.19090900	-1.88768300
C	1.72405200	-1.45847700	-2.86085200
C	0.35561500	0.53684500	-2.68817500
N	-0.35439100	-1.48618700	-1.63274900
C	0.75769800	-2.14417600	-2.09513400
C	1.47367200	-0.08501200	-3.14613000
H	0.16302300	1.56587000	-2.95009500
H	2.18631700	0.46620100	-3.75299700
C	-2.17135200	-2.82769500	-0.12749700
N	-0.20290500	-0.27508500	1.81393100
C	0.17180300	-1.49811600	1.97069400
C	-1.47826700	0.11823400	2.25874400
O	-1.78099500	1.30191800	2.23281300
O	-2.26265300	-0.86191000	2.65688100
C	-3.67040100	-0.64511900	3.06103300
H	-2.37829300	-0.31983900	-0.99320400
H	-0.59848000	2.98609300	-2.01532600
H	-3.01710100	1.72186100	-0.69197900
H	-3.62485100	1.09720100	-3.02140500
H	-2.20115900	1.95985100	-3.61960000
H	-4.54757800	3.15925100	-2.04884200
H	-4.19504300	3.44096200	-3.75337000
H	-3.43285000	5.34689600	-2.28768600
H	-2.09937100	4.61202800	-3.17558800
H	-1.40920000	4.98326200	-0.83616300
H	-2.80537800	4.07607400	-0.23649900
H	-2.28344800	-2.19168100	0.74582100
H	-1.92117600	-3.86699800	0.06652700
H	-0.46827600	-2.22156800	2.48146700
C	-3.69765000	0.16371300	4.35128700
H	-3.10440000	-0.32992700	5.12791000
H	-3.31456500	1.17474800	4.19745500
H	-4.73148200	0.23568900	4.70387800
C	-4.43990700	0.01857800	1.92490700
H	-4.27743500	-0.52038200	0.98485000
H	-5.50864900	-0.01987300	2.16049400
H	-4.15395200	1.06385100	1.79569400
C	-4.16452500	-2.06762800	3.28850300
H	-4.11720400	-2.64658000	2.36009300
H	-3.56215500	-2.57204500	4.05068400
H	-5.20393900	-2.04146500	3.62901600
C	1.45617800	-1.99468600	1.49799700
C	3.91150900	-3.01283600	0.66091900
C	2.29571400	-1.22624100	0.67777400
C	1.84768500	-3.28735100	1.87206000
C	3.07361500	-3.79347800	1.45528400
C	3.52100700	-1.73024200	0.27027400

H	1.97246300	-0.24783500	0.34221500
H	1.18979200	-3.88844900	2.49398700
H	3.37447300	-4.79476000	1.74663800
H	4.16642100	-1.13216000	-0.36494700
H	4.86749500	-3.40913900	0.33184300
C	4.94836500	3.12022000	0.86658800
H	5.56564400	3.73899300	0.22197300
C	5.49899800	2.43059800	1.92570100
H	6.56254600	2.50136600	2.12838300
C	4.68258100	1.63027100	2.74615800
H	5.12408800	1.08777800	3.57617400
C	3.32571700	1.52525100	2.51421500
H	2.68962900	0.90891700	3.14234100
C	0.94802700	-3.50682800	-1.78484400
H	0.20643400	-4.03230400	-1.19302400
C	2.08186200	-4.15087100	-2.22939600
H	2.23010700	-5.19806500	-1.98377800
C	3.05484000	-3.47246000	-2.99185800
H	3.94157900	-3.99982500	-3.32826500
C	2.87488900	-2.14444300	-3.30466200
H	3.61190700	-1.60340500	-3.89162600
H	-1.12881300	-2.11988100	-0.93674400

Activated nitronate adds to an activated *N*-Boc-phenylaldimine
(C-C bond formation transition state)
pro-(*R*)-TS174a

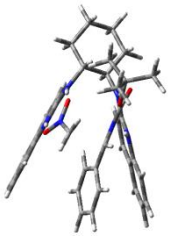

# opt=(calcfc,ts,noeigen) freq=noraman ωB97X-D/6-31g(d) scrf=(iefpcm,so
lvent=nitromethane,smd) geom=connectivity temperature=253

Zero-point correction= 0.764512 (Hartree/Particle)
Thermal correction to Energy= 0.795051
Thermal correction to Enthalpy= 0.795852
Thermal correction to Gibbs Free Energy= 0.705986
Sum of electronic and zero-point Energies= -2063.739404
Sum of electronic and thermal Energies= -2063.708865
Sum of electronic and thermal Enthalpies= -2063.708064
Sum of electronic and thermal Free Energies= -2063.797930

1 1

C	-1.22343600	2.86079600	1.20917600
C	0.22190600	1.02399000	2.07631800
N	0.35436800	-0.31480100	2.15051900

C	2.44637200	1.24110500	2.98433900
C	1.45909000	-0.95416000	2.67481700
C	1.32398700	1.83556700	2.50683300
C	2.55536500	-0.18172500	3.09637500
H	1.24666600	2.91315400	2.45987600
H	3.28338700	1.85407300	3.30598200
H	-0.33340500	-0.88295200	1.61369200
O	-1.89411600	-0.22119200	-2.14000800
N	-1.14673500	-1.12770600	-2.60935500
N	-0.93045200	1.49345700	1.60796900
H	-1.68000700	0.80821400	1.42179100
O	0.02067600	-0.84017700	-3.02926900
C	-1.63138800	2.87378200	-0.28038800
C	-1.95664500	4.29170500	-0.76081000
C	-3.06262600	4.90096700	0.10552200
C	-2.68493100	4.87987000	1.58883300
C	-2.34464700	3.46384600	2.05964700
N	-0.69680500	2.14388100	-1.13570700
C	0.62053000	2.30168200	-1.25935900
C	3.42472500	2.35461600	-1.56837600
C	1.38827200	3.38680100	-0.72120200
N	1.27976500	1.34780700	-1.94532500
C	2.64624100	1.32168100	-2.12026400
C	2.73805900	3.39662400	-0.87209500
H	0.89130800	4.19668300	-0.20774600
H	3.31669300	4.21710800	-0.45804900
H	0.73265500	0.55815600	-2.35232000
C	-1.54314900	-2.40644600	-2.54411300
N	-1.38325400	-1.58228000	0.25782200
C	-1.04955600	-2.69741600	-0.37058100
C	-2.71137500	-1.26996600	0.43396800
O	-3.04888900	-0.30253500	1.11787900
O	-3.57122200	-2.08494100	-0.17106800
C	-5.00677500	-1.79974700	-0.24509100
H	-1.08392100	1.28312100	-1.54643400
H	-0.32727200	3.46532500	1.34550700
H	-2.55367700	2.28598000	-0.35341700
H	-2.26609000	4.24290100	-1.80990300
H	-1.06365600	4.92587800	-0.71342600
H	-3.99049300	4.33185300	-0.04121800
H	-3.26098500	5.92747600	-0.22070300
H	-3.50454300	5.28067500	2.19465200
H	-1.81648000	5.53230400	1.75216800
H	-2.02919800	3.46619100	3.10830200
H	-3.23078200	2.81952800	1.98387600
H	-0.92240100	-3.12320300	-3.06243100
H	-2.60395100	-2.55840900	-2.41032800
H	-1.75077200	-3.52837800	-0.44017200
C	-5.63015500	-1.89670300	1.14325800
H	-5.42432600	-2.87580800	1.58888700
H	-5.24692500	-1.11772000	1.80497300
H	-6.71573900	-1.78080000	1.05822100
C	-5.23360100	-0.43980100	-0.89881700
H	-4.66026300	-0.37082300	-1.82855000
H	-6.29746900	-0.32677600	-1.13164500
H	-4.93336200	0.37664300	-0.23952600

C	-5.52193800	-2.91692400	-1.14629200
H	-5.06281800	-2.85729000	-2.13862600
H	-5.29887400	-3.89762800	-0.71380000
H	-6.60646800	-2.82794700	-1.26242100
C	0.38059100	-3.03997500	-0.49155600
C	3.08206800	-3.74173300	-0.61346700
C	0.75817200	-4.38594600	-0.54906500
C	1.36731000	-2.04767700	-0.51781400
C	2.71143700	-2.39841100	-0.57626200
C	2.10354900	-4.73544600	-0.60151200
H	-0.00739000	-5.15769700	-0.53774600
H	1.07628000	-1.00449200	-0.47357200
H	3.47134800	-1.62313600	-0.58347800
H	2.38890100	-5.78278700	-0.63149400
H	4.13284200	-4.01383200	-0.65211900
C	3.69785600	-0.83596200	3.59967100
H	4.54396400	-0.23725700	3.92447200
C	3.73375600	-2.21217000	3.67282700
H	4.61493900	-2.71484600	4.05777700
C	2.62348100	-2.96875900	3.25282800
H	2.65674700	-4.05199700	3.31590500
C	1.49001500	-2.35448400	2.76091700
H	0.63276700	-2.93242600	2.43080400
C	3.24586900	0.26512400	-2.82443400
H	2.63013900	-0.52978100	-3.23343100
C	4.61872500	0.25285600	-2.96461800
H	5.09050500	-0.56466800	-3.50078100
C	5.41453800	1.27870900	-2.41982600
H	6.49197000	1.24759000	-2.54427100
C	4.82451700	2.31692400	-1.73190000
H	5.42308700	3.11688800	-1.30592600

Activated nitronate adds to an activated *N*-Boc-phenylaldimine
(C-C bond formation transition state)
pro-(S)-TS174b

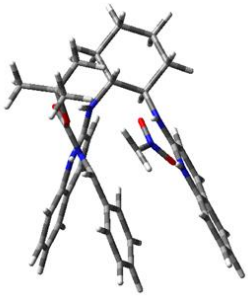

# opt=(calcfc,ts,noeigen) freq=noraman ωB97X-D/6-31g(d) scrf=(iefpcm,so
lvent=nitromethane,smd) geom=connectivity temperature=253

Zero-point correction= 0.765495 (Hartree/Particle)
Thermal correction to Energy= 0.795914
Thermal correction to Enthalpy= 0.796715

Thermal correction to Gibbs Free Energy= 0.706879
Sum of electronic and zero-point Energies= -2063.735425
Sum of electronic and thermal Energies= -2063.705007
Sum of electronic and thermal Enthalpies= -2063.704206
Sum of electronic and thermal Free Energies= -2063.794041

1 1

C	0.01243700	3.36680500	-0.53041300
C	-1.79092500	1.80656200	-1.20755800
N	-2.08189800	0.60963700	-1.74602700
C	-4.14854800	2.15096600	-0.82872000
C	-3.35915500	0.10697500	-1.86773500
C	-2.87683600	2.61869900	-0.73960300
C	-4.44125400	0.87025700	-1.39453000
H	-2.67730200	3.59796100	-0.32646800
H	-4.97154500	2.76262500	-0.47065300
H	-1.29701800	0.02305900	-2.11032600
N	-0.50679800	2.15214800	-1.14170100
H	0.18270300	1.47205900	-1.49337500
H	-0.71588900	3.72293200	0.19970500
C	1.33036000	3.05268400	0.20007200
C	1.85087800	4.29878800	0.92398400
H	1.13424000	4.60476600	1.69610900
H	2.78964500	4.04714200	1.42803200
C	2.06203100	5.44003700	-0.07576700
H	2.86025800	5.15854600	-0.77561600
H	2.40171000	6.33634900	0.45405400
C	0.78312400	5.74070800	-0.86200500
H	0.01872500	6.13001800	-0.17572600
H	0.96994500	6.52001200	-1.60842900
C	0.24231500	4.48530700	-1.55150700
H	0.95194200	4.13055300	-2.31048000
H	-0.70464500	4.69810300	-2.05908800
N	1.26300900	1.85516600	1.03515100
C	0.29656700	1.44746800	1.85755100
C	-1.65312900	0.34504800	3.56734800
C	-0.72268400	2.28108600	2.42158300
N	0.29002900	0.13743600	2.17409400
C	-0.62761500	-0.44715700	3.02055100
C	-1.66305100	1.73547200	3.23599100
H	-0.71283100	3.34407000	2.22663600
H	-2.43351100	2.36875400	3.66602700
N	1.89505800	-1.44056300	0.39304600
C	3.17965400	-0.94655000	0.41202700
O	3.45327000	0.07345600	1.04338400
O	4.06668800	-1.63857400	-0.29978700
C	5.43951300	-1.17069600	-0.51792400
H	2.02345000	1.18327200	0.88986300
C	1.63731800	-2.54409100	-0.28784800
H	2.43414600	-3.24599600	-0.53051700
C	1.82613600	-1.98423400	-2.46452000
H	2.88502300	-1.78797200	-2.38387100
H	1.44315600	-2.84122500	-2.99987800
N	1.02355500	-0.91297200	-2.42085000
O	-0.19055000	-1.02209100	-2.79431900
O	1.44197600	0.16888600	-1.91374700

H	2.06562100	2.78437800	-0.56773000
H	0.91963500	-0.49319100	1.62733200
C	0.27089000	-3.09391000	-0.27806900
C	-2.29180100	-4.20403400	-0.17436100
C	0.08119300	-4.45842000	-0.52423300
C	-0.83964600	-2.28455200	-0.01238300
C	-2.11217400	-2.84081800	0.05418100
C	-1.19350100	-5.01133100	-0.47153300
H	0.94064500	-5.08539100	-0.74830200
H	-0.70096600	-1.22145600	0.14605100
H	-2.96504400	-2.20891400	0.28144100
H	-1.33135800	-6.07264700	-0.65485400
H	-3.28632500	-4.63738900	-0.12341400
C	-0.55037800	-1.82022500	3.30266800
H	0.24922300	-2.41305600	2.86985400
C	-1.50348100	-2.38716400	4.12358200
H	-1.45252400	-3.44930000	4.34191500
C	-2.53661600	-1.60976400	4.68109700
H	-3.27351500	-2.07644400	5.32653000
C	-2.60843000	-0.26063400	4.40924700
H	-3.39704700	0.35382100	4.83367900
C	-3.56589200	-1.15352500	-2.45118300
H	-2.71684700	-1.72927200	-2.80556200
C	-4.85344800	-1.64026200	-2.54648200
H	-5.02078200	-2.61547700	-2.99304200
C	-5.94921500	-0.89294900	-2.07392300
H	-6.95274800	-1.29670500	-2.15958900
C	-5.74562400	0.34680000	-1.50692300
H	-6.58035900	0.93730800	-1.14047200
C	6.00164200	-2.22539400	-1.46456100
H	5.44107000	-2.24148300	-2.40528900
H	7.04893000	-2.00116500	-1.68893600
H	5.94967600	-3.21966800	-1.00937400
C	5.42290200	0.19896600	-1.19090500
H	5.05742000	0.97334400	-0.51436300
H	6.44113300	0.45592500	-1.50071500
H	4.78700300	0.17853500	-2.08263600
C	6.20268100	-1.16637700	0.80209300
H	7.25837100	-0.95078700	0.60763800
H	5.81064700	-0.41034100	1.48515100
H	6.13676900	-2.14829200	1.28271900

Proton Transfer transition state

TS-F

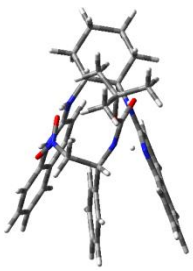

# opt=(calcfc,ts,noeigen) freq=noraman ωB97X-D/6-31g(d) scrf=(iefpcm,so
lvent=nitromethane,smd) geom=connectivity temperature=253

Zero-point correction=	0.765421 (Hartree/Particle)
Thermal correction to Energy=	0.795202
Thermal correction to Enthalpy=	0.796004
Thermal correction to Gibbs Free Energy=	0.709022
Sum of electronic and zero-point Energies=	-2063.764939
Sum of electronic and thermal Energies=	-2063.735157
Sum of electronic and thermal Enthalpies=	-2063.734356
Sum of electronic and thermal Free Energies=	-2063.821338

1 1

C	-0.88939500	2.84089000	1.41950400
C	0.00050200	0.62641500	2.15349200
N	-0.18085000	-0.69817100	2.03278000
C	2.06291100	0.23664700	3.34030700
C	0.68802500	-1.61069800	2.58197000
C	1.16754800	1.12028800	2.82973400
C	1.85451800	-1.17402600	3.24063600
H	1.32224900	2.18556000	2.93858800
H	2.95311600	0.60036300	3.84586600
H	-0.86692500	-1.04403500	1.15574100
O	-1.71702300	0.39012600	-2.43015300
N	-1.05515400	-0.59003900	-2.75105200
N	-0.94418600	1.40616800	1.61654900
H	-1.80431400	0.92537800	1.30044400
O	0.07866600	-0.51339100	-3.21817400
C	-1.02547500	3.16858800	-0.08283800
C	-0.97538400	4.67808100	-0.33988200
C	-2.07976900	5.38281500	0.45213900
C	-1.98363300	5.06113100	1.94496000
C	-2.00550300	3.55119200	2.19468800
N	-0.12409400	2.39249300	-0.94018600
C	1.20549800	2.32698900	-0.94396900
C	3.99882300	1.92997100	-1.04102100
C	2.07332500	3.07672700	-0.08651000
N	1.77803500	1.46892700	-1.81416800
C	3.13568200	1.22932600	-1.90055500
C	3.41483200	2.87242200	-0.13926600
H	1.65675300	3.80283400	0.59517600
H	4.06780800	3.43856200	0.51812900
H	1.17198800	0.93385200	-2.44198200
C	-1.61890200	-1.92052900	-2.47372500
N	-1.64503100	-1.34831800	-0.01618900
C	-1.28764300	-2.34172800	-0.99841900
C	-2.91132200	-0.96165900	0.14123000
O	-3.24806600	-0.05475800	0.92689800
O	-3.81716800	-1.64305500	-0.59997500
C	-5.20506300	-1.22388400	-0.71644400
H	-0.60542600	1.78531200	-1.60073200
H	0.06695100	3.21378900	1.78653300
H	-2.01821100	2.81682200	-0.38490600

H	-1.09380400	4.85612500	-1.41356200
H	0.00039900	5.08248000	-0.04605900
H	-3.05784900	5.05905100	0.07144100
H	-2.01367100	6.46392200	0.29040700
H	-2.80771600	5.53570000	2.48851200
H	-1.05094900	5.47948500	2.34744800
H	-1.88313600	3.33117600	3.26044000
H	-2.97150200	3.13210900	1.88176100
H	-1.17690900	-2.61840400	-3.18247900
H	-2.69471000	-1.83230300	-2.59936900
H	-1.87494000	-3.26465100	-0.89320000
C	-5.91979800	-1.35552300	0.62661200
H	-5.79060800	-2.36691000	1.02777000
H	-5.52977200	-0.63778900	1.34995200
H	-6.99176700	-1.17651900	0.48929300
C	-5.28476300	0.19354400	-1.27918400
H	-4.70911200	0.26366400	-2.20846000
H	-6.32876100	0.43982500	-1.50066100
H	-4.89434400	0.92385000	-0.56788500
C	-5.77529900	-2.22304400	-1.72020900
H	-5.25630100	-2.14542500	-2.68178500
H	-5.66812000	-3.24720800	-1.34754300
H	-6.83892100	-2.02411300	-1.88567900
C	0.18283800	-2.70414300	-0.86705100
C	2.88140800	-3.40675400	-0.57039400
C	0.58584800	-4.03594200	-0.97824900
C	1.15125100	-1.72672800	-0.62589200
C	2.49043200	-2.07267100	-0.47255600
C	1.92589100	-4.38735800	-0.82969900
H	-0.15826100	-4.80693100	-1.16410300
H	0.84748900	-0.69100400	-0.51450500
H	3.22605100	-1.30096400	-0.26507800
H	2.22089700	-5.43000000	-0.90621900
H	3.92463100	-3.68000100	-0.44110900
C	2.76034500	-2.12897900	3.74863000
H	3.65793500	-1.78212900	4.25316700
C	2.50885100	-3.47485100	3.59714400
H	3.21041400	-4.20936200	3.97948700
C	1.33344200	-3.90013400	2.94610300
H	1.13782400	-4.96207200	2.83143200
C	0.42627900	-2.98774800	2.45140100
H	-0.47938600	-3.31183800	1.94948700
C	3.63217400	0.28917400	-2.81472000
H	2.95168800	-0.25088100	-3.46547500
C	4.99213600	0.05755000	-2.85764800
H	5.38386900	-0.67179500	-3.55952300
C	5.87355500	0.74855100	-2.00560500
H	6.93894800	0.55041900	-2.05792000
C	5.38335600	1.67401100	-1.10966900
H	6.04898800	2.21777600	-0.44599100

Activated nitronate adds to an activated *N*-Boc-phenylaldimine

pro-(*R*)-TS174c

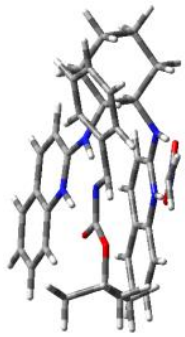

# opt=(calcfc,ts,noeigen) freq=noraman ωB97X-D/6-31g(d) scrf=(iefpcm,so
lvent=nitromethane,smd) geom=connectivity temperature=253

Zero-point correction=	0.766458 (Hartree/Particle)
Thermal correction to Energy=	0.796506
Thermal correction to Enthalpy=	0.797307
Thermal correction to Gibbs Free Energy=	0.710052
Sum of electronic and zero-point Energies=	-2063.736446
Sum of electronic and thermal Energies=	-2063.706399
Sum of electronic and thermal Enthalpies=	-2063.705598
Sum of electronic and thermal Free Energies=	-2063.792852

1 1

C	1.10197200	-2.99290500	1.13301200
C	-0.86243200	-1.68986400	1.85815200
N	-1.22004100	-0.40280200	1.98543500
C	-3.17757900	-2.25243700	1.48969200
C	-2.51854200	0.05033400	1.87612400
C	-1.88677100	-2.65749500	1.61741600
C	-3.54214100	-0.87632800	1.60767600
H	-1.61984000	-3.70353600	1.54631000
H	-3.95678600	-2.98458400	1.30006000
H	-0.46039100	0.30291100	2.06154000
O	0.75093300	1.53892300	1.99423900
N	1.98530700	1.26184200	2.04968900
N	0.44238600	-1.99002800	1.96874200
H	1.06026400	-1.19114000	2.17670200
O	2.36635400	0.07222700	2.24604000
C	1.68766100	-2.29771500	-0.12216000
C	2.39167900	-3.30336300	-1.03686100
C	3.51870800	-3.99002400	-0.26093300
C	2.98132500	-4.67265200	1.00031500
C	2.22711700	-3.68878600	1.89945600
N	0.73047100	-1.39986700	-0.77379000
C	-0.49287600	-1.68396300	-1.23113300
C	-3.17099700	-2.06975700	-2.02017700
C	-0.97903300	-2.99905900	-1.52240400
N	-1.33828000	-0.65072100	-1.39797500
C	-2.65764300	-0.78370600	-1.77291700
C	-2.27100400	-3.17231900	-1.90390500
H	-0.31351200	-3.84466800	-1.42781700

H	-2.63929200	-4.17228800	-2.11326200
H	-1.01191700	0.31396700	-1.17555300
C	2.87164700	2.22323400	1.73626700
N	1.47654400	1.49650000	-0.69604000
C	2.68172900	1.99907100	-0.46843300
C	0.40350500	2.35736900	-0.65155400
O	-0.74603200	1.96460500	-0.86820500
O	0.70278100	3.63029400	-0.40814300
C	-0.28686700	4.70862600	-0.41974200
H	0.94873200	-0.39644400	-0.65544000
H	0.36733000	-3.74209800	0.82897100
H	2.45262800	-1.60517800	0.24597200
H	2.78176100	-2.77906000	-1.91480500
H	1.69076400	-4.06360100	-1.39775500
H	4.27036900	-3.23937700	0.01932900
H	4.01829100	-4.72153500	-0.90487300
H	3.80201000	-5.12881700	1.56402400
H	2.30231400	-5.48510100	0.70797000
H	1.80079100	-4.20197200	2.76745300
H	2.92043800	-2.92524500	2.27786500
H	3.90349700	1.99331200	1.95836000
H	2.49350800	3.23258400	1.81486400
H	2.82940500	3.07714600	-0.48260800
C	-0.88176600	4.84899100	-1.81708200
H	-0.08798500	4.98070700	-2.56014700
H	-1.47638300	3.97314100	-2.08541100
H	-1.52887400	5.73184400	-1.84674500
C	-1.35365200	4.46888700	0.64303300
H	-0.88386500	4.23960800	1.60494500
H	-1.95272200	5.37806000	0.75903500
H	-2.01455700	3.64767000	0.36372500
C	0.55576000	5.92967300	-0.06612000
H	1.00914700	5.81253300	0.92380700
H	1.35428800	6.07441100	-0.80122700
H	-0.07227800	6.82584200	-0.05589500
C	3.88918400	1.19781200	-0.78523700
C	6.20795600	-0.23908200	-1.42779800
C	5.15400400	1.69336100	-0.44215500
C	3.80602500	-0.00409100	-1.49318000
C	4.95801600	-0.72212200	-1.80586600
C	6.30373400	0.97924600	-0.75413500
H	5.23259600	2.64286800	0.08110900
H	2.83938700	-0.36353600	-1.82840000
H	4.87623900	-1.65653300	-2.35335900
H	7.27614200	1.37269400	-0.47344200
H	7.10620400	-0.79953500	-1.66977400
C	-4.86228600	-0.40677400	1.45069500
H	-5.64988900	-1.12340900	1.23779500
C	-5.13509600	0.94002200	1.55402600
H	-6.14943400	1.30287900	1.42424500
C	-4.09685600	1.85181900	1.82490000
H	-4.31781600	2.91172800	1.90452700
C	-2.79718900	1.41953500	1.99222700
H	-1.99314800	2.11713800	2.20009200
C	-3.48107000	0.35105900	-1.85574400
H	-3.06742400	1.33377900	-1.65436500

C	-4.81357000	0.18276900	-2.16990900
H	-5.46107000	1.05254200	-2.22131800
C	-5.34831300	-1.09716200	-2.41394200
H	-6.40082700	-1.20461200	-2.65445100
C	-4.53634700	-2.20820400	-2.34567300
H	-4.93306200	-3.20193000	-2.53151500

Activated nitronate adds to an activated *N*-Boc-phenylaldimine

pro-(*S*)-TS174d

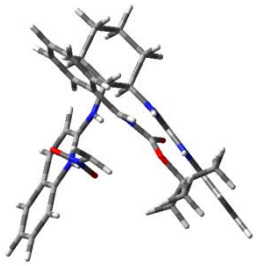

# opt=(calcfc,ts,noeigen) freq=noraman ωB97X-D/6-31g(d) scrf=(iefpcm,so
lvent=nitromethane,smd) geom=connectivity

Zero-point correction= 0.765776 (Hartree/Particle)
Thermal correction to Energy= 0.796306
Thermal correction to Enthalpy= 0.797107
Thermal correction to Gibbs Free Energy= 0.707318
Sum of electronic and zero-point Energies= -2063.728610
Sum of electronic and thermal Energies= -2063.698080
Sum of electronic and thermal Enthalpies= -2063.697279
Sum of electronic and thermal Free Energies= -2063.787068

1 1

C	0.62759200	-1.73276700	-2.45540500
C	2.59820700	-0.38929000	-1.73414600
N	3.00006700	0.77291600	-1.17735700
C	4.88063600	-1.15989600	-1.64163900
C	4.30608200	1.05850000	-0.83400500
C	3.58723900	-1.39666900	-1.97771800
C	5.29205400	0.08052700	-1.05676900
H	3.28802600	-2.32885900	-2.43908500
H	5.63197400	-1.92264000	-1.82352300
H	2.28179800	1.46778700	-0.95714700
N	1.30880900	-0.52043600	-2.01892600
H	0.71599000	0.27034700	-1.74526800
H	1.15568900	-2.59778200	-2.04498200
C	-0.80313800	-1.68651600	-1.88383600
H	-1.28647100	-0.80360800	-2.32093300
C	-1.63068000	-2.90467100	-2.30538900
H	-1.21862700	-3.82176000	-1.87033300
H	-2.64532300	-2.78548200	-1.91119300

C	-1.65027700	-3.03137000	-3.83084900
H	-2.17970600	-2.16958100	-4.25893700
H	-2.21090600	-3.92798200	-4.11602500
C	-0.23077900	-3.08640100	-4.40062200
H	0.27152400	-3.99420700	-4.03970800
H	-0.26208900	-3.15069100	-5.49351600
C	0.58134700	-1.85906400	-3.98098300
H	0.12827000	-0.94796000	-4.39326700
H	1.60542600	-1.91934600	-4.36527400
N	-0.83536100	-1.39829900	-0.45016300
C	-0.30940700	-2.09858500	0.55867000
C	0.73289000	-3.39968800	2.83399300
C	0.32698600	-3.37746600	0.43450700
N	-0.38458900	-1.55362300	1.78365300
C	0.09584500	-2.14940700	2.92700800
C	0.83062600	-3.99051500	1.53763700
H	0.40373200	-3.85272900	-0.53199300
H	1.31644300	-4.95668100	1.43795000
H	-0.83708100	-0.61559400	1.89840500
N	-1.82076900	1.38214000	-0.58733100
C	-0.70740700	2.16290800	-0.38805100
O	0.40423600	1.77303600	-0.75635100
O	-0.91219100	3.33600100	0.19290700
C	0.18862100	4.20786000	0.62050900
H	-1.20572800	-0.46129600	-0.24107700
C	-3.01001000	1.91710600	-0.39883300
H	-3.13014200	2.99895400	-0.35517900
C	-3.30937800	2.02473100	1.90156600
H	-2.77471900	2.95098600	2.05095400
H	-4.38095100	1.95113100	2.01726800
N	-2.61386600	0.89986900	2.11245500
O	-3.16470200	-0.22826100	2.14942000
O	-1.33195200	0.97374300	2.13935800
C	-4.22493800	1.14650500	-0.71574000
C	-6.56198800	-0.24542600	-1.36468500
C	-4.20544000	-0.24742600	-0.84088200
C	-5.42957900	1.83386800	-0.90828500
C	-6.59117500	1.14309900	-1.23405800
C	-5.36854100	-0.93738300	-1.16455300
H	-3.28415800	-0.79104600	-0.67472600
H	-5.45032900	2.91568300	-0.80110700
H	-7.51948900	1.68521200	-1.38749000
H	-5.34310800	-2.01906200	-1.26088700
H	-7.46882200	-0.78630100	-1.61948000
H	-0.55083400	-0.54234900	4.21310200
C	-0.05239700	-1.50553700	4.16703900
C	0.44407500	-2.11889700	5.29818400
C	1.09059500	-3.36860700	5.22379600
H	0.33321700	-1.62953400	6.26084200
H	1.47553200	-3.83017800	6.12719900
C	1.23306200	-4.00047100	4.00797800
H	1.72689400	-4.96488300	3.93291500
C	4.63338800	2.29818900	-0.26566500
H	3.85635100	3.03961000	-0.10204000
C	5.94799400	2.54788800	0.07458000
H	6.20963000	3.50430400	0.51625600

C	6.94949400	1.58321900	-0.14099800
H	7.97643500	1.80144600	0.13280900
C	6.62549300	0.36548700	-0.70041400
H	7.38639000	-0.38993000	-0.87327200
C	0.96104200	4.72049600	-0.59086600
H	0.28149400	5.19889100	-1.30420300
H	1.69022600	5.46694800	-0.25904000
H	1.49569400	3.91572100	-1.09884300
C	-0.54790600	5.35029400	1.31142900
H	0.17196000	6.09521900	1.66379800
H	-1.24243900	5.83744400	0.61948900
H	-1.11290500	4.98007400	2.17317500
C	1.07704500	3.46804600	1.61652600
H	1.77844400	4.17911100	2.06522400
H	0.46415700	3.02762500	2.40863700
H	1.65173300	2.67283900	1.13731700

Activated nitronate adds to an activated *N*-Boc-phenylaldimine
(B3LYP/6-31G(d) calculated C···C bond forming transition states)
pro-(*R*)-TS174a

#opt=(calcfc,ts,noeigen) freq=noraman b3lyp/6-31g(d) scrf=(iefpcm,sol
vent=nitromethane,smd) geom=connectivity temperature=253

---

1 1

C	0.27783200	2.94944400	1.40285400
C	-0.06818000	0.67117500	2.38695200
N	-0.68814000	-0.52437900	2.22489000
C	1.04959500	-0.23236500	4.33492500
C	-0.53756700	-1.59432700	3.08787000
C	0.85356700	0.80947200	3.47683900
C	0.35356600	-1.47189000	4.18257000
H	1.36249500	1.75243100	3.62560300
H	1.73811300	-0.12120800	5.16808700
H	-1.21973700	-0.67632300	1.33998500
O	-0.85496400	0.89156000	-2.51238400
N	-0.57295300	-0.25620900	-2.98158400
N	-0.36780200	1.63943400	1.51566600
H	-1.21369300	1.48633900	0.94404000
O	0.64089500	-0.65176000	-3.05252300
C	0.43248200	3.29855800	-0.10055300
C	1.04321700	4.69660600	-0.30993000
C	0.21811500	5.76562000	0.42118800
C	0.07878300	5.43649500	1.91312800
C	-0.53365100	4.04455600	2.12106200
N	1.08095000	2.23173000	-0.88231700
C	2.32905600	1.75222200	-0.81663300
C	4.90128300	0.56003500	-0.86844400
C	3.38221900	2.25277700	0.01935500
N	2.61384600	0.69264500	-1.61458800
C	3.84728100	0.07444500	-1.68047900
C	4.61560900	1.66977200	-0.01605000
H	3.19407300	3.08969200	0.67501100
H	5.40727700	2.05435700	0.62103700

H	1.84471400	0.28371000	-2.18782300
C	-1.58096500	-1.11097300	-3.27670700
N	-1.96457500	-0.79630400	-0.41234000
C	-2.04163300	-1.84061300	-1.24250600
C	-2.96406300	0.14839900	-0.41372200
O	-2.92723800	1.11639300	0.35817700
O	-3.96631600	-0.06664000	-1.28595900
C	-5.13196000	0.83849400	-1.41122800
H	0.43960200	1.72363800	-1.50863500
H	1.26923000	2.88149900	1.85534000
H	-0.58092500	3.32910400	-0.51659800
H	1.07749800	4.90019700	-1.38634700
H	2.07518300	4.72680500	0.05653300
H	-0.78071100	5.82922200	-0.03319600
H	0.69116800	6.74583500	0.28763200
H	-0.54358000	6.18822700	2.41324900
H	1.06806400	5.47530600	2.39096700
H	-0.58938400	3.79973300	3.18804700
H	-1.56094000	4.02793400	1.73187000
H	-1.29396500	-1.99990700	-3.82062100
H	-2.53929700	-0.64228700	-3.44689500
H	-3.00491700	-2.13294800	-1.65912700
C	-5.91246900	0.86771900	-0.09536800
H	-6.18885200	-0.14850300	0.20818900
H	-5.33068700	1.32918200	0.70460100
H	-6.83502400	1.44246000	-0.23384300
C	-4.67059900	2.22806500	-1.85521200
H	-4.05914700	2.15639900	-2.76150900
H	-5.54696600	2.84472900	-2.08408500
H	-4.08855500	2.72444900	-1.07667600
C	-5.95639200	0.16585600	-2.50986600
H	-5.39119000	0.11480300	-3.44704700
H	-6.23825500	-0.85158400	-2.21769800
H	-6.87215300	0.73805100	-2.69129000
C	-1.04706400	-2.92841500	-1.13727600
C	0.78183900	-5.05065100	-0.94505200
C	-1.39479600	-4.21452200	-1.58558600
C	0.23536800	-2.71609000	-0.60160900
C	1.14109400	-3.77227600	-0.50666500
C	-0.48928700	-5.26956300	-1.48550400
H	-2.38312100	-4.38196600	-2.00745700
H	0.51654900	-1.72325700	-0.26864900
H	2.13080100	-3.59793100	-0.09290700
H	-0.77415500	-6.26126000	-1.82640100
H	1.48974300	-5.87163900	-0.86783800
C	0.50646900	-2.56396000	5.06542000
H	1.18720400	-2.46381700	5.90629000
C	-0.19934000	-3.73525300	4.85757900
H	-0.08039700	-4.57311900	5.53770500
C	-1.07880500	-3.84132200	3.76088300
H	-1.63277000	-4.76227200	3.60334700
C	-1.25312000	-2.78666700	2.87892600
H	-1.93535400	-2.86338200	2.03827400
C	4.04973000	-1.02372500	-2.53627000
H	3.23211600	-1.38893400	-3.15004300
C	5.29852500	-1.62260600	-2.57700000

H	5.45939600	-2.47052200	-3.23643300
C	6.36023200	-1.14989400	-1.77800300
H	7.33016700	-1.63508300	-1.82742700
C	6.16292100	-0.07239500	-0.93390200
H	6.96873900	0.30378300	-0.30974500

Activated nitronate adds to an activated *N*-Boc-phenylaldimine
(B3LYP/6-31G(d) calculated C···C bond forming transition states)
pro-(*S*)-TS174b

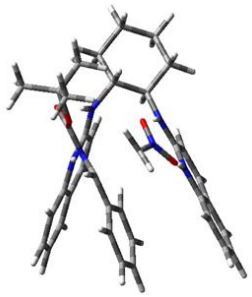

# opt=(calcfc,ts,noeigen) freq=noraman b3lyp/6-31g(d) scrf=(iefpcm,sol
vent=nitromethane,smd) geom=connectivity temperature=253

---

1 1

C	-1.35450500	3.14017800	-0.09868400
C	-2.85969900	1.27377700	-0.78438300
N	-2.95911600	0.07211100	-1.39936500
C	-5.22075000	1.13907100	-0.26304600
C	-4.13268500	-0.65039300	-1.50113300
C	-4.04303000	1.82335400	-0.18718600
C	-5.31564400	-0.12274600	-0.92705400
H	-3.99153300	2.78300600	0.30873500
H	-6.11580900	1.55984100	0.18673600
H	-2.09439800	-0.36344900	-1.79323700
N	-1.66443900	1.87511500	-0.77712200
H	-0.89693900	1.39267400	-1.26524800
H	-1.91909600	3.16907700	0.83770600
C	0.15837800	3.19797900	0.21844900
C	0.51887200	4.49429500	0.96985900
H	0.02283700	4.51205800	1.94770300
H	1.59908700	4.49704000	1.15458300
C	0.10308200	5.72939400	0.15759100
H	0.70714800	5.77890900	-0.75917700
H	0.32280300	6.63732100	0.73199100
C	-1.38434100	5.67823900	-0.21560700
H	-1.99427700	5.75894400	0.69532700
H	-1.64822100	6.53350400	-0.84909600
C	-1.73498500	4.37289400	-0.94444700
H	-1.19790100	4.31792600	-1.90101900
H	-2.80593500	4.33816000	-1.17323100
N	0.69572100	1.97819000	0.83874600
C	0.36356400	1.34943700	1.97258400
C	-0.07539200	-0.13425200	4.34291800
C	-0.55758500	1.82120200	2.96405500

N	0.97327000	0.15553100	2.19278900
C	0.81214800	-0.59750000	3.34001400
C	-0.75984000	1.09632600	4.10264900
H	-1.06513200	2.76359900	2.81610100
H	-1.44839000	1.46552400	4.85769400
N	2.30837300	-0.87136200	-0.25533700
C	3.26089800	0.07511400	-0.55611500
O	3.28111000	1.16503300	0.03127800
O	4.14634500	-0.26604700	-1.51068800
C	5.25904300	0.62138400	-1.92649400
H	1.54433000	1.61479300	0.38546200
C	2.27451400	-2.00380500	-0.96129800
H	3.15000300	-2.31079500	-1.53161600
C	1.39821700	-1.48536200	-2.93333900
H	2.24595500	-0.90651800	-3.26967600
H	1.16835700	-2.44164300	-3.38179800
N	0.33046800	-0.75891300	-2.52819300
O	-0.80738600	-1.33112000	-2.39475800
O	0.49607400	0.44901300	-2.16667200
H	0.67710400	3.22799600	-0.74689300
H	1.52371700	-0.25553000	1.40815200
C	1.37936000	-3.10597700	-0.55723200
C	-0.24545900	-5.26693900	0.20349500
C	1.71370800	-4.41946900	-0.93156600
C	0.20941000	-2.88792500	0.19096500
C	-0.59389600	-3.96332100	0.56965500
C	0.91081200	-5.49287100	-0.55010200
H	2.61349300	-4.59336800	-1.51713700
H	-0.06962300	-1.87687800	0.46414600
H	-1.49606000	-3.78404900	1.14845700
H	1.18649700	-6.50388800	-0.83751600
H	-0.87294500	-6.10263300	0.50172000
C	1.51270400	-1.80578500	3.50744100
H	2.19192400	-2.14532400	2.73204900
C	1.32417400	-2.53845100	4.66819200
H	1.86550400	-3.47063700	4.80152700
C	0.44633800	-2.09140100	5.67724700
H	0.31545900	-2.68097900	6.57944500
C	-0.24392600	-0.90410100	5.51550800
H	-0.92369400	-0.54405000	6.28278400
C	-4.14952800	-1.89055300	-2.16524200
H	-3.23579600	-2.28209000	-2.60136600
C	-5.34219100	-2.59054100	-2.25140200
H	-5.36000100	-3.54797500	-2.76396300
C	-6.52952900	-2.07982100	-1.68740900
H	-7.45240100	-2.64587000	-1.76851600
C	-6.51551900	-0.86113600	-1.03363600
H	-7.42111500	-0.45304500	-0.59342900
C	5.95735400	-0.20510200	-3.00703900
H	5.28163100	-0.40373700	-3.84610100
H	6.82621800	0.34199300	-3.38742200
H	6.30300100	-1.16297800	-2.60351500
C	4.70602800	1.92041200	-2.51583400
H	4.21517800	2.52977300	-1.75521000
H	5.52998000	2.49810500	-2.94956600
H	3.98794500	1.70373000	-3.31477100

C	6.19756600	0.86335800	-0.74241200
H	5.70876500	1.44120400	0.04436000
H	6.53865100	-0.08988000	-0.32268100
H	7.07859200	1.41662000	-1.08617800

Activated nitronate adds to an activated *N*-Boc-phenylaldimine
(M06-2X/6-31G(d) calculated C···C bond forming transition states)
pro-(*R*)-TS174a

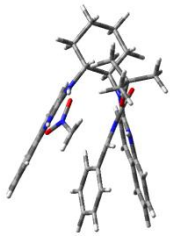

---

opt=(calcfc,ts,noeigen) freq=noraman 6-31g(d) scrf=(iefpcm,solvent=n
itromethane,smd) geom=connectivity m062x temperature=253

---

1 1

C	-1.12594700	2.72852700	1.43218600
C	0.26061600	0.84954200	2.29457800
N	0.45631100	-0.48241700	2.23999300
C	2.33142200	1.05646800	3.51492700
C	1.53486600	-1.13024200	2.80831300
C	1.24620800	1.65491900	2.96109700
C	2.51871900	-0.36309900	3.45924900
H	1.09231000	2.72399900	3.03386200
H	3.07847400	1.65695700	4.02690900
H	-0.18541100	-1.01889000	1.62616100
O	-1.90749800	-0.27155800	-2.25966500
N	-1.11777300	-1.15368200	-2.69523400
N	-0.83737700	1.33095200	1.72639100
H	-1.55399000	0.66208700	1.40109300
O	0.05396900	-0.82642300	-3.07164300
C	-1.69268700	2.79631200	-0.00223100
C	-2.07914900	4.22472100	-0.39864600
C	-3.07299700	4.79947400	0.61411700
C	-2.50150100	4.75329700	2.03224100
C	-2.12835600	3.32310200	2.42435100
N	-0.83783800	2.10670200	-0.97301700
C	0.44836400	2.33698600	-1.24321600
C	3.18457800	2.58259200	-1.89617900
C	1.21111400	3.45644400	-0.76381700
N	1.07706400	1.43959700	-2.02277200
C	2.41032200	1.50562300	-2.36491000
C	2.52737700	3.56094500	-1.08678900
H	0.73220400	4.21463900	-0.16159700
H	3.10301500	4.40923100	-0.72636700
H	0.54499700	0.61453400	-2.39659000
C	-1.46067800	-2.44542700	-2.62972500
N	-1.29711600	-1.49435400	0.11564900
C	-0.94147000	-2.62754000	-0.46752100
C	-2.63940100	-1.21352700	0.25035100

O	-3.02400300	-0.22419300	0.87338100
O	-3.46354900	-2.08765100	-0.32615700
C	-4.90553400	-1.85515600	-0.39610800
H	-1.22516300	1.24298500	-1.37348800
H	-0.19288700	3.29554900	1.48260900
H	-2.61252800	2.19873700	0.00052300
H	-2.51250800	4.19969700	-1.40354400
H	-1.19347400	4.86854500	-0.44043800
H	-4.00222000	4.21506500	0.57983000
H	-3.32702600	5.82741600	0.33662600
H	-3.22436300	5.15598400	2.74878600
H	-1.60674900	5.38837000	2.08444700
H	-1.69245100	3.28654100	3.42864600
H	-3.02547300	2.68916400	2.43127500
H	-0.79231200	-3.14018700	-3.11691500
H	-2.51464800	-2.64229700	-2.50104000
H	-1.62146900	-3.47973400	-0.50036700
C	-5.51017800	-1.88937300	1.00184200
H	-5.23328600	-2.81803100	1.51179400
H	-5.17643200	-1.04002400	1.59976100
H	-6.60134800	-1.85539700	0.92061300
C	-5.18468800	-0.54754300	-1.12734200
H	-6.24895300	-0.49889600	-1.37860800
H	-4.92880900	0.31757100	-0.51324600
H	-4.60030400	-0.50996200	-2.05196400
C	-5.39541400	-3.03937600	-1.21935700
H	-4.96376200	-3.01528500	-2.22539000
H	-5.11668800	-3.98251400	-0.73897700
H	-6.48484300	-3.00194300	-1.30963300
C	0.49827300	-2.93520400	-0.57734400
C	3.21601400	-3.57069200	-0.66113200
C	0.90774700	-4.27208600	-0.63042900
C	1.45926000	-1.91590700	-0.58613400
C	2.81323500	-2.23515700	-0.62981400
C	2.26226200	-4.58915800	-0.66227400
H	0.15783400	-5.06003200	-0.63043500
H	1.13521200	-0.88021100	-0.54725400
H	3.55597100	-1.44209400	-0.63110300
H	2.57488500	-5.62864100	-0.68654200
H	4.27325300	-3.81798700	-0.68493100
C	3.63427700	-1.01739300	4.01942100
H	4.38952700	-0.42116900	4.52372100
C	3.75852500	-2.38730800	3.92047900
H	4.61998900	-2.88929200	4.34815800
C	2.76311900	-3.13881800	3.26641500
H	2.86513800	-4.21720400	3.19179900
C	1.65379600	-2.52624500	2.71741100
H	0.87987300	-3.09859600	2.21394200
C	2.98173900	0.49645300	-3.15986500
H	2.36862300	-0.33289400	-3.50046200
C	4.32237300	0.58362700	-3.47822200
H	4.77466700	-0.19168000	-4.08898200
C	5.11214500	1.65853300	-3.02349000
H	6.16298500	1.70414300	-3.28941800
C	4.55020100	2.64527900	-2.24193600
H	5.14258000	3.48121400	-1.88063700

Activated nitronate adds to an activated *N*-Boc-phenylaldimine
(M06-2X/6-31G(d) calculated C···C bond forming transition states)
pro-(*S*)-TS174b

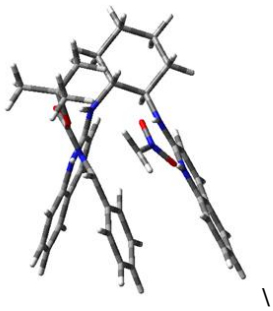

\

---

opt=(calcfc,ts,noeigen) freq=noraman 6-31g(d) scrf=(iefpcm,solvent=n
itromethane,smd) geom=connectivity m062x temperature=253

---

1 1

C	-1.02727300	2.95707900	-1.03150200
C	-2.68084600	1.10075800	-1.04201700
N	-2.88307900	-0.20123000	-1.31222400
C	-4.95596800	1.24181000	-0.25579800
C	-4.07790900	-0.85653000	-1.11043800
C	-3.76717000	1.85765600	-0.48573900
C	-5.15886600	-0.14339100	-0.56009500
H	-3.62127200	2.90836300	-0.26883000
H	-5.78387200	1.80550900	0.16577700
H	-2.08149300	-0.73347800	-1.70865100
N	-1.47581700	1.59430900	-1.30134000
H	-0.77611800	0.95878400	-1.71545200
H	-1.46950100	3.29243200	-0.08606800
C	0.50678400	2.91307800	-0.89294200
C	1.10768900	4.30324000	-0.66435700
H	0.77927400	4.71792100	0.29426200
H	2.19688700	4.20349800	-0.62127000
C	0.68459300	5.25103200	-1.78942500
H	1.10680100	4.89753900	-2.73948500
H	1.09795400	6.24728600	-1.60309900
C	-0.83921300	5.31484100	-1.90721300
H	-1.25973600	5.72858800	-0.98064600
H	-1.13201500	5.98542500	-2.72134500
C	-1.42302500	3.92349400	-2.15205300
H	-1.04452900	3.51973600	-3.10054300
H	-2.51578300	3.96019200	-2.22414500
N	0.95195600	1.89325500	0.05960000
C	0.70770200	1.80806600	1.36977700
C	0.28021800	1.37544300	4.12338400
C	0.05203200	2.80828400	2.16417800
N	1.10425000	0.67860200	1.98179000
C	0.91580900	0.41209500	3.31790100
C	-0.14469200	2.58513400	3.49088700
H	-0.28561000	3.72627800	1.70566800
H	-0.64320300	3.33969900	4.09332200

N	2.14196000	-1.09333700	0.06774700
C	3.39766800	-0.61496300	-0.26210000
O	3.77052600	0.48114300	0.12196700
O	4.11838100	-1.43824900	-1.03739700
C	5.43654400	-1.05246800	-1.53723500
H	1.36116400	1.05966600	-0.36663400
C	1.76166600	-2.29284100	-0.33854400
H	2.49751600	-3.04431900	-0.62885200
C	1.40537400	-2.11464900	-2.51182000
H	2.40079900	-1.73788900	-2.69617700
H	1.09391300	-3.09941200	-2.82941000
N	0.43422600	-1.19720800	-2.42601500
O	-0.78130200	-1.55099100	-2.50030800
O	0.73194200	0.00839400	-2.16608400
H	0.89546900	2.55050600	-1.85248800
H	1.53277700	-0.06289100	1.37082800
C	0.44634500	-2.79405500	0.10213300
C	-2.01183300	-3.76791800	1.00088700
C	0.20728400	-4.17162500	0.14287100
C	-0.56736200	-1.90465800	0.48342900
C	-1.78671500	-2.39202800	0.94260800
C	-1.01696400	-4.65679000	0.59278500
H	0.98979500	-4.85822100	-0.17142000
H	-0.39634300	-0.83349700	0.40184200
H	-2.56620400	-1.69880400	1.24685500
H	-1.19438300	-5.72723500	0.63038500
H	-2.96609100	-4.14590200	1.35624500
C	1.34455500	-0.81183800	3.85801000
H	1.82753100	-1.54149800	3.21421700
C	1.13786900	-1.05454200	5.20078900
H	1.46663400	-1.99707600	5.62740900
C	0.50841200	-0.09947000	6.02455300
H	0.35740300	-0.31330500	7.07738900
C	0.08477100	1.09943200	5.49244000
H	-0.40499600	1.84623300	6.11101700
C	-4.19722500	-2.21796800	-1.43262200
H	-3.34467100	-2.74740600	-1.84951400
C	-5.40200800	-2.85221300	-1.20284700
H	-5.50419600	-3.90484400	-1.44793600
C	-6.49718900	-2.15496800	-0.65570800
H	-7.43428500	-2.67394700	-0.48395300
C	-6.37682000	-0.81809300	-0.33889100
H	-7.21065700	-0.26534500	0.08478500
C	5.84527900	-2.25800300	-2.37326800
H	5.12603300	-2.42467400	-3.18173800
H	6.83162600	-2.08732800	-2.81401600
H	5.89072400	-3.15886600	-1.75326000
C	5.31661000	0.18880600	-2.41351600
H	5.03610900	1.06509100	-1.82724100
H	6.28012200	0.38005500	-2.89644700
H	4.56754900	0.02771100	-3.19668500
C	6.40271700	-0.85360400	-0.37563000
H	6.13414500	0.01957100	0.22062600
H	6.40763100	-1.73994900	0.26736200
H	7.41321900	-0.71309400	-0.77224900

124

Activated nitronate adds to an activated *N*-Boc-phenylaldimine with counterion
(B3LYP/6-31G(d) calculated C···C bond forming transition states)
pro-(*R*)-TS174a+counterion

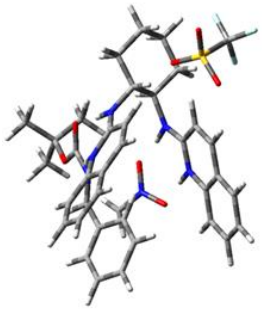

# opt=(calcfc,ts,noeigen) freq=noraman wb97xd/6-31g(d) scrf=(iefpcm,so
lvent=nitroethane) geom=connectivity temperature=253

Zero-point correction= 0.796551 (Hartree/Particle)
Thermal correction to Energy= 0.833730
Thermal correction to Enthalpy= 0.834531
Thermal correction to Gibbs Free Energy= 0.729361
Sum of electronic and zero-point Energies= -3025.113983
Sum of electronic and thermal Energies= -3025.076804
Sum of electronic and thermal Enthalpies= -3025.076003
Sum of electronic and thermal Free Energies= -3025.181173

0 1

C	1.31392200	1.91105500	0.85761200
C	0.10050800	0.02758500	1.92698800
N	-1.12473900	-0.49215100	2.14171700
C	1.06080100	-2.02659300	2.73736100
C	-1.34927400	-1.73816400	2.69318100
C	1.24576500	-0.78099300	2.23174600
C	-0.24493600	-2.55318800	2.99759600
H	2.24305200	-0.38992200	2.06594500
H	1.92551600	-2.64232900	2.96670800
H	-1.91844400	0.00385400	1.68954600
O	-2.27275500	1.69547700	-2.12391600
N	-2.99578000	0.71929300	-2.47678100
N	0.15664100	1.27052000	1.45786800
H	-0.73231200	1.78568900	1.35914300
O	-2.46459700	-0.31960600	-2.98555000
C	0.99745700	2.25342400	-0.61520800
C	2.21211900	2.88767900	-1.30136000
C	2.65290000	4.14264600	-0.54106500
C	2.92865100	3.83585900	0.93352900
C	1.71741300	3.18386600	1.60680100
N	0.40234300	1.14517300	-1.35882800
C	0.88077900	-0.08434300	-1.54555600

C	1.62651700	-2.77315800	-1.95647700
C	2.15496200	-0.55777100	-1.09892600
N	0.08216400	-0.95179800	-2.19801100
C	0.39556700	-2.27570500	-2.42075700
C	2.50008000	-1.85694400	-1.29331200
H	2.83504700	0.10812000	-0.59008700
H	3.46437600	-2.19695300	-0.92458800
H	-0.85132200	-0.62249000	-2.52540200
C	-4.30649000	0.73375000	-2.19498500
N	-3.03939500	0.83227800	0.44791300
C	-4.09059300	0.18091900	-0.02255500
C	-3.09722000	2.19703200	0.61098600
O	-2.16653200	2.81398900	1.13094900
O	-4.21466500	2.77406300	0.17553700
C	-4.36863100	4.22933200	0.10335800
H	-0.55881300	1.31182800	-1.68581900
H	2.15897900	1.22674700	0.90208400
H	0.19614600	3.00176300	-0.59729000
H	1.94802300	3.13074500	-2.33546300
H	3.04196000	2.17384500	-1.33819000
H	1.86554600	4.90502900	-0.61607500
H	3.54769100	4.56103400	-1.01349800
H	3.19783000	4.75374500	1.46649200
H	3.78346100	3.15313400	1.00691600
H	1.94405300	2.92327200	2.64567400
H	0.86737600	3.87991300	1.62200600
H	-4.88923700	-0.07069400	-2.61895700
H	-4.72844600	1.70656300	-1.99427500
H	-5.09001900	0.60748900	0.06059700
C	-4.36847100	4.82858800	1.50706700
H	-5.13429300	4.34878600	2.12502800
H	-3.39628900	4.70891700	1.98665500
H	-4.59978100	5.89648400	1.44119900
C	-3.27962800	4.81757900	-0.79052400
H	-3.23935800	4.27205700	-1.73793300
H	-3.50983400	5.86777300	-0.99564900
H	-2.30097800	4.76018400	-0.31145500
C	-5.74007800	4.38731400	-0.54649500
H	-5.74776200	3.94703700	-1.54854400
H	-6.51150400	3.89957400	0.05727300
H	-5.98690900	5.44927200	-0.63547800
C	-4.00353200	-1.28506200	-0.15627800
C	-3.85155200	-4.06952800	-0.29971000
C	-5.16454500	-2.05987500	-0.06645600
C	-2.76919200	-1.91737000	-0.34213500
C	-2.69330900	-3.30280700	-0.40808200
C	-5.08765300	-3.44678000	-0.13146500
H	-6.12697600	-1.57297100	0.06808400
H	-1.87132000	-1.31464200	-0.41234100
H	-1.72971200	-3.78481200	-0.53847200
H	-5.99156500	-4.04203900	-0.04798500
H	-3.79125900	-5.15258700	-0.34686100
C	-0.47203900	-3.83631100	3.53390600
H	0.38093900	-4.46504100	3.77150300
C	-1.75845400	-4.28116200	3.75082000
H	-1.93139300	-5.26999000	4.16159200

C	-2.85085600	-3.44934900	3.44411900
H	-3.86181700	-3.80418500	3.61570400
C	-2.65785100	-2.18581400	2.92557900
H	-3.49984000	-1.54607200	2.68394200
C	-0.51419300	-3.10976100	-3.08999900
H	-1.46301400	-2.70784500	-3.43036400
C	-0.18470000	-4.43578300	-3.28141900
H	-0.88413200	-5.08853700	-3.79356000
C	1.04018900	-4.95383600	-2.81982200
H	1.27624500	-6.00025300	-2.98009400
C	1.93397700	-4.13259900	-2.16764500
H	2.88265500	-4.51854100	-1.80679900
O	4.18750400	0.51491900	1.32385500
S	5.46347500	-0.10692100	0.91607800
O	6.56562200	0.08134500	1.86295200
O	5.32955700	-1.46092700	0.36103700
C	5.95550900	0.90946100	-0.54471900
F	6.00094700	2.20681000	-0.23039400
F	7.15649100	0.54474900	-0.99528100
F	5.07663000	0.75748000	-1.54526100

pro-(*S*)-TS174a+counterion

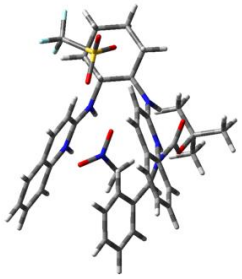

---

opt=(calcfc,ts,noeigen) freq=noraman wb97xd/6-31g(d) scrf=(iefpcm,solvent=nitroethane) geom=connectivity temperature=253

Zero-point correction= 0.796072 (Hartree/Particle)
Thermal correction to Energy= 0.833294
Thermal correction to Enthalpy= 0.834095
Thermal correction to Gibbs Free Energy= 0.728246
Sum of electronic and zero-point Energies= -3025.111185
Sum of electronic and thermal Energies= -3025.073963
Sum of electronic and thermal Enthalpies= -3025.073162
Sum of electronic and thermal Free Energies= -3025.179012

0 1

C	0.65369500	-2.64106600	-0.12566300
C	0.13442300	-0.88820000	1.60771300
N	-0.90371600	-0.17084500	2.08222300
C	1.63524900	0.68481400	2.64387500
C	-0.76548100	0.96380000	2.85403100
C	1.45894800	-0.45680100	1.92908400
C	0.52709000	1.44271300	3.13546100
H	2.31536600	-1.04384200	1.61986200

H	2.64712900	1.02056300	2.85065400
H	-1.84156300	-0.37496600	1.67285800
O	-2.09913100	-1.14027000	-1.97123200
N	-2.83190000	-0.18203900	-2.35193800
N	-0.16899200	-1.95477900	0.86730300
H	-1.15713100	-2.23231100	0.87310500
O	-2.30940400	0.88180400	-2.82115800
C	1.50351400	-1.69454800	-0.99569900
C	2.12006500	-2.48491900	-2.15594900
C	2.97887000	-3.63822900	-1.62711500
C	2.18278400	-4.55128000	-0.69028100
C	1.52904600	-3.76013700	0.44796600
N	0.68985200	-0.57999700	-1.46038000
C	1.04717800	0.70504800	-1.47382500
C	1.58064100	3.47220600	-1.54194500
C	2.27910500	1.21469500	-0.95044700
N	0.17329600	1.58229400	-1.99853400
C	0.38840700	2.94283400	-2.06586800
C	2.51725900	2.55000900	-0.97890100
H	3.00622600	0.55250900	-0.50474500
H	3.44328700	2.92897700	-0.55686900
H	-0.74519100	1.22629400	-2.34694100
C	-4.15782400	-0.23703300	-2.16103800
N	-3.29633600	-0.67228800	0.58405900
C	-4.15312900	0.18503200	0.05536500
C	-3.61884400	-2.00973300	0.62193600
O	-2.84092800	-2.83513000	1.09795000
O	-4.80460300	-2.32299900	0.10167100
C	-5.26438000	-3.70746100	-0.04166500
H	-0.26219000	-0.80333600	-1.78213700
H	3.37599400	-4.21396900	-2.46975200
H	3.83582800	-3.22408900	-1.08499900
H	1.40096000	-5.07060700	-1.26159100
H	2.83686800	-5.32400400	-0.27318200
H	-4.72833300	0.56858300	-2.59943500
H	-4.57510700	-1.22226600	-2.01945900
H	-5.20955200	-0.06823100	-0.02499500
C	-5.43666800	-4.34517800	1.33409700
H	-6.08269500	-3.72312000	1.96184100
H	-4.47472700	-4.47633600	1.83121200
H	-5.91048900	-5.32511800	1.21929200
C	-4.29906600	-4.48599700	-0.93201000
H	-3.33413900	-4.62676300	-0.44316200
H	-4.14410500	-3.95824400	-1.87876500
H	-4.72911400	-5.46792700	-1.15245800
C	-6.61544900	-3.53565000	-0.72945500
H	-6.49526000	-3.05381400	-1.70500100
H	-7.28355700	-2.92361200	-0.11593000
H	-7.08118600	-4.51358500	-0.88195500
C	-3.82142500	1.61959900	0.06096800
C	-3.22670500	4.34383100	0.21280200
C	-4.85037200	2.56732500	0.05637900
C	-2.49172900	2.05182200	0.10483400
C	-2.19693400	3.40592100	0.19770500
C	-4.55403000	3.92355600	0.13291700
H	-5.88484900	2.23701400	0.00669500

H	-1.69497800	1.31760300	0.07641500
H	-1.16328400	3.73047200	0.26114800
H	-5.35732000	4.65351600	0.13927700
H	-2.99589800	5.40226800	0.28470900
C	0.66426000	2.63076400	3.88195600
H	1.66132400	3.00216000	4.09893500
C	-0.45245500	3.30665300	4.32345600
H	-0.34511700	4.22384500	4.89243500
C	-1.73719700	2.80794700	4.03709200
H	-2.61240800	3.34501800	4.38779400
C	-1.90252300	1.64603900	3.31270800
H	-2.89073400	1.26319800	3.07930400
C	-0.58261000	3.78042800	-2.63758900
H	-1.50262100	3.35196900	-3.02114900
C	-0.35167100	5.13971200	-2.67359700
H	-1.09987200	5.79508500	-3.10753900
C	0.83376200	5.68911500	-2.14962000
H	0.99349500	6.76129800	-2.18743900
C	1.78737500	4.86559800	-1.59175500
H	2.70657600	5.27548900	-1.18415100
O	4.27385800	-1.89586000	1.16916300
S	5.24845300	-0.79195900	1.09449800
O	6.45313100	-0.97192700	1.90948400
O	4.64678500	0.55107100	1.14871500
C	5.86555100	-0.90877700	-0.64118600
F	6.40589200	-2.10724700	-0.87257300
F	6.78648800	0.02394600	-0.88572300
F	4.86022500	-0.73574800	-1.51197300
H	-0.08758800	-3.10298200	-0.79029500
H	2.32615900	-1.30651500	-0.39600500
H	1.31490800	-2.86857800	-2.79664200
H	2.72347100	-1.80419000	-2.76451200
H	0.90487100	-4.41392400	1.06555700
H	2.30237500	-3.32737700	1.09215800

Nitroenol adds to a catalyst bound *N*-Boc-phenylaldimine

pro-(*R*)-TS175a

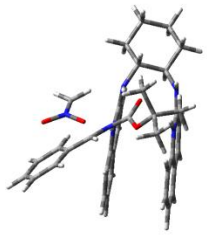

# opt=(calcfc,ts,noeigen) freq=noraman ωB97X-D/6-31g(d) scrf=(iefpcm,so
lvent=nitromethane,smd) geom=connectivity temperature=253

Zero-point correction= 0.766327 (Hartree/Particle)
Thermal correction to Energy= 0.796830
Thermal correction to Enthalpy= 0.797631
Thermal correction to Gibbs Free Energy= 0.707971

Sum of electronic and zero-point Energies= -2063.704867
Sum of electronic and thermal Energies= -2063.674364
Sum of electronic and thermal Enthalpies= -2063.673563
Sum of electronic and thermal Free Energies= -2063.763223

1 1

C	-2.71093800	-2.05865900	-1.69172900
C	-1.81230800	0.29797400	-1.58458700
N	-0.80945600	1.00759400	-1.03266700
C	-3.04040400	2.35469900	-1.86537700
C	-0.86044700	2.36718600	-0.80651100
C	-2.96204600	1.00982700	-2.04691000
C	-2.00168900	3.08243200	-1.21216300
H	-3.76731900	0.47074800	-2.52389800
H	-3.92010000	2.89167400	-2.20739700
H	0.06432000	0.51183900	-0.74929500
N	-1.66076200	-1.03391400	-1.62632800
H	-0.82969000	-1.37494500	-1.13705900
H	-2.16758000	-2.98378400	-1.46628100
C	-3.77534300	-1.89554800	-0.57641700
C	-4.69689100	-3.11387000	-0.55382600
H	-4.10839100	-3.99828300	-0.27391800
H	-5.45967200	-2.96893200	0.21807200
C	-5.34270800	-3.33034000	-1.92534700
H	-5.99699000	-2.47840700	-2.15472000
H	-5.97795300	-4.22190000	-1.89337000
C	-4.28905400	-3.47001000	-3.02731900
H	-3.69381100	-4.37553400	-2.84883300
H	-4.77360300	-3.59070100	-4.00185900
C	-3.35978800	-2.25280700	-3.06437400
H	-3.93914700	-1.36911800	-3.35253300
H	-2.57029100	-2.38442300	-3.81116300
N	-3.10057100	-1.71312700	0.71184900
C	-2.86598100	-0.51230800	1.26756900
C	-2.19601000	1.96430800	2.42609700
C	-3.76266500	0.59379400	1.16554800
N	-1.72852100	-0.33854500	1.95910500
C	-1.33563700	0.85709700	2.53282000
C	-3.43006600	1.78428700	1.73075500
H	-4.70545400	0.46180200	0.65242200
H	-4.11450900	2.62394100	1.65637600
N	1.57612700	-0.41090600	-0.22428000
C	1.17066100	-1.43483500	0.61039200
O	0.09631000	-2.01010400	0.41945200
O	1.98198300	-1.69126600	1.62261700
C	1.94441600	-2.95067300	2.38644100
H	-2.42635600	-2.44290700	0.92882400
C	2.86965400	-0.22464800	-0.33926000
H	3.56068500	-0.75122500	0.32134100
C	3.74576700	-2.14599600	-1.70417300
H	3.04140800	-2.79150900	-1.19957400
H	3.66473100	-1.92443200	-2.75928600
N	4.96581800	-2.02403600	-1.15316400
O	5.90982200	-1.49446300	-1.80393900
O	5.14330300	-2.35160700	0.06485200
H	-4.37570100	-1.00544200	-0.77622500

H	-1.05983400	-1.10798300	1.96728500
C	3.42994700	0.86821700	-1.13102100
C	4.57884000	2.99831900	-2.52227100
C	4.77653500	1.19963000	-0.92985700
C	2.66996200	1.59835300	-2.05718100
C	3.24200300	2.65818800	-2.74594900
C	5.34535100	2.26625200	-1.61965500
H	5.37059400	0.61378400	-0.23601200
H	1.63746100	1.32242600	-2.24514100
H	2.64869000	3.22224500	-3.45923000
H	6.38726500	2.52259000	-1.45377200
H	5.02193000	3.83266300	-3.05816600
C	-0.08595000	0.97107400	3.15856600
H	0.57748700	0.11287900	3.20727100
C	0.28595000	2.19284900	3.68191400
H	1.25507600	2.29262400	4.15996600
C	-0.56857800	3.30809400	3.60226500
H	-0.25451900	4.25748300	4.02281700
C	-1.79355700	3.19582400	2.98144900
H	-2.46057300	4.04863300	2.89891800
C	0.19570200	3.01074500	-0.14190600
H	1.06052600	2.43999400	0.17974400
C	0.09602700	4.36268200	0.11158400
H	0.90394100	4.86496100	0.63420900
C	-1.03929200	5.09607500	-0.28506500
H	-1.09678800	6.15807400	-0.07062300
C	-2.07389400	4.46457900	-0.93912300
H	-2.95829100	5.01333100	-1.24920600
C	3.07861400	-2.75469800	3.38411800
H	2.86542100	-1.91509200	4.05400300
H	3.19691400	-3.65910400	3.98831600
H	4.01757500	-2.55879000	2.85739900
C	0.61167800	-3.12317200	3.10852000
H	-0.19556700	-3.38089400	2.42072000
H	0.71043200	-3.93101800	3.84110900
H	0.34357600	-2.20972700	3.65144800
C	2.25595300	-4.09111600	1.42517400
H	1.46126700	-4.21524200	0.68366200
H	3.20272100	-3.88829300	0.91283900
H	2.34743800	-5.02679700	1.98620100

Nitroenol adds to a catalyst bound *N*-Boc-phenylaldimine

pro-(*S*)-TS175b

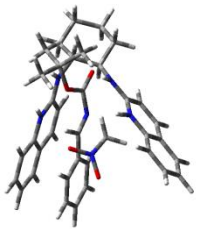

# opt=(calcfc,ts,noeigen) freq=noraman ωB97X-D/6-31g(d) scrf=(iefpcm,so
lvent=nitromethane,smd) geom=connectivity temperature=253

Zero-point correction= 0.766613 (Hartree/Particle)
Thermal correction to Energy= 0.797171
Thermal correction to Enthalpy= 0.797972
Thermal correction to Gibbs Free Energy= 0.709299
Sum of electronic and zero-point Energies= -2063.707311
Sum of electronic and thermal Energies= -2063.676754
Sum of electronic and thermal Enthalpies= -2063.675952
Sum of electronic and thermal Free Energies= -2063.764625

1 1

C	-3.72668500	-0.47207400	-0.47295400
C	-1.80228800	-1.50815200	-1.63979300
N	-0.51147300	-1.33117000	-1.97980300
C	-1.59631600	-3.83421000	-2.23344500
C	0.29858100	-2.33339800	-2.47279600
C	-2.36392500	-2.82027900	-1.75687700
C	-0.23367300	-3.62723100	-2.61779900
H	-3.40048100	-2.97973300	-1.48918100
H	-2.02066200	-4.82874300	-2.33550000
H	-0.06301400	-0.44298200	-1.68253000
N	-2.47214700	-0.44198600	-1.21062400
H	-2.00634700	0.47168900	-1.29884300
H	-3.76850400	-1.40988000	0.08844500
C	-3.75468500	0.72000200	0.50733900
C	-5.00518900	0.66649300	1.39039100
H	-4.99254300	-0.24059700	2.00663800
H	-4.99463400	1.52462500	2.06984600
C	-6.26321600	0.68319900	0.51629200
H	-6.32804600	1.65160700	0.00260800
H	-7.15140000	0.59705300	1.15102700
C	-6.24169200	-0.44019900	-0.52361400
H	-6.29897300	-1.41085000	-0.01267500
H	-7.11926800	-0.37005100	-1.17490100
C	-4.96707800	-0.39676400	-1.37073100
H	-4.92554700	0.53365300	-1.95205000
H	-4.94787600	-1.22867600	-2.08237600
N	-2.50534800	0.92205400	1.24946200
C	-1.81307800	0.07662700	2.01411100
C	-0.15340600	-1.57059700	3.59357500
C	-2.23911300	-1.23807000	2.38049300
N	-0.61002500	0.48921100	2.46058700
C	0.23850000	-0.26690500	3.24499500
C	-1.42641200	-2.02445600	3.13434500
H	-3.20981900	-1.59422200	2.06858800
H	-1.75243800	-3.02420700	3.40535700
N	0.57265600	1.00418700	-0.61389600
C	-0.13416600	2.15129900	-0.92000200
O	-1.25178100	2.08395800	-1.43363100
O	0.46192600	3.29160000	-0.60127800
C	-0.17118600	4.60222600	-0.79285200
H	-2.09118900	1.83675100	1.11314600

C	1.80869900	1.12997000	-0.18285900
H	2.24412100	2.11046300	0.01125600
C	3.13548500	1.73582400	-2.22752100
H	3.20012700	0.93046900	-2.94648100
H	2.42848400	2.54487400	-2.34071400
N	4.25470600	2.00825600	-1.53049400
O	4.27717600	3.01389300	-0.75267900
O	5.23839000	1.21884400	-1.56932800
H	-3.82148500	1.62538000	-0.10564800
H	-0.28389500	1.41285300	2.18371800
C	2.53739400	-0.01389200	0.37078600
C	3.92235000	-2.11945500	1.58519900
C	3.82908300	0.18686700	0.88026300
C	1.94092700	-1.27755800	0.50141400
C	2.62908500	-2.32287900	1.09894500
C	4.51750200	-0.86531200	1.47701400
H	4.28632500	1.16837900	0.80465700
H	0.92416500	-1.43034900	0.16063000
H	2.15301100	-3.29321400	1.20213100
H	5.51712300	-0.70193500	1.86839400
H	4.45616500	-2.93640100	2.06197800
C	1.47119200	0.25433000	3.66267700
H	1.75735400	1.26212200	3.37784400
C	2.30393900	-0.54064200	4.42271900
H	3.26323500	-0.14827700	4.74479100
C	1.93220500	-1.85132900	4.77986000
H	2.60548100	-2.45824300	5.37593400
C	0.71875700	-2.35929400	4.37179600
H	0.41634500	-3.36781100	4.63746900
C	1.63907300	-2.06444100	-2.78601800
H	2.03120800	-1.06118100	-2.65028800
C	2.43426400	-3.09196000	-3.25108800
H	3.47424800	-2.89327400	-3.49014600
C	1.91667200	-4.39047300	-3.41721400
H	2.55936000	-5.18255300	-3.78725800
C	0.60041600	-4.65441500	-3.10484500
H	0.18727200	-5.65201800	-3.22206000
C	0.88304700	5.55668400	-0.24438200
H	1.83061100	5.42933400	-0.77747300
H	0.54699100	6.59064600	-0.36765500
H	1.05604000	5.37170600	0.82082600
C	-0.40615200	4.85031600	-2.27881600
H	-1.14258700	4.15545400	-2.68694700
H	-0.77383100	5.87194900	-2.41895000
H	0.53185200	4.74443700	-2.83423500
C	-1.45393700	4.68026500	0.03019200
H	-2.22965700	4.02456600	-0.36998300
H	-1.25436800	4.40681500	1.07214400
H	-1.82706900	5.70944800	0.01438400

Nitroenol adds to a catalyst bound *N*-Boc-phenylaldimine
pro-(*R*)-TS175c

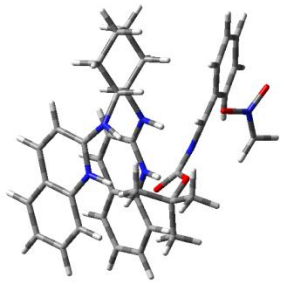

# opt=(calcfc,ts,noeigen) freq=noraman ωB97X-D/6-31g(d) scrf=(iefpcm,so
lvent=nitromethane,smd) geom=connectivity temperature=253

Zero-point correction= 0.765230 (Hartree/Particle)
Thermal correction to Energy= 0.795951
Thermal correction to Enthalpy= 0.796753
Thermal correction to Gibbs Free Energy= 0.707549
Sum of electronic and zero-point Energies= -2063.706205
Sum of electronic and thermal Energies= -2063.675483
Sum of electronic and thermal Enthalpies= -2063.674682
Sum of electronic and thermal Free Energies= -2063.763886

1 1

C	0.32499200	-2.49698400	-0.52708200
C	-1.32080000	-1.40353600	0.99525400
N	-1.63200900	-0.21508000	1.54691400
C	-3.58327900	-2.12555400	1.40900500
C	-2.87233800	0.09986200	2.06629200
C	-2.34117200	-2.40393000	0.93456800
C	-3.89727600	-0.85942100	1.99400600
H	-2.10601300	-3.37472200	0.51913200
H	-4.36090600	-2.88166000	1.35571300
H	-0.96876600	0.55835400	1.42073400
O	6.42146600	1.15465600	0.75177400
N	5.41712800	1.82033200	0.36828400
N	-0.08383800	-1.55749600	0.51519000
H	0.57182200	-0.79240600	0.71191900
O	5.16306700	1.91354000	-0.87944100
C	0.87263700	-1.70472300	-1.73850000
C	1.25861100	-2.64907200	-2.87735600
C	2.30678600	-3.65172500	-2.38478600
C	1.80367600	-4.43169600	-1.16719700
C	1.38060300	-3.48935100	-0.03787000
N	-0.00838200	-0.58664000	-2.12988900
C	-1.35562500	-0.61120000	-2.07784600
C	-4.14780000	-0.56539500	-1.74988000
C	-2.14183900	-1.72829000	-2.47991900
N	-1.99118400	0.46739300	-1.58982300
C	-3.35743300	0.54665600	-1.40559900
C	-3.49240800	-1.69855100	-2.31291400
H	-1.65110800	-2.58338800	-2.92370100
H	-4.09062400	-2.55426200	-2.61124900
H	-1.42185100	1.22018400	-1.18945000

C	4.56598300	2.34639600	1.26134200
N	1.58572800	0.89245900	0.92940700
C	2.80594700	0.59067300	0.55608800
C	0.93865200	1.92156100	0.28189700
O	-0.29717200	1.93709700	0.21775900
O	1.72965200	2.85426300	-0.20644200
C	1.29072000	3.93524900	-1.10295500
H	0.41055400	0.32115800	-1.96875500
H	-0.55545000	-3.06125800	-0.84371000
H	1.78724100	-1.20310300	-1.40462500
H	1.64645700	-2.05627000	-3.71175000
H	0.37479100	-3.18897200	-3.23781400
H	3.22329300	-3.10978300	-2.11397800
H	2.56784300	-4.33996600	-3.19547200
H	2.58298500	-5.10989400	-0.80347500
H	0.94780300	-5.05421400	-1.46187000
H	0.97214000	-4.04856200	0.81023900
H	2.25150000	-2.93071800	0.32289500
H	3.83680200	3.05369600	0.89791900
H	4.84817700	2.27496200	2.30254200
H	3.25970900	1.03254300	-0.33479900
C	0.73418600	3.32429900	-2.38405500
H	1.43748200	2.59353800	-2.79769600
H	-0.23158600	2.84037800	-2.22097000
H	0.58799500	4.11628400	-3.12520200
C	0.28863700	4.84128500	-0.39900800
H	0.69323100	5.18865700	0.55728200
H	0.10264900	5.71703800	-1.02938300
H	-0.66051400	4.33268000	-0.22025400
C	2.60306400	4.66400900	-1.37127000
H	2.96971300	5.14444700	-0.45812100
H	3.36368100	3.95649000	-1.71604600
H	2.45421100	5.43578400	-2.13240100
C	3.46028700	-0.58115400	1.13720600
C	4.62545600	-2.91697000	2.12038700
C	4.53860200	-1.16658600	0.46091800
C	2.97817700	-1.16792400	2.31768200
C	3.56319600	-2.32454500	2.80941300
C	5.11080400	-2.33902000	0.95039100
H	4.91849500	-0.69801300	-0.44128000
H	2.14135900	-0.70985300	2.83601700
H	3.18883400	-2.77512300	3.72362200
H	5.93937100	-2.79801300	0.41958900
H	5.07434600	-3.82985100	2.50090500
C	-5.17571100	-0.52682500	2.48563800
H	-5.96721500	-1.26803600	2.42741300
C	-5.40759400	0.71998800	3.02536400
H	-6.39213200	0.97632500	3.40241900
C	-4.36713700	1.66562100	3.08942300
H	-4.55753300	2.64518800	3.51634900
C	-3.10504800	1.36856400	2.61645000
H	-2.30175000	2.09756500	2.65673100
C	-3.92612500	1.68856600	-0.82293300
H	-3.29878800	2.53405500	-0.55904700
C	-5.28273100	1.69900100	-0.57477200
H	-5.73071000	2.57044100	-0.10846700

C	-6.09246600	0.59612100	-0.91099600
H	-7.15685900	0.62943400	-0.70390800
C	-5.53497900	-0.51829700	-1.49586500
H	-6.14441300	-1.37699300	-1.76091700

Nitroenol adds to a catalyst bound *N*-Boc-phenylaldimine

pro-(*S*)-TS175d

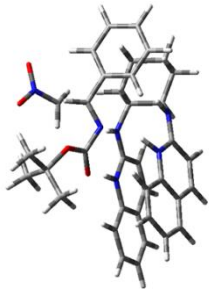

# opt=(calcfc,ts,noeigen) freq=noraman ωB97X-D/6-31g(d) scrf=(iefpcm,so
lvent=nitromethane,smd) geom=connectivity temperature=253

Zero-point correction= 0.766368 (Hartree/Particle)
Thermal correction to Energy= 0.796846
Thermal correction to Enthalpy= 0.797647
Thermal correction to Gibbs Free Energy= 0.708689
Sum of electronic and zero-point Energies= -2063.706972
Sum of electronic and thermal Energies= -2063.676495
Sum of electronic and thermal Enthalpies= -2063.675694
Sum of electronic and thermal Free Energies= -2063.764652

1 1

C	1.15769900	-3.09430100	0.39956500
C	-0.61784400	-1.87148100	1.62895300
N	-0.87132000	-0.58847600	1.93310000
C	-2.98781500	-2.29180100	1.60933700
C	-2.14061700	-0.07469700	2.12368700
C	-1.71909900	-2.76120800	1.46078300
C	-3.24484800	-0.92991500	1.95244500
H	-1.52549700	-3.80186300	1.23570500
H	-3.82975500	-2.96496000	1.47880200
H	-0.09896000	0.08557800	1.83027300
N	0.66889100	-2.25359000	1.49688100
H	1.35189500	-1.54930500	1.76863100
H	0.36085100	-3.77903100	0.09861100
C	1.54441300	-2.17822200	-0.78685500
C	2.12524700	-2.96294400	-1.96334600
H	1.38833300	-3.65808200	-2.37965900
H	2.39793200	-2.25764800	-2.75516700
C	3.34744400	-3.75340600	-1.48655700
H	4.12796400	-3.05029200	-1.16484900
H	3.75839100	-4.33323000	-2.31946800
C	2.98510700	-4.67885400	-0.32205200

H	2.26621700	-5.43305300	-0.66958000
H	3.87300900	-5.21802400	0.02446200
C	2.37534300	-3.90130100	0.84715900
H	3.12146200	-3.20652600	1.25738200
H	2.07809500	-4.57806700	1.65459300
N	0.48015100	-1.22391500	-1.12104700
C	-0.79507800	-1.47728600	-1.44805200
C	-3.54455800	-1.81797500	-1.95187500
C	-1.28926100	-2.73267400	-1.91840000
N	-1.67406700	-0.47211400	-1.28914100
C	-3.02987600	-0.58509500	-1.51269000
C	-2.61870500	-2.88450400	-2.15855600
H	-0.60316300	-3.55354100	-2.06670300
H	-2.99478300	-3.84166900	-2.50726200
N	1.00516800	1.31782800	0.60678000
C	0.14301600	2.30714800	0.16680400
O	-0.93678400	2.03151900	-0.35646000
O	0.55871800	3.53789300	0.40475600
C	-0.11804700	4.71583400	-0.16264300
H	0.64230600	-0.30744400	-0.70092900
C	2.29055500	1.50905600	0.38710500
H	2.65405900	2.47916200	0.04183500
C	2.55543100	1.12622500	-1.94538900
H	2.89909100	0.12465700	-2.17290800
H	1.52489300	1.40001700	-2.13099200
N	3.45543400	2.11532100	-2.19999500
O	3.08473700	3.31913800	-2.14194600
O	4.67035800	1.83594100	-2.38594500
H	2.34556900	-1.52745500	-0.41917500
H	-1.33367500	0.43891500	-0.92769300
C	3.26130100	0.59748600	1.04220600
C	5.06066100	-1.11732100	2.33373500
C	2.94845800	0.04737300	2.29169000
C	4.50371700	0.31242500	0.46475100
C	5.38927600	-0.54992700	1.10277000
C	3.84232800	-0.80678800	2.93317800
H	2.01186200	0.30916900	2.77657200
H	4.76767400	0.74880400	-0.49556700
H	6.34311300	-0.77822600	0.63642000
H	3.58528700	-1.22654800	3.90094000
H	5.75614900	-1.78871300	2.82841300
C	-3.87612000	0.50666400	-1.26435100
H	-3.46039200	1.44507300	-0.91145100
C	-5.23323500	0.34909400	-1.45282400
H	-5.89793100	1.18305000	-1.25080200
C	-5.76927700	-0.87658400	-1.89393400
H	-6.84027900	-0.97616500	-2.03540100
C	-4.93646400	-1.94523500	-2.14240500
H	-5.33410200	-2.89673200	-2.48263500
C	-2.31661200	1.28223600	2.43171700
H	-1.45236500	1.92523600	2.56388300
C	-3.59943600	1.77295300	2.55945300
H	-3.74595500	2.82344200	2.78977100
C	-4.71824200	0.93331200	2.39450200
H	-5.71719500	1.34338900	2.49937700
C	-4.54407800	-0.40029100	2.09828300

H	-5.39561600	-1.06008600	1.96204000
C	0.82737500	5.84861900	0.21811700
H	0.42058200	6.80178100	-0.13310600
H	0.95172600	5.90333100	1.30440300
H	1.80963200	5.69818100	-0.24140200
C	-0.20459200	4.57711300	-1.68007900
H	-0.96582500	3.85334600	-1.97718300
H	-0.46233900	5.54879800	-2.11369400
H	0.76607800	4.25889600	-2.07662300
C	-1.47957100	4.89133400	0.50035400
H	-2.15361800	4.06951900	0.25041200
H	-1.37195500	4.94743100	1.58891800
H	-1.92875900	5.82721000	0.15199300

Activated nitronate adds to an unactivated *N*-Boc-phenylaldimine

pro-(*R*)-TS176a

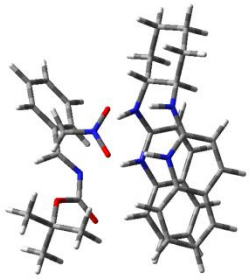

# opt=(calcfc,ts,noeigen) freq=noraman ωB97X-D/6-31g(d) scrf=(iefpcm,so
lvent=nitromethane,smd) geom=connectivity temperature=253

Zero-point correction= 0.768089 (Hartree/Particle)
Thermal correction to Energy= 0.797966
Thermal correction to Enthalpy= 0.798767
Thermal correction to Gibbs Free Energy= 0.712369
Sum of electronic and zero-point Energies= -2063.725239
Sum of electronic and thermal Energies= -2063.695362
Sum of electronic and thermal Enthalpies= -2063.694561
Sum of electronic and thermal Free Energies= -2063.780959

1 1

C	-3.48109900	-0.36822700	-1.55025300
C	-1.38008000	-1.63930700	-1.84959400
N	-0.05244800	-1.44281600	-1.84063500
C	-1.00370200	-3.91629800	-1.15251100
C	0.86911800	-2.41526500	-1.50261700
C	-1.87459100	-2.93719700	-1.51200300
C	0.40588600	-3.68912000	-1.12593700

H	-2.93909000	-3.12559900	-1.55490000
H	-1.37959700	-4.89935700	-0.88499100
H	0.31376300	-0.48015400	-1.97385500
O	1.17796600	1.05791700	-1.95668600
N	0.44171300	2.06277800	-1.77361000
N	-2.17226000	-0.60002400	-2.16924100
H	-1.66782900	0.27080000	-2.36159900
O	-0.82048200	1.93015800	-1.75570700
C	-3.34150700	0.74905500	-0.48582700
C	-4.66559000	1.00213700	0.23684300
C	-5.73403200	1.38765400	-0.79253900
C	-5.87607100	0.31914400	-1.88109400
C	-4.54043100	0.03259800	-2.57482300
N	-2.16016400	0.55859400	0.36520500
C	-1.81307400	-0.54509300	1.03862900
C	-0.92108000	-2.87918600	2.32729200
C	-2.74987700	-1.52765600	1.48319000
N	-0.50523700	-0.74278700	1.30078200
C	-0.01635400	-1.88109500	1.91954900
C	-2.31060100	-2.65074100	2.10631100
H	-3.80340600	-1.36465400	1.31143800
H	-3.02504500	-3.39902900	2.43569200
H	0.18469100	-0.01972100	1.01552500
C	1.00439800	3.23661300	-1.42029100
N	1.54507400	1.55440800	0.79629100
C	1.27297300	2.85151900	0.64655300
C	2.82128700	1.14046900	0.46675500
O	3.24653700	0.02621500	0.74165100
O	3.55851300	2.07137200	-0.16309700
C	4.89724900	1.80213000	-0.67047500
H	-1.38498100	1.13096000	0.03497800
H	-3.80161700	-1.28908300	-1.05764900
H	-3.10131200	1.67109500	-1.02499000
H	-4.52135100	1.80152800	0.97105600
H	-4.99771400	0.11130400	0.78029300
H	-5.45938700	2.34464200	-1.25587600
H	-6.69300000	1.53958000	-0.28607100
H	-6.61494300	0.63556200	-2.62479200
H	-6.25260700	-0.60899400	-1.43011900
H	-4.64813200	-0.77027500	-3.31145900
H	-4.19441100	0.92722900	-3.10986900
H	0.34273700	4.08830400	-1.48635100
H	2.04754300	3.32828700	-1.68727700
H	2.09479300	3.56449200	0.58440000
C	5.86042200	1.55188000	0.48628600
H	5.83309800	2.38718400	1.19447900
H	5.60966200	0.63094100	1.01597400
H	6.88076400	1.46547400	0.09762600
C	4.86749900	0.64274100	-1.66380800
H	4.06793100	0.79851200	-2.39579200
H	5.82257300	0.59785800	-2.19795300
H	4.70493300	-0.31075500	-1.15861700
C	5.24816400	3.10227000	-1.38819200
H	4.54749600	3.29101500	-2.20863400
H	5.20937200	3.94834200	-0.69419700
H	6.25874100	3.03961500	-1.80383900

C	0.03878500	3.41246800	1.26848800
C	-2.22569100	4.53152100	2.49113400
C	-0.72969500	2.66592800	2.16459500
C	-0.31497200	4.74836700	1.03428900
C	-1.43932600	5.30180300	1.63291800
C	-1.86074700	3.21668600	2.76369600
H	-0.42583100	1.65589500	2.41510500
H	0.29743300	5.35913300	0.37642200
H	-1.70149200	6.33662700	1.43365500
H	-2.45106300	2.61513800	3.44869200
H	-3.10776500	4.96209400	2.95589800
C	1.34229600	-4.66620000	-0.73190400
H	0.98186600	-5.64648800	-0.43441600
C	2.68824300	-4.36960200	-0.72095100
H	3.40919800	-5.11908500	-0.41177100
C	3.13119700	-3.08920600	-1.10255600
H	4.19213300	-2.85992200	-1.08252200
C	2.23802900	-2.11299700	-1.49256100
H	2.57664400	-1.11908000	-1.76226000
C	1.36481100	-2.04760500	2.09457400
H	2.04977700	-1.27551800	1.74944900
C	1.82389200	-3.21833500	2.66376200
H	2.89290400	-3.36197200	2.78812200
C	0.93652700	-4.23067700	3.07610500
H	1.32499100	-5.14198800	3.51874000
C	-0.41993600	-4.06093600	2.91182900
H	-1.12340000	-4.82775400	3.22225400

Activated nitronate adds to an unactivated *N*-Boc-phenylaldimine

pro-(*S*)-TS176b

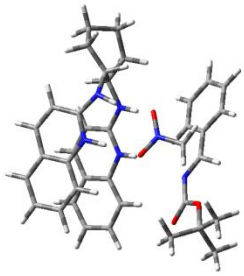

# opt=(calcfc,ts,noeigen) freq=noraman ωB97X-D/6-31g(d) scrf=(iefpcm,so
lvent=nitromethane,smd) geom=connectivity temperature=253

Zero-point correction= 0.766626 (Hartree/Particle)
Thermal correction to Energy= 0.797023
Thermal correction to Enthalpy= 0.797824
Thermal correction to Gibbs Free Energy= 0.708972
Sum of electronic and zero-point Energies= -2063.710699
Sum of electronic and thermal Energies= -2063.680302
Sum of electronic and thermal Enthalpies= -2063.679501

Sum of electronic and thermal Free Energies= -2063.768353

1 1

C	-3.27324400	-1.74494900	-1.35050600
C	-2.53188600	0.56607000	-1.88258400
N	-1.35874000	1.21931900	-1.86270200
C	-3.63109300	2.62436500	-1.28692000
C	-1.22135500	2.55577400	-1.54622900
C	-3.71850800	1.30290600	-1.60195000
C	-2.37572500	3.29730700	-1.23429100
H	-4.67454500	0.79956700	-1.63027400
H	-4.53336000	3.18312800	-1.05690000
H	-0.49223000	0.65866100	-1.89401800
O	0.98387000	-0.26742200	-1.30888000
N	0.95788200	-1.52632800	-1.46622900
N	-2.50129400	-0.76237700	-2.13185300
H	-1.55685500	-1.11938400	-2.27415800
O	-0.13604900	-2.15719700	-1.34663000
C	-3.28148400	-1.42503900	0.16298800
C	-3.72077300	-2.67248900	0.94311000
C	-4.84706700	-3.43778000	0.21320100
C	-5.61935400	-2.52467600	-0.74315300
C	-4.70333300	-2.00382300	-1.86462800
N	-1.96116900	-0.95643200	0.58513700
C	-1.70070600	0.21368100	1.17247100
C	-1.02825700	2.73808800	2.23402900
C	-2.70905400	1.04949400	1.75247400
N	-0.42708900	0.65638200	1.19378500
C	-0.04104900	1.87556900	1.72708000
C	-2.37829900	2.27265700	2.23787700
H	-3.73031700	0.69733600	1.79525800
H	-3.15120100	2.91310000	2.65224600
H	0.30012200	0.11651400	0.71140500
C	2.12071500	-2.19761700	-1.57881000
N	2.74181200	-0.99842500	0.84892400
C	2.68593300	-2.24839000	0.38777700
C	3.79629100	-0.21053600	0.46613400
O	4.01057500	0.89230600	0.95713300
O	4.57071300	-0.74071700	-0.50647900
C	5.67626200	-0.00771100	-1.11006000
H	-1.17237900	-1.46139300	0.16896800
H	-2.69890800	-2.66756500	-1.47375300
H	-3.99357400	-0.61731100	0.33442900
H	-2.84865400	-3.32247900	1.07489700
H	-4.04216300	-2.35562200	1.94076200
H	-4.41752700	-4.26624000	-0.36313000
H	-5.52594200	-3.88457200	0.94599700
H	-6.46654100	-3.05923800	-1.18409000
H	-6.03940100	-1.68124200	-0.18117200
H	-5.12686600	-1.09650200	-2.30271800
H	-4.64142300	-2.74081900	-2.67173600
H	2.01724400	-3.23357000	-1.87152100
H	2.95317500	-1.60919100	-1.93811800

H	3.59652600	-2.74949100	0.04996700
C	6.75667700	0.27864700	-0.07016200
H	7.05598700	-0.64877100	0.43028300
H	6.40456800	0.98841700	0.67992900
H	7.63799400	0.69825800	-0.56678200
C	5.15810700	1.26343000	-1.77890300
H	4.33984500	1.02145200	-2.46649100
H	5.96539000	1.72673200	-2.35599500
H	4.79724000	1.98146000	-1.04054700
C	6.19719600	-0.98591400	-2.15904700
H	5.42176200	-1.21250000	-2.89869600
H	6.51439900	-1.92241400	-1.68841400
H	7.05605900	-0.55164300	-2.68030300
C	1.66581700	-3.16048400	0.97577000
C	-0.25416900	-4.89652000	2.04359300
C	0.71245500	-2.69041600	1.88192200
C	1.65924300	-4.51506000	0.62445400
C	0.70583400	-5.37771200	1.15202200
C	-0.24423100	-3.55290500	2.41152500
H	0.74053900	-1.64843000	2.18304600
H	2.40346900	-4.88930600	-0.07468700
H	0.71010100	-6.42661000	0.87040000
H	-0.98143900	-3.17380600	3.11341800
H	-1.00119700	-5.56972000	2.45420700
C	-2.23343700	4.64494000	-0.84159600
H	-3.12469700	5.21590900	-0.59908900
C	-0.98109500	5.21061900	-0.75520200
H	-0.86846500	6.24280000	-0.44069400
C	0.16219800	4.44932500	-1.06835300
H	1.14532800	4.90131900	-0.98622800
C	0.05448100	3.13357800	-1.46800000
H	0.93505800	2.54168500	-1.69871200
C	1.30994900	2.24463400	1.73112700
H	2.07407100	1.56472800	1.36208900
C	1.65534300	3.48791000	2.22149100
H	2.70108800	3.78020100	2.22504500
C	0.68177500	4.37671000	2.71292600
H	0.97789800	5.35084100	3.08826300
C	-0.64446500	4.00232100	2.72479200
H	-1.41101000	4.66894800	3.10880700

Activated nitronate adds to an unactivated *N*-Boc-phenylaldimine

pro-(*R*)-TS176c

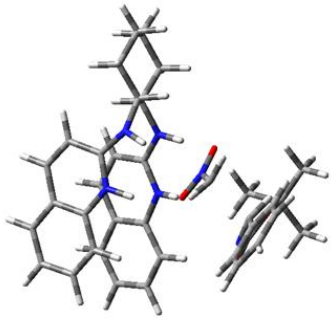

# opt=(calcfc,ts,noeigen) freq=noraman ωB97X-D/6-31g(d) scrf=(iefpcm,so
lvent=nitromethane,smd) geom=connectivity temperature=253

Zero-point correction= 0.766743 (Hartree/Particle)
Thermal correction to Energy= 0.797023
Thermal correction to Enthalpy= 0.797824
Thermal correction to Gibbs Free Energy= 0.709441
Sum of electronic and zero-point Energies= -2063.710941
Sum of electronic and thermal Energies= -2063.680661
Sum of electronic and thermal Enthalpies= -2063.679860
Sum of electronic and thermal Free Energies= -2063.768243

1 1

C	1.31698800	3.42838800	-0.34647700
C	1.93458900	1.46166300	-1.77334000
N	1.43049900	0.23643400	-1.99515100
C	4.13566000	0.58044000	-2.19073900
C	2.19613600	-0.87401300	-2.29152700
C	3.34059800	1.64519400	-1.89512800
C	3.59237100	-0.72235700	-2.38369400
H	3.75553000	2.63500200	-1.76281500
H	5.20861300	0.71865900	-2.28282900
H	0.44227300	0.08062100	-1.76551700
O	-0.84768000	-0.01908700	-0.29698400
N	-1.56288800	1.01362200	-0.09892700
N	1.08084900	2.44355800	-1.41867800
H	0.10134400	2.24278800	-1.57749700
O	-1.36181100	1.73628600	0.91266500
C	2.10671700	2.83719500	0.84613700
C	2.11376400	3.83939800	2.00207600
C	2.71649000	5.17431500	1.55480100
C	1.98196900	5.74606800	0.33936300
C	1.94489800	4.74158000	-0.81642000
N	1.52289300	1.55388200	1.23105200
C	2.15374500	0.37399900	1.21650900
C	3.29128900	-2.19738800	1.04867400
C	3.57498300	0.21409000	1.25097900
N	1.39676900	-0.73491000	1.13804500
C	1.89696200	-2.01893000	1.06228600
C	4.11119800	-1.03077700	1.15277700
H	4.20672300	1.08618400	1.35431400
H	5.19022500	-1.15284700	1.16245700
H	0.39622200	-0.59967700	0.94483500
C	-2.61902900	1.21181200	-0.92630900
N	-3.37567500	-1.31064100	-0.04938800
C	-3.97080300	-0.13063300	-0.22112400
C	-2.82452700	-1.59517900	1.17588700
O	-2.21965400	-2.63681800	1.40590000
O	-3.06508100	-0.66055000	2.12227900
C	-2.56601200	-0.75427500	3.48132700
H	0.49578400	1.53646700	1.25366600

H	0.30891500	3.65275500	0.01871700
H	3.13935400	2.66482500	0.53491700
H	1.08283700	3.98579000	2.35074100
H	2.68472500	3.41300000	2.83337700
H	2.68640100	5.88797800	2.38490300
H	3.77441900	5.02149800	1.30194700
H	0.95214200	6.00135000	0.62359000
H	2.46247400	6.67204400	0.00658900
H	2.96259200	4.56204600	-1.18331200
H	1.35815200	5.13287000	-1.65352600
H	-3.09077400	2.18123200	-0.82570100
H	-2.48461400	0.78207500	-1.90960100
H	-4.20573000	0.49434400	0.64367100
C	-1.04042500	-0.74070200	3.48475300
H	-0.68467800	0.14315900	2.94571000
H	-0.63778100	-1.64089500	3.01597900
H	-0.67190600	-0.68763500	4.51479000
C	-3.13883700	-1.98363400	4.18253300
H	-4.23029600	-1.99943900	4.08752700
H	-2.88983300	-1.94591100	5.24870900
H	-2.73497700	-2.90375100	3.75683600
C	-3.10221400	0.52478800	4.11875700
H	-4.19734700	0.53602200	4.10161600
H	-2.73668400	1.39977400	3.57158100
H	-2.77047700	0.59799800	5.15943800
C	-4.94720500	0.00369700	-1.34457100
C	-6.81261600	0.29170600	-3.41039000
C	-4.96754500	-0.90292900	-2.40826000
C	-5.86507300	1.05711900	-1.32831800
C	-6.79635900	1.19963900	-2.35342300
C	-5.89547000	-0.75932200	-3.43480000
H	-4.25443200	-1.72139300	-2.41666200
H	-5.85040900	1.76665300	-0.50412900
H	-7.51085500	2.01727200	-2.32608000
H	-5.90583700	-1.47137600	-4.25521500
H	-7.53950900	0.39944800	-4.21033400
C	4.38697100	-1.86383400	-2.62291300
H	5.46359000	-1.74437200	-2.69633700
C	3.79822400	-3.10181000	-2.74663500
H	4.40797500	-3.98241800	-2.91870800
C	2.39928200	-3.23286900	-2.64387400
H	1.94444500	-4.21402800	-2.73304100
C	1.59461500	-2.13418100	-2.42638300
H	0.51757000	-2.23480400	-2.33640100
C	1.02099300	-3.11084200	0.96140900
H	-0.05592300	-2.95003100	0.97455000
C	1.55902600	-4.37643200	0.84134000
H	0.89275000	-5.22963600	0.75942100
C	2.95212400	-4.57826400	0.81885500
H	3.35001600	-5.58267900	0.71793300
C	3.80797900	-3.50296600	0.92323300
H	4.88492700	-3.64172600	0.90610300

Activated nitronate adds to an unactivated *N*-Boc-phenylaldimine

pro-(*S*)-TS176d

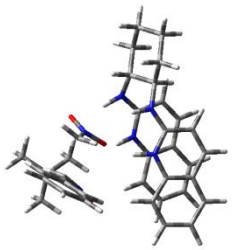

# opt=(calcfc,ts,noeigen) freq=noraman ωB97X-D/6-31g(d) scrf=(iefpcm,so
lvent=nitromethane,smd) geom=connectivity temperature=253

Zero-point correction= 0.767314 (Hartree/Particle)
Thermal correction to Energy= 0.797360
Thermal correction to Enthalpy= 0.798161
Thermal correction to Gibbs Free Energy= 0.711438
Sum of electronic and zero-point Energies= -2063.713262
Sum of electronic and thermal Energies= -2063.683216
Sum of electronic and thermal Enthalpies= -2063.682415
Sum of electronic and thermal Free Energies= -2063.769137

1 1

C	-2.42686700	2.83518600	-0.76710800
C	-1.65226700	0.69134500	-1.80101300
N	-0.62455700	-0.17435900	-1.79651300
C	-3.05050800	-1.06244800	-2.68039700
C	-0.71575200	-1.49523000	-2.18433500
C	-2.91727800	0.22987500	-2.27840500
C	-1.95364200	-1.97794800	-2.64383300
H	-3.74833300	0.92073600	-2.32825300
H	-4.01151200	-1.41576200	-3.04227000
H	0.22435500	0.10825400	-1.29051800
O	0.69747900	0.56807200	0.40519100
N	1.43379300	1.54151400	0.76857600
N	-1.43159600	1.92860000	-1.33570000
H	-0.46852700	2.16742300	-1.12293400
O	1.24472100	2.07327400	1.88729300
C	-2.08874900	3.10294400	0.72092400
C	-3.12705700	4.03033700	1.35637900
C	-3.19812100	5.34948700	0.58118100
C	-3.50591000	5.10898600	-0.89891900
C	-2.48968800	4.15671800	-1.53385100
N	-1.81472500	1.86683900	1.47552800
C	-2.47127100	0.70261800	1.29654300
C	-3.65584600	-1.80219400	0.81544200
C	-3.87995700	0.60197700	1.10378200
N	-1.74735800	-0.42873200	1.27314300
C	-2.27014000	-1.68228900	1.02908500
C	-4.44370700	-0.61536400	0.87439500
H	-4.48363900	1.49732600	1.15657300
H	-5.51662400	-0.69331200	0.72654200
H	-0.72642100	-0.32238800	1.28044600

C	2.46080800	1.87805900	-0.05212600
N	3.05827300	-0.85297800	0.03467600
C	3.75774800	0.27424300	0.12851500
C	2.51291100	-1.38812000	1.17833200
O	1.84740300	-2.41708500	1.17312100
O	2.82579500	-0.71230700	2.30433500
C	2.30565600	-1.06178200	3.61413200
H	-0.82806900	1.76772400	1.71500100
H	-3.40240800	2.34639300	-0.82648100
H	-1.12569900	3.62702900	0.73789000
H	-2.85103600	4.20528100	2.40103800
H	-4.11377600	3.55326100	1.35314200
H	-2.23663500	5.87237400	0.67338500
H	-3.96010500	5.99743000	1.02707900
H	-3.51024800	6.05822300	-1.44504900
H	-4.51128400	4.67752700	-0.99598200
H	-2.74817400	3.94673200	-2.57691000
H	-1.49144900	4.61441700	-1.52777100
H	2.99098800	2.77593100	0.24060000
H	2.25544800	1.70208800	-1.09940700
H	4.11424000	0.62336900	1.09946700
C	0.78404500	-0.94410200	3.62770600
H	0.49373500	0.03920300	3.24437500
H	0.32103600	-1.72484800	3.02127900
H	0.41596200	-1.04075600	4.65472400
C	2.78520100	-2.44952500	4.03182400
H	3.87611700	-2.51402200	3.95293000
H	2.50727200	-2.63409300	5.07523200
H	2.34150300	-3.22481000	3.40484500
C	2.91901600	0.01101100	4.50996000
H	4.01268900	-0.04489800	4.48564300
H	2.61255000	1.00482300	4.16772400
H	2.58737700	-0.12463800	5.54426300
C	4.63694400	0.64987700	-1.01808400
C	6.31004900	1.38724400	-3.13690500
C	4.47928600	0.06617900	-2.27857700
C	5.63875400	1.60592400	-0.82976800
C	6.47298100	1.97238000	-1.88271600
C	5.31096800	0.43319000	-3.33135300
H	3.70354300	-0.67931700	-2.42270600
H	5.76426700	2.06411500	0.14860500
H	7.25029500	2.71419400	-1.72387600
H	5.18172400	-0.02779500	-4.30649300
H	6.95981000	1.67204500	-3.95940900
C	-2.05747800	-3.33606300	-3.00845500
H	-3.01213600	-3.71314100	-3.36299100
C	-0.96189200	-4.16558600	-2.90362100
H	-1.04367000	-5.21210700	-3.17818800
C	0.26293700	-3.66345000	-2.42259800
H	1.11277900	-4.33159800	-2.32412400
C	0.39904600	-2.33862400	-2.06240800
H	1.32729700	-1.95211600	-1.64751700
C	-1.41893200	-2.79390500	0.92941900
H	-0.34512400	-2.67091900	1.05937100
C	-1.97160300	-4.02019300	0.62403000
H	-1.32252800	-4.88506600	0.53017700

C	-3.35822100	-4.16668700	0.42047500
H	-3.76664600	-5.14290000	0.18098600
C	-4.18979200	-3.07337700	0.51433900
H	-5.25896400	-3.16738600	0.35013800

4.4. Selected DFT Calculated Transition State Geometries & Thermochemical Data for HQuin-BAM Catalyzed *Aza*-Henry Reaction of Nitroethane with *N*-Boc Arylaldimines

Activated nitronate adds to an activated *N*-Boc phenylaldimine

(*R*,*S*)-TS188$_{trans}$

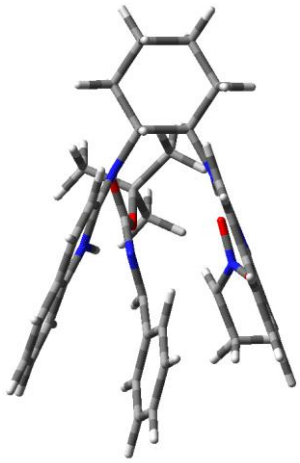

# opt=(calcfc,ts,noeigen) freq=noraman ωB97X-D/6-31g(d) scrf=(iefpcm,so
lvent=nitroethane) geom=connectivity temperature=253

Zero-point correction= 0.794967 (Hartree/Particle)
Thermal correction to Energy= 0.826323
Thermal correction to Enthalpy= 0.827124
Thermal correction to Gibbs Free Energy= 0.736688
Sum of electronic and zero-point Energies= -2102.986578
Sum of electronic and thermal Energies= -2102.955222
Sum of electronic and thermal Enthalpies= -2102.954421
Sum of electronic and thermal Free Energies= -2103.044857

Quasiharmonic free energy correction= 0.744570
SCF (B3LYP/6-31G*) = -2104.400085
SCF (ωB97X-D/6-311+G**) = -2104.299333
SCF (B3LYP-D3/6-311+G**) = -2105.09779

1 1

C	-1.10804700	3.08355000	1.01513300
C	0.29027800	1.30783400	2.06453800
N	0.39985900	-0.02391200	2.23308100
C	2.50546900	1.55573800	2.98271500
C	1.49213300	-0.64186300	2.80781700

C	1.39462100	2.13246100	2.45664600
C	2.59681300	0.14280900	3.18461100
H	1.32614000	3.20650600	2.35196300
H	3.34312600	2.18058800	3.27751400
H	-0.30083300	-0.61051900	1.72848500
O	-1.91120100	-0.31759900	-1.98527500
N	-1.19863800	-1.27208700	-2.41256000
N	-0.85253900	1.75953400	1.55403400
H	-1.61566500	1.07663300	1.41193700
O	-0.06082300	-1.03821800	-2.93461100
C	-1.54646000	2.94633300	-0.46093500
C	-1.83742000	4.31258700	-1.09120000
C	-2.90178500	5.05543200	-0.27814800
C	-2.49139400	5.18663000	1.19083700
C	-2.18932800	3.82015800	1.81182500
N	-0.65727000	2.09710400	-1.25010000
C	0.65944000	2.20463500	-1.42241700
C	3.45722000	2.14458800	-1.79520400
C	1.47126900	3.30661500	-0.99839500
N	1.27344000	1.18092200	-2.04652700
C	2.63439100	1.09698700	-2.24645400
C	2.81771700	3.26139500	-1.17604500
H	1.00904300	4.17408900	-0.55150500
H	3.42673500	4.09730000	-0.84548100
H	0.69385500	0.38218200	-2.38727600
C	-1.60256000	-2.54014300	-2.19758800
N	-1.39154400	-1.38589800	0.48425800
C	-1.07998900	-2.57036700	-0.02824100
C	-2.70925200	-1.02430900	0.61825800
O	-3.02581900	0.04529100	1.14425500
O	-3.59075900	-1.90991500	0.15825300
C	-5.02403200	-1.62347100	0.07105800
H	-1.08146100	1.21523800	-1.57197900
H	-0.18732100	3.66639400	1.06796000
H	-2.48712100	2.38313900	-0.44905500
H	-2.17117500	4.15845800	-2.12180200
H	-0.92369600	4.91733200	-1.13759600
H	-3.85207900	4.50890800	-0.34326500
H	-3.07264400	6.04410800	-0.71556400
H	-3.28231600	5.68262800	1.76231900
H	-1.59912200	5.82308100	1.26439200
H	-1.85210200	3.92668100	2.84780400
H	-3.09747800	3.20278500	1.82685500
H	-2.65906200	-2.60280200	-1.97428200
H	-1.79291900	-3.39399400	0.01363000
C	-5.61239000	-1.45336200	1.46919400
H	-5.38749900	-2.33046700	2.08465100
H	-5.21358300	-0.56297500	1.95682000
H	-6.70003600	-1.35717600	1.39217800
C	-5.25387600	-0.40301600	-0.81680700
H	-4.72345900	-0.52483300	-1.76579000
H	-6.32451500	-0.30344300	-1.02113600
H	-4.90280300	0.51036100	-0.33421000
C	-5.57324500	-2.88217600	-0.59402700
H	-5.13678700	-3.01583600	-1.58906400
H	-5.34776400	-3.76701700	0.00913600

H	-6.65876000	-2.80085700	-0.70179800
C	0.34547700	-2.93736800	-0.09936200
C	3.04613600	-3.64839200	-0.13403500
C	0.72430200	-4.27613300	0.03896800
C	1.33207300	-1.96070200	-0.28013900
C	2.67482600	-2.31459700	-0.29471900
C	2.06992300	-4.62900400	0.03041600
H	-0.03840100	-5.03934100	0.16910100
H	1.03614100	-0.92381500	-0.39025300
H	3.43337300	-1.54920800	-0.42438700
H	2.35595300	-5.66873900	0.15452700
C	3.72756900	-0.49113900	3.73870200
H	4.58043200	0.11461800	4.03018300
C	3.74433100	-1.85876600	3.90420000
H	4.61638700	-2.34610300	4.32649400
C	2.62537500	-2.62624900	3.53063900
H	2.64297400	-3.70272000	3.66547600
C	1.50309800	-2.03207800	2.99343900
H	0.64307600	-2.62379100	2.69944200
C	3.18272900	-0.03040700	-2.87819800
H	2.53072900	-0.83258300	-3.20821600
C	4.55050700	-0.09914600	-3.04418800
H	4.98386900	-0.97030700	-3.52443100
C	5.39107300	0.93830000	-2.59724600
H	6.46335100	0.86063600	-2.73947900
C	4.85124200	2.04658400	-1.98277700
H	5.48765800	2.85474900	-1.63547200
C	-0.89371700	-3.66389700	-2.87816600
H	0.18866000	-3.57859900	-2.76141500
H	-1.21973400	-4.61308200	-2.44306300
H	-1.12119300	-3.68770900	-3.95130400
H	4.09658500	-3.92291300	-0.13756700

(*S*,*R*)-TS188$_{anti}$

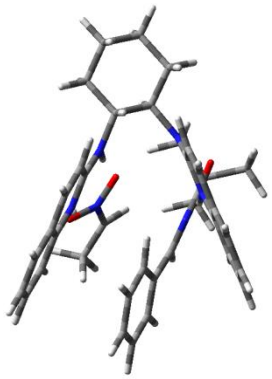

---

opt=(calcfc,ts,noeigen) freq=noraman ωB97X-D/6-31g(d) scrf=(iefpcm,solvent=nitroethane) geom=connectivity temperature=253

Zero-point correction= 0.794445 (Hartree/Particle)
Thermal correction to Energy= 0.826177
Thermal correction to Enthalpy= 0.826979
Thermal correction to Gibbs Free Energy= 0.734537

Sum of electronic and zero-point Energies= -2102.983671
Sum of electronic and thermal Energies= -2102.951939
Sum of electronic and thermal Enthalpies= -2102.951138
Sum of electronic and thermal Free Energies= -2103.043579

Quasiharmonic free energy correction= 0.743763
SCF (B3LYP/6-31G*) = -2104.399672
SCF (wB97XD/6-311+G**) = -2104.296489
SCF (B3LYP-D3/6-311+G**) = -2105.095569
1 1

C	-0.47550000	3.31182100	-0.67617200
C	-2.06675600	1.51176400	-1.25132200
N	-2.22915100	0.27741100	-1.75656600
C	-4.45221900	1.62844400	-0.91175600
C	-3.44643300	-0.36061000	-1.86191300
C	-3.23456400	2.22470700	-0.82533400
C	-4.60646000	0.30521600	-1.42800100
H	-3.14268600	3.23227700	-0.44438900
H	-5.33563000	2.16829600	-0.58448500
H	-1.38756600	-0.23865600	-2.10250200
N	-0.82279500	1.98660600	-1.16784700
H	-0.06018100	1.38084700	-1.50651200
H	-1.21460200	3.59379200	0.07709100
C	0.90848100	3.27979400	-0.00309200
C	1.24788500	4.65197500	0.59240200
H	0.54011700	4.89590300	1.39466600
H	2.24141900	4.59834900	1.04751300
C	1.19961300	5.73679400	-0.48766200
H	1.99666500	5.55154900	-1.21988700
H	1.40250500	6.71297700	-0.03620000
C	-0.15264100	5.75372600	-1.20525400
H	-0.93705900	6.05492900	-0.49775400
H	-0.14744700	6.49723300	-2.00825900
C	-0.49487500	4.37640100	-1.77914300
H	0.22833800	4.09451200	-2.55487700
H	-1.48453400	4.38633300	-2.24841900
N	1.07422100	2.16946500	0.92963900
C	0.21211700	1.70468000	1.83797600
C	-1.47417000	0.48297800	3.73772700
C	-0.87524900	2.43701000	2.41213200
N	0.40443100	0.43767500	2.24676500
C	-0.38183200	-0.20337200	3.17711200
C	-1.68600700	1.83290800	3.32173100
H	-1.01896700	3.47636000	2.15302000
H	-2.50715400	2.39180000	3.76003400
N	2.04692300	-1.01267800	0.49901600
C	3.28984600	-0.43915000	0.38055900
O	3.50140400	0.69848900	0.79851300
O	4.20805100	-1.19615900	-0.21905300
C	5.55647900	-0.70963100	-0.52563900
H	1.91359100	1.59664200	0.78192800
C	1.81719800	-2.21011400	-0.01870900
H	2.63722600	-2.90659200	-0.19278500
C	1.91125700	-1.95370400	-2.24960700
H	2.92762200	-1.59473700	-2.16509200
N	1.00338100	-0.96261200	-2.31907200

O	-0.18525000	-1.22462700	-2.69859500
O	1.30542100	0.19985800	-1.91398300
H	1.64392600	3.06847100	-0.78872300
H	1.07745600	-0.14109300	1.68379800
C	0.47621500	-2.79145200	0.14686900
C	-2.05563900	-3.90199200	0.54867300
C	0.31701600	-4.17930800	0.21256300
C	-0.65120500	-1.96712200	0.25332900
C	-1.90743000	-2.51863600	0.46419800
C	-0.94347400	-4.73165600	0.41682800
H	1.18601200	-4.82491300	0.11898100
H	-0.52864900	-0.89280800	0.17162300
H	-2.77266500	-1.87054800	0.56180800
H	-1.05780300	-5.80915900	0.47961900
C	-0.11067300	-1.53570400	3.52653400
H	0.73091600	-2.05017300	3.07458300
C	-0.93804700	-2.16871500	4.42890500
H	-0.74157200	-3.20175200	4.69636900
C	-2.03368900	-1.49673000	5.00531000
H	-2.66946300	-2.01497500	5.71488800
C	-2.29667000	-0.18786700	4.66714000
H	-3.13799100	0.34122000	5.10433600
C	-3.51407300	-1.66327100	-2.38206500
H	-2.60399200	-2.16442600	-2.69500500
C	-4.74329400	-2.28312100	-2.46313500
H	-4.80517900	-3.29058400	-2.86152700
C	-5.91668600	-1.63165500	-2.03649700
H	-6.87227700	-2.13903500	-2.11134000
C	-5.84899900	-0.35439600	-1.52575300
H	-6.74529300	0.15970400	-1.19226000
C	6.18605100	-1.90558900	-1.23296000
H	5.63335800	-2.15173000	-2.14529800
H	7.21957200	-1.67316500	-1.50575200
H	6.18851900	-2.78186400	-0.57748300
C	5.47213100	0.49125900	-1.46442900
H	5.03060300	1.35524200	-0.96594200
H	6.47980500	0.75525300	-1.80008900
H	4.87166600	0.24417600	-2.34626600
C	6.30235700	-0.39116700	0.76704300
H	7.34621100	-0.15962400	0.53327700
H	5.85685500	0.46411900	1.27677400
H	6.28562900	-1.25641900	1.43755600
C	1.60793400	-3.27217200	-2.87927300
H	1.54072000	-3.19261300	-3.97134600
H	2.40647200	-3.97966100	-2.63801200
H	0.65955200	-3.67728500	-2.51484100
H	-3.03809300	-4.33378800	0.71269100

(*R*,*R*)-TS188$_{syn}$

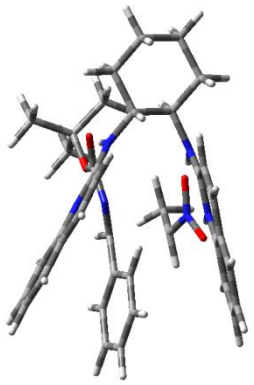

# opt=(calcfc,ts,noeigen) freq=noraman ωB97X-D/6-31g(d) scrf=(iefpcm,so
lvent=nitroethane) geom=connectivity temperature=253

Zero-point correction= 0.795758 (Hartree/Particle)
Thermal correction to Energy= 0.827070
Thermal correction to Enthalpy= 0.827871
Thermal correction to Gibbs Free Energy= 0.737075
Sum of electronic and zero-point Energies= -2102.979511
Sum of electronic and thermal Energies= -2102.948199
Sum of electronic and thermal Enthalpies= -2102.947398
Sum of electronic and thermal Free Energies= -2103.038193

Quasiharmonic free energy correction= 0.745913
SCF (B3LYP/6-31G*) = -2104.396034
SCF (wB97X-D/6-311+G**) = -2104.293754
SCF (B3LYP-D3/6-311+G**) = -2105.092579

1 1

C	-0.58095100	3.17854700	1.02711100
C	0.45644200	1.12969400	2.00676400
N	0.32735400	-0.20954400	2.09188600
C	2.60791400	0.93859300	3.07624400
C	1.24852800	-1.03660700	2.70251400
C	1.65745900	1.72640900	2.51117400
C	2.43553200	-0.47550300	3.20594400
H	1.78728900	2.79860900	2.45752000
H	3.51761400	1.38983200	3.46063000
H	-0.42366300	-0.64085700	1.51262000
O	-1.72335400	0.16078400	-2.35482500
N	-1.11989100	-0.89810600	-2.67968600
N	-0.56018900	1.79608800	1.46929100
H	-1.41647700	1.25777300	1.25363900
O	0.13268500	-0.87859200	-2.91000500
C	-0.94541900	3.20953100	-0.47556700
C	-1.00413300	4.64317800	-1.01364000
C	-2.00044100	5.47227300	-0.19716000
C	-1.66021900	5.44378300	1.29529400
C	-1.59061900	4.00928000	1.82538600
N	-0.13765300	2.29016700	-1.27520900
C	1.19241400	2.18858200	-1.31182900
C	3.97087400	1.71555900	-1.43231600

C	2.11445800	3.15632000	-0.79713100
N	1.70087200	1.08276600	-1.88434900
C	3.04666200	0.80048300	-1.96823600
C	3.45033600	2.91289700	-0.85472200
H	1.74505400	4.08464200	-0.38739600
H	4.14464100	3.64971600	-0.46253200
H	1.03574000	0.37715600	-2.27612200
C	-1.75993900	-2.08850700	-2.65631600
N	-1.57548600	-1.16446500	0.15808000
C	-1.46953200	-2.34346700	-0.44485900
C	-2.81932500	-0.63898400	0.41871400
O	-2.94047700	0.46215600	0.96021300
O	-3.85549800	-1.40587800	0.09005600
C	-5.24427700	-1.00825600	0.33791900
H	-0.66097000	1.50144800	-1.67850300
H	0.41043600	3.61032500	1.17421200
H	-1.95559400	2.79028500	-0.55379400
H	-1.29389700	4.61013100	-2.06825400
H	-0.01499600	5.11427300	-0.96785900
H	-3.01121900	5.07013900	-0.34761700
H	-2.00940100	6.50266700	-0.56624700
H	-2.40424700	6.00937800	1.86496900
H	-0.69269400	5.93757000	1.45850100
H	-1.30393000	3.99372400	2.88165600
H	-2.57632700	3.53130500	1.74879100
H	-2.33356200	-3.00532200	-0.50577000
C	-5.48010600	-0.84780300	1.83784400
H	-5.16578100	-1.75221200	2.36859700
H	-4.93481100	0.00850300	2.23645600
H	-6.54924200	-0.69883300	2.01853700
C	-5.58015800	0.25993600	-0.44332800
H	-5.37432300	0.12102500	-1.50942000
H	-6.64733600	0.47479700	-0.32945000
H	-5.00962600	1.11485700	-0.07839700
C	-6.03179600	-2.19761600	-0.20351700
H	-5.84054800	-2.33534900	-1.27180600
H	-5.75353000	-3.11554100	0.32323800
H	-7.10288200	-2.02643300	-0.06173400
C	-0.14565900	-2.99117400	-0.49405400
C	2.34058100	-4.26838000	-0.49864200
C	-0.06691400	-4.38611900	-0.57517200
C	1.03546400	-2.24251500	-0.43643800
C	2.27071900	-2.87887700	-0.43370400
C	1.16909800	-5.02183200	-0.57093600
H	-0.98085500	-4.97223800	-0.63038400
H	0.97552100	-1.16219500	-0.37936400
H	3.18015700	-2.28901700	-0.37559400
H	1.22042000	-6.10497700	-0.62216300
C	3.38897400	-1.32194900	3.80708000
H	4.30474900	-0.88812000	4.19719100
C	3.15541900	-2.67686400	3.89704000
H	3.89042100	-3.32816100	4.35736200
C	1.95859700	-3.21908600	3.39335700
H	1.77911700	-4.28648400	3.46871500
C	1.00642300	-2.41428600	2.80357100
H	0.08743900	-2.83263800	2.40710900

C	3.47844000	-0.39339200	-2.56806900
H	2.74852500	-1.09075800	-2.96624100
C	4.83105600	-0.65972700	-2.61850000
H	5.17392400	-1.58250500	-3.07497400
C	5.77148800	0.24442300	-2.08818200
H	6.82994200	0.01464800	-2.14368300
C	5.34719800	1.41739100	-1.50434700
H	6.06132700	2.12538900	-1.09495900
H	-1.13886100	-2.88986200	-3.03590800
C	-3.23863500	-2.13963200	-2.88059700
H	-3.64899400	-3.06829300	-2.47344500
H	-3.73703500	-1.30073100	-2.39851700
H	-3.46501600	-2.11639500	-3.95425000
H	3.30588700	-4.76520700	-0.49112100

(*S*,*S*)-TS188$_{syn}$

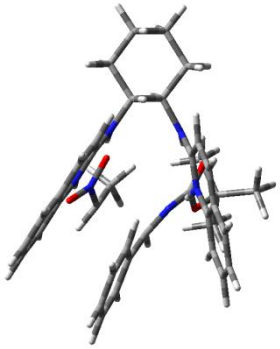

# opt=(calcfc,ts,noeigen) freq=noraman ωB97X-D/6-31g(d) scrf=(iefpcm,so
lvent=nitroethane) geom=connectivity temperature=253

Zero-point correction= 0.795037 (Hartree/Particle)
Thermal correction to Energy= 0.826544
Thermal correction to Enthalpy= 0.827345
Thermal correction to Gibbs Free Energy= 0.735644
Sum of electronic and zero-point Energies= -2102.977939
Sum of electronic and thermal Energies= -2102.946432
Sum of electronic and thermal Enthalpies= -2102.945631
Sum of electronic and thermal Free Energies= -2103.037332

Quasiharmonic free energy correction= 0.744917
SCF (B3LYP/6-31G*) = -2104.3963854
SCF (wB97X-D/6-311+G**) = -2104.291659
SCF (B3LYP-D3/6-311+G**) = -2105.090831

1 1

C	-0.99413200	3.32567700	-0.59590500
C	-2.47101400	1.36937900	-0.96883900
N	-2.56449200	0.12763600	-1.47737400
C	-4.75823000	1.18094900	-0.22675000
C	-3.70246800	-0.64815900	-1.41683300

C	-3.62342600	1.92144300	-0.32065600
C	-4.84327700	-0.13786600	-0.77170600
H	-3.58576700	2.92564600	0.07858600
H	-5.63029700	1.60003700	0.26602900
H	-1.72859600	-0.27932900	-1.95113000
N	-1.30514400	1.99866900	-1.10245100
H	-0.54704600	1.49007300	-1.58341100
H	-1.63684800	3.52096100	0.26531500
C	0.47647700	3.36911100	-0.13433900
C	0.80738300	4.73375200	0.48154600
H	0.21160600	4.89236700	1.38914000
H	1.85872500	4.73483000	0.78511000
C	0.53139800	5.85513300	-0.52516400
H	1.22642300	5.75710800	-1.36951500
H	0.73181800	6.82487200	-0.05890800
C	-0.90835600	5.80354200	-1.04394700
H	-1.60144100	6.02316300	-0.22061600
H	-1.06525500	6.57545800	-1.80399800
C	-1.24379400	4.42919100	-1.63007300
H	-0.62866100	4.23008400	-2.51696900
H	-2.29124700	4.38813400	-1.94784200
N	0.85647800	2.22700400	0.69308900
C	0.15659600	1.65358200	1.67482100
C	-1.19137500	0.23963900	3.70438900
C	-0.87893500	2.28963000	2.43077800
N	0.46615700	0.37907100	1.97448600
C	-0.14970200	-0.35252900	2.96702300
C	-1.52879200	1.59355600	3.40041700
H	-1.10422600	3.33196500	2.25807700
H	-2.31032600	2.08050800	3.97571100
N	2.09737500	-0.87561300	0.05329600
C	3.32199400	-0.25549000	0.15318200
O	3.40164200	0.92426900	0.49265300
O	4.37462700	-1.03671500	-0.08917100
C	5.75456600	-0.54726100	-0.02835300
H	1.69765700	1.71957600	0.39805800
C	1.97802800	-1.99216900	-0.65120300
H	2.87294100	-2.52187900	-0.97839600
C	1.78722200	-1.39401900	-2.78231300
N	0.70926300	-0.59535400	-2.61113000
O	-0.45754000	-1.08333200	-2.73815100
O	0.86736800	0.59658400	-2.22234100
H	1.09414900	3.25375300	-1.03273100
H	1.10556500	-0.12509000	1.31147000
C	0.76452400	-2.81369000	-0.50463500
C	-1.47116200	-4.44994700	-0.12668700
C	0.81723100	-4.17246900	-0.83411400
C	-0.43131300	-2.27794100	-0.01368200
C	-1.53682100	-3.09486000	0.18953100
C	-0.29370300	-4.98660900	-0.64635300
H	1.73881800	-4.59280800	-1.22875100
H	-0.49412800	-1.21848500	0.20543200
H	-2.45346500	-2.67146400	0.58751700
H	-0.23846800	-6.04170900	-0.89538300
C	0.24070900	-1.67887600	3.21009200
H	1.04236000	-2.12020600	2.62685500

C	-0.41844300	-2.39899800	4.18435200
H	-0.12781200	-3.42711900	4.37361600
C	-1.46095300	-1.82201200	4.93469600
H	-1.96261200	-2.40709100	5.69776300
C	-1.84031500	-0.51910600	4.70011500
H	-2.64100500	-0.06087000	5.27260300
C	-3.71064600	-1.92959300	-1.98983600
H	-2.81642000	-2.30864300	-2.47322500
C	-4.85908100	-2.68882600	-1.90518500
H	-4.87237800	-3.68176700	-2.34259700
C	-6.01046000	-2.19659000	-1.26174600
H	-6.90254900	-2.81117700	-1.20867500
C	-6.00282000	-0.93727500	-0.70344700
H	-6.88448400	-0.54297200	-0.20737000
C	6.56076100	-1.78914300	-0.39596200
H	6.27904400	-2.15015100	-1.39011800
H	7.62834300	-1.55048000	-0.40264500
H	6.38783700	-2.58963400	0.32981200
C	5.97295300	0.55912100	-1.05713600
H	5.35972700	1.43361100	-0.83394400
H	7.02607000	0.85713600	-1.04158200
H	5.73694800	0.20039500	-2.06353800
C	6.08029000	-0.09276400	1.39214900
H	7.15288400	0.11148400	1.46848800
H	5.53054800	0.81256900	1.65342900
H	5.83028800	-0.88206300	2.10824600
C	3.10687600	-0.75170700	-3.07089100
H	3.13939100	-0.36144300	-4.09604900
H	3.29248500	0.08469700	-2.39489300
H	3.91073600	-1.48414000	-2.96156800
H	1.53287500	-2.34485600	-3.23303200
H	-2.33716100	-5.08623300	0.02828600

Activated nitronate adds to an activated *N*-Boc *p*-OCF_3-arylaldimine

(*R*,*S*)-TS189$_{trans}$

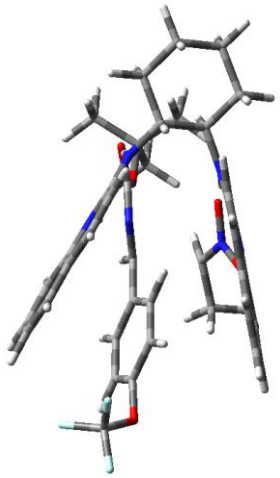

# opt=(calcfc,ts,noeigen) freq=noraman ωB97X-D/6-31g(d) scrf=(iefpcm,so
lvent=nitroethane) geom=connectivity temperature=253

Zero-point correction= 0.804720 (Hartree/Particle)
Thermal correction to Energy= 0.839418
Thermal correction to Enthalpy= 0.840219
Thermal correction to Gibbs Free Energy= 0.741662
Sum of electronic and zero-point Energies= -2515.132124
Sum of electronic and thermal Energies= -2515.097427
Sum of electronic and thermal Enthalpies= -2515.096625
Sum of electronic and thermal Free Energies= -2515.195182

Quasiharmonic free energy correction= 0.751948
SCF (wB97X-D/6-311+G**) = -2516.578595
SCF (B3LYP-D3/6-311+G**) = -2517.494824

1 1

C	-2.96354500	2.36411100	1.19210800
C	-0.85488900	1.35888100	2.06854100
N	-0.18293600	0.19750400	2.18624300
C	1.13185800	2.51874800	2.78920900
C	1.11684000	0.09857300	2.63985200
C	-0.16503100	2.57273200	2.38918100
C	1.82479900	1.27641000	2.93519400
H	-0.68250700	3.51955800	2.32397500
H	1.65747500	3.43999900	3.02161500
H	-0.60507400	-0.62790900	1.70915100
O	-2.33853000	-0.91801900	-1.94515700
N	-1.30616200	-1.45483400	-2.44338300
N	-2.12284000	1.28111200	1.67082200
H	-2.52450500	0.33704400	1.54712900
O	-0.40031000	-0.73308100	-2.97276800
C	-3.34078800	2.09796000	-0.28400600
C	-4.23547500	3.20941100	-0.84270400
C	-5.49902900	3.34510300	0.01199200
C	-5.15338300	3.58865700	1.48338200
C	-4.23782100	2.49162000	2.03350800
N	-2.19615600	1.76113500	-1.12599700
C	-1.07443800	2.44897700	-1.32753200
C	1.44418400	3.64622600	-1.75656600
C	-0.81607700	3.77886300	-0.86193300
N	-0.10095300	1.82911000	-2.02326300
C	1.14820100	2.36455100	-2.25439500
C	0.40402300	4.34025100	-1.06607500
H	-1.59595500	4.33290500	-0.36083400
H	0.59639000	5.34427700	-0.70064200
H	-0.28900400	0.87261900	-2.39429600
C	-1.12285900	-2.78222700	-2.29587900
N	-1.30286400	-1.76280500	0.45449900
C	-0.54091100	-2.67458700	-0.13266800
C	-2.63995300	-2.01180200	0.65370600
O	-3.35131000	-1.21074400	1.26318100
O	-3.08091700	-3.16378300	0.15569600
C	-4.50186400	-3.51967900	0.12590400
H	-2.20584500	0.79644300	-1.48850000

H	-2.41054100	3.30139700	1.26763100
H	-3.92931300	1.17260900	-0.28415700
H	-4.48862400	2.96865800	-1.87965500
H	-3.69858900	4.16554200	-0.85744200
H	-6.09173900	2.42479200	-0.07528000
H	-6.11842300	4.16114500	-0.37316000
H	-6.06704500	3.63782500	2.08415400
H	-4.65376200	4.56160700	1.58449100
H	-3.95656400	2.69999900	3.07049300
H	-4.76062000	1.52591500	2.02655800
H	-2.04087500	-3.29815400	-2.04952600
H	-0.82447500	-3.72708600	-0.12106300
C	-5.02888900	-3.69819900	1.54686400
H	-4.40533200	-4.41025100	2.09698700
H	-5.04320200	-2.74836000	2.08286600
H	-6.04776400	-4.09615600	1.50491000
C	-5.28027500	-2.47002100	-0.66339700
H	-4.79425700	-2.29045500	-1.62691900
H	-6.29560000	-2.83706700	-0.84357100
H	-5.34096100	-1.52604200	-0.11951900
C	-4.48997300	-4.85210600	-0.61758700
H	-4.09132600	-4.72678500	-1.62934500
H	-3.87340600	-5.58317700	-0.08576000
H	-5.50767400	-5.24570200	-0.69392900
C	0.89499700	-2.37883700	-0.28485300
C	3.59529100	-1.82934300	-0.54405600
C	1.83087500	-3.41680600	-0.25908700
C	1.33689000	-1.06194900	-0.45560900
C	2.68825400	-0.77897400	-0.58664900
C	3.18844600	-3.14606600	-0.37923900
H	1.49697300	-4.44271800	-0.13420300
H	0.61079900	-0.25862300	-0.47520400
H	3.03753000	0.23696200	-0.72607200
H	3.92748200	-3.93870200	-0.35487200
C	3.16862000	1.17809600	3.35052400
H	3.71664100	2.08810100	3.57552600
C	3.77235700	-0.05476200	3.45930600
H	4.81132300	-0.13011900	3.75977600
C	3.04287900	-1.22367200	3.17377200
H	3.52318200	-2.19180500	3.26354300
C	1.72435200	-1.15804000	2.77657400
H	1.16223200	-2.05831100	2.55329500
C	2.10978300	1.62622200	-2.96211600
H	1.86453200	0.63586000	-3.33231100
C	3.36167800	2.17524900	-3.15207200
H	4.11350300	1.60786800	-3.69084300
C	3.67818700	3.45431600	-2.65657900
H	4.66863800	3.86522600	-2.81824200
C	2.73049000	4.18169300	-1.97063500
H	2.95863300	5.17086500	-1.58558800
C	-0.03546600	-3.46784100	-3.05436400
H	0.11193500	-4.47249700	-2.64714300
H	-0.29303500	-3.56969700	-4.11600600
H	0.90656000	-2.91976000	-2.98427700
O	4.95470800	-1.58389400	-0.75541200
C	5.67252400	-1.09275300	0.27513600

F	6.93764600	-1.01657900	-0.11806300
F	5.60893100	-1.87549600	1.36052500
F	5.27311900	0.13161500	0.64631300

(*S,R*)-TS189$_{anti}$

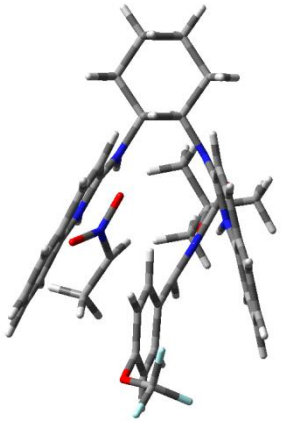

---

opt=calcfc freq=noraman ωB97X-D/6-31g(d) scrf=(iefpcm,solvent=nitroethane) geom=connectivity temperature=253

Zero-point correction= 0.804911 (Hartree/Particle)
Thermal correction to Energy= 0.839515
Thermal correction to Enthalpy= 0.840317
Thermal correction to Gibbs Free Energy= 0.741075
Sum of electronic and zero-point Energies= -2515.128926
Sum of electronic and thermal Energies= -2515.094321
Sum of electronic and thermal Enthalpies= -2515.093520
Sum of electronic and thermal Free Energies= -2515.192762

Quasiharmonic free energy correction= 0.751850
SCF (wB97X-D/6-311+G**) = -2516.576421
SCF (B3LYP-D3/6-311+G**) = -2517.492571

1 1

C	2.08412300	3.29234200	-0.19966200
C	-0.05615300	2.67050100	-1.27719400
N	-0.71486600	1.75415100	-2.00644600
C	-2.10657800	3.93135500	-1.11352800
C	-2.05815900	1.82518500	-2.30881300
C	-0.78024300	3.82653800	-0.83810400
C	-2.80499300	2.92311500	-1.84680900
H	-0.26987100	4.61094200	-0.29699700
H	-2.65467100	4.80356200	-0.77066000
H	-0.19089200	0.91887900	-2.35724200
N	1.22723000	2.43043200	-1.00037800
H	1.62964000	1.54799100	-1.34908100
H	1.44402200	3.88716100	0.45415600
C	3.02118300	2.44171400	0.67923700
C	3.85849100	3.34336700	1.59436800
H	3.20186200	3.88917400	2.28422100
H	4.51262700	2.71292200	2.20415200

C	4.67683000	4.33329300	0.76098500
H	5.40674200	3.77587800	0.15908900
H	5.24763400	4.99104100	1.42384900
C	3.78057800	5.15900600	-0.16560400
H	3.13025000	5.80679000	0.43788700
H	4.38844200	5.81716000	-0.79433300
C	2.91345900	4.25980200	-1.05232800
H	3.54344200	3.67676300	-1.73627300
H	2.23554200	4.85991200	-1.66857800
N	2.35248800	1.34669500	1.37422500
C	1.18162500	1.34415200	2.01288700
C	-1.33567900	1.07954900	3.25042400
C	0.48794700	2.50219500	2.48768400
N	0.61671400	0.13965000	2.22110500
C	-0.60626300	-0.04657500	2.82852500
C	-0.73248400	2.36176000	3.07012400
H	0.95432900	3.47373700	2.41143800
H	-1.25932700	3.24244800	3.42463600
N	1.72714300	-1.79976900	0.48765600
C	3.08868800	-1.93534300	0.63140800
O	3.73466000	-1.12358400	1.29186100
O	3.62361400	-2.97829100	0.00008000
C	5.07328000	-3.17748200	-0.10897200
H	2.80816400	0.43188000	1.26890200
C	1.05201900	-2.65007800	-0.26681700
H	1.43525700	-3.65054700	-0.46546700
C	1.70678300	-2.27490000	-2.39786000
H	2.71918900	-2.53355000	-2.12145500
N	1.47630400	-0.95001000	-2.38999200
O	0.43214300	-0.49183800	-2.96309300
O	2.23746400	-0.17717700	-1.73377600
H	3.71225500	1.92665400	0.00110500
H	1.04092500	-0.66648200	1.70465000
C	-0.40225500	-2.45132700	-0.37923000
C	-3.14287700	-2.07468900	-0.42625000
C	-1.25881900	-3.54467500	-0.53744700
C	-0.94336500	-1.16361400	-0.29367500
C	-2.31495000	-0.96663200	-0.30555900
C	-2.63637500	-3.36056800	-0.55555300
H	-0.84811400	-4.54624400	-0.62303900
H	-0.27353900	-0.31671500	-0.20390700
H	-2.74155300	0.02487900	-0.21803100
H	-3.31743900	-4.19778800	-0.65807200
C	-1.13045300	-1.34016200	2.97671000
H	-0.55620100	-2.19706600	2.63989700
C	-2.38660800	-1.49226900	3.52334600
H	-2.80736600	-2.48688200	3.62256700
C	-3.13368600	-0.37654900	3.94721800
H	-4.12089600	-0.52072600	4.37184700
C	-2.61189400	0.89117000	3.82086900
H	-3.17476000	1.75994900	4.14841600
C	-2.66802900	0.79307100	-3.04026000
H	-2.07535900	-0.05318400	-3.37187000
C	-4.02233300	0.86668800	-3.28978400
H	-4.50487700	0.06666400	-3.84159500
C	-4.78783900	1.95724100	-2.83399600

H	-5.85176500	1.99301800	-3.04137500
C	-4.18665600	2.97398800	-2.12546700
H	-4.76462500	3.82147400	-1.76969700
C	5.16826300	-4.42283000	-0.98487100
H	4.70432500	-4.24712100	-1.96064000
H	6.21848600	-4.68399000	-1.14374400
H	4.66753500	-5.26976000	-0.50609300
C	5.70607500	-1.97526000	-0.80539500
H	5.64867800	-1.08059600	-0.18356100
H	6.75864100	-2.19274600	-1.01098500
H	5.20329900	-1.77784300	-1.75777300
C	5.67244900	-3.43690800	1.26993000
H	6.72873800	-3.70076500	1.15705400
H	5.59736500	-2.55323500	1.90479000
H	5.16001200	-4.27304100	1.75628900
C	0.89370500	-3.15567600	-3.28638200
H	1.13220100	-4.20193700	-3.07476600
H	-0.17681700	-2.99964300	-3.12596400
H	1.10344200	-2.96658900	-4.34640900
O	-4.52820000	-1.90642200	-0.48818400
C	-5.16993300	-1.63886800	0.66881000
F	-4.89842000	-2.53931200	1.62166400
F	-4.85887500	-0.43296100	1.16624500
F	-6.47278800	-1.66125300	0.41949000

(*R*,*R*)-TS189$_{syn}$

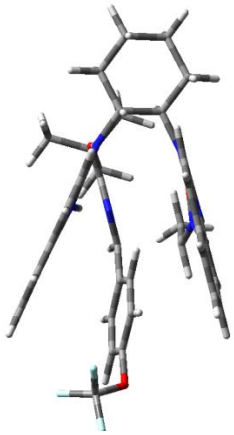

# opt=(calcfc,ts,noeigen) freq=noraman ωB97X-D/6-31g(d) scrf=(iefpcm,so
lvent=nitroethane) geom=connectivity temperature=253

Zero-point correction= 0.804778 (Hartree/Particle)
Thermal correction to Energy= 0.839548
Thermal correction to Enthalpy= 0.840349
Thermal correction to Gibbs Free Energy= 0.740876
Sum of electronic and zero-point Energies= -2515.125781
Sum of electronic and thermal Energies= -2515.091011
Sum of electronic and thermal Enthalpies= -2515.090210
Sum of electronic and thermal Free Energies= -2515.189683

Quasiharmonic free energy correction= 0.751941
SCF (wB97X-D/6-311+G**) = -2516.573011
SCF (B3LYP-D3/6-311+G**) = -2517.489455

1 1

C	-2.98179000	2.35878000	1.17536100
C	-0.85164500	1.34112800	1.99647200
N	-0.16774100	0.18046100	2.04793000
C	1.12070300	2.47405200	2.79517800
C	1.12479900	0.06432300	2.51908100
C	-0.17295500	2.54087100	2.38693500
C	1.81990600	1.22941000	2.88676000
H	-0.69800900	3.48587900	2.36846000
H	1.63798300	3.38488500	3.08115400
H	-0.57319800	-0.62075700	1.52261400
O	-2.27242800	-0.73568200	-2.26635000
N	-1.17853500	-1.22526400	-2.65908100
N	-2.11804700	1.27042200	1.59690300
H	-2.50183700	0.32595300	1.42463100
O	-0.19358900	-0.46301700	-2.92862100
C	-3.34512700	2.15866900	-0.31556400
C	-4.27299900	3.26614200	-0.82504500
C	-5.54201900	3.32044000	0.03085600
C	-5.20683100	3.50355000	1.51348600
C	-4.26271300	2.40728500	2.01503200
N	-2.18120900	1.90307200	-1.16106300
C	-1.05985200	2.61841700	-1.25476100
C	1.45160600	3.88314700	-1.46090900
C	-0.86988800	3.93810800	-0.73166700
N	-0.02479900	2.04194900	-1.89237300
C	1.22299600	2.61232300	-2.01889000
C	0.34854300	4.53196200	-0.82793400
H	-1.69990000	4.46065700	-0.27971100
H	0.48958900	5.52853800	-0.42095700
H	-0.16427600	1.08763500	-2.29522500
C	-0.98575300	-2.56323500	-2.66713300
N	-1.25401200	-1.72119200	0.18051600
C	-0.51208300	-2.61313900	-0.46208100
C	-2.56052400	-2.01789200	0.49667700
O	-3.25393600	-1.21829100	1.12856000
O	-2.99486000	-3.21389400	0.11275000
C	-4.35361900	-3.68713700	0.39992900
H	-2.15843200	0.96531900	-1.58349500
H	-2.45200000	3.30326700	1.30648400
H	-3.90284200	1.21592500	-0.36657800
H	-4.51567800	3.06578700	-1.87297900
H	-3.76735800	4.23846200	-0.79336500
H	-6.10457900	2.38684700	-0.10258900
H	-6.18676900	4.13375500	-0.31660700
H	-6.12305300	3.49935800	2.11241000
H	-4.73437300	4.48402600	1.66216500
H	-3.99278200	2.57225600	3.06269400
H	-4.75771800	1.42880400	1.95647400
H	-0.83021800	-3.65431200	-0.51699200
C	-4.54385000	-3.82116000	1.90863700
H	-3.76059000	-4.45673500	2.33402300

H	-4.51971800	-2.84698200	2.39882800
H	-5.51210800	-4.29077300	2.10819500
C	-5.38508100	-2.75964200	-0.23839400
H	-5.17126800	-2.62287800	-1.30336400
H	-6.37629500	-3.21453800	-0.14593500
H	-5.39932500	-1.78410600	0.24851500
C	-4.37967300	-5.05888900	-0.26746000
H	-4.23528100	-4.96819600	-1.34770700
H	-3.59207900	-5.70069300	0.13893900
H	-5.34635500	-5.53806600	-0.08712400
C	0.93694700	-2.36075300	-0.58154800
C	3.66811700	-1.92937500	-0.74020700
C	1.81810900	-3.44223600	-0.68757400
C	1.45119100	-1.05957600	-0.57255900
C	2.81855600	-0.83579000	-0.65502700
C	3.18888600	-3.23279400	-0.75729000
H	1.42815700	-4.45595500	-0.70385300
H	0.77226400	-0.22058700	-0.48828900
H	3.22171000	0.16983600	-0.65000300
H	3.88552600	-4.06062600	-0.82620600
C	3.15554600	1.11623300	3.32376500
H	3.69454700	2.01605700	3.60456800
C	3.76216300	-0.11884000	3.38750800
H	4.79377100	-0.20498300	3.70986900
C	3.04446100	-1.27529800	3.03133600
H	3.52711600	-2.24468700	3.08577900
C	1.73550000	-1.19495600	2.60554900
H	1.18301400	-2.08508800	2.32392700
C	2.24967600	1.91985200	-2.68045400
H	2.05404100	0.93936100	-3.10281800
C	3.49759600	2.50261200	-2.76493900
H	4.29909300	1.97152400	-3.26801700
C	3.74672000	3.77185400	-2.20841800
H	4.73502000	4.21081900	-2.28950800
C	2.73612500	4.45447900	-1.56844400
H	2.91229900	5.43584300	-1.13879200
H	-0.02691400	-2.83031300	-3.09321000
C	-2.14929500	-3.48429700	-2.85758000
H	-2.33609800	-3.64457700	-3.92689700
H	-1.94156900	-4.45922400	-2.40691800
H	-3.04801500	-3.07656700	-2.39882700
O	5.04502900	-1.73662300	-0.88678200
C	5.74980300	-1.39742600	0.21167700
F	5.57412200	-2.26298700	1.21894300
F	7.03421200	-1.38971800	-0.12174400
F	5.43051800	-0.18101200	0.67700000

(*S*,*S*)-TS189$_{syn}$

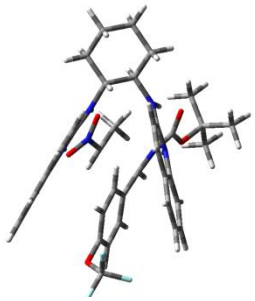

---

opt=(calcfc,ts,noeigen) freq=noraman ωB97X-D/6-31g(d) scrf=(iefpcm,solvent=nitroethane) geom=connectivity temperature=253

Zero-point correction= 0.804277 (Hartree/Particle)
Thermal correction to Energy= 0.839112
Thermal correction to Enthalpy= 0.839913
Thermal correction to Gibbs Free Energy= 0.740577
Sum of electronic and zero-point Energies= -2515.123506
Sum of electronic and thermal Energies= -2515.088671
Sum of electronic and thermal Enthalpies= -2515.087870
Sum of electronic and thermal Free Energies= -2515.187206

Quasiharmonic free energy correction= 0.751536
SCF (wB97X-D/6-311+G**) = -2516.571146
SCF (B3LYP-D3/6-311+G**) = -2517.487563

1 1

C	1.47469100	3.63365000	-0.03743100
C	-0.68693400	2.78847600	-0.91461800
N	-1.28307000	1.91750600	-1.74822800
C	-2.87240200	3.56437100	-0.25158000
C	-2.64938700	1.78334200	-1.87943800
C	-1.52155700	3.67369800	-0.15773100
C	-3.49200100	2.60094700	-1.10623400
H	-1.07562700	4.41693300	0.48813000
H	-3.50294100	4.22282500	0.33805700
H	-0.68661200	1.24975400	-2.28567400
N	0.64368500	2.74656900	-0.83590700
H	1.12660100	2.04176400	-1.41341700
H	0.86645800	4.02309400	0.78004300
C	2.66444500	2.85646900	0.56081300
C	3.49382700	3.76797600	1.47316500
H	2.88691400	4.08911800	2.32952600
H	4.33379600	3.19239400	1.87335000
C	3.99334200	4.99167600	0.69871900
H	4.69890900	4.66133500	-0.07514500
H	4.54850000	5.65199000	1.37225000
C	2.83819000	5.75149000	0.04137900
H	2.19799900	6.18737900	0.82015100
H	3.22251000	6.58440900	-0.55562400
C	1.99293100	4.83116500	-0.84333000
H	2.58702400	4.46052600	-1.68873200
H	1.13692700	5.37149500	-1.26095000
N	2.29145800	1.58435100	1.17581900
C	1.22473900	1.31149600	1.93162200

C	-1.07988000	0.50341200	3.33914500
C	0.45040700	2.27162500	2.65786900
N	0.85659900	0.01976500	2.00761300
C	-0.25572200	-0.43021000	2.68595200
C	-0.66926000	1.87170600	3.31782100
H	0.77918000	3.29993900	2.70352600
H	-1.26102600	2.60438700	3.85816800
N	1.99808700	-1.49578900	-0.07268500
C	3.33984700	-1.64941600	0.19758900
O	3.96188300	-0.75368100	0.76563800
O	3.85678000	-2.82657000	-0.14704500
C	5.26126700	-3.17441200	0.09022300
H	2.84071600	0.77297300	0.87010400
C	1.38339700	-2.28540400	-0.93682700
H	1.86707900	-3.19070300	-1.30355000
C	1.82261800	-1.47202300	-2.99240400
N	1.29340800	-0.24727600	-2.78185600
O	0.07609000	-0.03149800	-3.08583300
O	1.97150100	0.64271500	-2.19312800
H	3.30307900	2.55774100	-0.27910500
H	1.31003300	-0.63122100	1.32479600
C	-0.08955800	-2.26845700	-0.94722100
C	-2.85104600	-2.31021100	-0.72304600
C	-0.80810100	-3.41045600	-1.31206800
C	-0.78695500	-1.13419300	-0.52068400
C	-2.16632000	-1.14925700	-0.39183200
C	-2.19296900	-3.43765000	-1.19674300
H	-0.28195100	-4.29403800	-1.66127200
H	-0.23556900	-0.23441000	-0.27836300
H	-2.70067300	-0.27645200	-0.03981000
H	-2.76298000	-4.32278800	-1.45574200
C	-0.58380000	-1.79445500	2.66882600
H	0.06232800	-2.49790300	2.15383200
C	-1.74788100	-2.20726000	3.28066700
H	-2.02007300	-3.25676300	3.25239900
C	-2.59115700	-1.28663900	3.93165200
H	-3.50410800	-1.63437900	4.40220600
C	-2.25683900	0.04875100	3.97006900
H	-2.89457300	0.76733100	4.47561100
C	-3.17977500	0.81538800	-2.74715000
H	-2.51165000	0.18637800	-3.32581600
C	-4.54877900	0.66407900	-2.81683600
H	-4.96659900	-0.09042500	-3.47506800
C	-5.40901000	1.46753000	-2.04423100
H	-6.48222000	1.32828600	-2.11458800
C	-4.88820700	2.42666600	-1.20416700
H	-5.54003000	3.05470500	-0.60455500
C	5.35820300	-4.57807200	-0.49893900
H	5.11925800	-4.56485200	-1.56697300
H	6.37473100	-4.96284900	-0.37560900
H	4.66554300	-5.25712400	0.00738900
C	6.18203100	-2.21319300	-0.65672600
H	6.10167700	-1.19998700	-0.26062000
H	7.21653100	-2.55240200	-0.54430800
H	5.94167700	-2.20239400	-1.72433000
C	5.53736700	-3.19714800	1.59118200

H	6.54325700	-3.59137700	1.76628000
H	5.47280300	-2.19639300	2.02088400
H	4.82030400	-3.85082900	2.09806600
O	-4.24503900	-2.35781700	-0.66274900
C	-4.83099100	-2.26947900	0.54914100
F	-4.33291000	-3.15392100	1.42173400
F	-4.70284900	-1.05421500	1.10468300
F	-6.12540700	-2.51138200	0.38537000
C	3.31026600	-1.60377900	-3.07151300
H	3.68863300	-1.21329900	-4.02485200
H	3.79704100	-1.04436100	-2.27061300
H	3.59834800	-2.65535000	-2.99727800
H	1.18415100	-2.10306400	-3.59773100

Activated nitronate adds to an activated *N*-Boc *p*-Cl-arylaldimine

(*R*,*S*)-TS190$_{trans}$

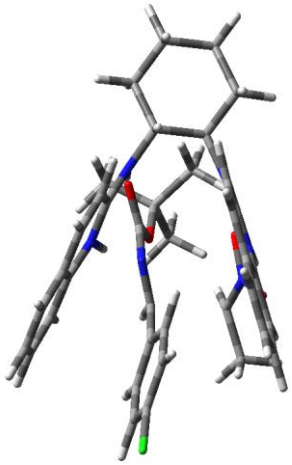

# opt=(calcfc,ts,noeigen) freq=noraman ωB97X-D/6-31g(d) scrf=(iefpcm,so
lvent=nitroethane) geom=connectivity temperature=253

Zero-point correction= 0.785518 (Hartree/Particle)
Thermal correction to Energy= 0.817803
Thermal correction to Enthalpy= 0.818604
Thermal correction to Gibbs Free Energy= 0.725591
Sum of electronic and zero-point Energies= -2562.578195
Sum of electronic and thermal Energies= -2562.545910
Sum of electronic and thermal Enthalpies= -2562.545109
Sum of electronic and thermal Free Energies= -2562.638123

Quasiharmonic free energy correction= 0.734587
SCF (B3LYP/6-31G*) = -2563.994162
SCF (wB97X-D/6-311+G**) = -2563.908378
SCF (B3LYP-D3/6-311+G**) = -2564.724095

1 1

C	-2.30878600	2.66308900	1.00615900

C	-0.40116800	1.44473300	2.04888700
N	0.12340600	0.21983100	2.24710800
C	1.65478400	2.40044000	2.86920700
C	1.37361800	-0.00761300	2.78742800
C	0.40019900	2.58452500	2.38402000
C	2.19292000	1.09389100	3.09094700
H	-0.00431700	3.57974400	2.26246600
H	2.26505400	3.26453500	3.11413600
H	-0.36449400	-0.56863800	1.77213400
O	-1.96801300	-0.84445300	-1.98323500
N	-0.98217600	-1.52041100	-2.39983400
N	-1.63814800	1.50047000	1.56145800
H	-2.14541600	0.60801400	1.44172600
O	0.02288500	-0.93312300	-2.91897400
C	-2.67254100	2.38064100	-0.46996100
C	-3.38114500	3.57971300	-1.10925000
C	-4.63348500	3.94335800	-0.30618100
C	-4.29786100	4.20580800	1.16436600
C	-3.57378000	3.01348600	1.79539700
N	-1.55598600	1.85466400	-1.25148400
C	-0.34189700	2.37528300	-1.42631500
C	2.33866600	3.18960100	-1.77479300
C	0.08081100	3.67740200	-1.00311400
N	0.56400900	1.59775000	-2.04985500
C	1.88499600	1.94182400	-2.23870600
C	1.37666000	4.05281100	-1.16714100
H	-0.63424000	4.35973300	-0.56825800
H	1.69232600	5.03659200	-0.83324900
H	0.26633800	0.65762600	-2.39334400
C	-0.95384900	-2.84863100	-2.17874900
N	-1.14311700	-1.65496000	0.50403000
C	-0.46146600	-2.67722300	0.00834700
C	-2.50832500	-1.74041600	0.64053000
O	-3.14969900	-0.83189400	1.17181000
O	-3.05595200	-2.85969500	0.17483100
C	-4.50653100	-3.04740600	0.08587300
H	-1.67762400	0.88324800	-1.57172700
H	-1.62985300	3.51536500	1.05469700
H	-3.38469200	1.54720500	-0.45649800
H	-3.63812200	3.32661000	-2.14227400
H	-2.70926700	4.44570800	-1.14879200
H	-5.35704300	3.12002300	-0.37316200
H	-5.11052500	4.82304800	-0.74951100
H	-5.21090200	4.42143700	1.72823300
H	-3.65968900	5.09674300	1.23953000
H	-3.29518900	3.22774000	2.83196600
H	-4.23377000	2.13583300	1.81094300
H	-1.93155800	-3.25119200	-1.95199000
H	-0.86355100	-3.68924500	0.05424600
C	-5.11277900	-3.10136800	1.48539100
H	-4.61757500	-3.87236000	2.08438600
H	-5.01801800	-2.13971200	1.99158700
H	-6.17458300	-3.35566300	1.40754400
C	-5.11764300	-1.94851500	-0.77985800
H	-4.57341100	-1.87108500	-1.72568500
H	-6.16208100	-2.19722400	-0.99258600

H	-5.08313700	-0.98176000	-0.27525200
C	-4.62412400	-4.40275700	-0.60474000
H	-4.17414000	-4.36899200	-1.60202300
H	-4.12234700	-5.17924500	-0.01924500
H	-5.67855500	-4.67345900	-0.71149400
C	1.00468900	-2.54678200	-0.06429800
C	3.76764900	-2.29052300	-0.06166900
C	1.81798400	-3.67224300	0.09191100
C	1.60171800	-1.29572100	-0.25274100
C	2.98188400	-1.15845900	-0.24847100
C	3.20262700	-3.55066800	0.10283200
H	1.36734200	-4.65110600	0.22729400
H	0.97420500	-0.42147800	-0.37483700
H	3.44172800	-0.18516000	-0.37552700
H	3.83266900	-4.42157500	0.24340900
C	3.48936500	0.86236300	3.59353700
H	4.12234300	1.71296700	3.82773300
C	3.94116600	-0.42578800	3.78072800
H	4.94104400	-0.60307900	4.16148300
C	3.10053100	-1.51548800	3.48699300
H	3.45948800	-2.52778100	3.64091000
C	1.82423600	-1.31806200	3.00329100
H	1.17717700	-2.15765700	2.77364500
C	2.76096800	1.04322000	-2.86820800
H	2.39157900	0.08208900	-3.21107500
C	4.08565300	1.39957600	-3.01462600
H	4.77220300	0.70739700	-3.49095800
C	4.56025900	2.64176800	-2.55153800
H	5.60631800	2.89834700	-2.67799600
C	3.69744000	3.52671100	-1.94322100
H	4.04959700	4.48923300	-1.58470000
C	0.09034300	-3.68648400	-2.83864200
H	1.08268600	-3.24360400	-2.72969100
H	0.09723700	-4.68111000	-2.38333600
H	-0.11302500	-3.80776500	-3.90996300
Cl	5.50914100	-2.11970500	-0.02306100

(*S*,*R*)-TS190$_{trans}$

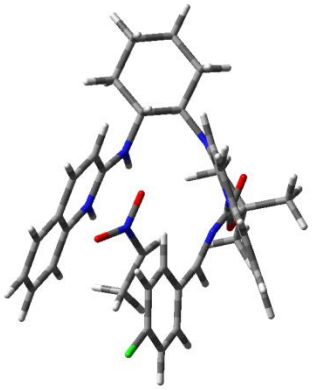

# opt=(calcfc,ts,noeigen) freq=noraman ωB97X-D/6-31g(d) scrf=(iefpcm,so
lvent=nitroethane) geom=connectivity temperature=253

Zero-point correction= 0.785325 (Hartree/Particle)
Thermal correction to Energy= 0.817896
Thermal correction to Enthalpy= 0.818698
Thermal correction to Gibbs Free Energy= 0.724266
Sum of electronic and zero-point Energies= -2562.575408
Sum of electronic and thermal Energies= -2562.542837
Sum of electronic and thermal Enthalpies= -2562.542036
Sum of electronic and thermal Free Energies= -2562.636468

Quasiharmonic free energy correction= 0.734082
SCF (B3LYP/6-31G*) = -2563.994457
SCF (wB97X-D/6-311+G**) = -2563.906099
SCF (B3LYP-D3/6-311+G**) = -2564.722367

1 1

C	0.68594100	3.47058400	-0.58201600
C	-1.31231500	2.18860700	-1.26545400
N	-1.78487700	1.06436300	-1.82934900
C	-3.58829500	2.92720500	-0.96043800
C	-3.12502200	0.77734400	-1.97714900
C	-2.25834000	3.17336500	-0.83157500
C	-4.07636400	1.71029400	-1.52806200
H	-1.91147100	4.10650600	-0.41016300
H	-4.30413500	3.67151100	-0.62537600
H	-1.10175200	0.35498500	-2.18234900
N	0.01054800	2.30389100	-1.13145300
H	0.59286500	1.52797300	-1.48031700
H	0.02570300	3.91699500	0.16497000
C	1.98986400	3.04781700	0.11989200
C	2.66636300	4.26018600	0.77231800
H	2.02672300	4.66016300	1.56901800
H	3.59595800	3.92838900	1.24433500
C	2.94187300	5.34982400	-0.26837200
H	3.68144100	4.97821000	-0.99012700
H	3.38662400	6.22173600	0.22138800
C	1.66615100	5.75105100	-1.01352100
H	0.96929200	6.23199300	-0.31380500
H	1.89572000	6.48845100	-1.78896100
C	0.98535900	4.53410300	-1.64484100
H	1.63006100	4.09289000	-2.41564600
H	0.04857900	4.82290500	-2.13352400
N	1.82257900	1.90730900	1.01682600
C	0.83752700	1.67273400	1.88808900
C	-1.21020100	0.91271000	3.66906100
C	-0.03003400	2.66124200	2.45224300
N	0.66129500	0.39227000	2.26157700
C	-0.31719200	-0.03268200	3.13298300
C	-1.02020300	2.27981100	3.30240500
H	0.13232600	3.70657800	2.23228100
H	-1.67732500	3.03165500	3.72874200
N	1.88954500	-1.41042700	0.48984700
C	3.24870700	-1.20797300	0.42993200
O	3.75322700	-0.19076000	0.90180800
O	3.93596600	-2.17258200	-0.17840100
C	5.37737300	-2.08039500	-0.43263800

H	2.47788900	1.13122600	0.86761100
C	1.35030500	-2.47587100	-0.07904100
H	1.93944600	-3.37440600	-0.26050000
C	1.60262900	-2.19390900	-2.30472400
H	2.67386900	-2.13796900	-2.17026100
N	1.00950200	-0.98771200	-2.35565500
O	-0.18869400	-0.89446000	-2.78338600
O	1.60417100	0.02940900	-1.88806800
H	2.66523900	2.66950200	-0.65691000
H	1.17317800	-0.33320700	1.70258300
C	-0.10825400	-2.63911500	0.01974400
C	-2.85273000	-2.94074800	0.30829100
C	-0.68360500	-3.91282600	0.00829400
C	-0.93804100	-1.51864800	0.14211500
C	-2.30727700	-1.66132400	0.30377800
C	-2.05722500	-4.07171300	0.15367000
H	-0.05379000	-4.79108400	-0.09948000
H	-0.49843800	-0.52838700	0.11498300
H	-2.94423500	-0.79277100	0.42520200
H	-2.50250800	-5.06003700	0.15435700
C	-0.44083500	-1.39652700	3.44143600
H	0.25290900	-2.11226500	3.01267700
C	-1.46097700	-1.80054000	4.27610400
H	-1.57060800	-2.85426000	4.51040800
C	-2.36295000	-0.86842400	4.82497200
H	-3.15546800	-1.20944800	5.48209100
C	-2.23658400	0.47063800	4.52957400
H	-2.92411100	1.20022400	4.94657200
C	-3.52309600	-0.44289500	-2.54681900
H	-2.77189400	-1.15465100	-2.87304700
C	-4.87048100	-0.71501500	-2.65877000
H	-5.18776700	-1.65776500	-3.09215000
C	-5.83847000	0.20721400	-2.21634100
H	-6.89230600	-0.02872900	-2.31606100
C	-5.44680800	1.40454800	-1.65991800
H	-6.18211300	2.12491300	-1.31468500
C	5.66052300	-3.37428800	-1.18935500
H	5.09212300	-3.40866100	-2.12425700
H	6.72589500	-3.43803000	-1.42883000
H	5.38848300	-4.24265400	-0.58155300
C	5.67380300	-0.86556000	-1.30811800
H	5.48368800	0.06623000	-0.77387500
H	6.72576600	-0.88986300	-1.60914600
H	5.05805400	-0.88794000	-2.21348100
C	6.13810200	-2.04898800	0.88970800
H	5.84354000	-2.89660700	1.51669600
H	7.21114500	-2.12818100	0.68937700
H	5.95040300	-1.12121300	1.43181400
C	0.96997000	-3.35483500	-2.99593100
H	-0.07294600	-3.48024800	-2.69204900
H	0.98774900	-3.23381500	-4.08613500
H	1.52078600	-4.26637200	-2.74702000
Cl	-4.58101300	-3.12630600	0.50454500

(*R*,*R*)-TS190$_{syn}$

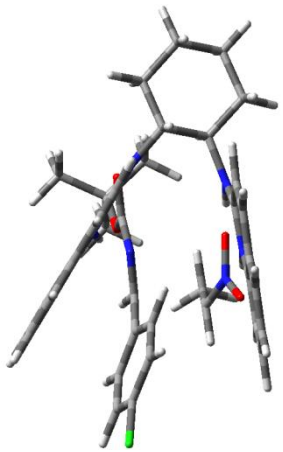

---

opt=(calcfc,ts,noeigen) freq=noraman ωB97X-D/6-31g(d) scrf=(iefpcm,solvent=nitroethane) geom=connectivity temperature=253

Zero-point correction= 0.786056 (Hartree/Particle)
Thermal correction to Energy= 0.818366
Thermal correction to Enthalpy= 0.819168
Thermal correction to Gibbs Free Energy= 0.726013
Sum of electronic and zero-point Energies= -2562.571584
Sum of electronic and thermal Energies= -2562.539274
Sum of electronic and thermal Enthalpies= -2562.538472
Sum of electronic and thermal Free Energies= -2562.631627

Quasiharmonic free energy correction= 0.735261
SCF (B3LYP/6-31G*) = -2563.989231
SCF (wB97X-D/6-311+G**) = -2563.902930
SCF (B3LYP-D3/6-311+G**) = -2564.718832

1 1

C	-2.00681800	2.84848300	1.05007800
C	-0.25071800	1.35550200	2.01213300
N	0.11720900	0.06406000	2.13194400
C	1.89611600	1.99095100	2.90638100
C	1.31575300	-0.35319200	2.67601600
C	0.68263600	2.36223400	2.42272200
C	2.25970500	0.61548600	3.05825400
H	0.41312000	3.40700000	2.35232400
H	2.60802700	2.75420700	3.20553400
H	-0.44424100	-0.62417700	1.59256400
O	-1.89002800	-0.40323400	-2.35603600
N	-0.92306000	-1.15409600	-2.66034100
N	-1.46662000	1.58734600	1.52629700
H	-2.06315000	0.76529200	1.33413100
O	0.22897400	-0.65677600	-2.88583500
C	-2.34302700	2.71366100	-0.45398600
C	-2.93808200	4.00825400	-1.01873500
C	-4.18157500	4.40948400	-0.21952700
C	-3.86788200	4.53697400	1.27342600

C	-3.26391200	3.24505300	1.83055900
N	-1.24036300	2.16062700	-1.23755300
C	0.02377200	2.58343100	-1.28975000
C	2.77582100	3.19583100	-1.39218000
C	0.50875000	3.82671300	-0.76878100
N	0.91285300	1.76403800	-1.87947100
C	2.26666800	2.00931100	-1.95019900
C	1.83824900	4.10493100	-0.81541900
H	-0.18544600	4.54464300	-0.35814400
H	2.20115300	5.04470300	-0.41041700
H	0.56649700	0.86343900	-2.28291300
C	-1.05438200	-2.49797900	-2.62074800
N	-1.29224300	-1.52110300	0.18833800
C	-0.72776200	-2.57546500	-0.38411200
C	-2.64753900	-1.51037700	0.43048000
O	-3.18090700	-0.54431400	0.97944500
O	-3.30836700	-2.60693300	0.07407900
C	-4.74861400	-2.77251800	0.29749600
H	-1.42605100	1.23566800	-1.64759400
H	-1.25750200	3.62842400	1.19155100
H	-3.11634900	1.93995300	-0.52539000
H	-3.18456900	3.84859700	-2.07275200
H	-2.20210100	4.82018900	-0.98177200
H	-4.96254100	3.65078800	-0.36339400
H	-4.57910400	5.35266000	-0.60746800
H	-4.77554000	4.78776100	1.83141500
H	-3.16011700	5.36248700	1.42849400
H	-3.00188800	3.35941000	2.88702300
H	-3.99422200	2.42772000	1.76303000
H	-1.26068600	-3.52450000	-0.44261000
C	-5.04475600	-2.75542600	1.79490100
H	-4.42855500	-3.49810500	2.31172800
H	-4.85466700	-1.77151800	2.22594300
H	-6.09677000	-3.01085600	1.95574000
C	-5.52840200	-1.70313800	-0.46341000
H	-5.24630600	-1.70088900	-1.52120200
H	-6.59758000	-1.92799900	-0.39737800
H	-5.35378400	-0.71079100	-0.04635900
C	-5.01856300	-4.15560300	-0.28751000
H	-4.79711000	-4.17549600	-1.35854200
H	-4.40406200	-4.91069600	0.21210200
H	-6.07179500	-4.41531400	-0.14676000
C	0.74565700	-2.64380400	-0.40303100
C	3.51476200	-2.80466300	-0.29026600
C	1.38246900	-3.88843900	-0.39969500
C	1.52438100	-1.48215100	-0.37789600
C	2.90887100	-1.55476300	-0.31921800
C	2.76746300	-3.97798400	-0.33448700
H	0.79111500	-4.79940600	-0.42860700
H	1.03670400	-0.51599900	-0.37778200
H	3.50699400	-0.65147600	-0.27859500
H	3.25870900	-4.94414600	-0.31149200
C	3.50450000	0.18998100	3.56500300
H	4.23593900	0.93648700	3.85879700
C	3.78262200	-1.15442800	3.68361800
H	4.74212000	-1.48085100	4.06981100

C	2.81787100	-2.10865500	3.31146300
H	3.03989000	-3.16584500	3.41252000
C	1.59038500	-1.72092300	2.81662500
H	0.84927700	-2.45487000	2.51873600
C	3.12024300	1.07266500	-2.55503500
H	2.70858000	0.16002900	-2.97384300
C	4.47540300	1.32973800	-2.58286900
H	5.14371400	0.60690500	-3.03929900
C	5.00405400	2.51068300	-2.02707900
H	6.07285100	2.69080800	-2.06333600
C	4.16481500	3.43303500	-1.44235400
H	4.55816100	4.34933700	-1.01289600
H	-0.16557800	-3.00307000	-2.97731700
C	-2.39390500	-3.12394500	-2.84825900
H	-2.43168800	-4.11554700	-2.38808200
H	-3.18754300	-2.51460400	-2.42018800
H	-2.58044000	-3.24781400	-3.92255400
Cl	5.25967900	-2.90248600	-0.18118500

(*S*,*S*)-TS190$_{syn}$

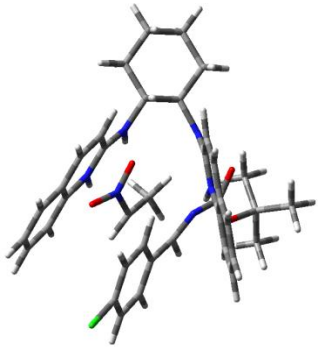

# opt=(calcfc,ts,noeigen) freq=noraman ωB97X-D/6-31g(d) scrf=(iefpcm,so
lvent=nitroethane) geom=connectivity temperature=253

Zero-point correction= 0.786583 (Hartree/Particle)
Thermal correction to Energy= 0.818723
Thermal correction to Enthalpy= 0.819524
Thermal correction to Gibbs Free Energy= 0.726826
Sum of electronic and zero-point Energies= -2562.569135
Sum of electronic and thermal Energies= -2562.536995
Sum of electronic and thermal Enthalpies= -2562.536194
Sum of electronic and thermal Free Energies= -2562.628892

Quasiharmonic free energy correction= 0.735820
SCF (B3LYP/6-31G*) = -2563.991954
SCF (wB97X-D/6-311+G**) = -2563.901493
SCF (B3LYP-D3/6-311+G**) = -2564.718086

1 1

C	0.03165200	3.66693000	-0.55979300
C	-1.88280700	2.14051800	-0.95919200
N	-2.28703300	0.98798900	-1.52202300
C	-4.12649600	2.46218600	-0.13508600

C	-3.57367900	0.49935000	-1.44417200
C	-2.85204700	2.91952200	-0.24777700
C	-4.53838500	1.22745800	-0.72550600
H	-2.56521900	3.86463600	0.19215400
H	-4.85743600	3.04892800	0.41304800
H	-1.58525400	0.40459900	-2.02963900
N	-0.59929100	2.47077000	-1.09612000
H	0.00119500	1.81237100	-1.61384800
H	-0.51413600	3.96709300	0.33751600
C	1.48658100	3.34375900	-0.16558500
C	2.17370400	4.57053600	0.44642600
H	1.68489400	4.84294400	1.38973000
H	3.20834500	4.30737800	0.68639200
C	2.12393200	5.75652400	-0.52129800
H	2.72081400	5.52003500	-1.41227700
H	2.58442300	6.63199200	-0.05292300
C	0.68665300	6.07163700	-0.94359700
H	0.11486200	6.41213600	-0.06971800
H	0.67439900	6.88992600	-1.67023500
C	0.00344200	4.84083400	-1.54550300
H	0.51025800	4.53818900	-2.47060600
H	-1.03795500	5.06101800	-1.80408400
N	1.60326800	2.13132500	0.64139400
C	0.83965800	1.75100400	1.66989700
C	-0.69793900	0.70055000	3.78731200
C	0.04588000	2.61933400	2.48494200
N	0.83283900	0.43778800	1.95938700
C	0.11127800	-0.12671700	2.98771200
C	-0.69732800	2.09897700	3.49777300
H	0.07654600	3.68661700	2.32005000
H	-1.29296400	2.76169400	4.11811900
N	1.97874600	-1.17895400	-0.02597700
C	3.33119200	-0.92614700	0.05469400
O	3.73800000	0.18850900	0.37541400
O	4.11413500	-1.97648000	-0.18327300
C	5.57695700	-1.90677800	-0.12103500
H	2.27045800	1.42920500	0.30706000
C	1.53639200	-2.22061600	-0.71026900
H	2.23273300	-2.98763400	-1.04910100
C	1.49428100	-1.59890900	-2.86250100
N	0.66174900	-0.54978600	-2.68420200
O	-0.59335900	-0.72186800	-2.80229900
O	1.12205000	0.56247200	-2.29951700
H	2.01845500	3.09300200	-1.09086200
H	1.28590100	-0.20513800	1.26533300
C	0.13777400	-2.64631700	-0.53461100
C	-2.45750700	-3.52638200	-0.08267200
C	-0.22867800	-3.95955700	-0.84349000
C	-0.83076200	-1.77358700	-0.02814700
C	-2.12517000	-2.20994600	0.21662500
C	-1.52440600	-4.40793300	-0.62029100
H	0.50932500	-4.64567100	-1.24958800
H	-0.57167500	-0.74227200	0.17697300
H	-2.86728800	-1.53432200	0.62639200
H	-1.80232100	-5.43048000	-0.84944100
C	0.16524400	-1.51240200	3.20555400

H	0.79272800	-2.13369700	2.57471600
C	-0.59368700	-2.05579100	4.22053700
H	-0.56126800	-3.12642400	4.39372400
C	-1.40581200	-1.24342100	5.03526000
H	-1.99040800	-1.69313900	5.83036900
C	-1.45577000	0.11648200	4.82357900
H	-2.07658200	0.75380800	5.44575900
C	-3.90125200	-0.71645800	-2.06513700
H	-3.13923200	-1.26662800	-2.60715000
C	-5.18930800	-1.19560800	-1.94999100
H	-5.44861900	-2.13828000	-2.42020800
C	-6.16773800	-0.48493200	-1.22868400
H	-7.17283500	-0.88440100	-1.14827800
C	-5.84748000	0.71178700	-0.62667700
H	-6.59265300	1.27217600	-0.07030300
C	5.98838900	-3.32828400	-0.49134300
H	5.62052400	-3.58579700	-1.48946600
H	7.07908300	-3.41205300	-0.49037700
H	5.58391500	-4.04697400	0.22794200
C	6.10749300	-0.90755900	-1.14545800
H	5.78965600	0.10907700	-0.90880400
H	7.20149500	-0.94247900	-1.14382000
H	5.76046100	-1.16708800	-2.15045000
C	6.01369800	-1.56840600	1.30192300
H	7.10030600	-1.67298700	1.38060900
H	5.73985500	-0.54598600	1.56643600
H	5.55126400	-2.25935800	2.01406000
C	2.93625800	-1.32494800	-3.14810300
H	3.51990200	-2.24248800	-3.03851400
H	3.07167500	-0.95576000	-4.17258900
H	3.33247400	-0.56586700	-2.47096700
H	0.99976700	-2.45368300	-3.30599300
Cl	-4.08845100	-4.08372700	0.21912600

Activated nitronate adds to an activated *N*-Boc *p*-NO_2-arylaldimine

(*R*,*S*)-TS191$_{trans}$

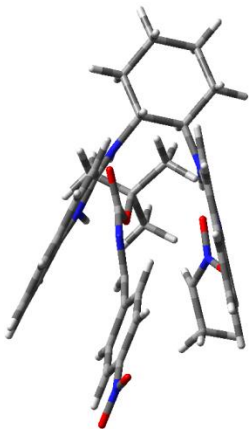

# opt=(calcfc,ts,noeigen) freq=noraman ωB97X-D/6-31g(d) scrf=(iefpcm,so
lvent=nitroethane) geom=connectivity temperature=253

Zero-point correction= 0.797769 (Hartree/Particle)
Thermal correction to Energy= 0.831277
Thermal correction to Enthalpy= 0.832078
Thermal correction to Gibbs Free Energy= 0.735688
Sum of electronic and zero-point Energies= -2307.424974
Sum of electronic and thermal Energies= -2307.391466
Sum of electronic and thermal Enthalpies= -2307.390665
Sum of electronic and thermal Free Energies= -2307.487054

Quasiharmonic free energy correction= 0.745754
SCF (B3LYP/6-31G*) = -2308.900617
SCF (wB97X-D/6-311+G**) = -2308.800293
SCF (B3LYP-D3/6-311+G**) = -2309.670383

1 1

C	-2.55189600	2.54965800	1.04445900
C	-0.56416300	1.43300600	2.05406100
N	0.00753100	0.23343200	2.27793700
C	1.50226000	2.47966500	2.72368300
C	1.29307300	0.06386700	2.75417900
C	0.21485000	2.60786200	2.31176600
C	2.09630200	1.19934200	2.95576700
H	-0.22602000	3.58560900	2.17832200
H	2.09747400	3.37078100	2.89827000
H	-0.46340800	-0.58301100	1.84345200
O	-2.00235500	-0.90317000	-1.96049300
N	-0.98293900	-1.52005300	-2.39071400
N	-1.81948800	1.43015100	1.61220500
H	-2.28762800	0.51481500	1.51507600
O	-0.00684600	-0.87132100	-2.89413200
C	-2.88229000	2.24872700	-0.43627900
C	-3.66120100	3.40057300	-1.08064100
C	-4.94249100	3.68201300	-0.29116800
C	-4.63911000	3.96132700	1.18306800
C	-3.84633600	2.81637800	1.81911400
N	-1.72791700	1.79868000	-1.20966400
C	-0.54947400	2.39619900	-1.37988200
C	2.07964500	3.37218500	-1.70254000
C	-0.21126500	3.72145500	-0.95345900
N	0.40650100	1.67760700	-2.00009100
C	1.70691000	2.09998500	-2.17229900
C	1.06041400	4.17577400	-1.10632000
H	-0.96966600	4.35784800	-0.52200000
H	1.31157400	5.17722000	-0.77042600
H	0.16494600	0.72489000	-2.35229600
C	-0.89049700	-2.84913200	-2.20527800
N	-1.17358600	-1.69935100	0.52090600
C	-0.44550600	-2.68219100	0.02651300
C	-2.53778100	-1.84979300	0.65332100
O	-3.21335600	-0.98742400	1.21496000
O	-3.03375900	-2.97157600	0.14464000
C	-4.47597200	-3.21966900	0.04211100
H	-1.79116000	0.82524100	-1.54138000
H	-1.93010500	3.44375400	1.10537500
H	-3.53780500	1.36967200	-0.43081200
H	-3.89032900	3.13305800	-2.11657400

H	-3.04622800	4.30815100	-1.11278200
H	-5.61182800	2.81473800	-0.36725900
H	-5.46889600	4.53108300	-0.73823100
H	-5.56981500	4.11536700	1.73804000
H	-4.06123900	4.89166000	1.26677100
H	-3.59403700	3.04486200	2.85928400
H	-4.44887300	1.89808200	1.82518100
H	-0.79968600	-3.71245200	0.04399100
C	-5.07617300	-3.37123800	1.43662800
H	-4.54682400	-4.14887400	1.99648900
H	-5.02372500	-2.43266800	1.99039600
H	-6.12591300	-3.66767800	1.34553700
C	-5.13736100	-2.10651600	-0.76650400
H	-4.59711300	-1.95459400	-1.70561100
H	-6.16815300	-2.39442100	-0.99548300
H	-5.15139200	-1.16659000	-0.21260200
C	-4.53001200	-4.54089000	-0.71853600
H	-4.08637700	-4.43272000	-1.71339100
H	-3.98900400	-5.32163500	-0.17518200
H	-5.57027600	-4.85727300	-0.83781600
C	1.01358800	-2.47460500	-0.05266400
C	3.74209300	-2.06693600	-0.05808800
C	1.88524600	-3.55885400	0.09054000
C	1.53536600	-1.18874600	-0.23637400
C	2.90308800	-0.97435000	-0.23415600
C	3.25858700	-3.36070500	0.09761600
H	1.48683200	-4.56015900	0.22035500
H	0.85707300	-0.35263300	-0.34547600
H	3.31747700	0.01870400	-0.34885600
H	3.94622800	-4.18615200	0.22991600
C	3.43299700	1.02417500	3.36721600
H	4.05571100	1.90070400	3.51794400
C	3.93721800	-0.24236000	3.56819500
H	4.96922300	-0.37689900	3.87296200
C	3.10912400	-1.36582600	3.38838600
H	3.50887800	-2.36026000	3.55712200
C	1.79506700	-1.22329600	2.99382300
H	1.15752400	-2.08890600	2.84834700
C	2.64344300	1.25469500	-2.78825600
H	2.33667700	0.27429200	-3.13848300
C	3.94781200	1.68719200	-2.91173800
H	4.68130300	1.03515400	-3.37446500
C	4.34163100	2.95498700	-2.44275000
H	5.37291900	3.27221100	-2.55178900
C	3.41871500	3.78862300	-1.85030900
H	3.70746800	4.77030700	-1.48727900
N	5.18723100	-1.84158700	-0.01825600
O	5.59353300	-0.69410600	-0.13936000
O	5.91691500	-2.81061300	0.13734600
C	0.20265900	-3.61745700	-2.86932000
H	0.01252700	-3.73292900	-3.94377800
H	1.16851400	-3.12171800	-2.74910000
H	0.26254000	-4.61758100	-2.43031900
H	-1.84511200	-3.30627600	-1.98472000

(*S*,*R*)-TS191$_{trans}$

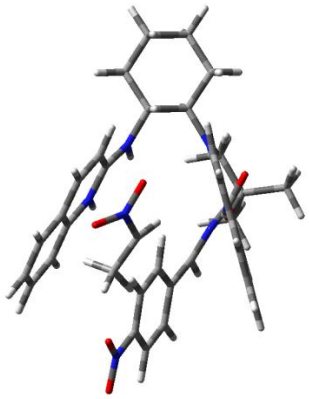

# opt=(calcfc,ts,noeigen) freq=noraman ωB97X-D/6-31g(d) scrf=(iefpcm,so
lvent=nitroethane) geom=connectivity temperature=253

Zero-point correction= 0.798073 (Hartree/Particle)
Thermal correction to Energy= 0.831594
Thermal correction to Enthalpy= 0.832396
Thermal correction to Gibbs Free Energy= 0.735424
Sum of electronic and zero-point Energies= -2307.421472
Sum of electronic and thermal Energies= -2307.387951
Sum of electronic and thermal Enthalpies= -2307.387150
Sum of electronic and thermal Free Energies= -2307.484121

Quasiharmonic free energy correction= 0.746425
SCF (B3LYP/6-31G*) = -2308.903187
SCF (wB97X-D/6-311+G**) = -2308.797466
SCF (B3LYP-D3/6-311+G**) = -2309.668504

1 1

C	1.35484800	3.40423100	-0.70795400
C	-0.83047400	2.42631700	-1.34890600
N	-1.46562400	1.35485100	-1.85344300
C	-2.97766200	3.47223200	-1.01374700
C	-2.83562300	1.24717800	-1.96129500
C	-1.62304600	3.54414000	-0.93122200
C	-3.64048800	2.31341000	-1.52320000
H	-1.14172300	4.43707700	-0.55728800
H	-3.57780600	4.31654900	-0.68822900
H	-0.89622500	0.54136200	-2.18273700
N	0.49951400	2.36549400	-1.26245600
H	0.94857200	1.48586500	-1.55556000
H	0.76134600	3.98960700	-0.00266300
C	2.52791500	2.75867600	0.05407900
C	3.40286100	3.83120500	0.71322200
H	2.82601500	4.37195200	1.47416900
H	4.23134000	3.33701600	1.22978100
C	3.92651300	4.81507900	-0.33703500

H	4.60271000	4.28451000	-1.02037100
H	4.51692200	5.59583100	0.15262200
C	2.78072200	5.43848000	-1.13821500
H	2.16817300	6.06273100	-0.47346100
H	3.17523700	6.09850100	-1.91704600
C	1.89444100	4.36414000	-1.77518500
H	2.46401800	3.78772000	-2.51544700
H	1.04882200	4.82039200	-2.30086200
N	2.11920100	1.68751300	0.95781000
C	1.09263700	1.65388300	1.80863000
C	-1.08142500	1.31508200	3.57116000
C	0.38515200	2.79323700	2.30827500
N	0.70258300	0.43574800	2.22944700
C	-0.34480800	0.21453500	3.09731500
C	-0.66786800	2.61574600	3.14948400
H	0.71871000	3.78747000	2.04841000
H	-1.19957900	3.48272600	3.52945100
N	1.69359300	-1.66363500	0.59180700
C	3.07357100	-1.63489900	0.56326800
O	3.68766800	-0.67998500	1.03146600
O	3.64688600	-2.68691700	-0.01302100
C	5.09289400	-2.76415700	-0.25891700
H	2.64088200	0.80985500	0.85859900
C	1.05026700	-2.65728700	0.01285800
H	1.53430300	-3.61639800	-0.16644900
C	1.38194900	-2.40469700	-2.23898500
N	0.96569700	-1.12778900	-2.28160000
O	-0.19717000	-0.86051700	-2.73469700
O	1.68592700	-0.21044700	-1.78331000
H	3.14487300	2.24194600	-0.69095700
H	1.11095500	-0.38943800	1.73428200
C	-0.42242300	-2.64308000	0.04684500
C	-3.17810800	-2.61755100	0.18865600
C	-1.14049400	-3.84093300	-0.03377600
C	-1.11284500	-1.43075300	0.16465200
C	-2.49407400	-1.41049800	0.25960700
C	-2.52671200	-3.83550100	0.03342600
H	-0.61314600	-4.78368600	-0.13900300
H	-0.55659200	-0.50203100	0.18495600
H	-3.03681800	-0.48220500	0.38046000
H	-3.09475700	-4.75506200	-0.02273000
C	-0.68572200	-1.09526100	3.46826200
H	-0.10646400	-1.93192500	3.09128400
C	-1.76529400	-1.29092300	4.30379400
H	-2.03903000	-2.30116900	4.58987800
C	-2.51401900	-0.20205800	4.78972200
H	-3.35695500	-0.38016400	5.44843400
C	-2.17442800	1.08387800	4.43179100
H	-2.74083300	1.93276800	4.80224400
C	-3.40849300	0.07456200	-2.48026700
H	-2.76723400	-0.74000500	-2.80121700
C	-4.78262300	-0.02078600	-2.54403200
H	-5.23492300	-0.92699300	-2.93321900
C	-5.60595000	1.03636300	-2.11087400
H	-6.68412000	0.93715900	-2.17193500
C	-5.04288100	2.18871800	-1.60973700

H	-5.66606700	3.01158700	-1.27302500
C	5.23452000	-4.10552000	-0.97055700
H	4.66393500	-4.11148200	-1.90468400
H	6.28682900	-4.28848300	-1.20622000
H	4.87426200	-4.91873900	-0.33330900
C	5.51935000	-1.61713700	-1.17117600
H	5.41984400	-0.65271200	-0.67110300
H	6.56649900	-1.75848900	-1.45562000
H	4.91481900	-1.60893500	-2.08419600
C	5.84894200	-2.77119600	1.06632600
H	6.90857600	-2.96501800	0.87288200
H	5.75524800	-1.81323800	1.57939200
H	5.46834200	-3.56502300	1.71682000
N	-4.63911800	-2.60139500	0.27075600
O	-5.23517200	-3.65957600	0.12574600
O	-5.19079000	-1.52983800	0.47811900
C	0.61337400	-3.45929700	-2.96127300
H	0.69461300	-3.34053900	-4.04894600
H	1.01373000	-4.44238200	-2.69811000
H	-0.44851400	-3.42840700	-2.70257900
H	2.44453800	-2.50471600	-2.06748900

(*R*,*R*)-TS191$_{syn}$

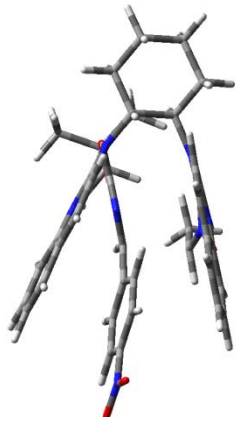

---

opt=(calcfc,ts,noeigen) freq=noraman ωB97X-D/6-31g(d) scrf=(iefpcm,solvent=nitroethane) geom=connectivity temperature=253

Zero-point correction= 0.797368 (Hartree/Particle)
Thermal correction to Energy= 0.830945
Thermal correction to Enthalpy= 0.831747
Thermal correction to Gibbs Free Energy= 0.734995
Sum of electronic and zero-point Energies= -2307.419354
Sum of electronic and thermal Energies= -2307.385776
Sum of electronic and thermal Enthalpies= -2307.384975
Sum of electronic and thermal Free Energies= -2307.481727

Quasiharmonic free energy correction= 0.745702
SCF (B3LYP/6-31G*) = -2308.895424
SCF (wB97X-D/6-311+G**) = -2308.794997
SCF (B3LYP-D3/6-311+G**) = -2309.665337

1 1

C	-2.27444900	2.74457900	1.07997700
C	-0.43926000	1.33928000	2.02707000
N	-0.02318600	0.06664200	2.18527100
C	1.72955400	2.07701200	2.78128700
C	1.22072700	-0.29074900	2.66800100
C	0.47440200	2.38971400	2.36741900
C	2.15563700	0.72068200	2.94487100
H	0.16339700	3.42186600	2.28738800
H	2.42958200	2.87438200	3.01127800
H	-0.56769200	-0.65505100	1.68103400
O	-1.93139200	-0.47574000	-2.34577300
N	-0.91672400	-1.15921300	-2.65675500
N	-1.67400200	1.51282200	1.56441300
H	-2.23371600	0.66317800	1.38709000
O	0.20369300	-0.58561600	-2.86716900
C	-2.59260700	2.59620800	-0.42700400
C	-3.26141600	3.85476000	-0.99187200
C	-4.52755400	4.18644300	-0.19744200
C	-4.22645700	4.33015000	1.29638000
C	-3.55483700	3.07253300	1.85409100
N	-1.45323800	2.11732900	-1.20695200
C	-0.22132400	2.62690300	-1.26263900
C	2.48919200	3.40741700	-1.33806400
C	0.18084100	3.89825400	-0.73955400
N	0.72016500	1.87041300	-1.85496100
C	2.05752000	2.19663100	-1.90886000
C	1.49139800	4.25781200	-0.77309100
H	-0.55924800	4.56987400	-0.33061500
H	1.79133600	5.21701900	-0.36248100
H	0.43409600	0.95084700	-2.26341500
C	-0.96338300	-2.50729700	-2.64713700
N	-1.31438700	-1.57394100	0.20023300
C	-0.67402100	-2.57912100	-0.36797200
C	-2.67263100	-1.65590500	0.43375700
O	-3.26316500	-0.73709900	1.00178100
O	-3.25800200	-2.78108800	0.04442900
C	-4.68832000	-3.04235800	0.25126100
H	-1.57660000	1.18367100	-1.62094700
H	-1.56743500	3.56151400	1.22918400
H	-3.31737700	1.77750600	-0.50683800
H	-3.49483800	3.68133500	-2.04668300
H	-2.57348000	4.70763600	-0.95318000
H	-5.26655700	3.38750000	-0.34439800
H	-4.97318900	5.10722600	-0.58664400
H	-5.14866900	4.52938800	1.85116800
H	-3.56642000	5.19369800	1.45491600
H	-3.30451500	3.19889100	2.91194100
H	-4.24023300	2.21743200	1.78191500
H	-0.04121700	-2.95135600	-3.00010600
H	-1.13549600	-3.56255200	-0.45495500
C	-4.99110200	-3.08675900	1.74648600
H	-4.33453800	-3.80723800	2.24464400
H	-4.86042900	-2.10668000	2.20737600
H	-6.02690800	-3.40790700	1.89371000

C	-5.52504400	-1.99927900	-0.48481500
H	-5.23961200	-1.95236100	-1.54069100
H	-6.57988100	-2.28604700	-0.42994300
H	-5.40744900	-1.01026400	-0.04033000
C	-4.86884700	-4.42123200	-0.37578200
H	-4.64263700	-4.39437800	-1.44569400
H	-4.20972400	-5.15100900	0.10413300
H	-5.90406600	-4.75073400	-0.24863200
C	0.80204700	-2.52461400	-0.38956000
C	3.55821200	-2.43719800	-0.26034000
C	1.54458500	-3.71074600	-0.40565100
C	1.46936700	-1.29552600	-0.34118400
C	2.85163400	-1.24280000	-0.27149900
C	2.92912200	-3.67565400	-0.33227400
H	1.03496200	-4.66801900	-0.45459900
H	0.89394600	-0.38023400	-0.32211300
H	3.37487400	-0.29795000	-0.20378100
H	3.51353600	-4.58658800	-0.32153100
C	3.45211000	0.35364100	3.35895500
H	4.17913800	1.13275000	3.56644300
C	3.78655100	-0.97664200	3.49343300
H	4.78733400	-1.25775800	3.80263700
C	2.82675500	-1.97376600	3.23953500
H	3.09250000	-3.01898400	3.35801800
C	1.54990500	-1.64311200	2.83578600
H	0.81113500	-2.40971800	2.62731800
C	2.97200300	1.31321100	-2.50464000
H	2.61846100	0.38255100	-2.93660200
C	4.31154300	1.64311800	-2.50335200
H	5.02721600	0.95869500	-2.94683200
C	4.76360800	2.84793100	-1.93129600
H	5.82187200	3.08472300	-1.94296700
C	3.86383600	3.72135500	-1.36148000
H	4.19783900	4.65585700	-0.92104500
N	5.01575800	-2.38719100	-0.15026500
O	5.55054300	-1.28854800	-0.08647200
O	5.62868000	-3.44545700	-0.12478600
C	-2.25958000	-3.21566700	-2.87828400
H	-2.22399500	-4.21914400	-2.44423400
H	-3.08839200	-2.67346100	-2.42727300
H	-2.44876700	-3.32499000	-3.95375000

(*S,S*)-TS191$_{syn}$

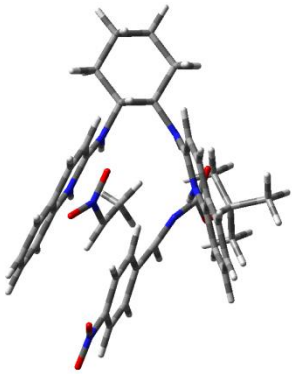

# opt=(calcfc,ts,noeigen) freq=noraman ωB97X-D/6-31g(d) scrf=(iefpcm,so
lvent=nitroethane) geom=connectivity temperature=253

Zero-point correction= 0.798215 (Hartree/Particle)
Thermal correction to Energy= 0.831582
Thermal correction to Enthalpy= 0.832383
Thermal correction to Gibbs Free Energy= 0.736432
Sum of electronic and zero-point Energies= -2307.416979
Sum of electronic and thermal Energies= -2307.383612
Sum of electronic and thermal Enthalpies= -2307.382811
Sum of electronic and thermal Free Energies= -2307.478763

Quasiharmonic free energy correction= 0.746549
SCF (B3LYP/6-31G*) = -2308.899724
SCF (wB97X-D/6-311+G**) = -2308.793614
SCF (B3LYP-D3/6-311+G**) = -2309.664365

1 1

C	0.71587300	3.66931900	-0.66366000
C	-1.40829200	2.43109500	-1.00566800
N	-1.97926000	1.33246200	-1.53146200
C	-3.57553800	3.10235000	-0.18853900
C	-3.32436700	1.04356300	-1.44325100
C	-2.24925100	3.36560300	-0.31880700
C	-4.16651300	1.92480000	-0.74240200
H	-1.82523100	4.27283700	0.08889000
H	-4.20998800	3.80442200	0.34386700
H	-1.37063300	0.64033300	-2.02187100
N	-0.09131700	2.56444800	-1.15497200
H	0.40544300	1.80093300	-1.63804700
H	0.20135600	4.11676500	0.18901500
C	2.08374700	3.13798000	-0.19045300
C	2.93318100	4.27221600	0.39394700
H	2.45232200	4.67846700	1.29252300
H	3.89847800	3.86158300	0.70509600
C	3.12156300	5.38507900	-0.64188900
H	3.71132700	4.99686200	-1.48284000
H	3.69784900	6.20419200	-0.20046900
C	1.77664600	5.90143300	-1.16100500
H	1.23519500	6.39487200	-0.34215400
H	1.93380800	6.65727600	-1.93693800
C	0.91856600	4.76259100	-1.71860600
H	1.39904500	4.31859600	-2.59990300
H	-0.06149100	5.13404900	-2.03678800
N	1.97955900	1.96027500	0.66917200
C	1.10263700	1.73401200	1.65025600
C	-0.72977700	1.00868700	3.66612300
C	0.40161100	2.74261800	2.38469100
N	0.87532000	0.44754800	1.97324800
C	0.00246500	0.03814400	2.95881800
C	-0.48822000	2.37940300	3.34616700
H	0.61672700	3.78546100	2.20134300
H	-1.01623200	3.14764800	3.90268100
N	1.85916900	-1.42476500	0.08315800
C	3.23523100	-1.34486600	0.19576300

O	3.77078100	-0.28564900	0.50993900
O	3.88131900	-2.48866900	-0.00704200
C	5.34206300	-2.60170100	0.09018700
H	2.54473300	1.15190700	0.39015800
C	1.31426600	-2.40717100	-0.60515700
H	1.91682500	-3.25569600	-0.92803200
C	1.39386800	-1.81022900	-2.79648800
H	0.78078300	-2.58117000	-3.24533800
N	0.72963900	-0.64818200	-2.62388000
O	-0.53551600	-0.62390100	-2.76747200
O	1.34838700	0.37815000	-2.22134900
H	2.60243500	2.76164400	-1.07998300
H	1.26642200	-0.28112900	1.33432900
C	-0.13730600	-2.64124100	-0.49457900
C	-2.83059600	-3.15883500	-0.17468800
C	-0.66199300	-3.88870400	-0.85117200
C	-0.99523500	-1.64744900	-0.01044800
C	-2.34314100	-1.90700000	0.17750800
C	-2.01389500	-4.15508500	-0.69904300
H	-0.00430100	-4.65995800	-1.24034300
H	-0.60350400	-0.66566500	0.22193700
H	-3.01126100	-1.15554700	0.57753300
H	-2.43167400	-5.11722600	-0.96604800
C	-0.17339700	-1.32960400	3.21852800
H	0.40200500	-2.06287800	2.66280000
C	-1.08794700	-1.71302400	4.17706000
H	-1.23618800	-2.76880100	4.37820200
C	-1.82977700	-0.75649800	4.89610100
H	-2.54214500	-1.08138600	5.64638300
C	-1.64981200	0.58623000	4.64765600
H	-2.21260100	1.33400500	5.19799200
C	-3.83402600	-0.12319000	-2.03572900
H	-3.16689800	-0.79018800	-2.57200200
C	-5.17839600	-0.40282700	-1.90500600
H	-5.57931800	-1.30656600	-2.35196000
C	-6.03573400	0.46280600	-1.19950400
H	-7.08881700	0.22110000	-1.10676800
C	-5.53712900	1.61315600	-0.62969800
H	-6.18749500	2.29158400	-0.08616400
C	5.58162700	-4.06987300	-0.24593700
H	5.21505900	-4.29829000	-1.25154900
H	6.65295800	-4.28728300	-0.20806800
H	5.06857700	-4.71861800	0.47036300
C	6.01393300	-1.69696400	-0.93884400
H	5.82498300	-0.64331400	-0.72821200
H	7.09420100	-1.87031100	-0.91154800
H	5.65749000	-1.93120800	-1.94661200
C	5.78468500	-2.29267200	1.51786100
H	6.85029200	-2.51938000	1.62169000
H	5.62568700	-1.24158100	1.76275400
H	5.23044700	-2.91442000	2.22806900
N	-4.25528300	-3.43385500	0.00741200
O	-4.69414000	-4.49737600	-0.40847500
O	-4.93812700	-2.58531500	0.56429100
C	2.86728600	-1.76716700	-3.04449800
H	3.30233000	-2.76008100	-2.90445900

H	3.08227900	-1.44513200	-4.07131400
H	3.35888000	-1.06405200	-2.36966300

5. References

[1] (a) Pimentel, G. C.; McClellan, A. L. *The Hydrogen Bond*; Freeman: San Francisco, 1960. (b) Jeffrey, G. A. *An Introduction to Hydrogen Bonding*; Oxford University: New York, 1997.

[2] (a) Schreiner, P. R.; *Chem. Soc. Rev.* **2003**, *32*, 289; (b) Pihko, P. M. *Angew. Chem. Int. Ed.* **2004**, *43*, 2062.

[3] Lewis, G. N. *Valence and the Structure of Atoms and Molecules*; Chemical Catalog Co: New York, 1923.

[4] (a) Pauling, L. *Proc. Natl. Acad. Sci.* **1928**, *14*, 359, (b) Pimentel, G. C.; McClellan, A. L. *The Hydrogen Bond*; Freeman: San Francisco, 1960.

[5] Steiner, T. *Angew. Chem. Int. Ed.* **2002**, *41*, 48.

[6] (a) Weinhold, F.; Klein, R. A. *Molecular Physics*, **2012**, *110*, 565. (b) Weinhold, F.; Klein, R. A. *Chem. Educ. Res. Pract*, **2014**, *15*, 276.

[7] Jeffrey, G. A.; Saenger, W. *Hydrogen Bonding in Biological Structures*; Springer-Verlag: Berlin, 1991.

[8] Desiraju.; Steiner, T. *The Weak Hydrogen Bond in Structural Chemistry and Biology*; Oxford University Press Inc: New York, 1999.

[9] Rozas, I.; Alkorta, I.; Elguero, J. *J. Am. Chem. Soc.* **2000**, *122*, 11154.

[10] Bader, R. F. W. *Atoms in Molecules, A Quantum Theory*; Oxford University Press: Oxford, 1990.

[11] Gilli, P.; Pretto, L.; Bertolasi, V.; Gilli.; G. *Accounts of Chemical Research*. **2009**, *42*, 33.

[12] a) Shibasaki, M.; Sasai, H.; Arai, T. *Angew.Chem. Int. Ed. Engl.* **1997**, *36*, 1236. b) GrMger, H. *Chem. Eur. J.* **2001**, *7*, 5246. c) Rawlands, G. J. *Tetrahedron* **2001**, *57*, 1865. d) Ma, J.-A.; Cahard, D. *Angew. Chem. Int. Ed.* **2004**, *43*, 4566.

[13] Wong, H.-Y.; Halcomb, R. H.; Ichikawa, Y.; Kajimoto, T. *Angew. Chem. Int. Ed. Engl.* **1995**, *34*, 412.

[14] Blackburn, G. M.; Gait, M. J. *Nucleic Acids in Chemistry and Biology*; Oxford Press: Oxford, UK, 1996.

[15] (a) Ferr, A. R.; Amar, T-D.; Zhou, T, K.; Doudna, J. A. *Nature.* **1998**, *395*, 567. (b) Perrotta, A. T.; Shih, I.-H.; Been, M. D. *Science.* **1999**, *286*, 123.

[16] (a) Jeffrey, G.; Saenger, W. *Hydrogen Bonding in Biological Structures*; Springer: Berlin, 1991. (b) Desiraju, G. R.; Steiner, T. *The Weak Hydrogen Bond in Structural Chemistry and Biology*; Oxford University Press: Oxford, 1999.

[17] (a) Pihko, P. M. *Angew. Chem.* **2004**, *43*, 2026. (b) Schreiner, P. R. *Chem. Soc. Rev.* **2003**, *32*, 289. (c) Taylor, M. S.; Jacobsen, E. N. *Angew. Chem., Int. Ed.* **2006**, *45*, 1520.

[18] (a) Doyle, A. G.; Jacobsen, E. N. *Chem. Rev.* **2007**, *107*, 5713. (b) Ha-Yeon Cheong, P.; Legault, C. Y.; Um, J. M.; Celebi-Olcum, N.; Houk, K. N. *Chem. Rev.* **2011**, *111*, 5042.

[19] (a) Rozas, I.; Alkorta, I.; Elguero, J. *J. Phys. Chem. A* **1998**, *102*, 9925. (b) Gilli, G.; Gilli, P. J. *Mol. Struct.* **2000**, *552*, 1.

[20] (a) Seayad, J.; List, B. *Org. Biomol. Chem.* **2005**, *3*, 719. (b) Dalko, P. I.; Moisan, L. *Angew. Chem., Int. Ed.* **2004**, *43*, 5138.

[21] (a) Yu, X.; Wang, W. *Chem. Asian J.* **2008**, *3*, 516. (b) Doyle, A. G.; Jacobsen, E. N. *Chem. Rev.* **2007**, *107*, 5713. (c) Connon, S. J. *Org. Biomol. Chem.* **2007**, *5*, 3407.

[22] Moyano, A.; Rios, R. *Chem. Rev.* **2011**, *111*, 4703.

[23] (a) Seebach,D.; Beck, A. K.; Heckel, A. *Angew. Chem. Int. Ed.* **2001**, *40*, 92. (b) Brunel, J. M. *Chem. Rev.* **2005**, *105*, 857.

[24] Ishihara, K.; Nakamura, S.; Yamamoto, H. *J. Am. Chem. Soc.* **1999**, *121*, 4906.

[25] (a) McDougal, N. T.; Schaus, S. E. *J. Am. Chem. Soc.* **2003**, *125*, 12094. (b) McDougal, N. T.; Trevellini, W.; Rodgen, S. A.; Kliman, L. T.; Schaus, S. E. *Adv. Synth. Catal.* **2004**, *346*, 1231.

[26] Akiyama, T.; Itoh, J.; Yokata, K.; Fuchibe, K. *Angew. Chem. Int. Ed.* **2004**, *43*, 1566.

[27] Uraguchi, D.; Terada, M. *J. Am. Chem. Soc.* **2004**, *126*, 5356.

[28] (a) Huang, Y.; Rawal, V. H. *J. Am. Chem. Soc.* **2002**, *124*, 9662. (b) Thadani, A. N.; Stankovic, A. R.; Rawal, V. H. *PNAS.* **2004**, *101*, 5846.

[29] (a) Gordillo, R.; Dudding, T.; Anderson, C. D.; Houk, K. N. *Org. Lett.* **2007**, *9*, 501. (b) Anderson, C. D.; Dudding, T.; Gordillo, R.; Houk, K. N. *Org. Lett.* **2008**, *10*, 2749. (c) Domingo, L. R.; Andres, J. *J. Org. Chem.* **2003**, *68*, 8662. (d) Polo, V.; Domingo, L. R.; Andres, J. *J. Phys. Chem. A* **2005**, *109*, 10438.

[30] (a) Inoue, S.; Oku, J.-I. *J. Chem. Soc., Chem. Commun.* **1981**, 228. (b) Tanaka, K.; Mori, A.; Inoue, S. *J. Org. Chem.* **1990**, *55*, 181.

[31] Iyer, M. S.; Gigstad, K. M.; Namdev, N. D.; Lipton, M. *J. Am. Chem. Soc.* **1996**, *118*, 4910.

[32] Shvo, Y.; Becker, G. M.; Elgavi, A. *Tetrahedron: Asymmetry* **1996**, *7*, 911.

[33] (a) Sigman, M. S.; Jacobsen, E. N. *J. Am. Chem. Soc.* **1998**, *120*, 4901. (b) Sigman, M.S.; Vachal, P.; Jacobsen, E. N. *Angew. Chem. Int. Ed.* **2000**, *39*, 1279. c) Vachal, P.; Jacobsen, E. N. *Org. Lett.* **2000**, *2*, 867. d) Vachal, P.; Jacobsen, E. N. *J. Am. Chem. Soc.* **2002**, *124*, 10012.

[34] Ha-Yeon Cheong, P.; Legault, C. Y.; Um, J. M.; Celebi-Olcum, N.; Houk, K. N. *Chem. Rev.* **2011**, *111*, 5042.

[35] (a) Vachal, P.; Jacobsen, E. N. *J. Am. Chem. Soc.* **2002**, *124*, 10012. (b) Fuerst, D. E.; Jacobsen, E. N. *J. Am. Chem. Soc.* **2005**, *127*, 8964. (c) Yoon, T. P.; Jacobsen, E. N. *Angew.*

Chem., Int. Ed. **2005**, *44*, 466. (d) Wenzel, A. G.; Lalonde, M. P.; Jacobsen, E. N. *Synlett* **2003**, *12*, 1919. (e) Taylor, M. S.; Jacobsen, E. N. *J. Am. Chem. Soc.* **2004**, *126*, 10558.

[36] (a) De, C. K.; Seidel, D. *J. Am. Chem. Soc.* **2011**, *133*, 14538. (b) Knowles, R. R.; Lin, S.; Jacobsen, E. N. *J. Am. Chem. Soc.* **2010**, *132*, 5030. (c) Peterson, E. A.; Jacobsen, E. N. *Angew. Chem., Int. Ed.* **2009**, *48*, 6328. (d) Brown, A. R.; Kuo, W.; Jacobsen, E. N. *J. Am. Chem. Soc.* **2010**, *132*, 9286. (e) Brown, A. R.; Kuo, W.-H.; Jacobsen, E. N. *J. Am. Chem. Soc.* **2010**, *132*, 9286.

[37] Okino, T.; Hoashi, Y.; Takemoto, Y. *Tetrahedron Lett.* **2003**, *44*, 2817.

[38] (a) Curran, D. P.; Kuo, L. H. *J. Org. Chem.* **1994**, *59*, 3259. (b) Schreiner, P. R.; Wittkopp, A. *Org. Lett.* **2002**, *4*, 217-220. (c) Wittkopp,A.; Schreiner, P. R. *Chem. Eur. J.* **2003**, *9*, 407.

[39] (a) Okino, T.; Hoashi, Y.; Takemoto, Y. *J. Am. Chem. Soc.* **2003**, *125*, 12672. (b) Okino, T.; Nakamura, S.; Furukawa, T.; Takemoto, Y. *Org. Lett.* **2004**, *6*, 625.

[40] a) Okino, T.; Hoashi, Y.; Furukawa, T.; Xu, X.; Takemoto, Y. *J. Am. Chem. Soc.* **2005**, *127*, 119. b) Okino, T.; Hoashi, Y.; Takemoto, Y. *J. Am. Chem. Soc.* **2003**, *125*, 12672. c) Okino, T.; Nakamura, S.; Furukawa, T.; Takemoto, Y. *Org. Lett.* **2004**, *6*, 625.

[41] (a) Shibasaki, M.; Sasai, H.; Arai, T. *Angew. Chem., Int. Ed.* **1997**, *36*, 1236. (b) Shibasaki, M.; Yoshikawa, N. *Chem. Rev.* **2002**, *102*, 2187. (c) Shibasaki, M.; Matsunaga, S.; Kumagai, N. *Synlett* **2008**, 1583.

[42] (a) Schuster, T.; Kurz, M.; Göbel, M. W. *J. Org. Chem.* **2000**, *65*, 1697. (b) Sohtome, Y.; Hashimot, Y.; Nagasawa, K. *Adv. Synth. Catal.* **2005**, *347*, 1643. (c) Terada, M.; Nakano, M.; Ube, H. *J. Am. Chem. Soc.* **2006**, *128*, 16044.

[43] Corey, E. J.; Grogan, M. J. *Org. Lett.* **1999**, *1*, 157.

[44] Li, J.; Jiang, W.-Y.; Han, K.-L.; He, G.; Zhong, Li, C. *J. Org. Chem.* **2003**, *68*, 8786.

[45] Jiang, Li. J.; Han, W.-Y.; He, K.-L.; Zhong, G.; Li, C. *J. Org. Chem.* **2003**, *68*, 8786.

[46] Schuster, T.; Kurz, M.; Göbel, M. W. *J. Org. Chem.* **2000**, *65*, 1697.

[47] Nugent, B. M.; Yoder, R. A.; Johnston, J. N. *J. Am. Chem. Soc.* **2004**, *126*, 3418.

[48] Takaaki, I.; Fujioka, S.; Sekiguchi, Y.; Kotsuki, H. *J. Am. Chem. Soc.* **2004**, *126*, 9558.

[49] (a) Schuster, T.; Kurz, M.; Göbel, M. W. *J. Org. Chem.* **2000**, *65*, 1697. (b) Schuster, T.; Bauch, M.; DVrner, G.; Göbel, M. W. *Org. Lett.* **2000**, *2*, 179.

[50] Schuster, T.; Kurz, M.; Göbel, M. W. *J. Org. Chem.* **2000**, *65*, 1697.

[51] Tsogoeva, S. B.; Durner, G.; Bolte, M.; Göbel, M. W., *Eur. J. Org. Chem.* **2003**, 1661.

[52] (a) Tsogoeva, S. B.; Durner, G.; Bolte, M.; Göbel, M. W. Eur. *J. Org. Chem.* **2003**, 1661. (b) Akalay, D.; Durner, G.; Bats, J. W.; Bolte, M.; Göbel, M. W., *J. Org. Chem.* **2007**, *72*, 5618.

[53] Nugent, B. M.; Yoder, R. A.; Johnston, J. N. *J. Am. Chem. Soc.* **2004**, *126*, 3418.

[54] (a) Hess, A. S.; Yoder, R. A.; Johnston, J. N. *Synlett* **2006**, *1*, 147. (b) Dobish, M. C.; Johnston, J. N. *Org. Lett.* **2010**, *12*, 5744. (c) Shen, B.; Makley, D. M.; Johnston, J. N. *Nature* **2010**, *465*, 1027. (d) Davis, T. A.; Johnston, J. N. *Chem. Sci.* **2011**, *2*, 1076. (e) Davis, T. A.; Danneman, M. W.; Johnston, J. N. *Chem. Commun.* **2012**, *48*, 5578. (f) Davis, T. A.; Vilgelm, A. E.; Richmond, A.; Johnston, J. N. *J. Org. Chem.* **2013**, *78*, 10605. (g) Vara, B. A.; Mayasundari, A.; Tellis, J. C.; Danneman, M. W.; Arredondo, V.; Davis, T. A.; Min, J.; Finch, K.; Guy, R. K.; Johnston, J. N. *J. Org. Chem.* **2014**, *79*, 6913.

[55] (a) Dobish, M. C.; Johnston, J. N. *J. Am. Chem. Soc.* **2012**, *134*, 6068. (b) Davis, T. A.; Wilt, J. C.; Johnston, J. M. *J. Am. Chem. Soc.* **2010**, *132*, 2880.

[56] Ono, N. *The Nitro Group in Organic Synthesis*; John Wiley & Sons: New York, 2001.

[57] Henry, L. *Chem. Ber.* **1905**, *38*, 2027.

[58] Henry, L. *Bull. Acad. Roy. Belg.* **1896**, *32*, 33.

[59] Mousset, T. *Bull. Acad. Roy. Belg.* **1901**, 622.

[60] (a) Cerf de Mauny, H. *Bull. Soc. Chim. Fr.* **1937**, *4*, 1451. (b) Cerf de Mauny, H. *Bull. Soc. Chim. Fr.* **1937**, *4*, 1460.

[61] Senkus, M. *J. Am. Chem. Soc.* **1946**, *68*, 10.

[62] Johnson, H. *J. Am. Chem. Soc.* **1946**, *68*, 12.

[63] Johnson, H. G. *J. Am. Chem. Soc.* **1946**, *68*, 14.

[64] Hurd, C. D.; Strong, J. S. *J. Am. Chem. Soc.* **1950**, *72*, 4813.

[65] Adams, H.; Anderson, J. C.; Peace, S.; Pennell, A. M. K. *J. Org. Chem.* **1998**, *63*, 9932.

[66] (a) Anderson, J. C.; Peace, S.; Pih, S. *Synlett* **2000**, *6*, 850. (b) Anderson, J. C.; Howell, G. P.; Blake, A. J.; Wilson, C. *J. Org. Chem.* **2005**, *70*, 549.

[67] (a) Yamada, K.; Harwood, S. J.; Gröger, H.; Shibasaki, M. *Angew. Chem. Int. Ed.* **1999**, *38*, 3504. (b) Yamada, K.; Moll, G.; Shibasaki, M. *Synlett* **2001**, *SI*, 980. (c) Shibasaki, M.; Kanai, M. *Chem. Pharm. Bull.* **2001**, *49*, 511.

[68] Knudsen, K. R.; Risgaard, T.; Nishiwaki, N.; Gothelf, K. V.; Jørgensen, K. A. *J. Am. Chem. Soc.* **2001**, *123*, 5843.

[69] Nishiwaki, N.; Knudsen, K. R.; Gothelf, K. V.; Jørgensen, K. A. *Angew. Chem. Int. Ed.* **2001**, *40*, 2992.

[70] Okino, T.; Nakamura, S.; Furukawa, T.; Takemoto, Y. *Org. Lett.* **2004**, *6*, 625.

[71] Yoon, T. P.; Jacobsen, E. N. *Angew. Chem., Int. Ed.* **2005**, *44*, 466.

[72] Xu, X.; Furukawa, T.; Okino, T.; Miyabe, H.; Takemoto, Y. *Chem. Eur. J.* **2006**, *12*, 466.

[73] (a) Bode, C. M.; Ting, A.; Schaus, S. E. *Tetrahedron* **2006**, *62*, 11499. (b) Bernardi, L.; Fini, F.; Herrera, R. P.; Ricci, A.; Sgarzani, V. *Tetrahedron* **2006**, *62*, 375.

[74] Chang, Y.-W.; Yang, J.-J.; Dang, J.-N.; Xue, Y.-X. *Synlett* **2007**, 2283.

[75] Robak, M. T.; Trincado, M.; Ellman, J. A. *J. Am. Chem. Soc.* **2007**, *129*, 15110.

[76] (a) Wang, C.; Zhou, Z.; Tang, C. *Org. Lett.* **2008**, *10*, 1707. (b) Rampalakos, C.; Wulff, W. D. *Adv. Synth. Catal.* **2008**, *350*, 1785.

[77] Wang, C.-J.; Dong, X.-Q.; Zhang, Z.-H.; Xue, Z.-Y.; Teng, H.-L. *J. Am. Chem. Soc.* **2008**, *130*, 8606.

[78] Jiang, X.; Zhang, Y.; Wu, L.; Zhang, G.; Liu, X.; Zhang, H.; Fu, D.; Wang, R. *Adv. Synth. Catal.* **2009**, *351*, 2096.

[79] (a) Palomo, C.; Oiarbide, M.; Laso, A.; López, R. *J. Am. Chem. Soc.* **2005**, *127*, 17622. (b) Fini, F.; Sgarzani, V.; Pettersen, D.; Herrera, R. P.; Bernardi, L.; and Ricci, A. *Angew. Chem., Int. Ed.* **2005**, *44*, 7975.

[80] Gomez-Bengoa, E.; Linden, A.; López, R.; Múgica-Mendiola, I.; Oiarbide, M.; Palomo, C. *J. Am. Chem. Soc.* **2008**, *130*, 7955.

[81] Wei, Y.; He, W.; Liu, Y.; Liu, P.; Zhang, S. *Org. Lett.* **2012**, *14*, 704.

[82] Takada, K.; Nagasawa, K. *Adv. Synth. Catal.* **2009**, *351*, 345.

[83] Nugent, B. M.; Yoder, R. A.; Johnston, J. N. *J. Am. Chem. Soc.* **2004**, *126*, 3418.

[84] (a) Dobish, M. C.; Johnston, J. N. *Org. Lett.* **2010**, *12*, 5744. (b) Davis, T. A.; Wilt, J. C.; Johnston, J. M. *J. Am. Chem. Soc.* **2010**, *132*, 2880. (c) Shen, B.; Makley, D. M.; Johnston, J. N. *Nature* **2010**, *465*, 1027. (d) Davis, T. A.; Johnston, J. N. *Chem. Sci.* **2011**, *2*, 1076. (e) Dobish, M. C.; Johnston, J. N. *J. Am. Chem. Soc.* **2012**, *134*, 6068. (f) Davis, T. A.; Vilgelm, A. E.; Richmond, A.; Johnston, J. N. *J. Org. Chem.* **2013**, *78*, 10605. (g) Vara, B. A.; Mayasundari, A.; Tellis, J. C.; Danneman, M. W.; Arredondo, V.; Davis, T. A.; Min, J.; Finch, K.; Guy, R. K.; Johnston, J. N. *J. Org. Chem.* **2014**, *79*, 6913.

[85] a) Clemente, F. R.; Houk, K. N. *J. Am. Chem. Soc*. **2005**, *127*, 11294. b) Ha-Yeon Cheong, P.; Legault, C. Y.; Um, J. M.; Celebi-Olcum, N.; Houk, K. N. *Chem. Rev.* **2011**, *111*, 5042. b) Yamanaka, M.; Yoshida, U.; Sato, M.; Shigeta, T.; Yoshida, K.; Furuta, T.; Kawabata, T. *J. Org. Chem.* **2015**, *80*, 3075. c) Bahmanyar, S.; Houk, K. N. *J. Am. Chem. Soc.* **2001**, *123*, 11273. d) Gomez-Bengoa, E.; Linden, A.; Lopez, R.; Mugica-Mendiola, I.; Oiarbide, M.; Palomo, C. *J. Am. Chem. Soc.* **2008**, *130*, 7955.

[86] a) Griffiths, D. J. In *Introduction to Quantum Mechanics Second Edition*; Pearson Prentice Hall: Upper Saddle River, 2005. b) Levine, I. N. *Quantum Chemistry Fifth Edition*; Prentice Hall: Upper Saddle River, 2000. Foresman, J. B.; Frisch, In *Exploring Chemistry with Electronic Structure Methods Second Edition*; Gaussian: Pittsburgh, 1996.

[87] a) Odagi, M.; Furukori, K.; Yamamoto,Y.; Sato, M.; Iida, K.; Yamanaka, M.; Nagasawa, K. *J. Am. Chem. Soc.* **2015**, *137*, 1909. b) Gordillo, R.; Houk, K. N. *J. Am. Chem. Soc*. **2006**, *128*, 3543. c) Uyeda, C.; Jacobsen, E. N. *J. Am. Chem. Soc.* **2011**, *133*, 5062.

[88] Grimme, S. *Wiley Interdiscip. Rev. Comput. Mol. Sci.* **2011**, *1*, 211.

[89] (a) Grimme, S. *J. Comput. Chem.* **2004**, *25*, 1463-1473. (b) Grimme, S. *J. Comput. Chem.* **2006**, *27*, 1787-1799.

[90] (a) Li, A.; Muddana, H. S.; Gilson, M. K. *J. Chem. Theory Comput.* **2014**, *10*, 1563. (b) Krenske, E. H.; Houk, K. N. *Acc. Chem. Res.* **2013**, *46*, 979. (c) Cohen, A. J.; Mori-Sánchez, P.; Yang, W. *Chem. Rev.* **2012**, *112*, 289. (d) Johnson, E. R.; Mackie, I. D.; DiLabio, G. A. *J. Phys. Org. Chem.* **2009**, *22*, 1127. (e) Foster, M. E.; Sohlberg, K. *Phys. Chem. Chem. Phys.* **2010**, *12*, 307. (f) Kruse, H.; Goerigk, L.; Grimme, S. *J. Org. Chem.* **2012**, *77*, 10824.

[91]Armstrong, A.; Boto, R.; Dingwall, P.; Contreras-García, J.; Harvey, M. J.; Mason, N. J.; Rzepa, H. S. *Chem. Sci.* **2014**, *5*, 2057.

[92] a) Medve, M.; Budzák, S.; Laurent, A. D.; Jacquemin, D. *J. Phys. Chem. A,* **2015**, 119, 3112. b) Lam, Y.; Houk, K. N. *J. Am. Chem. Soc.* **2015**, *137*, 2116. c) Breugst, M.; Houk, K. N. *J. Org. Chem.* **2014**, *79*, 6302. d) Lam, Y.; Houk, K. N. *J. Am. Chem. Soc.* **2014**, *136*, 9556.

[93] Grimme, S.; Antony, J.; Ehrlich, S.; Krieg, H. *J. Chem. Phys.* **2010**, *132*, 154104.

[94] Chai, J.-D.; Head-Gordon, M. *Phys. Chem. Chem. Phys.* **2008**, *10*, 6615.

[95] Ha-Yeon Cheong, P.; Legault, C. Y.; Um, J. M.; Celebi-Olcum, N.; Houk, K. N. *Chem. Rev.* **2011**, *111*, 5042.

[96] Zhang, X.; Du, H.; Wang, Z.; Wu, Y.-D.; Ding, K. *J. Org. Chem.* **2006**, *71*, 2862.

[97] Gordillo, R. D. T.; Anderson, C. D.; Houk, K. N. *Org. Lett.* **2007**, *9*, 501.

[98] Gomez-Bengoa, E. *Eur. J. Org. Chem.* **2009**, 1207.

[99] (a) Gordillo, R.; Dudding, T.; Anderson, C. D.; Houk, K. N. *Org. Lett.* **2007**, *9*, 501. (b) Anderson, C. D.; Dudding, T.; Gordillo, R.; Houk, K. N. *Org. Lett.* **2008**, *10*, 2749. (c) Domingo, L. R.; Andres, J. *J. Org. Chem.* **2003**, *68*, 8662. (d) Polo, V.; Domingo, L. R.; Andres, J. *J. Phys. Chem. A* **2005**, *109*, 10438.

[100] Anderson, C. D.; Dudding, T.; Gordillo, R.; Houk, K. N. *Org. Lett.* **2008**, *10*, 2749.

[101] (a) Akiyama, T.; Itoh, J.; Yokota, K.; Fuchibe, K. *Angew. Chem.* **2004**, *116*, 1566. (b) Uraguchi, D.; Terada, M. *J. Am. Chem. Soc.* **2004**, *126*, 5356.

[102] (a) Gridnev, I. D. K., M.; Sorimachi, K.; Terada, M. *Tetrahedron Lett.* **2007**, *48*, 497. (b) Yamanaka, M.; Itoh, J.; Fuchibe, K.; Akiyama, T. *J. Am. Chem. Soc.* **2007**, *129*, 6756. (c) Chen, X.-H.; Wei, Q.; Luo, S.-W.; Xiao, H.; Gong, L.-Z. *J. Am. Chem. Soc.* **2009**, *131*, 13819. (d)

Simon, L.; Goodman, J. M. *J. Am. Chem. Soc.* **2008**, *130*, 8741. (e) Marcelli, T.; Hammar, P.; Himo, F. *Adv. Synth. Catal.* **2009**, *351*, 525.

[103] Yamanaka, M.; Itoh, J.; Fuchibe, K.; Akiyama, T. *J. Am. Chem. Soc.* **2007**, *129*, 6756.

[104] (a) Gridnev, I. D. K. M.; Sorimachi, K.; Terada, M. *Tetrahedron Lett.* **2007**, *48*, 497. (b) Yamanaka, M.; Itoh, J.; Fuchibe, K.; Akiyama, T. *J. Am. Chem. Soc.* **2007**, *129*, 6756.

[105] Chen, X.-H.; Wei, Q.; Luo, S.-W.; Xiao, H.; Gong, L.-Z. *J. Am. Chem. Soc.* **2009**, *131*, 13819.

[106] Li, N.; Chen, X.-H.; Song, J.; Luo, S.-W.; Fan, W.; Gong, L.-Z. *J. Am. Chem. Soc.* **2009**, *131*, 15301.

[107] Shi, F.-Q.; Song, B.-A. *Org. Biomol. Chem.* **2009**, *7*, 1292.

[108] (a) Kelly, T. R.; Meghani, P.; Ekkundi, V. S. *Tetrahedron Lett.* **1990**, *31*, 3381. (b) Etter, M. C. *Acc. Chem. Res.* **1990**, *23*, 120. (c) Etter, M. C.; Urbanczyk-Lipkowska, Z.; Zia-Ebrahimi, M.; Panunto, T. W. *J. Am. Chem. Soc.* **1990**, *112*, 8415. (d) Curran, D. P.; Kuo, L. H. *J. Org. Chem.* **1994**, *59*, 3259.

[109] (a) Sigman, M. S.; Jacobsen, E. N. *J. Am. Chem. Soc.* **1998**, *120*, 4901. (b) Vachal, P.; Jacobsen, E. N. *J. Am. Chem. Soc.* **2002**, *124*, 10012.

[110] Raheem, I. T.; Thiara, P. S.; Peterson, E. A.; Jacobsen, E. N. *J. Am. Chem. Soc.* **2007**, *129*, 13404.

[111] Zuend, S. J.; Jacobsen, E. N. *J. Am. Chem. Soc.* **2009**, *131*, 15358.

[112] (a) Schreiner, P. R.; Wittkopp, A. *Org. Lett.* **2002**, *4*, 217. (b) Schreiner, P. R. *Chem. Soc. Rev.* **2003**, *32*, 289.

[113] Fu, A. P.; Thiel, W. J. *Mol. Struct. (Theochem)* **2006**, *765*, 45.

[114] Ha-Yeon Cheong, P.; Legault, C. Y.; Um, J. M.; Celebi-Olcum, N.; Houk, K. N. *Chem. Rev.* **2011**, *111*, 5042.

[115] (a) Chen, D.; Lu, N.; Zhang, G.; Mi, S. *Tetrahedron: Asymmetry* **2009**, *20*, 1365. (b) Zhu, R.; Zhang, D.; Wu, J.; Liu, C. *Tetrahedron: Asymmetry* **2007**, *18*, 1655. (c) Xu, X.; Yabuta, T.; Yuan, P.; Takemoto, Y. *Synlett* **2006**, *1*, 137. (d) Simon, L.; Goodman, J. M. *Org. Biomol. Chem.* **2009**, *7*, 483. (e) Wang, S.-X.; Chen., F.-E. *Adv. Synth. Catal.* **2009**, *351*, 547.

[116] (a) Yalalov, D. A.; Tsogoeva, S. B.; Schmatz, S. *Adv. Synth. Catal.* **2006**, *348*, 826. (b) Hamza, A.; Schubert, G.; Soos, T.; Papai, I. *J. Am. Chem. Soc.* **2006**, *128*, 13151. (c) Liu, T.-Y.; Li, R.; Chai, Q.; Long, J.; Li, B.-J.; Wu, Y.; Ding, L.-S.; Chen, Y.-C. *Chem. Eur. J.* **2006**, *13*, 319.

[117] Tsogoeva, S. B.; Wei, S. *Chem. Commun*, **2006**, 1451.

[118] Okino, T.; Hoashi, Y.; Furukawa, T.; Xu, X.; Takemoto, Y. *J. Am. Chem. Soc.* **2005**, *127*, 119.

[119] Hamza, A.; Schubert, G.; Soos, T.; Papai, I. *J. Am. Chem. Soc.* **2006**, *128*, 13151.

[120] Liu, T.-Y.; Li, R.; Chai, Q.; Long, J.; Li, B.-J.; Wu, Y.; Ding, L.-S.; Chen, Y.-C. *Chem.—Eur. J.* **2007**, *13*, 319.

[121] Zhu, R.; Zhang, D.; Wu, J.; Liu, C. *Tetrahedron: Asymmetry* **2007**, *18*, 1655.

[122] Tan, B.; Lu, Y.; Zeng, X.; Chua, P. J.; Zhong, G. *Org. Lett.* **2010**, *12*, 2682.

[123] Simon, L.; Goodman, J. M. *Org. Biomol. Chem.* **2009**, *7*, 483.

[124] Martin Breugst and K. N. Houk, *J. Org. Chem.* **2014**, *79*, 6302.

[125] Kitagaki, S.; Ueda, T.; Mukai, C. *Chem. Commun.* **2013**, *49*, 4030.

[126] Simon, L.; Goodman, J. M. *J. Org. Chem.* **2007**, *72*, 9656.

[127] Chuma, A.; Horn, H. W.; Swope, W. C.; Pratt, R. C.; Zhang, L.; Lohmeijer, B. G. G.; Wade, C. G.; Waymouth, R. M.; Hedrick, J. L.; Rice, J. E. *J. Am. Chem. Soc.* **2008**, *130*, 6749.

[128] Almasi, D; Alonso, D. A.; Gomez-Bengoa, E.; Najera, C. *J. Org. Chem.* **2009**, *74*, 6163.

[129] Hamza, A.; Schubert, G.; Soos, T.; Papai, I. *J. Am. Chem. Soc.* **2006**, *128*, 13151.

[130] Chen, X.; Wang, J.; Zhu, Y.; Shang, D.; Gao, B.; Liu, X.; Feng, X.; Su, Z.; Hu, C. *Chem.—Eur. J.* **2008**, *14*, 10896.

[131] (a) Uraguchi, D.; Sakaki, S.; Ooi, T. *J. Am. Chem. Soc.* **2007**, *129*, 12392. (b) Uraguchi, D.; Ueki, Y.; Ooi, T. *J. Am. Chem. Soc.* **2008**, *130*, 14088.

[132] Simón. L.; Paton. R. S. *Org. Chem.* **2015**, *80*, 2756.

[133] (a) Hintermann, L.; Ackerstaff, J.; Boeck, F. *Chem. Eur. J.* **2013**, *19*, 2311. (b) Sengupta, A.; Sunoj, R. B. *J. Org. Chem.* **2012**, *77*, 10525.

[134] Cook, T. C.; Andrus, M. B.; Ess, D. H. *Org. Lett.* **2012**, *14*, 5836.

[135] Lam, Y.-H.; Houk. K. N. *J. Am. Chem. Soc.* **2014**, *136*, 9556.

[136] Lam, Y.-H.; Houk, K. N. *J. Am. Chem. Soc.* **2015**, *137*, 2116.

[137] Belding, L.; Taimoory, S. M.; Dudding, T. *ACS Catal.* **2015**, *5*, 343.

[138] Nugent, B. M.; Yoder, R. A.; Johnston, J. N. *J. Am. Chem. Soc.* **2004**, *126*, 3418.

[139] Tomasi, J.; Mennucci, B.; Cance, E. *J. Mol. Struct.* **1999**, *464*, 211.

[140] Glendening, E. D.; Reed, A.E.; Carpenter, J.E.; Weinhold, F. NBO Version 3.1.

[141] (a) Gilli, P.; Pretto, L.; Gilli, G. *J. Mol. Struct.* **2007**, *844-845*, 328. (b) Chen, J.; McAllister, M.A.; Lee, J. K.; Houk, K. N. *J. Org. Chem.* **1998,** *63*, 4611. (c) Gilli, P.; Pretto, L.; Bertolasi, V.; Gilli, G. *Accounts of Chemical Research.* **2009**, *42*, 33.

[142] Newberry, R. W.; VanVeller, B.; Guzei, I.A.; Raines. R. T. *J. Am. Chem. Soc.* **2013**, *135*, 7843.

[143] Biegler-König, F.; Schönbohm, J.; Bayles, D. *J. Comput. Chem*, **2001**, *22*, 545.

[144] (a) Lammertsma, K.; Prasad, B. V. *J. Am. Chem. Soc.* **1993**, *115*, 2348. (b) Turnbull, D.; Maron, S. H. *J. Am. Chem. Soc.* **1943**, *65*, 212.

[145] (a) Knudsen, K. R.; Risgaard, T.; Nishiwaki, N.; Gothelf, K. V.; Jørgensen, K. A. *J. Am. Chem. Soc.* **2001**, *123*, 5843. (b) Nishiwaki, N.; Knudsen, K. R.; Gothelf, K. V.; Jørgensen, K. A. *Angew. Chem. Int. Ed* **2001**, *40*, 2992.

[146] (a) Ribeiro, R. F.; Marenich, A. V.; Cramer, C. J.; Truhlar, D. G. *J. Phys. Chem. B* **2011**, *115*, 14556. (b) Zhao, Y.; Truhlar, D. G. *Phys. Chem. Chem. Phys.* **2008**, *10*, 2813.

[147] (a) Waller, M.; Grimme, S. *Weak Intermolecular Interactions: A Supermolecular Approach. In Handbook of Computational Chemistry;* Leszczynski, J., Ed.; Springer: Dordrecht, The Netherlands, 2012; 443. (b) Grimme, S. *Wiley Interdiscip. Rev.: Comput. Mol. Sci.* **2011**, *1*, 211.

[148] (a) Contreras-García, J.; Johnson, E. R.; Keinan, S.; Chaudret, R.; Piquemal, J-P.; Beratan, D.N.; Yang, W. *J. Chem. Theory Comput.* **2011**, *7*, 625. (b) Shakourian-Fard, M.; Kamath, G.; Jamshidi, Z. *J. Phys. Chem. C* **2014**, *118*, 26003.

[149] Bader, R. F. W. *Atom in Molecules: A Quantum Theory*; Oxford University Press: New York, 1990.

[150] Johnson, E. R.; Keinan, S.; Mori-Sánchez, P.; Contreras-García, J.; Cohen, A. J.; Yang, W. *J. Am. Chem. Soc.* **2010**, *132*, 6498. b) Contreras-García, J.; Johnson, E. R.; Keinan, S.; Chaudret, R.; Piquemal, J.-P.; Beratan, D. N.; Yang, W. *J. Chem. Theory Comput.* **2011**, *7*, 625.

[151] (a) Klug, A. *Angew. Chem., Int. Ed. Engl.* **1983**, *22*, 565. (b) Maharaj, P. D.; Mallajosyula, J. K.; Lee, G.; Thi, P.; Zhou, Y.; Kearney, C. M.; McCormick, A. A. *Int. J. Mol. Sci.* **2014**, *15*, 18540. (c) Yonetani, T.; Laberge, M. *Biochim. Biophys. Acta, Proteins Proteomics* **2008**, *1784*, 1146.

[152] Frisch, M. J.; Trucks, G. W.; Schlegel, H. B.; Scuseria, G. E.; Robb, M. A.; Cheeseman, J. R.; Scalmani, G.; Barone, V.; Mennucci, B.; Petersson, G. A.; Nakatsuji, H.; Caricato, M.; Li, X.; Hratchian, H. P.; Izmaylov, A. F.; Bloino, J.; Zhang, G.; Sonnenberg, J. L.; Hada, M.; Ehara, M.; Toyota, K.; Fukuda, R.; Hasegawa, J.; Ishida, M.; Nakajima, T.; Honda, Y.; Kitao, O.; Nakai, H.; Vreven, T.; Montgomery, J. A.; Peralta, Jr., J. E.; Ogliaro, F.; Bearpark, M.; Heyd, J. J.; Brothers, E.; Kudin, K. N.; Staroverov, V. N.; Kobayashi, R.; Normand, J.; Raghavachari, K.; Rendell, A.; Burant, J. C.; Iyengar, S. S.; Tomasi, J.; Cossi, M.; Rega, N.; Millam, J. M.; Klene, M.; Knox, J.e.; Cross, J. B.; Bakken, V.; Adamo, C.; Jaramillo, J.; Gomperts, R.; Stratmann, R. E.; Yazyev, O.; Austin, A. J.; Cammi, A. R.; Pomelli, C.; Ochterski, J. W.; Martin, R. L.; Morokuma, K.; Zakrzewski, V. G.; Voth, G. A.; Salvador, P.; Dannenberg, J. J.; Dapprich, S.; Daniels, A. D.; Farkas, Ö.; Foresman, J. B.; Ortiz, J. V.; Cioslowski, J.; Fox, D. J.*Gaussian 09, Revision C.02*; Gaussian, Inc.: Wallingford, CT, 2009.

[153] Chai, J.-D.; Head-Gordon, M. *Phys. Chem. Chem. Phys.* **2008**, *10*, 6615.

[154] Bader, R. F. W. *Atoms in Molecules, A Quantum Theory*; Oxford University Press: Oxford, 1990.

[155] Schrödinger Materials Science Suite 2014-2, Schrödinger, LLC, New York, NY, 2014.

6. Appendix.

Table 8A. The evaluated resonance stabilization energy and C_{Ph}-C_{CN}-N_{CN}-C_{CO} dihedral angle of the *N*-Boc phenylaldimine electrophile within the optimized transition state geometries.

***N*-Boc p-OCF_3 arylaldimine/$EtNO_2$**

Donor NBO	Acceptor NBO	*E(2)* (kcal/mol)	C_{ph}-C_{CN}-N_{CN}-C_{CO} (degree)	Donor NBO	Acceptor NBO	*E(2)* (kcal/mol)	C_{ph}-C_{CN}-N_{CN}-C_{CO} (degree)
(*R*,*S*)-TS189$_{anti}$			-178°	(*S*,*R*)-TS189$_{anti}$			-179°
BD N32-C33	BD* N32-C34	1.49		BD N36-C42	BD* N36-C37	1.51	
BD N32-C33	BD* C34-O35	49.6		BD N36-C42	BD* C37-O38	49.3	
BD C33-C63	BD* N32-C33	1.50		BD C42-C51	BD* N36-C37	4.43	
BD C33-C63	BD* N32-C34	4.31		BD C42-C51	BD* N36-C42	1.51	
BD C63-C66	BD* N32-C33	28.4		BD C51-C53	BD* N36-C42	28.6	
BD C63-C65	BD* C33-C63	2.71		BD C51-C53	BD* C42-C51	2.73	
BD C63-C65	BD* C33-C63	2.89		BD C51-C54	BD* C42-C51	2.86	
E(2)(delocalization)		91.0		E(2)(delocalization)		91.0	

***N*-Boc p-OCF_3 arylaldimine/$EtNO_2$**

Donor NBO	Acceptor NBO	E(2) (kcal/mol)	C_{ph}-C_{CN}-N_{CN}-C_{CO} (degree)	Donor NBO	Acceptor NBO	E(2) (kcal/mol)	C_{ph}-C_{CN}-N_{CN}-C_{CO} (degree)
(*R*,*R*)-TS189$_{syn}$			-170°	(*S*,*S*)-TS189$_{syn}$			-166°
BD N32-C33	BD* N32-C34	1.42		BD N36-C42	BD* N36-C37	1.58	
BD N32-C33	BD* C34-O35	50.9		BD N36-C42	BD* C37-O38	46.5	
BD C33-C62	BD* N32-C33	1.43		BD C42-C50	BD* N36-C37	4.45	
BD C33-C62	BD* N32-C34	4.24		BD C42-C50	BD* N36-C42	1.52	
BD C62-C64	BD* N32-C33	1.61		BD C50-C52	BD* N36-C42	27.7	
BD C62-C64	BD* C33-C62	2.57		BD C50-C52	BD* C42-C50	2.68	
BD C62-C65	BD* C33-C62	2.91		BD C50-C53	BD* C42-C50	2.87	
BD C62-C65	BD* N32-C33	24.9		E(2)(delocalization)		87.3	
E(2)(delocalization)			90.0				

***N*-Boc *p*-Cl arylaldimine/$EtNO_2$**

Donor NBO	Acceptor NBO	*E(2)* (kcal/mol)	C_{ph}-C_{CN}-N_{CN}-C_{CO} (degree)	Donor NBO	Acceptor NBO	*E(2)* (kcal/mol)	C_{ph}-C_{CN}-N_{CN}-C_{CO} (degree)
(*R*,*S*)-TS190$_{anti}$			-178°	(*S*,*R*)-TS190$_{anti}$			-179°
BD N32-C33	BD* N32-C34	1.50		BD N36-C42	BD* N36-C37	1.50	
BD N32-C33	BD* C34-O35	49.3		BD N36-C42	BD* C37-O38	49.3	
BD C33-C63	BD* N32-C33	1.48		BD C42-C51	BD* N36-C37	4.42	
BD C33-C63	BD* N32-C34	4.36		BD C42-C51	BD* N36-C42	1.55	
BD C63-C66	BD* C33-C63	2.90		BD C51-C53	BD* N36-C42	29.5	
BD C63-C65	BD* N32-C33	28.5		BD C51-C53	BD* C42-C51	2.76	
BD C63-C65	BD* C33-C63	2.70		BD C51-C54	BD* C42-C51	2.89	
E(2)(delocalization)		91.0		E(2)(delocalization)		92.0	

N-Boc p-Cl arylaldimine/$EtNO_2$

Donor NBO	Acceptor NBO	E(2) (kcal/mol)	C_{ph}-C_{CN}-N_{CN}-C_{CO} (degree)	Donor NBO	Acceptor NBO	E(2) (kcal/mol)	C_{ph}-C_{CN}-N_{CN}-C_{CO} (degree)
(*R*,*R*)-TS190$_{syn}$			-169°	(*S*,*S*)-TS190$_{syn}$			-166°
BD N32-C33	BD* N32-C34	1.42		BD N36-C42	BD* N36-C37	1.59	
BD N32-C33	BD* C34-O35	50.8		BD N36-C42	BD* C37-O38	45.7	
BD C33-C63	BD* N32-C33	1.41		BD C42-C50	BD* N36-C37	4.25	
BD C33-C63	BD* N32-C34	4.31		BD C42-C50	BD* N36-C42	1.57	
BD C63-C66	BD* C33-C63	24.9		BD C51-C52	BD* N36-C42	31.2	
BD C63-C65	BD* N32-C33	2.90		BD C51-C52	BD* C42-C50	2.63	
BD C63-C65	BD* C33-C63	2.61		BD C51-C53	BD* C42-C50	2.93	
E(2)(delocalization)		88.3		E(2)(delocalization)		89.9	

N-Boc p-NO_2 arylaldimine/$EtNO_2$

Donor NBO	Acceptor NBO	E(2) (kcal/mol)	C_{ph}-C_{CN}-N_{CN}-C_{CO} (degree)	Donor NBO	Acceptor NBO	E(2) (kcal/mol)	C_{ph}-C_{CN}-N_{CN}-C_{CO} (degree)
(*R*,*S*)-TS191$_{anti}$			-178°	(*S*,*R*)-TS191$_{anti}$			-179°
BD N32-C33	BD* N32-C34	1.47		BD N36-C42	BD* N36-C37	1.47	
BD N32-C33	BD* C34-O35	46.7		BD N36-C42	BD* C37-O38	46.9	
BD C33-C62	BD* N32-C33	1.44		BD C42-C50	BD* N36-C37	4.38	
BD C33-C62	BD* N32-C34	4.43		BD C42-C50	BD* N36-C42	1.50	
BD C62-C64	BD* N32-C33	26.5		BD C50-C52	BD* N36-C42	27.0	
BD C62-C65	BD* C33-C62	2.75		BD C51-C52	BD* C42-C50	2.58	
BD C62-C64	BD* C33-C62	2.56		BD C50-C53	BD* C42-C50	2.74	
E(2)(delocalization)		86.0		E(2)(delocalization)		87.0	

N-Boc p-NO_2 arylaldimine/$EtNO_2$

Donor NBO	Acceptor NBO	E(2) (kcal/mol)	C_{ph}-C_{CN}-N_{CN}-C_{CO} (degree)	Donor NBO	Acceptor NBO	E(2) (kcal/mol)	C_{ph}-C_{CN}-N_{CN}-C_{CO} (degree)
(*R*,*R*)-TS191$_{syn}$			-170°	(*S*,*S*)-TS191$_{syn}$			-168°
BD N32-C33	BD* N32-C34	1.41		BD N36-C42	BD* N36-C37	1.53	
BD N32-C33	BD* C34-O35	46.0		BD N36-C42	BD* C37-O38	43.1	
BD C33-C63	BD* N32-C33	1.39		BD C42-C51	BD* N36-C37	4.25	
BD C33-C63	BD* N32-C34	4.41		BD C42-C51	BD* N36-C42	1.56	
BD C63-C65	BD* C33-C63	2.48		BD C51-C53	BD* N36-C42	27.8	
BD C63-C65	BD* N32-C33	26.0		BD C51-C54	BD* C42-C51	2.79	
BD C63-C66	BD* C33-C63	2.74		BD C51-C53	BD* C42-C51	2.48	
E(2)(delocalization)		84.0		E(2)(delocalization)		83.0	

Table 9A. Distortion/interaction analysis of the stereo-determining transition states in addition of nitronate to (a) *N*-Boc *p*-OCF_3-arylaldimine (**TS189**), (b) *p*-Cl-arylaldimine (**TS190**), and (c) *p*-NO_2-arylaldimine (**TS191**).

	(*R*,*S*)-TS189$_{anti}$	(*S*,*R*)-TS189$_{anti}$	ΔE	(*R*,*R*)-TS189$_{syn}$	(*S*,*S*)-TS189$_{syn}$	ΔE
Interaction Energy (E_{int}) (kcal/mol)	-65.7	-65.5	0.20	-64.3	-64.2	0.10
Catalyst Distortion ($E_{dist/cat}$) (kcal/mol)	5.23	5.71	0.47	5.22	5.76	0.54
Substrate Distortion/Interaction ($E_{dist/int}$) (kcal/mol)	1.03	2.26	1.22	2.15	3.28	1.13

	(*R*,*S*)-TS190$_{anti}$	(*S*,*R*)-TS190$_{anti}$	ΔE	(*R*,*R*)-TS190$_{syn}$	(*S*,*S*)-TS190$_{syn}$	ΔE
Interaction Energy (E_{int}) (kcal/mol)	-64.5	-64.0	0.50	-63.0	-62.1	0.90
Catalyst Distortion ($E_{dist/cat}$) (kcal/mol)	5.20	5.75	0.55	5.22	5.43	0.21
Substrate Distortion/Interaction ($E_{dist/int}$) (kcal/mol)	1.12	2.00	0.88	2.11	2.19	0.10

	(*R*,*S*)-TS191$_{anti}$	(*S*,*R*)-TS191$_{anti}$	ΔE	(*R*,*R*)-TS191$_{syn}$	(*S*,*S*)-TS191$_{syn}$	ΔE
Interaction Energy (E_{int}) (kcal/mol)	-63.3	-62.3	1.20	-61.9	-61.1	0.75
Catalyst Distortion ($E_{dist/cat}$) (kcal/mol)	5.17	5.37	0.20	5.18	5.34	0.16
Substrate Distortion/Interaction ($E_{dist/int}$) (kcal/mol)	1.24	2.02	0.78	2.23	2.31	0.10

Table 10A. NCI interaction critical points ((+/-)ρ_{ICP}) and QTAIM ρ_{BCP} representing the intra-host and host-guest non-covalent interactions in **TS190, TS191**.

	Non-Covalent Interactions	$(-)\rho_{ICP}$	ρ_{BCP}
(*R*,*S*)-**TS190**$_{anti}$	**Intra-Host**		
	A[a]	-0.0038	0.0043
	B	-0.0111	0.0116
	Host-Guest		
	C	-0.0071	0.0072
	D	-0.0068	0.0075
(*S*,*R*)-**TS190**$_{anti}$	**Intra-Host**		
	A	-	-
	B	-0.0102	0.0109
	Host-Guest		
	C	-0.0058	0.0078
	D	-0.0052	0.0062

	Non-Covalent Interactions	$(-)\rho_{ICP}$	ρ_{BCP}
(*R*,*R*)-**TS190**$_{syn}$	**Intra-Host**		
	A[a]	-0.0043	0.0049
	B	-0.0109	0.0109
	Host-Guest		
	C	-0.0069	0.0071
	D	-0.0074	0.0081
(*S*,*S*)-**TS190**$_{syn}$	**Intra-Host**		
	A	-	-
	B	-0.0104	0.0108
	Host-Guest		
	C	-0.0068	0.0072
	D	-0.0044	0.0054

	Non-Covalent Interactions	$(-)\rho_{ICP}$	ρ_{BCP}
(*R*,*S*)-**TS191**$_{anti}$	**Intra-Host**		
	A[a]	-0.0041	0.0051
	B	-0.0111	0.0108
	Host-Guest		
	C	-0.0074	0.0072
	D	-0.0069	0.0080
(*S*,*R*)-**TS191**$_{anti}$	**Intra-Host**		
	A	-0.0104	0.0107
	B		
	Host-Guest		
	C	-0.0061	0.0073
	D	-0.0048	0.0060

	Non-Covalent Interactions	$(-)\rho_{ICP}$	ρ_{BCP}
(*R*,*R*)-**TS191**$_{syn}$	**Intra-Host**		
	A[a]	-0.0047	0.0055
	B	-0.0111	0.0110
	Host-Guest		
	C	-0.0069	0.0074
	D	-0.0073	0.0087
(*S*,*S*)-**TS191**$_{syn}$	**Intra-Host**		
	A	-0.0105	0.0107
	B		
	Host-Guest		
	C	-0.0052	0.0070
	D	-0.0068	0.0059

[a] *The low density values (i.e., $\rho(r) < 0.005$ au) and the negative sign of λ_2 associated with this intra-host interaction were diagnostic of weakly attractive bonding interactions, such as induced dipole-induced dipole (London dispersion forces) interactions.*